

The genus *Phasgonophora* Westwood, 1832 (Hymenoptera, Chalcididae) in Saudi Arabia: re-evaluation of its limits and description of three new species

Muhammad Athar Gul^{1,2}, Ahmed Mostafa Soliman^{2,3}, Neveen Samy Gadallah⁴,
Hathal Mohammed Al Dhafer², Gérard Delvare⁵

1 Department of Environmental and Biological Sciences, University of Eastern Finland, P.O. Box 1627, FI-70211 Kuopio, Finland **2** Plant Protection Department, College of Food and Agriculture Sciences, King Saud University, P.O. BOX 2460, Riyadh 11451, Saudi Arabia **3** Zoology Department, Faculty of Science (Boys), Al-Azhar University, P.O. Box 11884, Nasr City, Cairo, Egypt **4** Entomology Department, Faculty of Science, Cairo University, Giza, Egypt **5** Centre de Coopération Internationale en Recherche Agronomique pour le Développement (CIRAD), Montpellier SupAgro, INRA, IRD, Univ. Montpellier, Montpellier, France

Corresponding author: Neveen Samy Gadallah (n_gadallah@hotmail.com)

Academic editor: P. Jansta | Received 17 July 2019 | Accepted 25 February 2020 | Published 27 April 2020

<http://zoobank.org/8C7E1DDE-BCFA-47C0-A38D-18458AD9221E>

Citation: Gul MA, Soliman AM, Gadallah NS, Al Dhafer HM, Delvare G (2020) The genus *Phasgonophora* Westwood, 1832 (Hymenoptera, Chalcididae) in Saudi Arabia: re-evaluation of its limits and description of three new species. Journal of Hymenoptera Research 76: 1–38. <https://doi.org/10.3897/jhr.76.38340>

Abstract

A phylogenetic study based on 25 species of Phasgonophorinae (Hymenoptera: Chalcididae) and 36 characters was carried out for ensuring the generic placement of three new species from Saudi Arabia. As a result of this study, the genera *Trigonura* Sichel, 1866, *Bactrochalcis* Kieffer, 1912, *Centrochalcis* Cameron, 1913, *Centrochalcidia* Gahan & Fagan, 1923, *Chalcidellia* Girault, 1924, *Urochalcis* Nikol'skaya, 1952, *Trigonurella* Bouček, 1988, and *Muhabbetella* Koçak & Kemal, 2008 are synonymized with *Phasgonophora* Westwood, 1832. This genus is recorded in Saudi Arabia for the first time, represented here by *P. rubens* (Klug), and newly described species *P. baiocchii* Soliman & Gul, **sp. nov.**, *P. granulifera* Delvare, **sp. nov.**, and *P. magnanii* Gadallah & Gul, **sp. nov.** An illustrated key to species of the Arabian Peninsula is provided. The relevant specimens were mostly reared from buprestid species infesting *Acacia* sp. and *Dodonaea viscosa* in Al-Baha, Asir and Riyadh regions, Saudi Arabia.

Keywords

Al-Baha, Asir, Riyadh, Buprestidae, new species, *Phasgonophora*, Phasgonophorini, phylogeny

Introduction

Phasgonophorinae were first recognized as discrete group by Steffan (1951) who listed their features and classified them within Brachymeriinae. They were later classified within Chalcidinae (Bouček 1988, 1992; Narendran 1989; Wijesekara 1997a; Delvare 2017), but quite recently were raised to subfamily level (Cruaud et al. 2020) appearing as the sister group of Brachymeriinae *s.s.* (sensu Wijesekara 1997b, as Phasgonophorini). This rather small subfamily includes 66 described species, but many of them, particularly in *Phasgonophora*, still await description, especially in the tropics where the subfamily is the most diverse. The subfamily was extensively studied by Steffan (1951, 1956, 1973).

Phasgonophorinae are parasitoids of wood-boring beetles belonging to the families Buprestidae, Curculionidae (including Scolytinae), Cerambycidae and Anthribidae (Steffan 1951, 1973; Burks 1959; Mateu 1972; Bouček 1988, 1992; Narendran 1989; Roscoe 2014; Narendran and van Achterberg 2016).

The subfamily currently includes two tribes (Cruaud et al. 2020), Phasgonophorini and Stypiurini, namely the *Phasgonophora* and *Stypiura* groups of Steffan (1951). Phasgonophorini themselves would comprise a single genus based on the phylogenetic results using the ultra-conserved elements (UCE) (Cruaud et al. 2020). Furthermore, *Trigonura* appeared polyphyletic, merging on two different branches, the first one together with *Muhabbetella* Koçak & Kemal, 2008 (replacement name for *Trigonurella* Bouček, 1988 nec Maa, 1963) on one hand, and *Phasgonophora* Westwood, 1832 on the other hand.

Phasgonophorini have the following features: a hardly sclerotized body, most often with rasp-like sculpture on pronotum and mesonotum; malar sulcus absent; antennal scrobes quite deep and entirely delimited by carinae; antennal toruli on about the level of lower ocular line; both mandibles with three teeth; propodeum often strongly sloping; mesopleuron frequently with a ventral shelf that is regularly longer than epicnemium; procoxa with a deep depression anteriorly, delimited by an oblique carina raised into a flange; metatibia without spur; postmarginal vein short, only surpassing stigmal vein in length; petiole very short, either entirely concealed dorsally or visible here as a ring-like sclerite, but better visible ventrally; first tergite with dorsolateral costulae and syntergum often elongated into a stylus; ovipositor sheaths and valvulae straight.

Phasgonophora with 38 described species is distributed in arid and temperate zones of Asia (21 species), New World (11 species), Africa (2 species) and Australia (4 species). The genus parasitizes xylophagous beetles of the families Anthribidae, Buprestidae, Cerambycidae and Curculionidae (including Scolytinae) (Waterston 1922; Steffan 1951; Burks 1959; Mateu 1972; Narendran and van Achterberg 2016).

Until now *Phasgonophora* was represented by only two species in the Arabian Peninsula, *P. ninae* (Nikol'skaya, 1952) and *P. rubens* (Klug, 1834), reported by Delvare (2017) from the United Arab Emirates (under *Trigonura*). In the present study, the genus is recorded for the first time from Saudi Arabia (from Al-Baha, Asir and Riyadh regions) with four species, namely *P. rubens* (Klug), and the newly described *P. baiocchii* Soliman & Gul, sp. nov., *P. granulifera* Delvare, sp. nov., and *P. magnanii* Gadallah & Gul, sp. nov., mainly reared from Buprestidae attacking *Acacia* sp. (Fabaceae) or *Dodonaea viscosa* (L.) Jacq. (Sapindaceae) dead wood.

A phylogenetic study based on morphology was carried out for exploring the possible congruence between molecular and morphological data and hypothesizing the systematic placement of the species collected in Saudi Arabia.

Material and methods

Phylogenetic study

Sampling (Table 1). Outgroups include *Brachymeria minuta* (Linnaeus, 1761) (Brachymeriinae), and within the Phasgonophorinae, three species of Stypriurini, namely *Kopinata partirubra* Bouček, 1988, and two *Stypiuura* species that were chosen together with 21 species of Phasgonophorini belonging to the genera presently recognized. *Phasgonophora sulcata* Westwood, 1835, *Phasgonophora (Trigonura) crassicauda* Sichel, 1866, and *Chalcis euthyrrhini* Dodd, 1921, respectively type species of *Phasgonophora* Westwood, 1832, *Trigonura* Sichel, 1866, and *Chalcidellia* Girault, 1924 are included in the sample, which also comprises the specimens that were used for the phylogenetic inference with Ultra Conserved Elements (UCE) (Cruaud et al. 2020). The material from Saudi Arabia was reared from xylophagous Coleoptera of the family Buprestidae (*Chrysobothris* sp.) attacking *Acacia* sp. and *D. viscosa* dead wood collected by Daniele Baiocchi and Gianluca Magnani (Roma, Italy) or collected using sweep net on *Calotropis procera* (Aiton) (Apocynaceae) trees from different wadis in Al Baha, Asir and Riyadh regions.

Table 1. Specimens used for the phylogenetic study. Generic names as in the present literature.

| Specimen | Specimen status | Subfamily | Tribe | Country | Year collect | Molecular code |
|--|-----------------|------------------|-----------------|---------------------|--------------|----------------|
| <i>Brachymeria minuta</i> (Linnaeus, 1761) | | Brachymeriinae | Brachymeriini | France | 1986 | |
| <i>Kopinata partirubra</i> Bouček, 1988 | paratype | Phasgonophorinae | Stypriurini | PNG | 1981 | |
| <i>Stypiuura</i> GDEL00236 | | Phasgonophorinae | Stypriurini | French Guiana | 2005 | GDEL00236 |
| <i>Stypiuura</i> GDEL00580 | | Phasgonophorinae | Stypriurini | French Guiana | 2010 | GDEL00580 |
| <i>Trigonura</i> GDEL00487 | | Phasgonophorinae | Phasgonophorini | Cameroon | 2003 | GDEL00487 |
| <i>Trigonura</i> GDEL00489 | | Phasgonophorinae | Phasgonophorini | Cameroon | 2003 | GDEL00489 |
| <i>Trigonura steffani</i> Narendran, 1987 | holotype | Phasgonophorinae | Phasgonophorini | India, Kerala | 1985 | |
| <i>Trigonura javensis</i> Narendran, 1987 | holotype | Phasgonophorinae | Phasgonophorini | Indonesia, Java | 1930 | |
| <i>Trigonura bakeri</i> Masi, 1926 | holotype | Phasgonophorinae | Phasgonophorini | Philippines | | |
| <i>Trigonura tarsata</i> (Dalla Torre, 1898) | | Phasgonophorinae | Phasgonophorini | Canada, Quebec | 1948 | |
| <i>Trigonura elegans</i> (Provancher, 1887) | | Phasgonophorinae | Phasgonophorini | USA | | |
| <i>Trigonura nishidai</i> Narendran, 1989 | | Phasgonophorinae | Phasgonophorini | Laos | 2013 | JRAS5401_0101 |
| <i>Muhabbetella</i> JRAS5401_0301 | | Phasgonophorinae | Phasgonophorini | Laos | 2013 | JRAS5401_0301 |
| <i>Trigonura rubens</i> (Klug, 1834) | | Phasgonophorinae | Phasgonophorini | Saudi Arabia | 2017 | |
| <i>Trigonura ninae</i> (Nikols'kaya, 1952) | | Phasgonophorinae | Phasgonophorini | UAE | 2006 | |
| <i>Phasgonophora ruficauda</i> (Cameron, 1905) | | Phasgonophorinae | Phasgonophorini | Guinea | 1986 | |
| <i>Trigonura euthyrrhini</i> (Dodd, 1921) | | Phasgonophorinae | Phasgonophorini | PNG | 2018 | JRAS7369 |
| <i>Trigonura crassicauda</i> (Sichel, 1866) | holotype | Phasgonophorinae | Phasgonophorini | Mexico | | |
| <i>Phasgonophora baiocchi</i> sp. nov. | holotype | Phasgonophorinae | Phasgonophorini | Saudi Arabia | 2017 | |
| <i>Phasgonophora magnanii</i> sp. nov. | holotype | Phasgonophorinae | Phasgonophorini | Saudi Arabia | 2016 | |
| <i>Phasgonophora granulis</i> sp. nov. | holotype | Phasgonophorinae | Phasgonophorini | Saudi Arabia | 2016 | |
| <i>Trigonura</i> Nkolbisson | | Phasgonophorinae | Phasgonophorini | Cameroon | 1965 | |
| <i>Trigonura</i> Kenya Mt Elgon | | Phasgonophorinae | Phasgonophorini | Kenya | 2011 | |
| <i>Phasgonophora sulcata</i> Westwood, 1832 | | Phasgonophorinae | Phasgonophorini | USA, Virginia | 1986 | |
| <i>Phasgonophora</i> nr. <i>sulcata</i> Westwood, 1832 | | Phasgonophorinae | Phasgonophorini | USA, North Carolina | 2014 | JRAS5708_0101 |

Phylogenetic inference. A matrix of 36 characters (Tables 2, 3) was analyzed with maximum parsimony in PAUP* version 4.0a (Swofford 2001). PAUP analysis was first performed with equally weighted and non-additive character states. Eight characters that were initially stated irreversible, as reversals involving a separation of claval segments and gastral tergites following their fusion or the reappearance of the metatibial spur after its loss, are biologically inconceivable. A traditional heuristic search was conducted using 100 random addition sequences (RAS) to obtain an initial tree and “tree bisection and reconnection (TBR)” as branch swapping option. We then used a successive weighting method with the weight assigned to each character proportional to the maximum rescaled consistency index. We also screened the effect of ordering/non-ordering of characters. Robustness of the topology (equally weighted characters) was assessed by bootstrap procedures (100 replicates).

Examination and imaging

Specimens were examined using a Leica M205 C stereomicroscope. Some specimens were photographed using a digital microscope Keyence VHX-5000. Photographs were digitally optimized (artifacts removal, background standardization) using the photoshop V-program. The photos made with the aforementioned equipment were used for measurements of the types (holotypes and some paratypes). Further photographs were taken using Canon EOS camera attached to a Leica MZ 125 stereomicroscope. Individual source images were then stacked using HeliconFocus v.6.22 (HeliconSoft Ltd) extended depth of field software. Further image processing was done using the software Adobe photoshop CS5.1 (v.12.1) and Adobe photoshop Lightroom v.5.2 Final [ChingLiu]. The distribution of *Phasgonophora* species in Saudi Arabia was plotted (Fig. 17) using DIVA-GIS (v.7.17).

Morphological terminology

Morphological terminology follows Burks (1959) and Delvare (2017); body sculpture terminology follows Harris (1979).

Species identification

We examined the types of 18 species of *Phasgonophora sensu lato*, thus including those described in *Trigonura*. The relevant species included all those described from the New World, the west Palaearctic and the Afrotropical regions, and part of those described from the Oriental region. We used keys and descriptions provided by Narendran (1989), Narendran and van Achterberg (2016) for comparison of species described from Saudi Arabia to the rest of the Oriental species.

Table 2. Characters and their states used for phylogenetic inference of the Phasgonophorini.

| | |
|------|--|
| [1] | Mandibular formula. (0) mandibles 2.2; (1) mandibles 3.3. [unordered] |
| [2] | Upper tooth of mandible. (0) sharp or narrowly rounded at apex; (1) truncate at apex. [unordered] |
| [3] | Lower face: presence of differentiate median stripe. (0) strip absent; (1) alutaceous strip present; (2) narrow, non-sculptured strip present. [unordered] |
| [4] | Preorbital carina or ridge. (0) absent; (1) present. [unordered] |
| [5] | Malar sulcus. (0) present, at least partly; (1) completely absent. [irreversible] |
| [6] | Antennal insertion. (0) not or hardly above lower ocular line; (1) much above lower ocular line. [unordered] |
| [7] | Interantennal projection. (0) ventral surface triangular, not compressed ventrally; (1) ventral surface moderately compressed laterally; (2) ventral surface strongly compressed, forming a lamina. [unordered] |
| [8] | Interocellar distance (between median and lateral ocellus). (0) not especially short, at least as large as ocellus diameter; (1) very short, shorter than ocellus diameter. [unordered] |
| [9] | Carina behind ocellar triangle. (0) carina absent; (1) carina present; (2) carina present and raised to form a bump behind ocellar triangle. [unordered] |
| [10] | Sculpture of occiput behind ocellar triangle. (0) occiput punctured behind ocellar triangle; (1) occiput punctured strigulose mesally behind ocellar triangle; (2) occiput strigulose mesally behind ocellar triangle (with vertical carinulae there). [unordered] |
| [11] | Sculpture of occiput on lateral surface. (0) occiput punctured; (1) occiput punctured strigulose, the puncturation alternating with vertical carinulae; (2) occiput entirely strigulose. [unordered] |
| [12] | Length of flagellomeres. (0) flagellomeres relatively short, F1 at most 1.5× as long as wide; (1) flagellomeres elongate, F1 more than 2× as long as wide. [unordered] |
| [13] | Segmentation of clava. (0) clava 3-segmented; (1) clava at most 2-segmented (rarely 1-segmented). [irreversible] |
| [14] | Pronotum: median depression. (0) absent; (1) present. [unordered] |
| [15] | Pronotal collar: anterior margin. (0) collar with rounded or blunt anterior margin sometimes not differentiate mesally; (1) collar strongly angulate with collum, angle acute; (2) pronotum sloping from posterior margin, collar not differentiate, at least mesally. [unordered] |
| [16] | Pronotum: hind margin. (0) margin slightly concave; (1) margin strongly concave. [unordered] |
| [17] | Mesonotum: sculpture. (0) mesonotum entirely punctured; (1) mesonotum at least partly cristate; (2) mesonotum entirely strigose. [unordered] |
| [18] | Mesoscutellum: anterior margin. (0) mesoscutellum truncate anteriorly on transscutal line; (1) anterior margin of mesoscutellum forming a blunt angle as the axillar grooves are meeting or almost so on transscutal line. [unordered] |
| [19] | Setation of axilla. (0) sparse to moderately dense; (1) quite dense. [unordered] |
| [20] | Mesodiscrimen. (0) visible as raised carina dorsally and a fovea ventrally on mesal surface of epicnemium; (1) visible as a low ridge on mesal surface of epicnemium. [unordered] |
| [21] | Epicnemial carina laterally. (0) not or moderately raised; (1) strongly raised. [unordered] |
| [22] | Epicnemial carina ventrally. (0) not or slightly raised, not forming or forming small tooth in lateral view; (1) strongly raised forming a projecting tooth in lateral view. [unordered] |
| [23] | Length of ventral shelf of mesepisternum. (0) ventral shelf not or not much longer than epicnemium; (1) ventral shelf much longer than epicnemium and several times long as long as mesocoxa. [unordered] |
| [24] | Procoxa. (0) coxa depressed on front side, depression margined posterodorsally by faint carina; (1) coxa deeply depressed on front side, depression margined posterodorsally by raised carina forming flange. [unordered] |
| [25] | Dorso-apical margin of protibia. (0) not forming projection; (1) forming a short and apically blunt projection; (2) well expanded with sharp apex. [unordered] |
| [26] | Outer dorsal surface of metacoxa. (0) flattened posteriorly, on less than half-length; (1) convex. [unordered] |
| [27] | Metatibia spur. (0) one spur present; (1) spur absent. [irreversible] |
| [28] | Postmarginal vein. (0) longer than marginal vein; (1) about twice as long as stigmal vein (not or hardly longer than marginal vein). [irreversible] |
| [29] | Number of gastral tergites in female. (0) seven, Gt1 and Gt2 not fused; (1) less than seven as Gt1 and Gt2 are fused. [irreversible] |
| [30] | First gastral tergite ornamentation. (0) no ornamentation, tergite regularly convex dorsally; (1) tergite with basal transverse carina and longitudinal ridges joining it. |
| [31] | First tergite: lateral line. (0) absent; (1) present. [unordered] |
| [32] | Penultimate tergite: depth of puncturation. (0) deep as usual; (1) superficial. [unordered] |
| [33] | Spiracle on penultimate tergite. (0) of usual size, quite visible; (1) very small with aperture smaller than diameter of punctures. [unordered] |
| [34] | Syntergum length. (0) syntergum not especially elongate, not more than 2 times as long as its basal width; (1) syntergum elongate as a stylus much more than twice its basal width. [unordered] |
| [35] | Position of cercal plates. (0) near anterior margin of syntergum; (1) situated about at mid length of syntergum; (2) situated near apex of syntergum. [unordered] |
| [36] | Ovipositor sheaths. (0) sheaths as usual, not especially curved; (1) sheaths curved downwards. [unordered] |

Acronyms for museums and other institutions

Natural History Museum, London, United Kingdom (**BMNH**); Efflatoun Bey collection, Entomology Department, Faculty of Science, Giza, Egypt (**EFC**); King Saud

University for Arthropods, Plant Protection Department, College of Food and Agriculture Sciences, King Saud University, Riyadh, Saudi Arabia (**KSMA**); Museum für Naturkunde, Berlin, Germany (**MNB**); National Museum of Natural History, Smithsonian Institution, Washington, United States of America (**USNM**).

Table 3. Data matrix for the phylogenetic inference of the Phasgonophorini (Chalcididae).

| | 1 1 1 1 1 1 1 1 1 1 1 2 2 2 2 2 2 2 2 2 2 2 2 2 2 2 3 3 3 3 3 3 3 | | | | | | | | | | | | | | | | | | | | | | | | | | | | | | | | | | | | |
|--|---|---|---|---|---|---|---|---|---|---|---|---|---|---|---|---|---|---|---|---|---|---|---|---|---|---|---|---|---|---|---|---|---|---|---|---|---|
| | 1 | 2 | 3 | 4 | 5 | 6 | 7 | 8 | 9 | 0 | 1 | 2 | 3 | 4 | 5 | 6 | 7 | 8 | 9 | 0 | 1 | 2 | 3 | 4 | 5 | 6 | 7 | 8 | 9 | 0 | 1 | 2 | 3 | 4 | 5 | 6 | |
| <i>Brachymeria minuta</i> | 0 | 0 | 0 | 0 | 0 | 0 | 2 | 0 | 0 | 0 | 0 | 0 | 0 | 0 | 0 | 0 | 0 | 0 | 0 | 0 | 0 | 0 | 0 | 0 | 0 | 0 | 0 | 0 | 0 | 0 | 0 | 0 | 0 | 0 | 0 | 0 | 0 |
| <i>Kopinata partirubra</i> | 0 | 0 | 0 | 0 | 0 | 0 | 0 | 1 | 0 | 2 | 1 | 1 | 0 | 0 | 0 | 1 | 2 | 0 | 0 | ? | ? | ? | ? | ? | 1 | 1 | 0 | ? | 2 | 1 | 0 | 0 | 1 | 0 | 1 | 1 | 1 |
| <i>Styptiura</i> GDEL00236 | 0 | 0 | 1 | 0 | 1 | 1 | 0 | 1 | 1 | 2 | 0 | 1 | 0 | 0 | 0 | 1 | 0 | 1 | 0 | 1 | 0 | 0 | 0 | 1 | 1 | 0 | 0 | 2 | 0 | 0 | 0 | 1 | 1 | 1 | 1 | 2 | |
| <i>Styptiura</i> GDEL00580 | 0 | 0 | 1 | 0 | 1 | 1 | 1 | 1 | 1 | 2 | 0 | 1 | 0 | 0 | 0 | 1 | 0 | 0 | 1 | 0 | 0 | 0 | 1 | 1 | 0 | 0 | 2 | 0 | 0 | 0 | 1 | 1 | 1 | 1 | 2 | | |
| <i>Trigonura</i> GDEL00487 | 1 | 0 | 0 | 1 | 0 | 1 | 0 | 0 | 1 | 0 | 0 | 0 | 0 | 1 | 1 | 0 | 0 | 1 | 0 | 0 | 0 | 1 | 1 | 0 | 0 | 1 | 1 | 0 | 2 | 0 | 0 | 1 | 0 | 0 | 0 | 0 | |
| <i>Trigonura</i> GDEL00489 | 1 | 0 | 1 | 1 | 1 | 0 | 0 | 0 | 1 | 0 | 0 | 0 | 0 | 0 | 1 | 1 | 0 | 0 | 1 | 0 | 0 | 0 | 1 | 1 | 0 | 1 | 1 | 0 | 2 | 0 | 0 | 1 | 0 | 0 | 0 | 0 | |
| <i>Trigonura euthyrrhini</i> | 1 | 1 | 0 | 0 | 1 | 0 | 1 | 0 | 0 | 1 | 0 | 0 | 0 | 0 | 1 | 1 | 0 | 0 | 1 | 0 | 0 | 0 | 1 | 1 | 0 | 1 | 1 | 0 | 2 | 0 | 0 | 1 | 0 | 0 | 0 | 0 | |
| <i>Muhabbetella</i> JRAS5401 | 1 | 0 | 1 | 1 | 1 | 0 | 1 | 1 | 0 | 1 | 0 | 0 | 0 | 0 | 0 | 1 | 1 | 0 | 0 | 1 | 0 | 0 | 0 | 1 | 1 | 0 | 1 | 2 | 0 | 0 | 1 | 0 | 0 | 0 | 0 | 0 | |
| <i>Trigonura steffani</i> | 1 | 0 | 1 | 1 | 1 | 0 | 0 | 0 | 0 | 1 | 0 | 0 | 0 | 0 | 0 | 1 | 1 | 0 | 0 | ? | 0 | 0 | 0 | 1 | 1 | 0 | 1 | 2 | 0 | 0 | 1 | 0 | 0 | 0 | 0 | 0 | |
| <i>Trigonura javensis</i> | 1 | 0 | 1 | 1 | 1 | 0 | 0 | 0 | 0 | 1 | 0 | 0 | 0 | 0 | 0 | 1 | 1 | 0 | 0 | ? | 0 | 0 | 0 | 1 | 1 | 0 | 1 | 2 | 0 | 0 | 1 | 0 | 0 | 0 | 0 | 0 | |
| <i>Trigonura tarsata</i> | 1 | 0 | 1 | 0 | 1 | 0 | 0 | 0 | 1 | 0 | 1 | 0 | 0 | 0 | 1 | 1 | 0 | 0 | 1 | 0 | 0 | 0 | 1 | 1 | 0 | 1 | 1 | 0 | 2 | 0 | 0 | 1 | 1 | 0 | 1 | 0 | 0 |
| <i>Trigonura elegans</i> | 1 | 0 | 0 | 1 | 1 | 0 | 0 | 0 | 1 | 0 | 0 | 0 | 0 | 0 | 1 | 1 | 1 | 0 | 1 | 0 | 0 | 0 | 1 | 1 | 0 | 1 | 1 | 0 | 2 | 0 | 0 | 1 | 1 | 0 | 0 | 0 | 0 |
| <i>Trigonura nishidai</i> | 1 | 0 | 0 | 0 | 1 | 0 | 1 | 0 | 0 | 2 | 0 | 0 | 1 | 0 | 0 | 1 | 1 | 0 | 0 | ? | 1 | ? | 0 | 1 | 2 | 0 | 1 | 2 | 0 | 0 | 1 | 0 | 0 | 1 | 0 | 1 | |
| <i>Trigonura bakeri</i> | 1 | 0 | 0 | 0 | 1 | 0 | 2 | 0 | 0 | 1 | 0 | 1 | 1 | 0 | 0 | 1 | 1 | 1 | 0 | 2 | 0 | 0 | 0 | 1 | 2 | 0 | 1 | 2 | 0 | 0 | 1 | 1 | 0 | 1 | 0 | 1 | |
| <i>Trigonura</i> Nkolbisson | 1 | 1 | 2 | 0 | 2 | 0 | 2 | 0 | 2 | 2 | 2 | 1 | 1 | 0 | 1 | 1 | 1 | 1 | 0 | 1 | 0 | 0 | 1 | 1 | 1 | 0 | 1 | 2 | 0 | 0 | 1 | 1 | 1 | 0 | 0 | 1 | |
| <i>Trigonura</i> Kenya Mt Elgon | 1 | 1 | 2 | 0 | 2 | 0 | 2 | 0 | 2 | 2 | 2 | 1 | 1 | 0 | 1 | 1 | 1 | 1 | 0 | 1 | 0 | 0 | 1 | 1 | 2 | 0 | 1 | 2 | 0 | 0 | 1 | 1 | 1 | 1 | 0 | 2 | |
| <i>Trigonura ninae</i> | 1 | 0 | 0 | 0 | 1 | 0 | 2 | 1 | 0 | 0 | 0 | 1 | 1 | 0 | 0 | 1 | 1 | 1 | 0 | 2 | 0 | 1 | 0 | 1 | 2 | 0 | 1 | 2 | 0 | 0 | 1 | 0 | 1 | 1 | 0 | 1 | |
| <i>Phasgonophora baiocchii</i> | 1 | 0 | 0 | 0 | 1 | 0 | 1 | 0 | 1 | 2 | 1 | 0 | 1 | 0 | 0 | 1 | 1 | 0 | 0 | 1 | 0 | 0 | 2 | 1 | 0 | 0 | 1 | 2 | 0 | 1 | 2 | 0 | 0 | 1 | 0 | 0 | 0 |
| <i>Phasgonophora magnanii</i> | 1 | 0 | 0 | 0 | 1 | 0 | 1 | 0 | 1 | 2 | 1 | 1 | 1 | 0 | 1 | 1 | 1 | 0 | 1 | 1 | 0 | 2 | 0 | 0 | 0 | 1 | 2 | 0 | 1 | 2 | 0 | 0 | 1 | 0 | 1 | 0 | 1 |
| <i>Phasgonophora granulis</i> | 1 | 0 | 0 | 0 | 1 | 0 | 2 | 0 | 2 | 2 | 2 | 1 | 1 | 1 | 0 | 1 | 1 | 0 | 1 | 2 | 1 | 1 | 1 | 1 | 2 | 0 | 1 | 2 | 0 | 0 | 1 | 0 | 1 | 1 | 0 | 1 | |
| <i>Trigonura rubens</i> | 1 | 1 | 0 | 0 | 1 | 0 | 2 | 0 | 0 | 2 | 2 | 1 | 1 | 1 | 0 | 1 | 1 | 0 | 0 | ? | 1 | 1 | 1 | 1 | 2 | 0 | 1 | 2 | 0 | 0 | 1 | 0 | 1 | 1 | 0 | 1 | |
| <i>Trigonura crassicauda</i> | ? | ? | 0 | 0 | 1 | 0 | 2 | 0 | 1 | 2 | 2 | 1 | ? | 1 | 0 | 1 | 1 | 1 | ? | 2 | 1 | ? | 1 | 1 | 2 | 0 | 1 | 2 | 0 | 0 | ? | ? | ? | 1 | 0 | ? | |
| <i>Trigonura ruficauda</i> | 1 | 0 | 0 | 0 | 1 | 0 | 2 | 0 | 1 | 2 | 2 | 1 | 1 | 1 | 0 | 1 | 1 | 1 | 1 | 2 | 0 | 1 | 1 | 1 | 2 | 0 | 1 | 2 | 0 | 0 | 1 | 0 | 1 | 1 | 0 | 1 | |
| <i>Phasgonophora sulcata</i> | 1 | 0 | 0 | 0 | 1 | 0 | 2 | 0 | 1 | 2 | 1 | 1 | 1 | 1 | 0 | 1 | 1 | 0 | 0 | 2 | 0 | 1 | 1 | 1 | 2 | 1 | 1 | 2 | 0 | 1 | - | ? | 1 | 1 | 0 | 1 | |
| <i>Phasgonophora</i> nr <i>sulcata</i> | 1 | 0 | 0 | 0 | 1 | 0 | 2 | 0 | 1 | 2 | 1 | 1 | 1 | 1 | 0 | 1 | 1 | 1 | ? | 2 | 0 | 1 | 1 | 1 | 2 | 1 | 1 | 2 | 0 | 1 | - | ? | 1 | 1 | 0 | 1 | |

Abbreviations

F1–F3 = first to third funicular segments; Gt = gastral tergite; MGV = marginal vein of fore wing; OOL = distance between lateral ocelli and inner eye margin; PMV = postmarginal vein; POL = distance between lateral ocelli; Rs = radial sector; r-m = radio-medial cross vein; SMV = submarginal vein of fore wing; STV = stigmal vein.

Results

Phylogeny of Phasgonophorini

The initial analysis provided 33 equally parsimonious trees with a length of 88 steps, and values of 0.489, 0.831 and 0.406 respectively for the consistency (CI), reten-

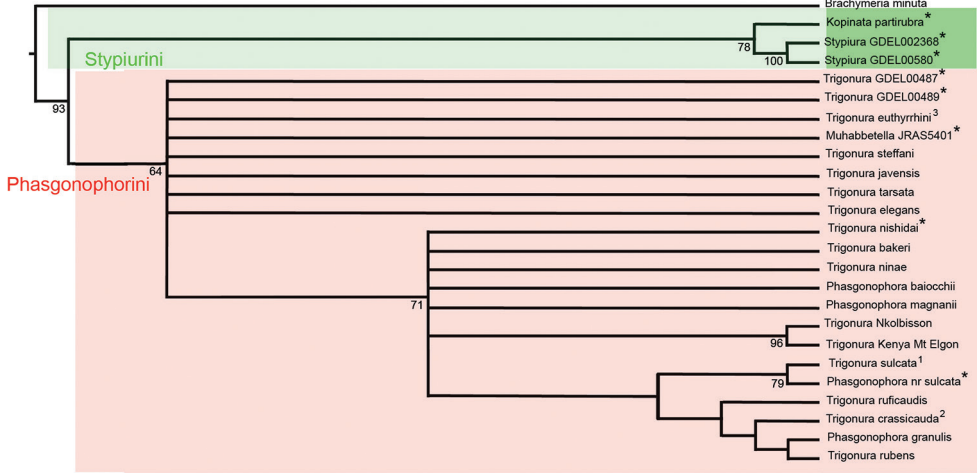


Figure 1. Strict consensus tree of the Phasgonophorini achieved from phylogenetic inference using parsimony. Bootstrap support below nodes. A, B, C denote the supported clades; * denote specimens used for the phylogenetic study using the Ultra Conserved Elements (Cruaud et al. 2020); 1, type species of *Phasgonophora* Westwood; 2, type species of *Trigonura* Sichel; 3, type species of *Chalcidellia* Girault.

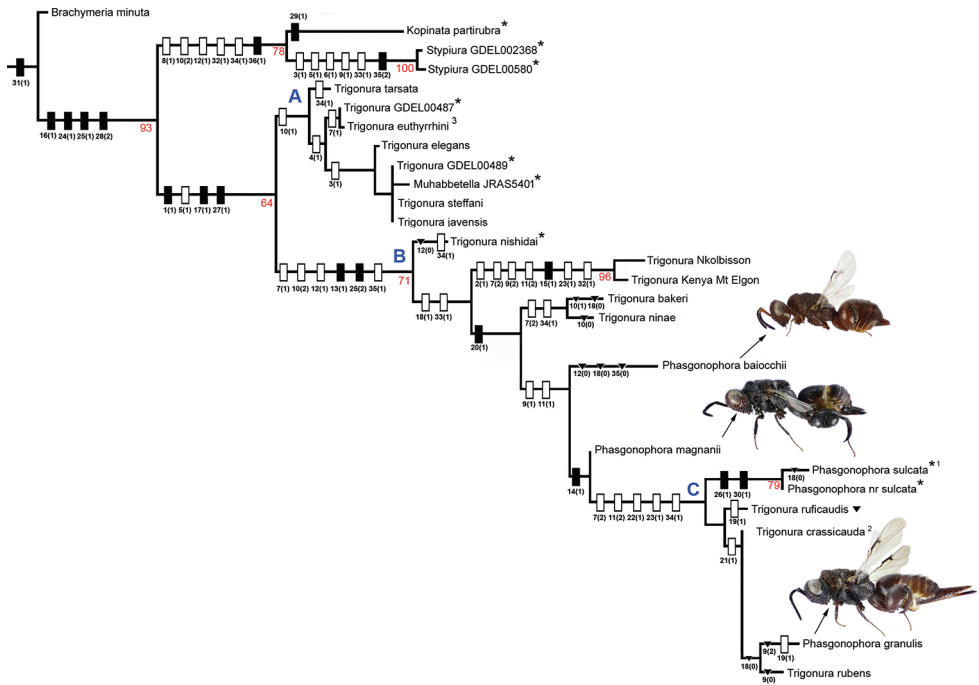


Figure 2. Preferred tree of the Phasgonophorini from phylogenetic inference using parsimony after successive weighting. Legend identical with Fig. 1. Black rectangles denote synapomorphies, white rectangles homoplastic derived states and dark triangles putative reversals.

tion (RI), and rescaled consistency (RC) indices. Stypriurini and Phasgonophorini are retrieved monophyletic with moderately strong supports (respectively 78, 64 for the bootstrap values) in the strict consensus tree (CST) (Fig. 1). Regarding Phasgonophorini, the tree shows a basal polytomy, including seven species, identified as *Trigonura* and one as *Muhabbetella* when using the traditional classification. The tree then shows a basal clade (Fig. 2, clade B), itself with a polytomy including seven species. Two of the newly described species from Saudi Arabia are retrieved here; all species in clade B would be assigned to *Trigonura* with the available keys (Bouček 1988; Narendran 1989). Finally, a second, terminal clade (Fig. 2, clade C) especially includes *P. sulcata* and *T. crassicauda* – the type species of *Phasgonophora* and *Trigonura* – together with *P. granulifera*, one of the new described species from Saudi Arabia. This clade would otherwise comprise most of the species presently identified as *Trigonura*.

The successive weighting procedure provided three trees with length of 34.232, CI, RI, and RC, respectively of 0.665, 0.933 and 0.658. Ordering versus non-ordering characters do not change the topology. The preferred tree is presented as the Fig. 2. It is entirely congruent, for the appropriate species, with the tree achieved when using the UCE (Cruaud et al. 2020). Here the polytomies observed in the CST are solved, but the corresponding nodes do not have any support as they are sustained by a few derived, mostly homoplastic character states. Again *P. granulifera* appears as sister to *T. rubens*, while *P. magnanii* as sister to clade C, a relationship sustained by the presence of a median depression on the pronotum. *P. baiocchii* merges on a node just basal to *P. magnanii*, but its position varies when the characters are equally weighted. Thus, it is sometimes sister to *P. magnanii*, sister to *T. nishidai* Narendran, 1989 or even merges on a basal node within the clade C, hence sister to the other species of the clade B taken together.

***Phasgonophora* Westwood, 1832**

Phasgonophora Westwood, 1832: 432 (fig. 77). Type species: *Phasgonophora sulcata* Westwood, 1832, by monotypy.

= *Phasganophora* [sic] subg. *Trigonura* Sichel, 1866: 358–376. Type species: *Phasganophora (Trigonura) crassicauda* Sichel, 1866, by monotypy, syn. nov.

= *Trigonura* Kirby, 1883: 54, 59–60 (raised to genus level), syn. nov.

= *Bactrochalcis* Kieffer, 1912: 463. Type species: *Bactrochalcis reticulata* Kieffer, by monotypy. Synonymized with *Trigonura* by Steffan, 1951: 147, syn. nov.

= *Centrochalcis* Cameron, 1913: 92. Type species: *Centrochalcis ruficaudis* Cameron, by monotypy. Synonymized with *Trigonura* by Waterston, 1922: 10, syn. nov.

= *Centrochalcidea* Gahan & Fagan, 1923. Replacement name for *Centrochalcis* Cameron, 1913, nec Cameron, 1905, syn. nov.

= *Chalcidellia* Girault, 1924: 3. Type species: *Chalcis euthyrrhini* Dodd, 1921, by original designation. Synonymized with *Trigonura* by Bouček, 1988: 63–64, syn. nov.

- = *Urochalcis* Nikol'skaya, 1952: 91. Type species: *Urochalcis ninae* Nikol'skaya, 1952, by original designation. Synonymized with *Trigonura* by Nikol'skaya, 1960: 90, syn. nov.
- = *Trigonurella* Bouček, 1988: 64. Type species: *Trigonurella elegans* Bouček, 1988, by original designation, syn. nov.
- = *Muhabbetella* Koçak & Kemal, 2008: 3. Replacement name for *Trigonurella* Bouček, 1988 nec *Trigonurella* Maa, 1963, syn. nov.

The above synonymies are just the taxonomic implications resulting from phylogenetic inference using UCE (Cruaud et al. 2020) and the present study from morphological data. In these two studies, *Trigonura* appears paraphyletic relative to *Phasgonophora* and *Muhabbetella*. In addition, the type species of *Phasgonophora* and *Trigonura* are included in supported clade B (values of the bootstrap 100 and 71 respectively for the UCE and the morphology tree) (Figs 1, 2). Thus, *Trigonura* cannot be sustained anymore and the species belonging to the clade B must be classified in *Phasgonophora* which may just be considered as a derived form of *Trigonura*. It would have been possible to classify the species belonging to the clade A in another genus and *Chalcidellia* Girault is available for that. Bouček (1988) was confronted to the same dilemma and wrote the following: "For some time I thought that *Chalcidellia* could be retained as a subgenus of *Trigonura*, because its type species [*Chalcis euthyrrhini* Dodd] differs from the typical *Trigonura* in having a distinct flat and punctured interantennal space and in the female the epipygium [syntergum] is short, with cercal tubercles placed right at the beginning of the sculptured part. The antennae are relatively short and very slightly thickened apically. On the contrary, the type species of *Trigonura* and many other tropical species have the interantennal space narrow, the female epipygium is prolonged with cercal tubercles removed distinctly from base, and the antennae long and filiform or even tapering apically. However, more recently I found species combining these features in varying degrees, which makes me regard *Chalcidellia* as only a species group of *Trigonura*". The distribution of character states within the morphological matrix just confirm Bouček's observations (Tables 2, 3). His opinion is shared here and is reinforced by the fact that the clade A is not at all supported and forms a polytomy in the strict consensus tree (Fig. 1).

Taxonomic study of Saudi Arabian species

Key to the species of *Phasgonophora* Westwood from the Arabian Peninsula (based on females)

- 1 Gaster shortly acute (Figs 5A, 12A). Syntergum short, about 1.1–1.4× as long as wide when seen from dorsal view (Fig. 5A) **2**
- Gaster lanceolate (Figs 15C, 16A, B). Syntergum evidently longer, 2.5–4.0× as long as wide when seen from dorsal view (Figs 9A, 15C, 16B) **3**

- 2 Body entirely red (Figs 3A–C, E, 5A). Fore wing with setae white, sparse and short (Fig. 4C). Propodeum without spiracular teeth (Fig. 4A). Pronotal collar without median depression, regularly convex (Fig. 4B). Mesoscutellum truncate anteriorly (Fig. 3E). Pedicel about 1.8 × as long as wide (Fig. 3D). Anellus hardly transverse, about 0.8 × as long as wide (Fig. 3D)
 ***P. baiocchii* Soliman & Gul, sp. nov.**
- Meso- and metasoma mostly black (Figs 10E, 11A, 12A). Fore wing with dark setae (Fig. 11B). Propodeum with sharp spiracular teeth (Fig. 10E, F). Pronotal collar with evident median depression (Fig. 10E). Mesoscutellum bluntly angulate anteriorly (Fig. 10E). Pedicel as long as wide (Fig. 10D). Anellus quite transverse, about 0.45 × as long as wide (Fig. 10D)
 ***P. magnanii* Gadallah & Gul, sp. nov.**
- 3 Propodeum without spiracular teeth (Fig. 16B). Pronotum sloping from posterior margin mesally, uniformly convex (Fig. 16B, C). Mesoscutellum convex, and bluntly angulate anteriorly as axillar grooves are joining to each other on transscutal line (Fig. 16B) ***P. ninae* (Nikol'skaya)**
- Propodeum with sharp spiracular teeth (Fig. 7E). Pronotum with collar separated by evident angulation from collum (Figs 7E, 8A, 14A) **4**
- 4 Body 7.0–9.6 mm in length. Gena sparsely punctured (Fig. 14A, B). Pronotum with shallow median depression (Fig. 14D). Pronotal collar and mesonotum clearly cristate (transverse crests) (Fig. 14A), not at all punctured. Setation of axilla not especially dense, not masking integument beneath (Fig. 14D). Propodeum strongly sloping posteriorly, almost vertical. Epicnemial carina moderately raised ventrally. Fore wing without pigmented tracks of Rs and r-m (Fig. 15B). Gt_1 with curved carinulae dorsally, sparsely setose laterally (Fig. 15C)
 ***P. rubens* (Klug)**
- Body 9.5–13.6 mm in length. Gena densely punctured (Figs 7D, 8A). Pronotal collar with evident median depression (Fig. 7E). Pronotal collar and mesonotum cristate-punctured, the anterior wall of punctures raised (Fig. 8A). Axillae densely setose, setation masking integument beneath (Fig. 7E). Propodeum less strongly sloping than in alternate. Epicnemial carina strongly raised ventrally, forming sharp tooth mesally (Fig. 8A). Fore wing with evident pigmented tracks of Rs and r-m (Fig. 8D); Gt_1 with superficial, irregular wrinkles, densely setose laterally (Fig. 9A) ***P. granulis* Delvare, sp. nov.**

Review of *Phasgonophora* species from Saudi Arabia

Table 4 represents the absolute measurements of the female holotypes and male paratypes. Selected ratios are quoted in Tables 5–7. They are not repeated in the following descriptions.

Table 4. Measurements of the types of the described species of *Phasgonophora* (in μm).

| Character | <i>Phasgonophora baiocchii</i> holotype ♀ | <i>Phasgonophora granulifera</i> holotype ♀ | <i>Phasgonophora magnanii</i> holotype ♀ | <i>Phasgonophora baiocchi</i> paratype ♂ | <i>Phasgonophora magnanii</i> paratype ♂ |
|--|---|---|--|--|--|
| head width | 1537 | 1705 | 1897 | 1276 | 1821 |
| head maximal length | 784 | 989 | 1038 | 691 | 1054 |
| head length on median line | 511 | 608 | 654 | 447 | 717 |
| eye length | 532 | 648 | 737 | 455 | 690 |
| temple length | 121 | 182 | 64 | 138 | 163 |
| frontovertex width | 774 | 926 | 1026 | 740 | 989 |
| distance between lateral ocelli | 263 | 455 | 353 | 289 | 370 |
| ocular – lateral ocellus distance | 137 | 74 | 186 | 122 | 168 |
| diameter of lateral ocellus | 158 | 182 | 167 | 122 | 152 |
| distance between median and lateral ocelli | 95 | 142 | 109 | 102 | 98 |
| head height | 1058 | 1269 | 1477 | 1079 | 1284 |
| eye height | 571 | 744 | 781 | 584 | 798 |
| distance lower edge antennal torulus – ventral margin of clypeus (ATC) | 314 | 481 | 500 | 317 | – |
| distance lower edge antennal torulus – lower edge of median ocellus (ATOM) | 538 | 603 | 719 | 455 | – |
| length of malar space | 455 | 513 | 781 | 396 | – |
| width of oral fossa | 551 | 679 | 781 | 505 | – |
| scape length | 570 | 730 | 815 | 444 | – |
| pedicel length | 127 | 131 | 109 | 98 | 110 |
| pedicel width | 80 | 108 | 125 | 76 | 106 |
| anellus length | 59 | 59 | 62 | 33 | 37 |
| anellus width | 75 | 98 | 125 | 79 | 102 |
| 2 nd flagellomere (= F1) length | 159 | 280 | 308 | 139 | 301 |
| 2 nd flagellomere width | 102 | 127 | 161 | 133 | 163 |
| 8 th flagellomere (= F7) length | 110 | 172 | 232 | 136 | 272 |
| 8 th flagellomere width | 112 | 105 | 151 | 133 | 159 |
| clava length | 310 | 292 | 446 | 234 | 472 |

***Phasgonophora baiocchii* Soliman & Gul, sp. nov.**

<http://zoobank.org/75C97023-EFBA-437E-A031-23A13760231B>

Figs 3A–E, 4A–E, 5A–D, 6A–C

Type material. *Holotype* ♀: KINGDOM OF SAUDI ARABIA, RIYADH, Ad Diriyah, Al Uyaynah, Wadi Al Hesiya (40 NW of Riyadh) [24°55'22.44"N, 46°12'15.13"E, Alt. 790 m], 8.IV.2017, reared from *Anthaxia* sp. (Buprestidae), e.l. *Acacia*, leg. D. Baiocchi [KSMA]; *Paratype* 1♂, same data as for holotype [KSMA].

Diagnosis. Body mostly red; fore wing hyaline with white setation (Fig. 4C); setation on body and wings sparse and short (Figs 3A–C, E, 4C); flagellomeres moder-

Table 5. Calculated ratios for the females of *Phasgonophora* from measurements of Table 4.

| Ratio | <i>Phasgonophora baiocchi</i> holotype ♀ | <i>Phasgonophora granulis</i> holotype ♀ | <i>Phasgonophora magnanii</i> holotype ♀ |
|--|---|---|---|
| head width : head maximal length | 1.960 | 1.724 | 1.827 |
| head width : head length on median line | 3.010 | 2.804 | 2.902 |
| head width : head height | 1.453 | 1.343 | 1.285 |
| fronto-vertex width : eye height | 1.356 | 1.245 | 1.313 |
| ocular – lateral ocellus distance : diameter of lateral ocellus | 0.520 | 0.406 | 1.115 |
| distance between median and lateral ocelli : diameter of lateral ocellus | 0.600 | 0.781 | 0.654 |
| ATC : ATOM | 0.583 | 0.798 | 0.696 |
| length of malar space : eye height | 0.798 | 0.690 | 1.000 |
| length of malar space : width of oral fossa | 0.826 | 0.755 | 1.000 |
| scape length : eye height | 1.000 | 0.981 | 1.043 |
| pedicel length : pedicel width | 1.585 | 1.218 | 0.873 |
| anellus length : anellus width | 0.789 | 0.600 | 0.492 |
| F1 length : F1 width | 1.558 | 2.200 | 1.914 |
| F7 length : F7 width | 0.982 | 1.638 | 1.539 |
| mesosoma length : mesosoma (= mesoscutum) width | 1.600 | 1.640 | 1.612 |
| mesosoma length : mesosoma height | 1.538 | 2.335 | 2.265 |
| pronotum width : pronotum maximal length | 1.707 | 1.714 | 1.849 |
| pronotum width : pronotum length on median line | 3.559 | 2.754 | 2.688 |
| pronotum width : mesoscutum width | 1.077 | 0.977 | 1.042 |
| mesoscutum length : pronotum length on median line | 1.729 | 1.475 | 1.375 |
| mesoscutellum length : mesoscutellum width | 0.898 | 0.810 | 0.978 |
| fore wing length : fore wing width | 2.858 | 2.690 | 2.263 |
| marginal vein length : costal cell length | 0.348 | 0.269 | 0.284 |
| marginal vein length : stigmal vein length | 3.512 | 3.016 | 3.643 |
| marginal vein length : postmarginal vein length | 4.800 | 2.603 | 4.857 |
| metacoxa length : metacoxa width | 2.153 | 1.747 | 2.000 |
| metafemur length : metafemur width | 1.764 | 1.774 | 1.684 |
| syntergum length : mesotibia length | 0.276 | 1.226 | 0.546 |

ately long (Fig. 3D); clava 1-segmented in both sexes (Figs 3D, 6B); mesoscutellum moderately convex, truncate anteriorly (Fig. 4A); propodeal spiracular tooth absent (Figs 4A, 6C); fore wing setation sparse and very short, distributed on both sides without line of setae on Rs (Fig. 4C); Gt_1 dorsally smooth (Fig. 5A); syntergum 0.276× as long as mesotibia (Fig. 5A, B).

Etymology. This species is dedicated to Daniele Baiocchi, who reared this species from *Anthaxia* spp. (Buprestidae) infesting *Acacia* sp. (Fabaceae).

Condition of holotype. Specimen glued on rectangular card, metasoma glued separately. Head and mesosoma partly covered with a thin artifactual layer in bottom of areoles, appearing artificially dull rather than glossy by places; second to fifth terga with sides wide apart from each other, probably resulting from immersion in some medium.

Description of holotype ♀: Body length 5.0 mm. **Colour.** Body reddish brown; antennal scape and pedicel, anellus and basal half of F1 reddish (Fig. 3D), the rest of flagellum dark brown, almost black (Fig. 3D); mandibular teeth black (Fig. 3B); palpi brown; mesoscutellum apically and metanotum dark (Fig. 3E); wings hyaline (Fig. 4C), SMV testaceous, MG, STV and PMV dark brown (Fig. 4C); tegula brownish; all legs

Table 6. Calculated ratios for the males of *Phasgonophora* from measurements of Table 4.

| Ratio | <i>Phasgonophora baiocchii</i> paratype ♂ | <i>Phasgonophora magnanii</i> paratype ♂ |
|--|---|--|
| head width : head maximal length | 1.847 | 1.727 |
| head width : head length on median line | 2.855 | 2.538 |
| head width : head height | 1.183 | 1.418 |
| fronto-vertex width : eye height | 1.267 | 1.240 |
| ocular – lateral ocellus distance : diameter of lateral ocellus | 1.000 | 1.107 |
| distance between median and lateral ocelli : diameter of lateral ocellus | 0.833 | 0.643 |
| ATC : ATOM | 0.696 | – |
| length of malar space : eye height | 0.678 | – |
| length of malar space : width of oral fossa | 0.784 | – |
| scape length : eye height | 0.759 | – |
| pedicel length : pedicel width | 1.286 | 1.038 |
| anellus length : anellus width | 0.414 | – |
| F1 length : F1 width | 1.041 | 1.850 |
| F7 length : F7 width | 1.020 | 1.718 |
| mesosoma length : mesosoma (= mesoscutum) width | 1.671 | 1.781 |
| mesosoma length : mesosoma height | 1.521 | 1.605 |
| pronotum width : pronotum maximal length | 3.296 | 4.064 |
| pronotum width : pronotum length on median line | 1.047 | 1.130 |
| pronotum width : mesoscutum width | 1.556 | 2.574 |
| mesoscutum length : pronotum length on median line | 0.878 | 1.000 |
| mesoscutellum length : mesoscutellum width | 2.650 | 2.892 |
| fore wing length : fore wing width | 0.307 | 0.367 |
| marginal vein length : costal cell length | 2.629 | 3.143 |
| marginal vein length : stigmal vein length | 4.182 | 2.973 |
| marginal vein length : postmarginal vein length | 2.154 | 1.901 |
| metacoxa length : metacoxa width | 1.875 | 1.784 |

reddish, but tarsi testaceous; metafemur with black teeth on ventral margin (Fig. 4E); metasoma reddish brown (Fig. 5A, B), tip of ovipositor sheaths black (Fig. 5B).

Head (Fig. 3A–C). Slightly wider than maximal width of mesosoma; with sparse, short and thin setae; vertex and frons densely punctured (Fig. 3A, B), lower face and especially gena sparsely punctured, with interspaces as large as punctures on its mesal surface; lower face and frons strongly convex, without preorbital ridges (Fig. 3B); both mandibles 3-toothed, teeth of same length, somewhat blunt at apex (Fig. 3B); clypeus roundly protruding at free margin (Fig. 3B); tentorial pits well visible (Fig. 3B); genal carina strongly raised (Fig. 3C); scrobal cavity completely transversely strigose, reaching median ocellus (Fig. 3B); lateral margins of depression slightly converging dorsally; interantennal projection as wide as diameter of antennal torulus, subtriangular, and with punctulate front surface, with sharp carina above it, 0.33× as long as scape (Fig. 3B); occiput vertically strigulose behind ocellar triangle, punctured laterally (Fig. 3A).

Antenna (Fig. 3D). Apex of scape reaching level of median ocellus; pedicel 1.58× as long as wide, without basal bottle neck; anellus hardly transverse, tapering basally; flagellomeres pubescent, bearing numerous, not raised, multiporous plate sensilla in several intricate rows; F1 somewhat tapering basally, 1.59× as long as wide, slightly longer than each of F2 and F3; clava 1-segmented, conical, not much longer than F7 and very narrowly truncate at apex.

Table 7. Comparison between the sexes of *P. baiocchii* sp. nov. and *P. magnanii* through ratios calculated from measurements of Table 4.

| Ratio | <i>Phasgonophora baiocchii</i> holotype ♀ | <i>Phasgonophora baiocchii</i> paratype ♂ | <i>Phasgonophora magnanii</i> holotype ♀ | <i>Phasgonophora magnanii</i> paratype ♂ |
|--|---|---|--|--|
| head width : head maximal length | 1.960 | 1.847 | 1.827 | 1.727 |
| head width : head length on median line | 3.010 | 2.855 | 2.902 | 2.538 |
| head width : head height | 1.453 | 1.183 | 1.285 | 1.418 |
| fronto–vertex width : eye height | 1.356 | 1.267 | 1.313 | 1.240 |
| ocular – lateral ocellus distance : diameter of lateral ocellus | 0.520 | 1.000 | 1.115 | 1.107 |
| distance between median and lateral ocelli : diameter of lateral ocellus | 0.600 | 0.833 | 0.654 | 0.643 |
| ATC : ATOM | 0.583 | 0.696 | 0.696 | – |
| length of malar space : eye height | 0.798 | 0.678 | 1.000 | – |
| length of malar space : width of oral fossa | 0.826 | 0.784 | 1.000 | – |
| scape length : eye height | 1.000 | 0.759 | 1.043 | – |
| pedicel length : pedicel width | 1.585 | 1.286 | 0.873 | 1.038 |
| anellus length : anellus width | 0.789 | 0.414 | 0.492 | 0.360 |
| F1 length : F1 width | 1.558 | 1.041 | 1.914 | 1.850 |
| F7 length : F7 width | 0.982 | 1.020 | 1.539 | 1.718 |
| mesosoma length : mesosoma (= mesoscutum) width | 1.600 | 1.671 | 1.612 | 1.781 |
| mesosoma length : mesosoma height | 1.538 | 1.521 | 2.265 | – |
| pronotum width : pronotum maximal length | 1.707 | 3.296 | 1.849 | 1.605 |
| pronotum width : pronotum length on median line | 3.559 | 1.047 | 2.688 | 4.064 |
| pronotum width : mesoscutum width | 1.077 | 1.556 | 1.042 | 1.130 |
| mesoscutum length : pronotum length on median line | 1.729 | 0.878 | 1.375 | 2.574 |
| mesoscutellum length : mesoscutellum width | 0.898 | 2.650 | 0.978 | 1.000 |
| fore wing length : fore wing width | 2.858 | 0.307 | 2.263 | 2.892 |
| marginal vein length : costal cell length | 0.348 | 2.629 | 0.284 | 0.367 |
| marginal vein length : stigmal vein length | 3.512 | 4.182 | 3.643 | 3.143 |
| marginal vein length : postmarginal vein length | 4.800 | 2.154 | 4.857 | 2.973 |
| metacoxa length : metacoxa width | 2.153 | 1.875 | 2.000 | 1.901 |
| metafemur length : metafemur width | 1.764 | – | 1.684 | 1.784 |
| syntergum length : mesotibia length | 0.276 | – | 0.546 | – |

Mesosoma (Figs 3E, 4A, B). Slightly convex in lateral view (Fig. 4B), pronotum and mesonotum bearing short thin setae, adpressed on pronotum and suberect on mesonotum (Fig. 3E); pronotum entirely punctured, its dorsal outline regularly convex, without median depression (Fig. 3E); lateral panel with oblique crenulae ventrally; mesonotum cristate-punctured, the transverse crests moderately raised (Fig. 4B); notauli not much impressed (Fig. 3E); tegula bearing three very short setae basally; mesoscutellum short, convex in lateral view (Fig. 4B), truncate anteriorly as the axillae are widely separated, broadly rounded at apex, with fine longitudinal carinae; postscutellum as trapezoidal areola with secondary sculpture (Fig. 3E); propodeum not much sloping, without anterolateral spiracular tooth (Figs 3E, 4A), with irregular costula and poorly delimited median areola; mesepisternum with mesodiscrimen as faint carina dorsally, bifurcate ventrally delimiting a shallow fovea (Fig. 4A); epicnemial carina strongly raised at mid-height, moderately raised ventrally (Fig. 4B); ventral shelf virtu-

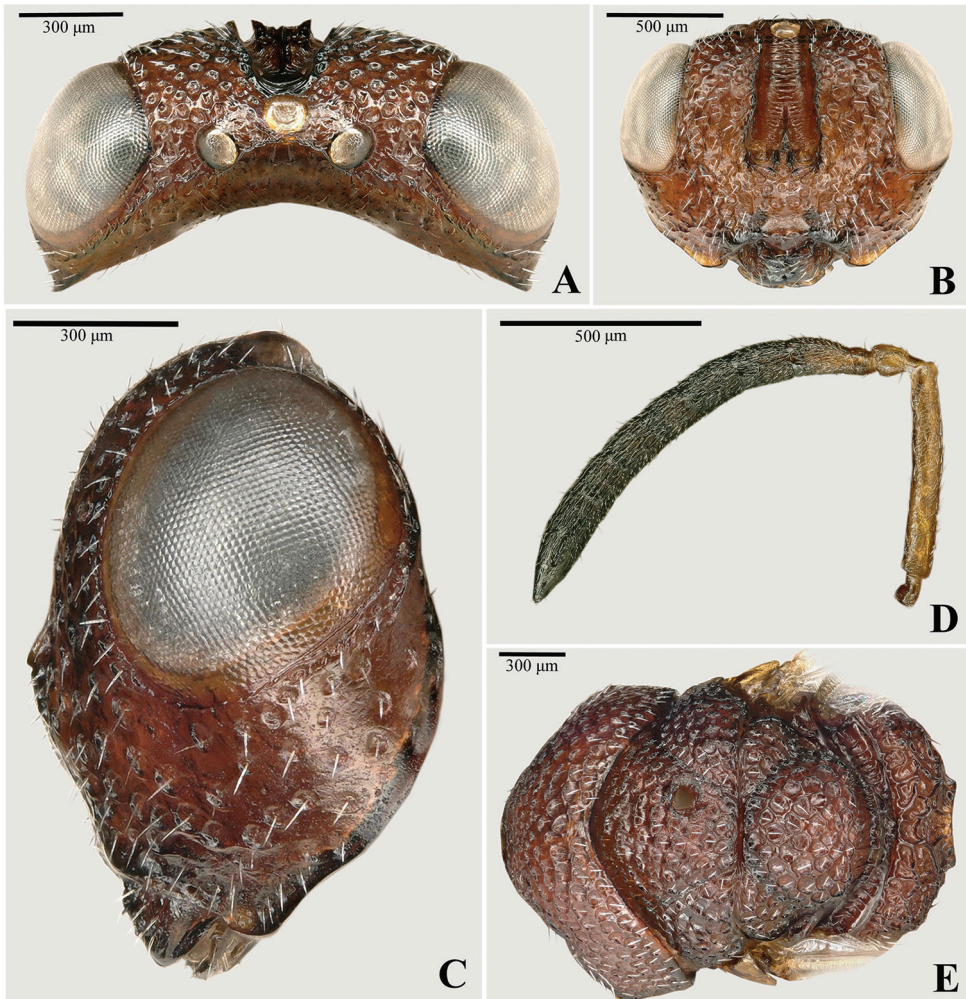


Figure 3. A–E *Phasgonophora baiocchii* Soliman & Gul, sp. nov., female (holotype) **A** head (dorsal view) **B** head (frontal view) **C** head (lateral view) **D** antenna **E** mesosoma (dorsal view).

ally smooth; adscrobal area of mesepisternum, entire mesepimeron and metepimeron with dense setiferous punctures, the setae are short and addressed as on pronotum (Fig. 4B); femoral scrobe of mesopleuron entirely strigose (Fig. 4B).

Wings (Fig. 4C). Fore wing lacking marginal fringe, with microtrichiae on both sides, MG_V 0.35× as long as SM_V, PM_V 0.20× as long as MG_V, ST_V slightly longer than PM_V; hind wing with three similar closely set hamuli.

Legs (Fig. 4D, E). Procoxa deeply depressed anteriorly, the depression delimited laterodorsally by strongly raised carina (Fig. 4D). Protibia with thin apicodorsal socketed spine (Fig. 4D). Mesotibia without dorsal pegs. Hind leg bearing sparse, thin and suberect setae on ventral side of coxa, femur and tibia (Fig. 4E); metafemur sparsely

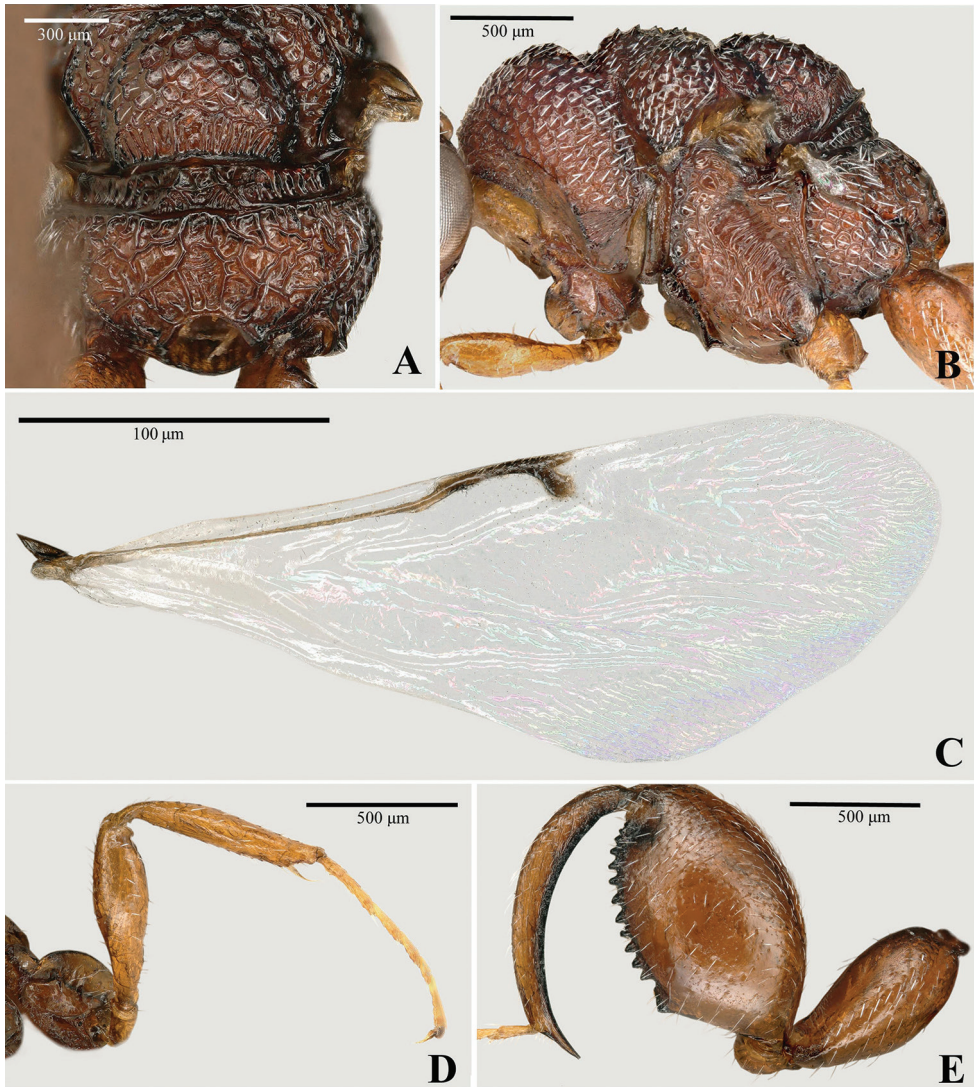


Figure 4. A–E *Phasgonophora baiocchii* Soliman & Gul, sp. nov., female (holotype) **A** mesosoma (part, dorsal view) **B** mesosoma (lateral view) **C** fore wing **D** proleg **E** hind leg.

punctulate on outer side, its ventral margin with a row of 11 regularly distributed equal teeth, basal tooth not prominent, no basal inner tooth (Fig. 4E). All tarsi thin, bearing slender claws.

Metasoma (Fig. 5A, B). Petiole quite transverse in dorsal view, ventral surface virtually smooth. Gaster short, only slightly longer than mesosoma; Gt_1 2.6× as wide as long, as long as Gt_2 and Gt_3 combined, smooth on disc, solely with a row of three thin and short setae on either side (Fig. 5A); Gt_{2-5} smooth, except for the setiferous punctures in front of their posterior margin, laterally with a complete row of setae and a partial row in front of it (Fig. 5A); penultimate tergite entirely densely and deeply

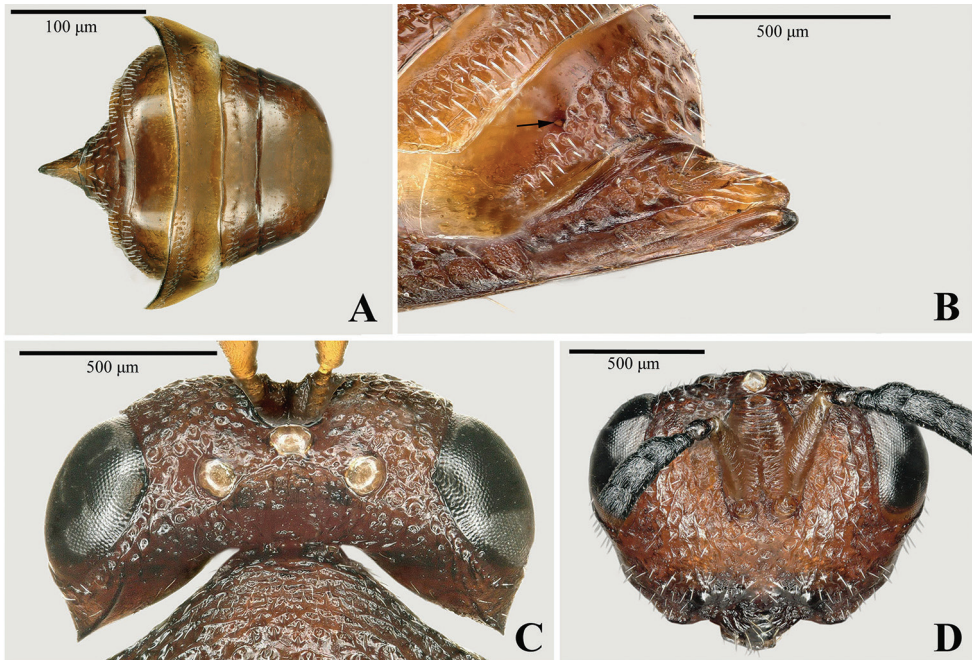


Figure 5. A–D *Phasgonophora baiocchii* Soliman & Gul, sp. nov. **A, B** female (holotype): **A** metasoma (dorsal view) **B** syntergum (lateral view) **C, D** male (paratype): **C** head (dorsal view) **D** head (frontal view).

punctured, with three rows of setiferous punctures, spaces between punctures smooth and shiny; spiracle very small, hardly visible at lateral edge of punctured surface as its peritreme is not raised; syntergum very short, only 0.276× as long as mesotibia, its basal part, in front of cercal plates (Fig. 5B); extremely short, median ridge present; tergum coarsely punctured laterally; sternites smooth and bare; tip of hypopygium at about half length of gaster.

Male (Figs 5C, D, 6A–C). Length 4.2 mm; similar to female except for the following characters: black parts better expanded especially on occiput, pronotum and mesonotum; scape bright reddish brown (Fig. 6B); head less transverse in dorsal view with anterior outline of frons more convex and temples relatively longer (Fig. 5C), gena mostly smooth, with very sparse punctures (Fig. 6A); frons with faint preorbital ridges, carina above interantennal projection almost reaching dorsal margin of scrobal depression (Fig. 5D); scape fusiform, 3.4 × as long as wide, anellus transverse, strongly tapering basally (Fig. 6B).

Recognition. None of the described *Phasgonophora* from the Afrotropical region have the short syntergum exhibited by *P. baiocchii*. Considering the Oriental species, the species would run, using Narendran (1989), either to *Trigonura steffani* Narendran, or *T. javensis* Narendran, 1987. The first species (holotype examined) is quite different, especially the deeply impressed notauli and the strongly convex mesoscutellum. In the second species (holotype examined), the lower face has a differentiate median strip similar to that of *Muhattabella*, and fore wing bears dark setae among other characters.



Figure 6. A–C *Phasgonophora baiocchii* Soliman & Gul, sp. nov., male (paratype) **A** head (fronto-lateral view) **B** antenna **C** head and mesosoma (dorsal view).

From this species group, especially in *P. euthyrrhinii*, the type species of *Chalcidiella*, *P. baiocchii* differs from all species examined by the non-segmented clava, the mesodiscrimen, not raised as median crest, and the white setae of the fore wing *versus* clava 3-segmented, mesodiscrimen raised as a carina dorsally and fore wing setation dark.

Distribution. Only known from Saudi Arabia, in Riyadh Region (Fig. 17).

Host. *Anthaxia* (*Haplanthaxia*) *abdita* Bílý, 1982 and *A.* (*H.*) *kneuckeri* ssp. *zabran-skyi* Bílý, 1995 (Coleoptera, Buprestidae).

***Phasgonophora granulis* Delvare, sp. nov.**

<http://zoobank.org/5EB72879-1E9C-4A89-BCD8-FF37534B7172>

Figs 7A–E, 8A–D, 9A, B

Type material. *Holotype* ♀: KINGDOM OF SAUDI ARABIA, AL-BAHA, Al Mikhwa (Shada Al-Ala Natural Reserve) [19°50'51"N, 41°18'06.12"E, Alt. 1358 m], 14.IV.2016,

e.l. *Acacia*, leg. D. Baiocchi [KSMA]. **Paratypes:** 7♀, same data as holotype [KSMA]; 2♀, same data as holotype [BMNH]; 2♀, same data as holotype [USNM]; 3♀, same data as holotype [EFC]; 2♀, same data as holotype but differing as for the coordinates [19°51'39.96"N, 41°18'15.84"E, Alt. 1248 m] and collection date, 29.III.2017 [KSMA]; 2♀, KINGDOM OF SAUDI ARABIA, ASIR, Muhayil, Wadi Sabian (28 km SSE of Muhayil) [18°17'54.89"N, 42°07'41.11"E, Alt. 809 m], 05.IV.2017, e.l. *Acacia*, leg. D. Baiocchi [KSMA].

Diagnosis. Gaster longer than mesosoma and acuminate, with syntergum longer than mesotibia (1.15×) (Fig. 9A, B); gena densely and entirely punctured (Figs 7D, 8A); occiput completely strigulose (Fig. 7A); flagellum filiform, with all flagellomeres much longer than wide, F1 2.5× as long as wide (Fig. 7C); mesosomal dorsum somewhat flattened (Fig. 8A); pronotal collum and mesonotum cristate punctured (Fig. 8A); axillae densely setose, setation masking integument posteriorly (Fig. 7E); propodeum with sharp spiracular teeth (Fig. 7E); mesepisternum with epicnemial carina forming sharp tooth mesoventrally (Fig. 8A); fore wing with dense but short setation, and pigmented track of Rs and r-m (Fig. 8D); Gt₁ with weak wrinkles dorsally (Fig. 9A); Gt₆ with deep punctures and very small, hardly visible, spiracle; cerci removed from base of syntergum, situated at half of its length (Fig. 9A, B).

Etymology. The name is chosen in reference to the secondary sculpture of the areoles on the head and mesonotum, giving to them a dull, granulose appearance (see Fig. 8B).

Condition of holotype. Specimen glued on rectangular card. Head and mesosoma partly covered with a thin layer on the bottom of areoles; second to fifth tergites with sides wide apart from each other, probably resulting from immersion in some medium.

Description of female holotype. Body 8.4 mm. **Colour.** Head and mesosoma entirely black (Fig. 7A–E), metasoma brown (Fig. 9A), with syntergum darker laterally (Fig. 9B); tegula brownish (Fig. 8A); fore and mid legs dark brown, but knees, apex of tibiae and tarsi testaceous; hind leg dark brown (Fig. 8C), ventral femoral teeth and ventral side of tibia black (Fig. 8C), tarsus lighter; antenna entirely black (Fig. 7C); wings hyaline, veins dark brown (Fig. 8D).

Head (Figs 7A, B, D, 8A). Hardly wider than mesosoma; with moderately dense setation, the setae long, thin and suberect, regularly distributed according to punctures; lower face and frons strongly convex, without preorbital ridges (Fig. 7D); vertex, frons and lower face densely punctured (Fig. 7B, D), gena more coarsely punctured (Fig. 8A); both mandibles 3-toothed (Fig. 7D), lower tooth the largest and somewhat removed from the mid one; clypeus hardly protruding at free margin (Fig. 7D); edge of oral fossa thickened (Fig. 7D); tentorial pits absent (Fig. 7B); scrobal depression entirely transversely strigose, reaching median ocellus (Fig. 7B); interantennal projection (Fig. 7B) strongly compressed laterally, narrower than antennal torulus, punctulate on front surface (one row of punctures only), narrowly produced upwards, but without flange above it; vertex with short but distinct carina behind median ocellus (Fig. 7A); POL 6× OOL (Fig. 7A); occiput entirely strigulose, except for a row of punctures behind posterior edge of eye (Fig. 7A).

Antenna (Fig. 7C). Scape linear, its apex with level of vertex; pedicel 1.2× as long as wide, with slight basal bottle neck; anellus slightly transverse, 0.8× as long as wide,

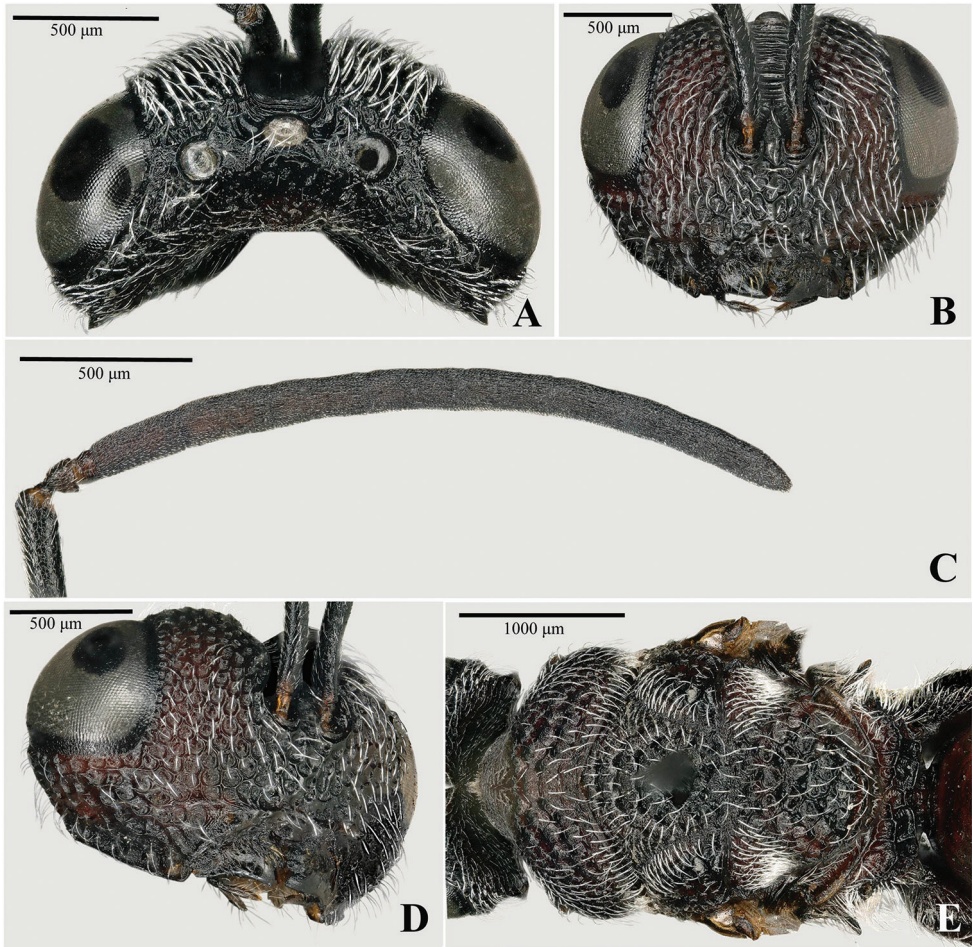


Figure 7. A–E *Phasgonophora granulis* Delvare, sp. nov., female (holotype) **A** head (dorsal view) **B** head (frontal view) **C** antenna **D** head (frontolateral view) **E** mesosoma (dorsal view).

tapering basally; funicular segments pubescent, bearing numerous, not raised multiporous plate sensilla in several intricate rows; F1 2.2× as long as wide, shorter than F2; F2 as long as F3; F7 1.64× as long as wide; clava 2-segmented (suture nevertheless hardly distinct), narrowly rounded apically.

Mesosoma (Figs 7E, 8A). With setae about twice as long puncture diameter, curved and suberect; setae regularly distributed on punctures, but pronotum in front of prepectus, axillae and propodeum laterally around the spiracle, densely setose, the setae adpressed there; dorsum of mesosoma somewhat flattened (Fig. 8A), with dorsal outline of pronotal collar and mesonotum straight; punctures with secondary, very fine, sculpture on their bottom (visible only at very high magnification: 800×) (as in Fig. 8B), thus appearing dull; pronotal collum transversely strigose (Fig. 7E); pronotal collar and mes-

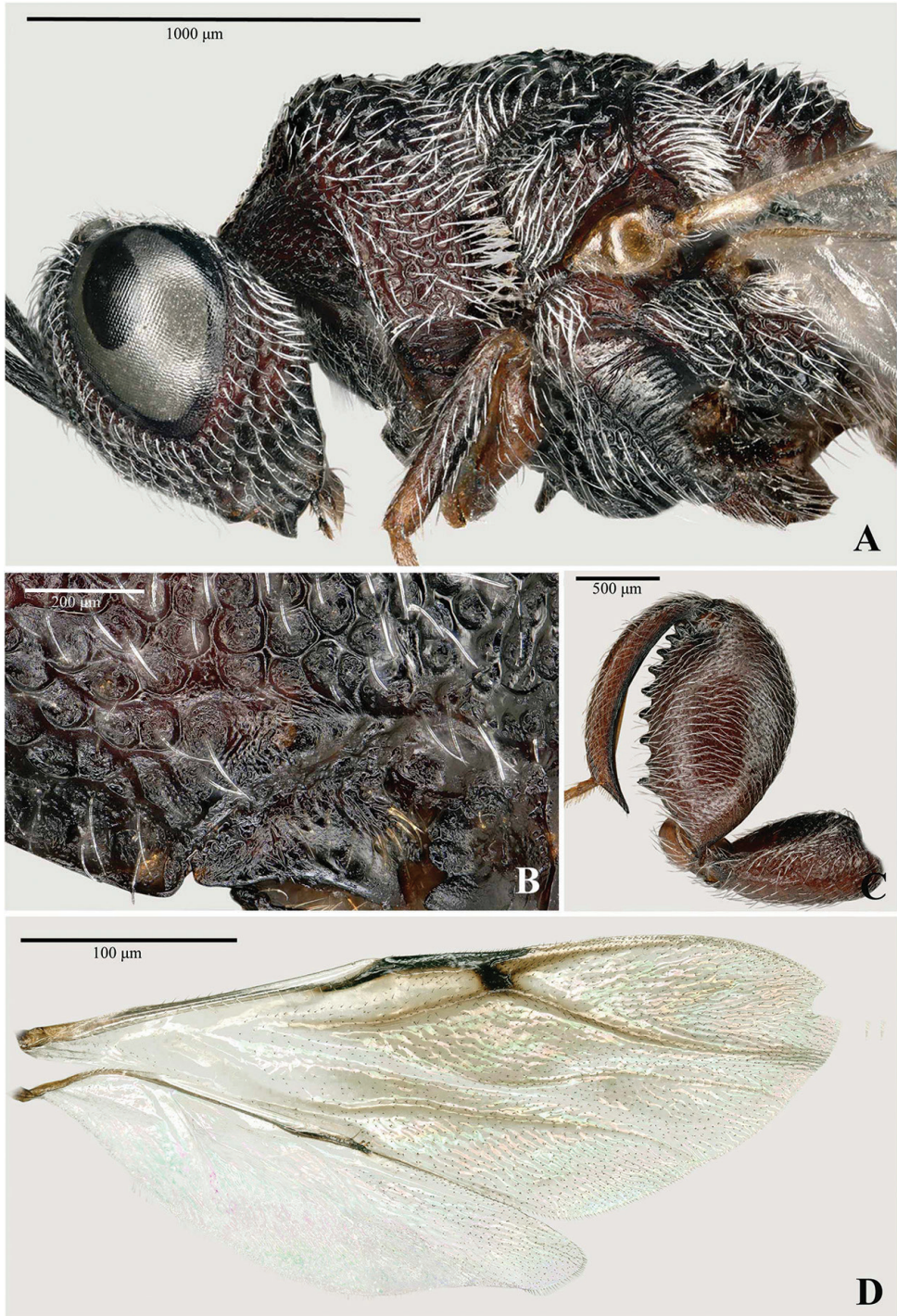


Figure 8. A–D *Phasgonophora granulis* Delvare, sp. nov., female (holotype) **A** head and mesosoma (lateral view) **B** head (part of integument, showing granulate foveae) **C** hind leg **D** fore and hind wings.

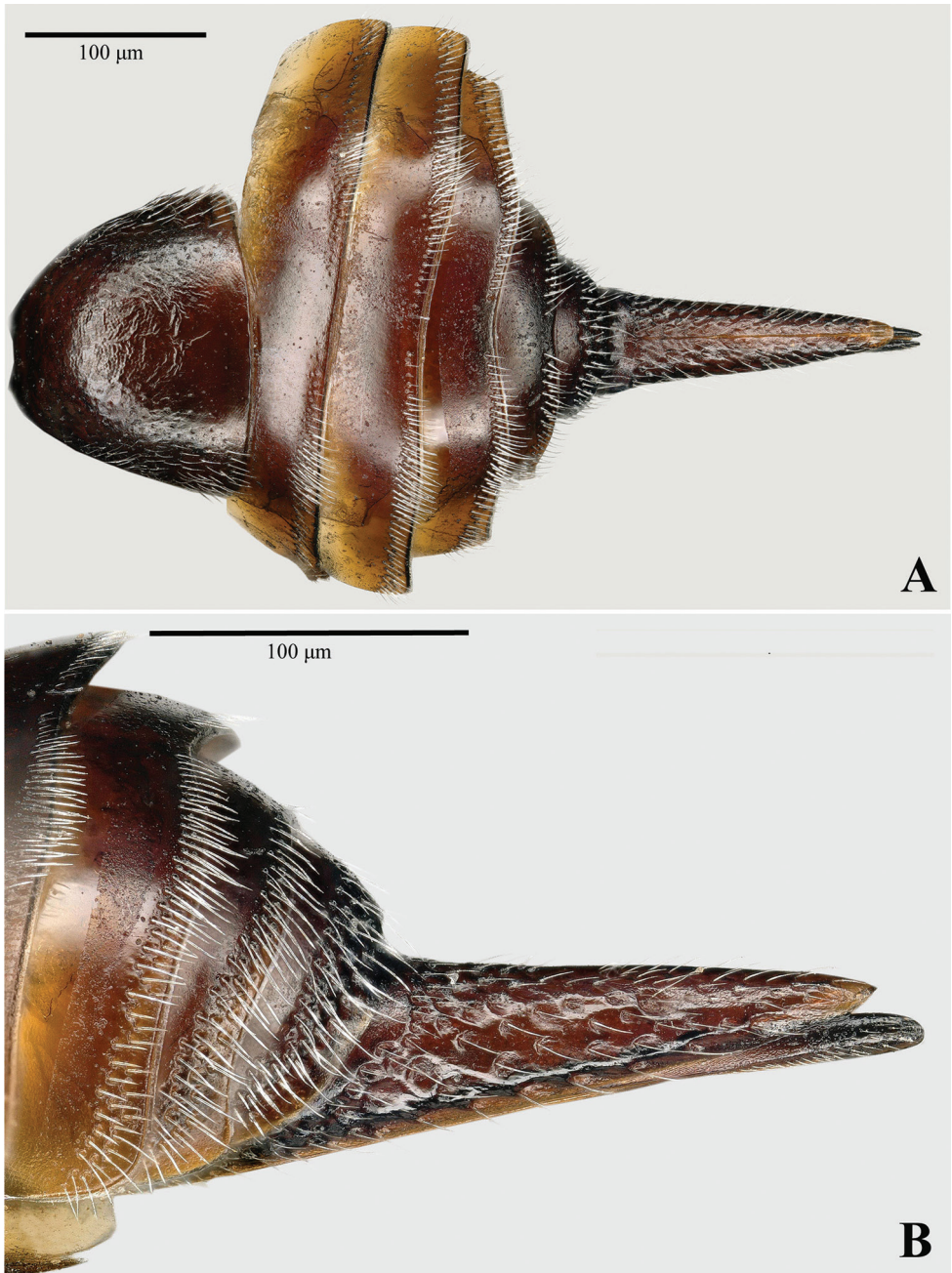


Figure 9. A, B *Phasgonophora granulis* Delvare, sp. nov., female (holotype) **A** metasoma (dorsal view) **B** syntergum (lateral view).

onotum uniformly cristate punctured, the anterior wall of punctures forming crests (Fig. 8A); pronotal collar with shallow mesal depression, its sides strongly convex (Fig. 8A); pronotal carina visible laterally, forming a tooth in dorsal view; lateral panel mostly flat,

with longitudinal carinulae dorsally and raised curved carina ventrally; notauli impressed (Fig. 7E); tegula with a tuft of about 10 setae anteriorly (Fig. 8A); mesoscutellum truncate anteriorly, rounded apically, its posterior margin raised and surpassing postscutellum (Fig. 7E); propodeum strongly sloping anteriorly, more strongly so posteriorly, with sharp spiracular tooth (Fig. 7E) and two irregular costulae; mesepisternum with mesodiscrimen as faint carina all over, without ventral fovea; epicnemial carina moderately raised laterally, strongly protruding mesoventrally, appearing as a sharp tooth in lateral view (Fig. 8A); ventral shelf in mesepisternum very weakly sculptured; adscrobal area, mesepimeron, and metepimeron coarsely areolate, the later bearing long setae; femoral depression of mesepisternum with only a few low carinae (Fig. 8A).

Wings (Fig. 8D). Fore wing densely setose but bare on basal cell, basal and cubital folds, marginal cell with a single, incomplete row of setae on the underside; setae generally very short on the disc of the wing, somewhat longer below MG_V, PM_V and R_s track; setae uniformly short on the underside of wing; MG_V 0.27× as long as SM_V; PM_V 0.38× as long as MG_V; ST_V 0.33× as long as PM_V; hind wing with 4 hamuli, the basal one the largest, removed from the followings.

Legs (Fig. 8C). Procoxa with deep depression anteriorly, margined dorsolaterally with carina raised into flange. Protibia with sharp, non-socketed apical spine. Mesotibia without dorsal pegs. Metacoxa sparsely punctured ventrally, densely so on outer surface of metafemur, with dense and fine setiferous punctures, ventral edge with irregular row of unequal teeth, outer ventral margin with a row of 8–10 teeth, basal tooth not prominent but wider than other teeth; inner basal tooth absent; apical truncation of metatibia forming a curved spine. Tarsi slender.

Metasoma (Fig. 9A, B). Petiole not visible dorsally. Gaster lanceolate, longer than mesosoma; G₁ with weak wrinkles dorsally, setose laterally, the setae progressively longer towards the side (Fig. 9A); G₂₋₅ smooth, with posterior rows of setiferous punctures, a tuft of sublateral setae longer (Fig. 9A); posterior margin of tergites hardly concave; penultimate tergite smooth anteriorly, with moderately coarse setiferous punctures posteriorly; spiracle hardly visible in sublateral position, its aperture much smaller than puncture diameter; syntergum elongate (Fig. 9A, B), 1.23× as long as mesotibia, densely and deeply punctured, with dorsal median ridge (Fig. 9A); cerci removed from base of syntergum, situated at half of its length.

Male. Unknown.

Distribution. Known from Saudi Arabia only in Al-Baha and Asir Regions (Fig. 17).

Host. *Anthaxia (Haplanthaxia) abdita* Bílý, 1982 and *A. (H.) kneuckeri* ssp. *zabranskyi* Bílý, 1995 (Coleoptera, Buprestidae).

***Phasgonophora magnanii* Gadallah & Gul, sp. nov.**

<http://zoobank.org/EFfB564A-B742-47FB-8C59-A9DED8A2B07C>

Figs 10A–F, 11A–D, 12A–D, 13A, B

Type material. *Holotype* ♀: KINGDOM OF SAUDI ARABIA, ASIR, Abha (Garf Raydah Natural Reserve) [18°12'14.04"N, 42°24'42.84"E, Alt. 2809 m], 16.IV.2016,

e.l. *Dodonaea viscosa*, reared from *Chrysobothris* sp. (Buprestidae), leg. G. Magnani [KSMA]; **Paratypes:** 1♀, same data as holotype but differing as for the collection date, 11–13.IV.2019 and the collector, D. Baiocchi [KSMA]; 1♂, same data as holotype [KSMA].

Diagnosis. Body mostly black with head predominantly red (Figs 10A–F, 12A); setation of wings dark (Fig. 11B); frons strongly convex (Fig. 10C), and occiput quite concave (Fig. 10A); vertex with transverse mesal carina behind ocellar triangle (Fig. 10A); pedicel short with basal bottle neck (Fig. 10D); funicular segments elongate (Fig. 10D); clava 2-segmented (Fig. 10D); pronotum with mesal depression (Fig. 10E), notauli hardly impressed (Fig. 10E); mesoscutellum bluntly angulate anteriorly (Fig. 10E); propodeum with sharp spiracular teeth (Fig. 10E, F); surface of propodeum with long and dense setae lateral to costula (Fig. 10F); mesepisternum with mesodiscrimen as moderately raised carina, without ventral depression (Fig. 11A); epicnemial carina not raised laterally, but raised mesoventrally; forming a tooth in lateral view (Fig. 11A); gaster short with syntergum about half as long as mesotibia (Fig. 12A); vertex of male without transverse carina behind ocellar triangle (Fig. 12B); clava 1-segmented (Fig. 12D).

Etymology. The new species is dedicated to Gianluca Mangani (Roma, Italy) who reared this species from *Chrysobothris* sp. (Buprestidae) infesting *Dodonaea viscosa* (L.) Jacq. (Sapindaceae).

Condition of holotype. Specimen glued on rectangular card; head and mesosoma partly covered with a thin artifactual layer on bottom of areoles, appearing artificially dull by places; second to fifth tergites with sides widely separated from each other, probably resulting from immersion in some medium.

Description of holotype ♀: Body length 6.5 mm. **Colour.** Head mostly red (Fig. 10A–C), ocellar triangle, occiput laterally, gena ventrally, interantennal projection and supraclypeal strip, black (Fig. 10A–C); antenna black (Fig. 10D), scape and pedicel with faint brownish tint; meso- and metasoma black (Figs 10E, 12A), pronotal collar and shoulder (Fig. 10E), mesoscutum laterally and anteromedially (Fig. 10E), mesoscutellum dorso-laterally (Fig. 10E), posterior margin of Gt₁, gaster laterally, tip of syntergum and ovipositor sheaths basally, brownish (Fig. 12A); fore wing slightly infusate, with track of Rs pigmented, veins dark brown to black (Fig. 11B); tegula glassy yellowish brown (Fig. 10E); fore and mid legs dark brown to black, tarsi brown (Fig. 11C); hind leg black (Fig. 11D), coxa apically, femur ventrally, tibia dorsally brownish, tarsus brown.

Head (Fig. 10A–C). Subequal to maximal width of mesosoma; with moderately dense long thin and suberect setae (Fig. 10A–C), setae longer towards oral fossa; lower face and frons strongly convex, without preorbital ridges (Fig. 10C); both mandibles 3-toothed, lower tooth the largest and somewhat removed from the mid one (Fig. 10B); clypeus protruding at free margin, but projection truncate (Fig. 10B); tentorial pits present, but not well distinct from other punctures (Fig. 10B); lower face and gena densely punctured (Fig. 10B, C), interspaces 0.2× punctures diameter; gena with deep sulcus along genal carina (Fig. 10C); scrobal depression piriform, entirely transversely strigose, reaching median ocellus (Fig. 10A); interantennal projection foveolate, nearly

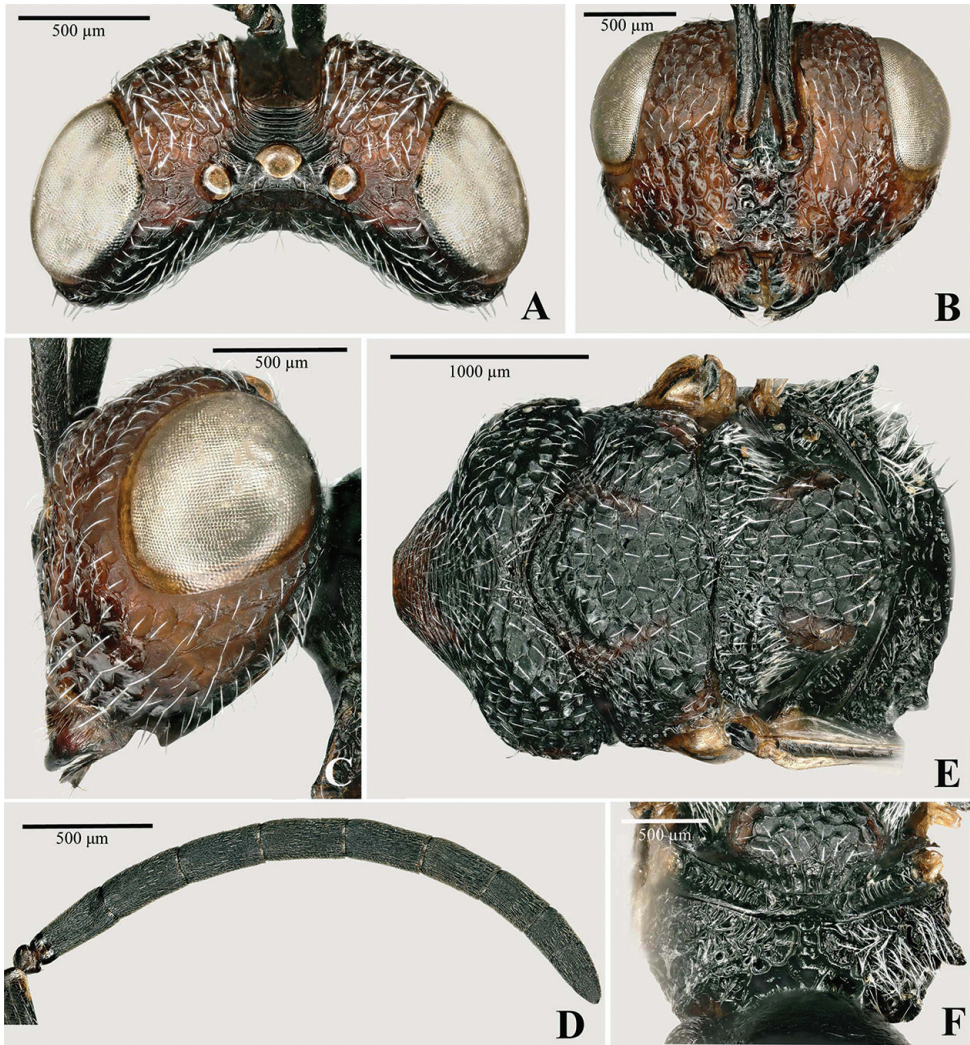


Figure 10. A–F *Phasgonophora magnanii* Gadallah & Gul, sp. nov., female (holotype) **A** head (dorsal view) **B** head (frontal view) **C** head (lateral view) **D** antenna **E** mesosoma (dorsal view) **F** propodeum (posterodorsal view, showing spiracular teeth).

as wide as diameter of antennal torulus, $0.45\times$ as long as scape (Fig. 10B); vertex and frons densely areolate (Fig. 10B), vertex with distinct curved carina behind ocellar triangle (Fig. 10A); occiput with vertical carinulae behind ocellar triangle; punctured-strigose laterally, with oblique crests (Fig. 10A).

Antenna (Fig. 10D). Apex of scape reaching level of median ocellus; anellus strongly transverse; pedicel short, with strong basal bottle neck; flagellomeres pubescent, bearing numerous, not raised, multiporous plate sensilla in several intricate rows; F1 $1.8\times$ as long as wide, scarcely shorter than F2 or F3 ($0.93\times$); clava 2-segmented, narrowly rounded apically.

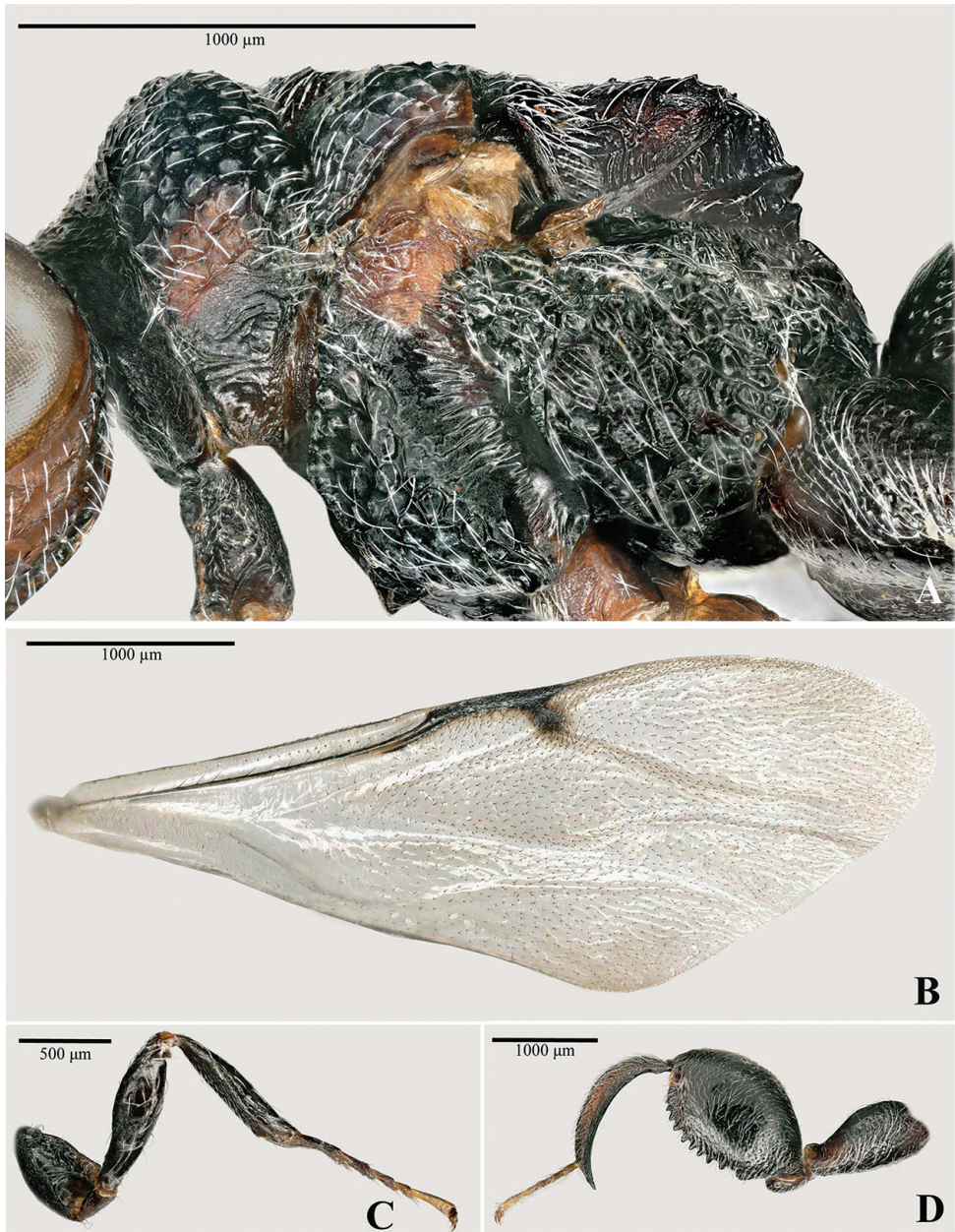


Figure 11. A–D *Phasgonophora magnanii* Gadallah & Gul, sp. nov., female (holotype) **A** mesosoma (lateral view) **B** fore wing **C** fore leg **D** hind leg.

Mesosoma (Figs 10E, F, 11A). Pronotum and mesonotum bearing short, adpressed and thin setae (Fig. 10E); pronotum with deep median depression, only angulate laterally for distinction of collar, which is densely punctured, the anterior walls of which

are raised into crests, especially on either side of the median depression (Fig. 10E); pronotal collum transversely strigose; lateral panel flat, with a single oblique carina (Fig. 11A); dorsal outline of mesonotum straight, mesoscutum and mesocutellum being flattened, crests transverse and hardly raised on mesoscutum, better raised and interrupted between each puncture on mesocutellum (Fig. 11A); notauli hardly impressed posteriorly; tegula with a patch of about 10 setae posteriorly; mesoscutellum rhombic and angulate anteriorly as axillar grooves are joining to each other on transscutal line (Fig. 10E); frenum distinctly sloping; posterior margin of mesoscutellum rounded (Fig. 10E); propodeum moderately sloping, with sharp spiracular teeth and raised but irregular costulae (Fig. 10E, F); surface of propodeum with long and dense setae lateral to costulae (Fig. 10E); mesepisternum with mesodiscrimen appearing as moderately raised carina, without ventral depression (Fig. 11A); epicnemial carina not raised laterally, but raised mesoventrally, forming a tooth in lateral view (Fig. 11A); ventral shelf of mesepisternum punctured-strigose (Fig. 11A); adscrobal area, mesepimeron, and metepimeron coarsely areolate, bearing long, thin and erect setae (Fig. 11A).

Wings (Fig. 11B). Fore wing densely setose, but basal cell, basal and cubital folds bare; marginal cell with a single row of hairs on the underside; MG_V 0.35× as long as SMV, PMV 0.2× as long as MG_V, STV 1.3× as long as PMV; hind wing with three hamuli, the basal one larger and somewhat removed from the followings.

Legs (Fig. 11C, D). Procoxa depressed anteriorly, the depression delimited latero-dorsally by a raised carina (Fig. 11C). Protibia with apicodorsal, not socketed spine. Mesotibia without pegs. Metacoxa densely punctured on outer ventral side, with long fine setae along its whole surface (Fig. 11D); metafemur with dense fine setiferous punctures on outer side, ventral margin with a row of 11 teeth, basal tooth not prominent but wider than other teeth, no inner basal tooth (Fig. 11D). Apical truncation of metatibia forming a curved spine (Fig. 11D).

Metasoma (Fig. 12A). Petiole not visible from above, entirely concealed within propodeal foramen. Gaster slightly longer than mesosoma; Gt₁ 1.35× as wide as long, as long as Gt₂₋₅ combined, faintly transversely striolate mesally, broadly setose postero-laterally; Gt₂₋₅ with 1 row of setae in front of the slightly concave posterior margin; penultimate tergite densely and coarsely punctured on the whole dorsal surface; spiracle very small, hardly distinct; syntergum short, 0.55× as long mesotibia, without median ridge, densely coarsely punctured laterally; sternites sparsely finely punctulate; tip of hypopygium 0.60 of gaster length.

Male (Figs 12B–D, 13A, B). Length 5.8 mm. Differs from female mostly through the following characters: interantennal projection better raised and laterally compressed (Fig. 12C); gena with dense umbilicate punctures (Fig. 12C); carina behind ocellar triangle vestigial (Figs 12B, 13A); flagellomeres shorter with clava only 1-segmented (Fig. 12D); mesosoma more elongate with dorsal outline slightly convex in lateral view; Gt₂₋₅ with 2–3 rows of setiferous punctures posteriorly (Fig. 13B).

Recognition. None of the Afrotropical species described in *Trigonura* or *Phasgonophora* has the short syntergum exhibited by *P. magnanii*. In the key of the Oriental species provided by Narendran (1989), it would run to *T. samarensis* Narendran, 1987.

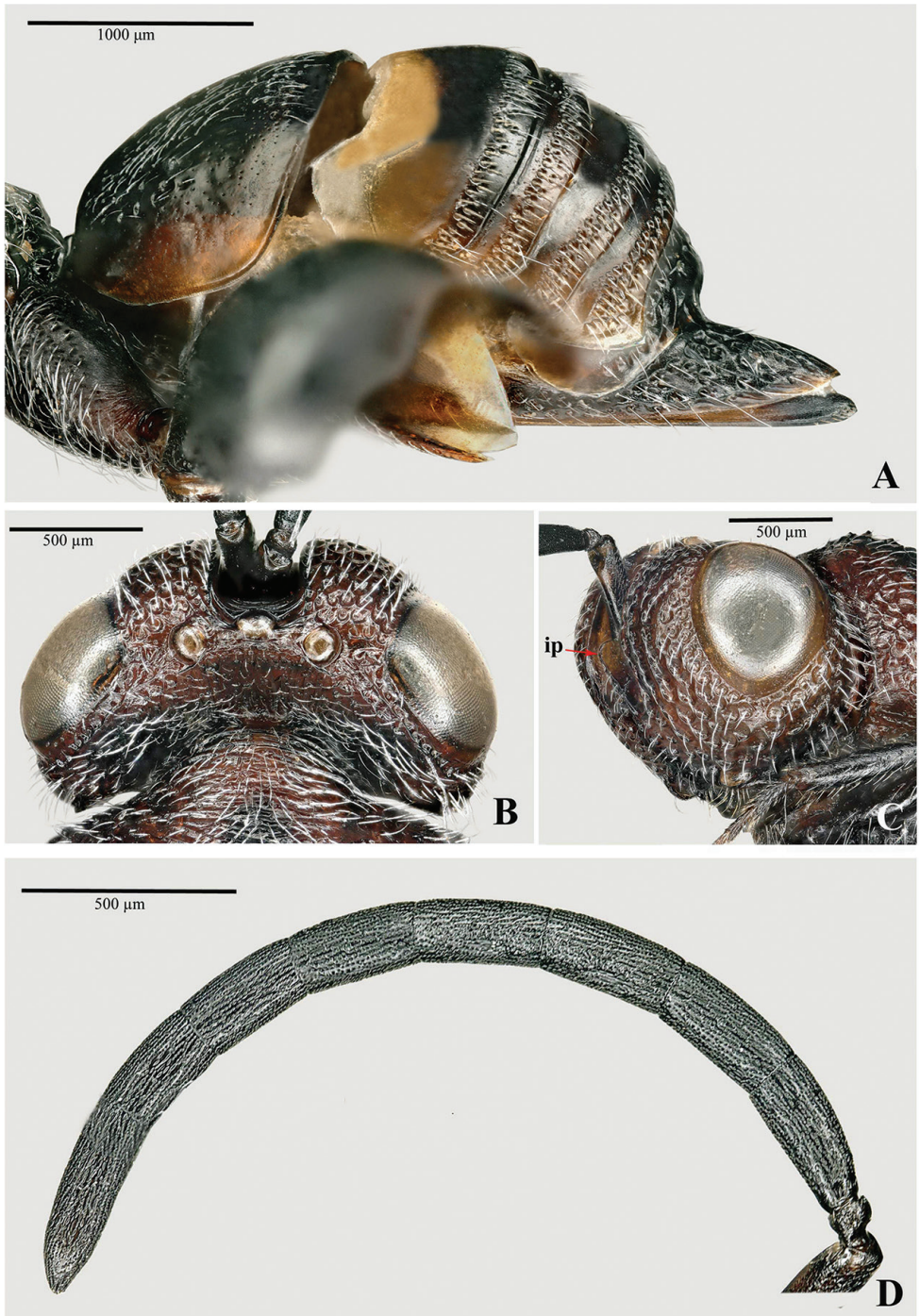


Figure 12. A–D *Phasgonophora magnanii* Gadallah & Gul, sp. nov. **A** female (holotype) metasoma (lateral view) **B, C** male (paratype): **B** head (dorsal view) **C** head (lateral view) **D** antenna.

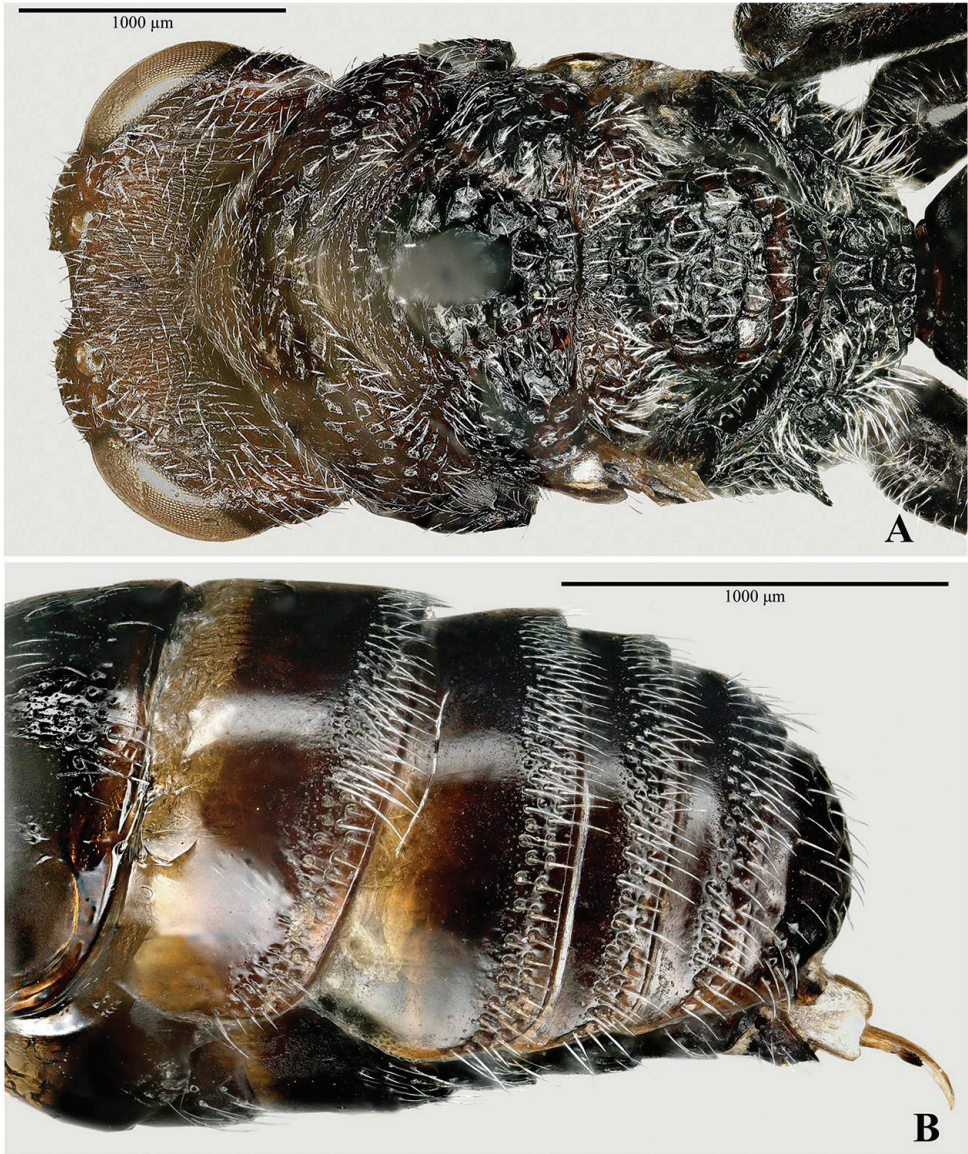


Figure 13. A, B *Phasgonophora magnanii* Gadallah & Gul, sp. nov., male (paratype) **A** head and mesosoma (dorsal view) **B** metasoma (dorsolateral view).

It differs from this species by the gaster being longer than the mesosoma *versus* shorter in *samarensis*; it also lacks the infuscate spot around the stigma, and Gt_1 is transversely striolate on the disc *versus* smooth and shiny in *T. samarensis*.

Distribution. Only known from Saudi Arabia in Asir Region (Fig. 17).

Host. *Chrysobothris* (*Abothris*) sp. (Coleoptera, Buprestidae).

***Phasgonophora rubens* (Klug, 1834)**

Figs 14A–D, 15A–C

Chalcis rubens Klug, 1834: tab. 37, fig. 7, n. 2.*Phasganophora rubens* (Klug), Sichel, 1866: 368.*Urochalcis maura* Nikol'skaya, 1952: 91–92.

Material examined. Type material. Two conspecific, pinned, ♀ syntypes, labelled “Abissynien /Ambukohl /Ehrbg. L [manuscript, black ink, green label] ‘rubens Kl’ [manuscript, black pencil] ‘type’ [red label] ‘GBIF-ChalcISE /ID: Chalc0656’ [MNB].

Other material (all from Saudi Arabia): 1♀, 2♂, AL-BAHA, 2 km E of Nawan [19°32'48"N, 41°11'34"E, Alt. 117 m], 31.III.2017, e.l. *Acacia*, leg. D. Baiocchi [KSMA]; 1♂, ASIR, Abha, N of Khamis Mushait [18°25'25"N, 42°42'05"E, Alt. 1944 m], 17.IV.2016, e.l. *Acacia*, leg. D. Baiocchi [KSMA]; 2♀, 3♂, RIYADH, Ad Diriyah, Al Uyaynah, Al Bodah (30 km NW Riyadh) [24°53'33"N, 46°17'39.84"E, Alt. 761 m], 10.IV.2016, e.l. *Acacia*, leg. D. Baiocchi [KSMA]; 1♂, the same previous data but differing as for collection date (08.IV.2017) [KSMA]; 13♀, 14♂, RIYADH, Ibex Reserve Protected Area (W of Hutat Bani Tamim) [23°27'26"N, 46°33'37"E, Alt. 721 m], 11.IV.2017, e.l. *Acacia*, leg. D. Baiocchi [KSMA]; 3♀, 2♂, RIYADH, Ibex Reserve Protected Area (W of Hutat Bani Tamim) [23°21'06.62"N, 46°21'35.94"E, Alt. 709 m], 11.IV.2017, e.l. *Acacia*, leg. D. Baiocchi [KSMA]; 1♀, RIYADH, Rimah, Rawdat Khuraim (100 km NE Riyadh) [25°22'59.06"N, 47°16'42.58"E, Alt. 559 m], 18.II.2012, sweep net (A), *Calotropis procera*, leg. unknown [KSMA]; 1♂, RIYADH, Rimah, Rawdat Khuraim (100 km NE Riyadh) [25°25'56.64"N, 47°13'51.96"E, Alt. 572 m], 28.IV.2012, pitfall trap (B), leg. unknown [KSMA]; 1♀, same data but differing as for the trap (Malaise trap (B)) [KSMA]; 9♀, 7♂, RIYADH, Rimah, Rawdat Khuraim (100 km NE Riyadh) [25°23'13"N, 47°16'45"E, Alt. 550 m], 09.IV.2016, e.l. *Acacia*, leg. D. Baiocchi [KSMA]; 2♀, 1♂, RIYADH, Rimah, Rawdat Khuraim (100 km NE Riyadh) [25°22'59.06"N, 47°16'42.58"E, Alt. 559 m], 09.IV.2016, e.l. *Acacia*, leg. D. Baiocchi [EFC]; RIYADH, Rimah, Rawdat Khuraim (100 km NE Riyadh) [25°22'59.06"N, 47°16'42.58"E, Alt. 559 m], 09.IV.2017, e.l. *Acacia*, leg. D. Baiocchi [12♀, 13♂ in KSMA; 1♀, 1♂ in EFC]; 6♀, 8♂, RIYADH, Wadi Al Hesiya (40 NW of Riyadh) [24°55'22.44"N, 46°12'15.13"E, Alt. 790 m], 08.IV.2017, e.l. *Acacia*, leg. D. Baiocchi [KSMA]; 1♀, RIYADH, Wadi Huraymila (86 km NW of Riyadh) [25°04'44.20"N, 46°03'29.80"E, Alt. 798 m], 08.IV.2017, e.l. *Acacia*, leg. D. Baiocchi [KSMA].

Diagnosis. *Female* with gena sparsely setose (Fig. 14B); flagellomeres long, F1 2× as long as wide (Fig. 14C); pronotal collar angulate with collum, with shallow median depression (Fig. 14D); mesonotum flattened dorsally, entirely cristate (Fig. 14A); propodeum with spiracular teeth (Fig. 15A), sloping posteriorly; fore wing with moderately dense setation, without pigmented track of Rs and r-m (Fig. 15B); metasoma lanceolate (Figs 14A, 15C); Gt₁ with evident curved carinae dorsally, sparsely setose laterally



Figure 14. A–D *Phasgonophora rubens* (Klug), female **A** lateral habitus **B** head (anterolateral view) **C** antenna **D** mesosoma (dorsal view).

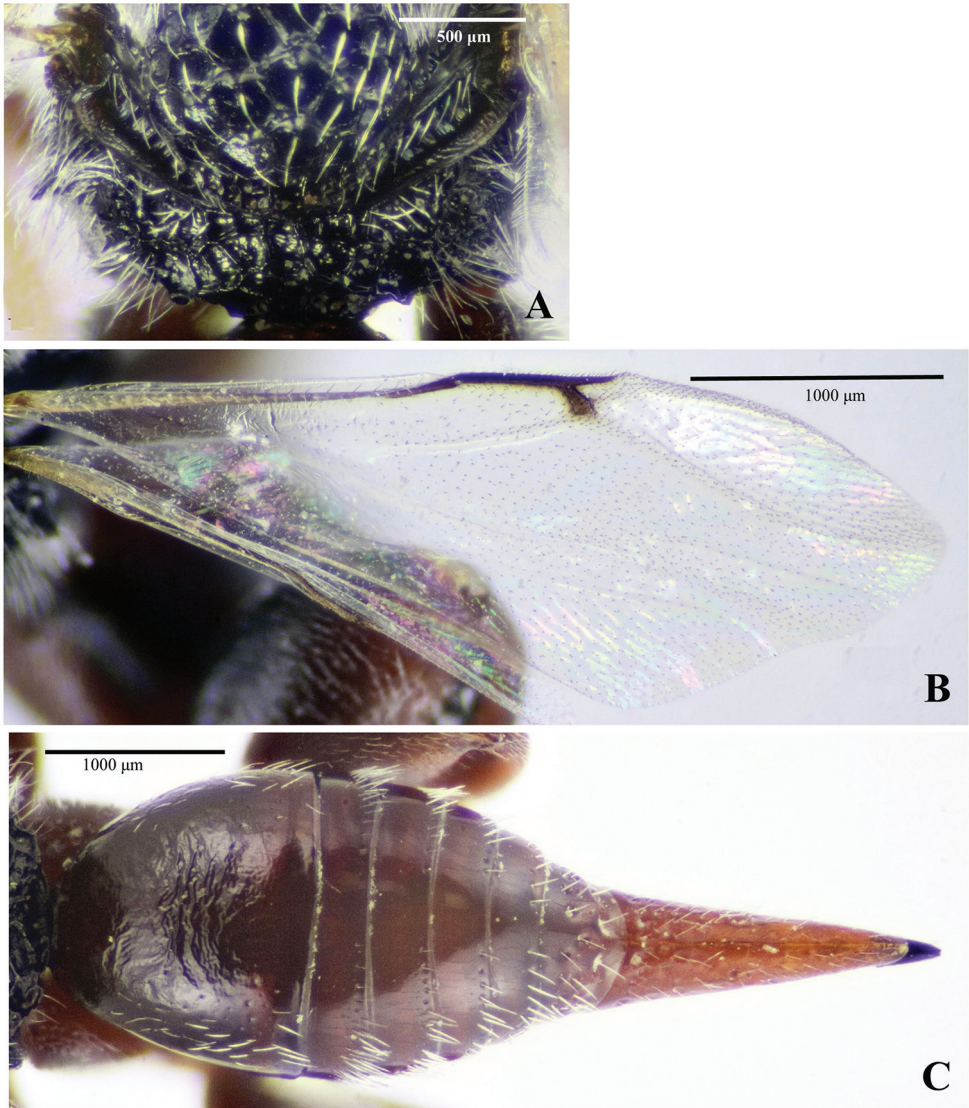


Figure 15. A–C *Phasgonophora rubens* (Klug), female **A** mesoscutellum and propodeum (dorsal view) **B** fore wing **C** metasoma (dorsal view).

(Fig. 15C); penultimate tergite densely and deeply punctured (Fig. 15C); syntergum (Fig. 14A) longer than mesotibia (1.25×), sparsely shallowly punctured (punctures dense at base), with median ridge (Fig. 15C). *Male*. Length 3.1–4.6 mm. Similar to female but antenna stouter; denser pale setae on fore wing; propodeal spiracular teeth slightly shorter; metasomal petiole narrow.

Distribution. General distribution. ALGERIA: mostly northwestern and central Sahara, less common in southern Sahara and Sahel (Mateu, 1972); EGYPT: surrounds

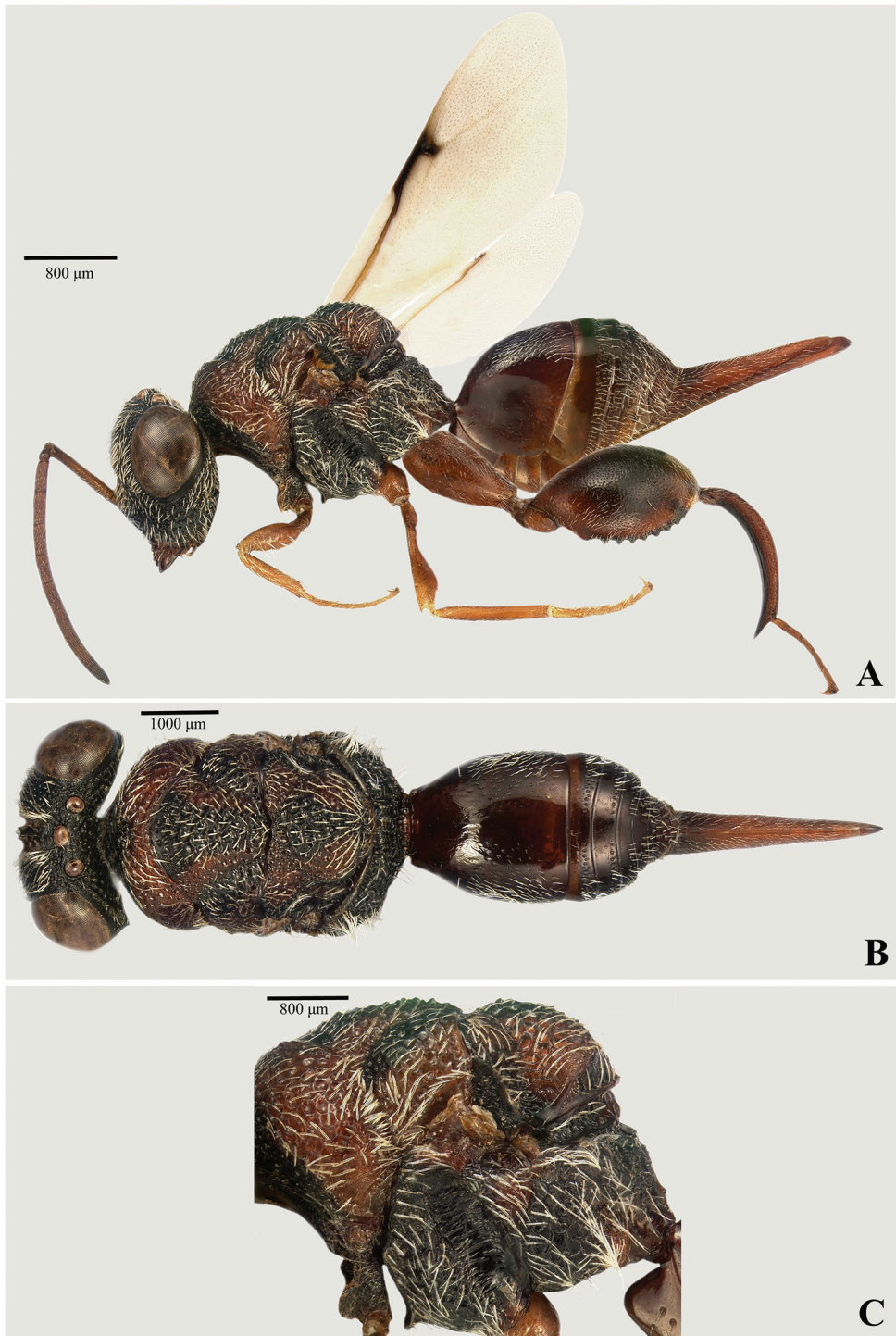


Figure 16. A–C *Phasgonophora niniae* (Nikol'skaya), female **A** lateral habitus **B** dorsal habitus **C** mesosoma (lateral view).

of Cairo (Masi 1931); ISRAEL: Wadi Fukra (Bouček 1956); TUNISIA: Bled Ejdla (Nikol'skaya 1952); SAUDI ARABIA (**new record**; Asir, Al-Baha and Riyadh Regions, Fig. 16); SUDAN (Klug 1834); UAE (Delvare 2017).

Biology. Hosts. *Anthaxia* [as *Cratomerus*] *angustipennis* (Klug, 1829) (Buprestidae) (Nikol'skaya 1952); *Anthaxia* spp., especially *A. angustipennis* and *A. pseudocongregata* Descarpentries & de Miré, 1963, *A. pulex* Abeille de Perrin, 1893, *Acmaeodera* spp., especially *A. adspersula* (Illiger, 1803), *A. flavipennis* (Klug, 1829), *A. convolute* (Klug, 1829) (Mateu 1972), *Anthaxia* (*Haplanthaxia*) *abdita* Bílý, 1982, *A. (H.) kneuckeri zabraskyi* Bílý, 1995, and *A. (H.) marginifera metallescens* Abeille de Perrin, 1907 (present study).

Associated plants. *Vachellia* [= *Acacia*] *farnesiana* (L.) Willd, 1806 (Masi 1931), *Acacia tortilis* (Forssk.) Hayne, 1825 [ssp. *Acacia raddiana* Savi] and *A. ehrenbergiana* Haine [= *A. flava* (Forssk.) Schwein.]; it was also reared from cages with *Tamarix pauciovulata* and *Rhus tripartitus* R. Sch. infested by *Buprestis hilaris* Klug, 1829 but with possible contamination from cultures of infested *A. tortilis* (Mateu, 1972) in the neighborhood.

Female behavior and larval development (Mateu 1972). Mating occurs only once and soon after the female looks for hosts. She oviposits preferably in cracks; the duration of oviposition is short (5–10 minutes); the stylets are not always vertical but forms an obtuse angle with the surface of the wood. A single, caudate larva develops within the host. The female apparently chooses for old instar larvae. At the end of the development, the larva fully occupies the body of the pupa of the buprestid host, which is at that time mummified. The larva of the host is thus preserved until its complete development. In this respect, the mature larva of the host is able to dig the gallery that is normally used by the adult for emergence but used here by the chalcidid. The progeny emerges during late spring from eggs deposited in summer (August) of the previous year; the species is thus univoltine.

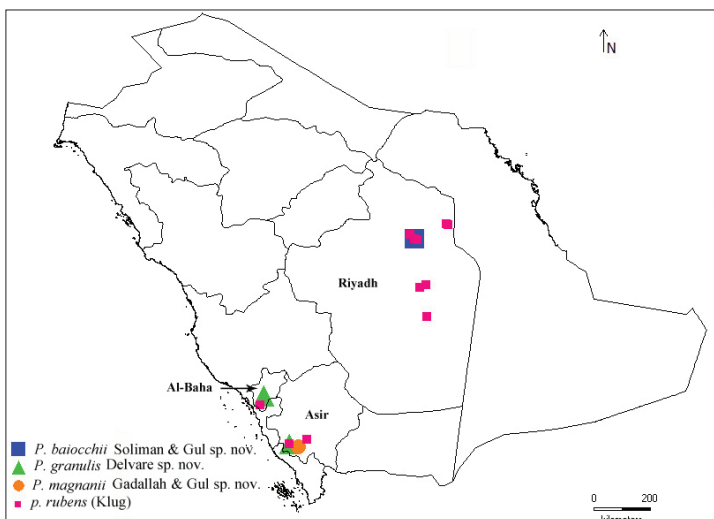


Figure 17. Distribution map of *Phasgonophora* species in Saudi Arabia.

Discussion

Systematic placement of the new species

The three new species, as well as *P. rubens*, undoubtedly belong to the genus *Phasgonophora*, sharing with its type species: 1) a laterally compressed interantennal projection (homoplastic); 2) a transverse carina behind ocellar triangle on the vertex (homoplastic); 3) a strigulose occiput behind the ocellar triangle (homoplastic); 4) a punctured strigulose or even strigulose occiput laterally (homoplastic); 5) a partial fusion of the claval segments (fusion complete in *P. baiocchii*) (a true synapomorphy within the subfamily); 6) the mesodiscrimen appearing as a low carina dorsally and as a vestigial fovea ventrally (a true synapomorphy of a part of clade B); 7) the apical projection of the protibia forming a sharp tooth (a true synapomorphy of a part of clade B); 8) a very small spiracle on the penultimate tergite with the peritreme not raised (homoplastic).

Phasgonophora granulis is retrieved as the sister species of *P. rubens* but this relationship is solely supported by a reversal on the mesoscutellum (anteriorly truncate). *Phasgonophora granulis* might otherwise have been the sister species of *P. ruficaudis* (Cameron, 1905) as the setation of the axilla in these species (and in some undescribed Afrotropical *Phasgonophora* as well) is quite dense; nevertheless, this conflicts with a derived state on the epicnemial carina (here strongly raised laterally) shared by *P. granulis* and *P. rubens*. Apparently, a radiation occurred in what appears in the tree as the sister group of *Phasgonophora sensu stricto* (*P. sulcata* and its sister species) with a high diversity of forms in the Afrotropical fauna.

Phasgonophora magnanii is retrieved as sister group of the well supported clade C (Fig. 2). This relationship is sustained by a single synapomorphy, the presence of a median depression on the pronotum. The position of *P. magnanii* within the clade B, in which most species exhibit a long syntergum, is *a priori* surprising for a species with a short syntergum; one would have positioned it within the clade A. Yet *P. magnanii* shows all derived states of this clade and, in addition, a number of those exhibited by the clade C. Such a placement on the tree finally has sense.

Phasgonophora baiocchii is a quite enigmatic species according to its amazing combination of character states that would prompt it within the clade A, as it is the case when using the available key (Narendran 1989). However, this species likewise shares the derived states sustaining the clade B and, to a less degree than for *P. magnanii*, some of those of the clade C. This suggests that it necessary merges on a node situated between the origins of these clades. Resulting from a lack of support, the topology in this part of the tree is unstable; it is therefore difficult to assess the exact placement of *P. baiocchii*. Molecular data are here requested.

Hosts and biology

Detailed biological data and hosts are available for *T. rubens*, the latter apparently restricted to Buprestidae belonging to the genera *Anthaxia* and *Acmaeodera* (Bupresti-

dae). The same host family (genus *Anthaxia*) was retrieved for *P. baiocchii* and *P. granulis*. Mateu (1972) stated that the larvae of these buprestids are able to develop within dried wood and certainly are adapted to the desert areas; *T. rubens* itself is adapted to their life-cycle and phenology. On the other hand, a strong discrepancy appears in the data from Saudi Arabia between the relatively large number of *P. rubens* reared from *Acacia* (n = 94) and the number of specimens (respectively 2 and 19) of the other species (*P. baiocchii* and *P. granulis*) reared from the same tree. In addition, *P. rubens* was collected in nine places *versus* a single site for *P. baiocchii* and two sites for *P. granulis*. This questions whether the tree species actually is their usual associated tree; in that case, they would really be quite rare. In the alternate, if the relevant *Acacia* is a marginal associate plant one would look for other trees where they would inhabit.

Acknowledgements

Sincere gratitude to Daniele Baiocchi and Gianluca Mangani (Roma, Italy) for providing us with the *Phasgonophora* specimens reared from buprestid beetles attacking *Acacia* and *Dodonaea viscosa* trees. The authors express their appreciation to Natalie Dale-Skey (Natural History Museum, London, UK), Claire Villemant and Agnièle Touret-Alby (Muséum National d'Histoire Naturelle de Paris); Lukas Kirschey (Museum für Naturkunde, Berlin, Germany) for the loan of types and their kind and helpful welcome during the visits of GD, Gary Gibson (Canadian National Collection of Insects, Ottawa, Canada) and Michael Gates (United States Museum of Natural History, Washington D.C., USA) for the loan of types. Sincere appreciation extended to the Deanship of Scientific Research at King Saud University for funding this research group number RGP-1437-009.

References

- Bouček Z (1956) A contribution to the knowledge of the Chalcididae, Leucospidae and Eucharitidae (Hymenoptera, Chalcidoidea) of the Near East. Bulletin of the Research Society of Israel 5B: 227–259.
- Bouček Z (1988) Australasian Chalcidoidea (Hymenoptera) – A Biosystematic Revision of Genera of Fourteen Families, with a Reclassification of Species. CAB International (Wallingford): 1–832.
- Bouček Z (1992) The New World genera of Chalcididae. Memoirs of the American Entomological Institute 53: 49–118.
- Burks BD (1959) The North American species of *Trigonura* (Hymenoptera; Chalcididae). Annals of the Entomological Society of America 52(1): 75–81. <https://doi.org/10.1093/aesa/52.1.75>
- Cameron P (1905) Description of a new genus and three new species of Chalcididae from South Africa. (Hym.). Zeitschrift für Systematische Hymenopterologie und Dipterologie 5(4): 230–232.

- Cameron P (1913) On some new and other species of Hymenoptera in the collections of the Zoological Branch of the Forest Research Institute. Dehra Dun. Part I. On the Parasitic Hymenoptera reared at Dehra Dun, northern India, from the lac (*Tachardia*) and sal insects. Indian Forest Records 4(2): 91–110.
- Cruaud A, Delvare G, Nidelet N, Sauné L, Ratnasingham S, Chartois M, Blaimer B, Gates M, Brady S, Faure S, van Noort S, Rossi JP, Rasplus J-Y (2020) Ultra-Conserved Elements and morphology reciprocally illuminate conflicting phylogenetic hypotheses in Chalcidoidea (Hymenoptera, Chalcidoidea). Cladistics (in press). <https://doi.org/10.1101/761874>
- Delvare G (2017) Order Hymenoptera, family Chalcididae. Arthropod Fauna of the UAE 6: 225–274.
- Dodd AP (1921) A new chalcid parasite of *Euthyrrhinus mediatundus*. Bulletin of Entomological Research 12(1): 67–68.
- Gahan AB, Fagan MM (1923) The type species of the genera of Chalcidoidea or chalcidflies. Bulletin of the United States National Museum, Washington 124: 1–173. <https://doi.org/10.5479/si.03629236.124.i>
- Girault AA (1924) *Homo perniciosus* and new Hymenoptera. Brisbane, private publication, 4 pp.
- Harris RA (1979) A glossary of surface sculpturing. California Department of Food & Agriculture Occasional Papers in Entomology 28: 1–31.
- Kieffer JJ (1912) Description de deux nouveaux chalcidides. Annales de la Société Entomologique de France 80: 463–466.
- Kirby WF (1883) Remarks on the genera of the subfamily Chalcidinae, with synonymic notes and descriptions of new species of leucospinae and Chalcidinae. Journal of the Linnean Society (Zoology) 17: 53–78.
- Klug F (1834) Pars zoologica. Insecta. In: Ehrenberg CG (Ed.) Symbolae Physicae seu Icones et Descriptiones Corporum Naturalium Novorum aut Minus Cognitorum Quae ex Itineribus per Libyam Aegyptum Nubiam Dongalam Syriam Arabiam et Habessiniam. Dec., Berlin, 5pp.
- Koçak AÖ, Kemal M (2008) Nomenclatural notes on the genus group names in the order Hymenoptera (Chalcidoidea). Miscellaneous Papers Centre for Entomological Studies, Ankara 149: 3–7.
- Masi L (1931) Sur quelque Brachymeriinae de l’Égypte (Hym.-Chalc.). Bulletin de la Société Entomologique d’Égypte 1930: 214–218.
- Mateu J (1972) Les insectes xylophages des *Acacia* dans les régions sahariennes. Publicações do Instituto de Zoologia «Dr. Augusto Nobre», Faculdade de Ciências de Porto 116: 1–713.
- Narendran TC (1987) Oriental Chalcididae (Hymenoptera: Chalcidoidea). Zoological Monograph, Department of Zoology, University of Calicut (Kerala): 1–441.
- Narendran TC (1989) Oriental chalcidid wasps of the genus *Trigonura* Sichel (Hymenoptera: Chalcididae). Entomon 12(3): 279–293.
- Narendran TC, van Achterberg C (2016) Revision of the family Chalcididae (Hymenoptera, Chalcidoidea) from Vietnam, with the description of 13 new species. ZooKeys 576: 1–202. <https://doi.org/10.3897/zookeys.576.8177>
- Nikol’skaya MN (1952) Chalcids of the fauna of USSR (Chalcidoidea). Opredeliteli po Faune SSSR 44: 1–575.

- Nikol'skaya MN (1960) Hymenoptera 7, 5. Chalcids of fam. Chalcididae and Leucospidae. Fauna SSSR (N.S.), 76: 1–221.
- Roscoe LE (2014) *Phasgonophora sulcata* Westwood (Hymenoptera: Chalcididae): a Potential Augmentative Biological Control Agent for the Invasive *Agrilus planipennis* Fairmaire (Coleoptera: Buprestidae) in Canada. Ph.D Thesis, University of Toronto, Canada, 228 pp.
- Sichel J (1866) Études Hyménoptérologiques. Annales de la Société Entomologique de France, 5(4): 331–492.
- Steffan JR (1951) Note sur la classification des Brachymeriinae (Hym. Chalcididae). Bulletin de la Société Entomologique de France 55: 146–150.
- Steffan JR (1956) Note synonymique sur les Cratocentrini et les Phasgonophorini (Hym. Chalcididae). Bulletin de la Société Entomologique de France 61: 238–242.
- Steffan JR (1973) Révision des genres *Stypiura* Kirby et *Parastypiura* Steffan (Hym. Chalcididae) de la région néotropicale. Annales de la Société Entomologique de France (N.S.) 9: 391–412.
- Swofford DL (2001) PAUP. Phylogenetic analysis using parsimony and other methods. Version 4.0 beta version. Sinauer Associates, Sunderland.
- Waterston J (1922) On Chalcidoidea (Mainly bred at Dehra Dun, U.P., from pests of Sal, Toon, Chir and Sundi). Indian Forest Records 9: 1–44.
- Westwood JO (1832) Page Plate 77. In : Griffith E, Pidgeon E (Eds) The class Insecta arranged by the Baron Cuvier with supplementary additions to each order and notices of new genera and species by Goerge Gray, Esq. Volume the second. The Animal Kingdom arranged in conformity with its organization, by the Baron Cuvier, with supplementary additions to each order by Edward Griffith and others, 15: 796 pp, 128 plates. (London).
- Wijsekara GAW (1997a) Phylogeny of the Chalcididae (Insecta: Hymenoptera) and its congruence with contemporary hierarchial classification. Contribution of the American Entomological Institute 29: 1–61.
- Wijsekara GAW (1997b) Generic relationship within the tribes Cratocentrini and Phasgonophorini (Hymenoptera: Chalcididae). Journal of the Hymenoptera Research 6(2): 297–335.

The genus *Indabracon* van Achterberg (Hymenoptera, Braconidae, Braconinae) in China, with description of four new species

Yang Li^{1,4}, Pu Tang^{1,2}, Xue-Xin Chen^{1,2,3,4}

1 Institute of Insect Sciences, Zhejiang University, Hangzhou 310058, China **2** State Key Lab of Rice Biology, Zhejiang University, Hangzhou 310058, China **3** Ministry of Agriculture Key Lab of Molecular Biology of Crop Pathogens and Insects, Zhejiang University, Hangzhou 310058, China **4** Zhejiang Provincial Key Laboratory of Biology of Crop Pathogens and Insects, Zhejiang University, Hangzhou 310058, China

Corresponding author: Xue-xin Chen (xxchen@zju.edu.cn)

Academic editor: J. Fernandez-Triana | Received 4 February 2020 | Accepted 25 March 2020 | Published 27 April 2020

<http://zoobank.org/BF46486F-0940-4DAF-9144-10780157BEA0>

Citation: Li Y, Tang P, Chen X-X (2020) The genus *Indabracon* van Achterberg (Hymenoptera, Braconidae, Braconinae) in China, with description of four new species. Journal of Hymenoptera Research 76: 39–56. <https://doi.org/10.3897/jhr.76.50794>

Abstract

The species of the braconid genus *Indabracon* van Achterberg, 1992 (Hymenoptera: Braconidae, Braconinae) from China are revised and 6 species are recognized, including 4 new species (*Indabracon albugilvus* sp. nov., *I. discolor* sp. nov., *I. nigricans* sp. nov. and *I. semicircularis* sp. nov.), which are described and illustrated. A key to the Chinese species of the genus *Indabracon* is provided.

Keywords

Hymenoptera, Braconidae, Braconinae, Braconini, *Indabracon*, new species, China

Introduction

Indabracon van Achterberg, 1992, is a small genus in the tribe Braconini Nees (Hymenoptera: Braconidae: Braconinae) with only three described species all occurring in the Oriental region (Yu et al. 2016). The biology of this genus is still unknown.

During the course of the study of the Chinese Braconidae, six species of this genus have been found in China, of which four species are new to science (*I. albogilvus* sp. nov., *I. discolor* sp. nov., *I. nigricans* sp. nov. and *I. semicircularis* sp. nov.). In the present paper, the new species are described and illustrated, and a key to the Chinese species of *Indabracon* is provided.

Material and methods

For the recognition of the subfamily Braconinae and the tribe Braconini, see van Achterberg (1990, 1993) and Chen & van Achterberg, (2019), for the terminology and measurements used in this paper, see van Achterberg (1988, 1993), and for additional references, see Yu et al. (2016). The following abbreviations are used: POL = postocellar line; OOL = ocular-ocellar line; OD = minimum diameter of posterior ocellus; T1 = first metasomal tergite; T2 = second metasomal tergite; T3 = third metasomal tergite; T4 = fourth metasomal tergite; T5 = fifth metasomal tergite; T6 = sixth metasomal tergite; T7 = seventh metasomal tergite. The medial length of the third metasomal tergite is measured from the posterior border of the second suture to the posterior margin of the tergite.

Photographs were made with a Keyence VHX-2000 digital microscope and the photos were slightly processed (mainly cropped and the background modified) in Photoshop CS6. For the descriptions and measurements, a Leica M125 stereomicroscope was used. The specimens are deposited in the Institute of Zoology, Chinese Academy of Sciences, Beijing (IZCAS).

Results

Genus *Indabracon* van Achterberg, 1992

Figs 1–8

Indabracon van Achterberg, 1992: 384; Yang, Chen and Liu 2006: 319; Chen and Yang, 2006: 122. Type species: *Spinaria trimaculata* Cameron, 1900.

Diagnosis. Body medium-sized, body length 6.0–10.0 mm; terminal flagellomere often strongly acute apically; in lateral view scapus gradually narrowed basally, without double margin at inner side apically and concave apico-laterally, ventrally weakly to distinctly longer than dorsally; eye glabrous, not or weakly emarginated; face with few rugae and rugulae or some punctures; clypeus moderately narrow, without dorsal carina; malar suture absent or present, sometimes sculptured; labio-maxillary complex normal, not elongate; frons nearly flat, with some setae and a strong median groove; mesosoma largely smooth and shiny; notauli shallow, and only present anteriorly; pleural sulcus smooth, absent medially; mesosternal sulcus smooth, shallow; antes-

cutal depression and metapleural flange narrow, sometimes protruding anteriorly; scutellar sulcus moderately wide and crenulate; metanotum strongly convex medially, and with a short median carina anteriorly; propodeum largely smooth, without medio-longitudinal carina or groove, sometimes with short crenulae posteriorly; propodeal spiracle round, near middle of propodeum, and without tubercle above it; angle between veins 1-SR and C+SC+R of fore wing about 50°; fore wing vein 1-SR+M slightly to strongly bent subbasally; fore wing vein cu-a interstitial or narrowly postfurcal; fore wing vein 1-M straight; fore wing vein CU1b medium-sized to long (slightly shorter than vein 3-CU1), slender and reclivous; fore wing vein m-cu converging to vein 1-M posteriorly; fore wing vein 1-R1 much longer than pterostigma, ending distad of apex of vein 3-M; vein 3-CU1 of fore wing slender; fore wing vein r oblique and shorter than width of pterostigma; second submarginal cell of fore wing long, and subparallel-sided; hind wing vein SC+R1 distinctly longer than vein 1r-m; hind wing with 2 bristles baso-anteriorly and with 3 hamuli on vein R1, membrane largely glabrous near vein cu-a; tarsal claws without lobe, with setae, but often pectinate basally; metasomal tergites often largely sculptured; T1 movably joined to T2; T1 median area strongly convex and sculptured, with angulate sides and a medio-longitudinal carina; T1 lateral areas wide; T1 with dorsal carinae but absent basally; T2 with small smooth medio-basal area, often smooth, rarely rugose, and connected to median carina posteriorly, lateral grooves wide; second metasomal suture deep and crenulate; T3–4 with antero-lateral grooves, and latero-posterior corner protruding, more or less smooth; T2–4 with sharp lateral crease; T3–5 with transverse posterior grooves (sometimes absent on T3); hypopygium medium-sized and apically acute, not emarginate medio-apically; ovipositor normal, subapically upper valve with nodus, and its lower valve with teeth ventrally.

Biology. Unknown.

Distribution. Oriental.

Key to Chinese species of the genus *Indabracon* van Achterberg

- 1 Pterostigma entirely dark brown, or apical 1/5 slightly paler or pale brown; T1 largely smooth, with a few striae antero-laterally and medially..... **2**
- At least basal half of pterostigma yellow and remainder dark brown, sometimes with black spots basally and its apical third; T1 largely coarsely sculptured, especially median area and lateral grooves **4**
- 2 Smooth postero-lateral areas of T3 large; scutellum pale yellowish brown; fore wing vein 1-SR+M at most weakly curved; T1 pale yellowish brown laterally and its median area black; ovipositor sheath about 0.75 times as long as fore wing ***I. trimaculatus***
- Smooth postero-lateral areas of T3 small; scutellum black or reddish brown; fore wing vein 1-SR+M strongly curved basally; T1 entirely whitish yellow; ovipositor sheath 0.4–0.6 times as long as fore wing **3**

- 3 Head largely reddish brown, face reddish yellow; mesoscutum reddish brown; hind wing vein 2-SC+R longer than vein 1r-m; in dorsal view length of eye 3.0 times temple; temples strongly narrowed behind eyes.....*I. discolor* sp. nov.
- Head largely yellow; mesoscutum yellow, but middle lobe anteriorly and lateral lobes with a black spot; hind wing vein 2-SC+R shorter than vein 1r-m; in dorsal view length of eye 2.6 times temple; temples linearly narrowed behind eyes.....*I. albogilvus* sp. nov.
- 4 Fore wing vein 1-SR+M at most weakly curved basally; basal half of pterostigma yellow and its apical half dark brown *I. bicolor*
- Fore wing vein 1-SR+M strongly curved basally; pterostigma largely yellow and its apical third mainly black **5**
- 5 Scutellum black medially; T1 reddish yellow laterally; T4–5 entirely black; fore wing vein CU1b half as long as vein 3-CU1 *I. nigricans* sp. nov.
- Scutellum yellow medially; T1 black laterally; T4–5 pale yellow laterally, T4 with a large black mark medially, not reaching posterior margin of tergite, and T5 with a semicircular black mark medio-basally; fore wing vein CU1b 0.7 times as long as vein 3-CU1.....*I. semicircularis* sp. nov.

***Indabracon albogilvus* sp. nov.**

<http://zoobank.org/A7DFE4DC-0454-4FDE-A274-63B024080C8A>

Figs 1, 2

Type material. Holotype. ♀, China, Yunnan Prov., Xishuangbanna Meng’ a, 1050–1080m, 17.X.1958, Chen Zhizi, No. IOZ(E)1964562 (IZCAS). **Paratypes:** 1 ♀, China, Yunnan Prov., Xishuangbanna Yunjinghong, 900m, 28.VI.1958, Zhang Yiran, No. IOZ(E)1964578 (IZCAS). 1 ♀, China, Yunnan Prov., Xishuangbanna Damenglong, 650m, 10.IV.1958, Hong Chunpei, No. IOZ(E)1964560 (IZCAS).

Diagnosis. This new species is very similar to *I. trimaculatus* (Cameron, 1900), but can be separated from the latter by the following characters: scutellum black (pale yellowish brown in *I. trimaculatus*); fore wing vein cu-a curved basally, slightly postfurcal (straight and interstitial in *I. trimaculatus*); fore wing vein 1-SR+M strongly curved basally (more or less straight, or weakly curved in *I. trimaculatus*); smooth posterolateral areas of T3 small (large in *I. trimaculatus*); ovipositor sheath 0.4–0.5 times as long as fore wing (about 0.8 times in *I. trimaculatus*).

Description. Holotype, ♀, length of body 6.4 mm, of fore wing 6.6 mm, of ovipositor sheath 2.4 mm.

Head. Antenna with 42 segments; apical antennal segment strongly acute, 2.1 times longer than its maximum width (Fig. 2l); third segment 1.1 and 1.2 times longer than fourth and fifth, respectively, the latter 1.3 times longer than wide; length of maxillary palp 0.8 times height of head; malar suture present, and with sparse, short setae (Fig. 2i); clypeus height: inter-tentorial distance: tentorio-ocular distance = 3: 5: 3; clypeus with sparse, long setae; eye hardly emarginated (Fig. 2g); face with some

punctures, especially laterally (Fig. 2g); eye height: shortest distance between eyes: head width = 20: 18: 41; frons largely smooth except for a few weak punctures, with a strong narrow median groove (Fig. 2h); vertex largely smooth except for a few weak punctures, and with some sparse short setae; POL: OD: OOL = 4: 4: 11; length of malar space 1.6 times basal width of mandible; length of eye 2.4 times temple in dorsal view; temples largely glabrous except for a few short setae, and directly narrowed behind eyes (Fig. 2h).

Mesosoma. Length of mesosoma 1.8 times its height (Fig. 2c); notauli impressed anteriorly half (Fig. 2d); mesoscutum smooth, with sparse long setae (Fig. 2d); scutellar sulcus wide, deep, and with crenulae (Fig. 2d); scutellum distinctly convex, sparsely punctate, and with dense short setae posteriorly; metanotum strongly convex medially, and with a short median carina anteriorly (Fig. 2d); propodeum largely smooth except for some crenulae posteriorly, and with sparse setae medially, and dense, long setae laterally (Fig. 2d).

Wings. Fore wing (Fig. 2a): SR1: 3-SR: r = 12: 9: 2; 1-SR+M weakly curved after arising from 1-M, and 1.5 times longer than 1-M; 2-SR: 3-SR: r-m = 8: 18: 5; CU1b 0.8 times as long as 3-CU1; cu-a weakly postfurcal, and slightly bent basally towards base of wing. Hind wing (Fig. 2b): 1r-m more or less straight; SC+R1: 2-SC+R: 1r-m = 19: 5: 7.

Legs. Length of fore femur: tibia: tarsus = 18: 21: 25; length of hind femur: tibia: basitarsus = 25: 37: 12; length of femur, tibia and basitarsus of hind leg 3.8, 6.7 and 4.0 times their maximum width, respectively.

Metasoma. Length of T1 0.9 times its apical width, median area convex and striate-rugose, lateral areas largely smooth but anteriorly striate-rugose (Fig. 2j); lateral grooves of T1 sparsely and weakly crenulate anteriorly (Fig. 2j); T2 largely coarsely sculptured, but medio-basal area smooth (Fig. 2e); antero-lateral grooves of T2 developed and crenulate (Fig. 2e); second suture deep and crenulate, wide and straight medially, narrow laterally (Fig. 2e); T3–4 with antero-lateral grooves, and latero-posterior corner small; T3–5 coarsely sculptured, and with crenulate transverse subposterior groove (Fig. 2e); T6–7 largely smooth, and with sparse long setae posteriorly; hypopygium acute apically, not reaching level of apex of metasoma; ovipositor sheath 0.4 times as long as fore wing.

Colour. Largely black (Fig. 1); head yellow, but antenna, eyes, and mandible apically black; prothorax, notaulic area, median mesoscutal lobe posteriorly and tegulae yellow (Fig. 2c, d, g, h); fore legs (except for first segment of tarsus posteriorly, second–fifth segment of tarsus, and claws black) yellow; T1 whitish yellow, T6–7 pale yellow posteriorly (Fig. 2e, j); wing membrane fuscate, pterostigma (except basal yellow patch) and veins dark brown (Fig. 2a, b).

Variation. Length of body of female 6.4–8.3 mm, of fore wing of female 6.5–7.6 mm, and of ovipositor sheath 2.4–3.1 mm; antenna of female with 40–44 segments; length of mesosoma 1.6–1.8 times its height; fore wing vein CU1b 0.6–0.8 times as long as vein 3-CU1; tegulae sometimes black, and pterostigma sometimes uniformly black.

Biology. Unknown.



Figure 1. *Indabracon albogilvus* sp. nov., ♀, holotype, habitus lateral.

Distribution. China (Yunnan).

Etymology. Named after the whitish yellow colour of the T1: “albogilvus” is Latin for “whitish yellow”.

***Indabracon bicolor* Yang, Chen & Liu, 2006**

Indabracon bicolor Yang, Chen & Liu, 2006a: 321; Chen et Yang, 2006: 123.

Biology. Unknown.

Distribution. China (Fujian).

Note. The type specimens of this species were collected in SE China (Fujian).

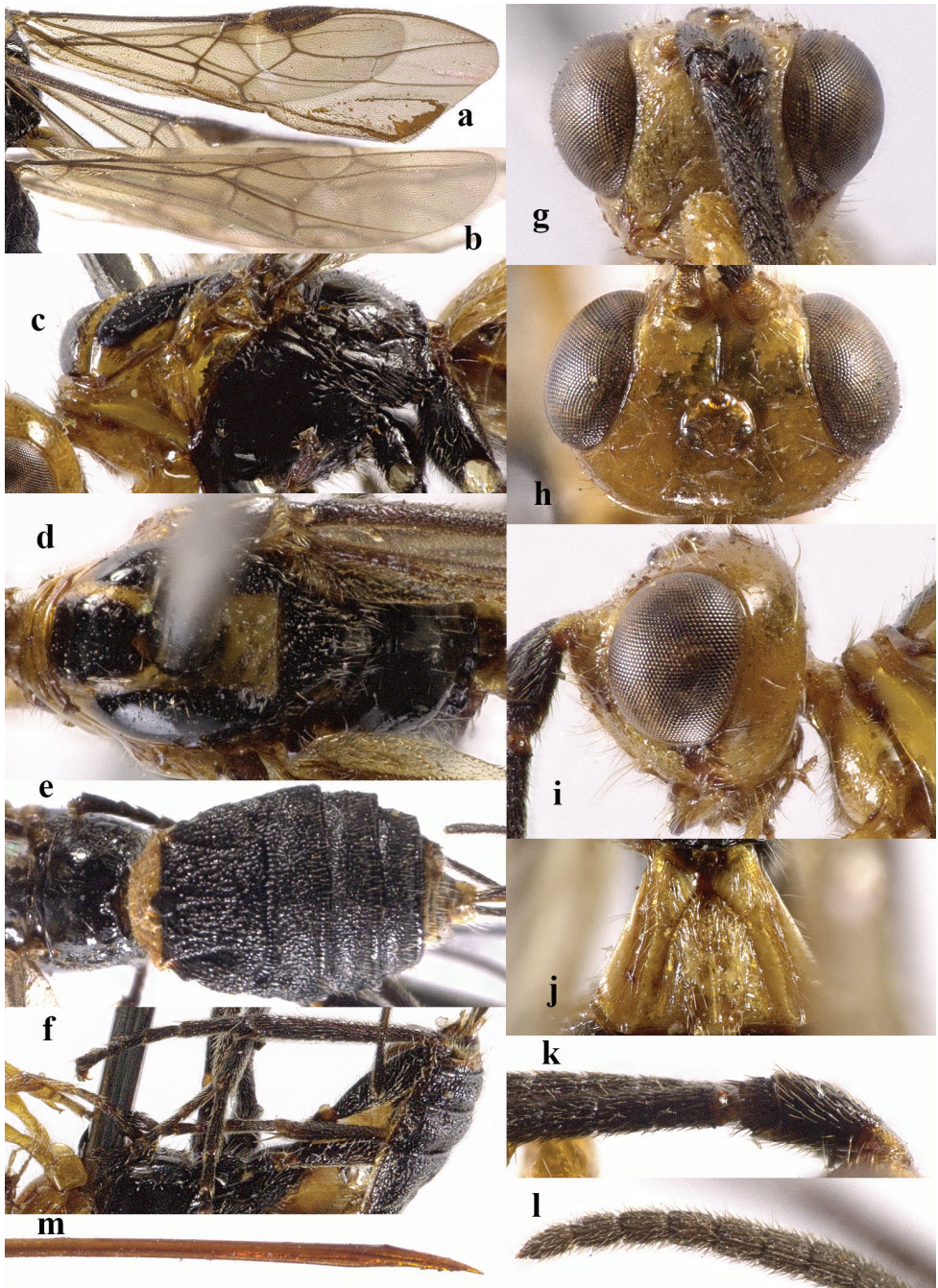


Figure 2. *Indabracon albobilvus* sp. nov., ♀, holotype **a** fore wing **b** hind wing **c** mesosoma, lateral view **d** mesosoma, dorsal view **e** metasoma, dorsal view **f** hind leg, lateral view **g** head, front view **h** head, dorsal view **i** head, lateral view **j** first metasomal tergite, dorsal view **k** scapus outer side, lateral view **l** apex of antenna **m** apex of ovipositor, lateral view.

***Indabracon discolor* sp. nov.**

<http://zoobank.org/397DBCAC-5BB8-4675-87BD-3B9FA19B2A49>

Figs 3, 4

Type material. Holotype. ♀, China, Yunnan Prov., Xishuangbanna Meng'a, 1050–1080m, 20.VIII.1958, Pu Fuji, No. IOZ(E)1964571 (IZCAS). **Paratypes:** 1♀, same label data, but Wang Shuyong, No. IOZ(E)1964563 (IZCAS).

Diagnosis. This new species is very similar to *I. albogilvus* sp. nov., but can be separated from the latter by the following characters: head largely reddish brown, but face reddish yellow (largely yellow in *I. albogilvus*); mesoscutum reddish brown (yellow, but lobes with black spot in *I. albogilvus*); hind wing vein 2-SC+R longer than vein 1r-m (shorter than vein 1r-m in *I. albogilvus*); in dorsal view length of eye 3.0 times temple and temples strongly narrowed behind eyes (length of eye 2.6 times temple and temples gradually narrowed behind eyes in *I. albogilvus*).

Description. Holotype, ♀, length of body 9.7 mm, of fore wing 9.1 mm, of ovipositor sheath 5.6 mm.

Head. Antenna with 56 segments; apical antennal segment strongly acute, 1.8 times longer than its maximum width (Fig. 4l); third segment 1.2 and 1.3 times longer than fourth and fifth, respectively, the latter as long as wide; length of maxillary palp 0.8 times height of head; malar suture rather weak, punctate and with short setae (Fig. 4i); clypeus height: inter-tentorial distance: tentorio-ocular distance = 3: 14: 7; clypeus with dense, long setae; eye hardly emarginated (Fig. 4g); face coarsely rugose, with some striae and long setae laterally (Fig. 4g); eye height: shortest distance between eyes: head width = 22: 18: 39; frons largely smooth except for a few weak punctures, with some sparse short setae and a strong median groove (Fig. 4h); vertex largely smooth except for a few weak punctures, and with some sparse short setae; POL: OD: OOL = 3: 4: 6; length of malar space 1.3 times basal width of mandible; length of eye 3.0 times temple in dorsal view; temples largely glabrous except for a few long setae, and directly narrowed behind eyes (Fig. 4h).

Mesosoma. Length of mesosoma 1.7 times its height (Fig. 4c); notauli impressed anteriorly half (Fig. 4d); mesoscutum smooth, with sparse long setae (Fig. 4d); scutellar sulcus wide, deep, and with crenulae (Fig. 4d); scutellum distinctly convex, moderately densely punctate, and with dense short setae posteriorly; metanotum strongly convex medially, and with a short median carina anteriorly (Fig. 4d); propodeum largely smooth except for a few weak punctures and some crenulae medio-posteriorly, and with sparse setae medially, and dense, long setae laterally (Fig. 4d).

Wings. Fore wing (Fig. 4a): SR1: 3-SR: r = 29: 26: 4; 1-SR+M strongly angled after arising from 1-M, and 1.5 times longer than 1-M; 2-SR: 3-SR: r-m = 8: 26: 7; CU1b 0.5 times as long as 3-CU1; cu-a weakly postfurcal, and rather weakly bent basally towards base of wing. Hind wing (Fig. 4b): 1r-m more or less straight; SC+R1: 2-SC+R: 1r-m = 23: 10: 7.



Figure 3. *Indabracon discolor* sp. nov., ♀, holotype, habitus lateral.

Legs. Length of fore femur: tibia: tarsus = 21: 25: 30; length of hind femur: tibia: basitarsus = 33: 50: 18; length of femur, tibia and basitarsus of hind leg 3.7, 8.3 and 6.0 times their maximum width, respectively.

Metasoma. Length of T1 1.1 times its apical width, median area convex and coarsely rugose, lateral areas largely smooth except for with a few striae anteriorly (Fig. 4j); lateral grooves of T1 sparsely crenulate (Fig. 4j); T2 largely coarsely sculptured, but medio-basal area smooth (Fig. 4e); antero-lateral grooves of T2 strongly developed and crenulate (Fig. 4e); second suture deep and crenulate, wide and straight medially, narrow laterally (Fig. 4e); T3–4 with antero-lateral grooves, and latero-posterior corner medium-sized; T3–5 coarsely sculptured, and with crenulate transverse subposterior groove (Fig. 4e); T6–7 largely weakly rugose, and with sparse long setae posteriorly; hypopygium acute apically, not reaching level of apex of metasoma; ovipositor sheath 0.6 times as long as fore wing.

Colour. Largely black (Fig. 3); head and mesosoma largely reddish brown, but antenna, eyes, mandible apically and propodeum black, face reddish yellow (Fig. 4c, d, g); fore femur and tibia somewhat infuscate; T1 whitish yellow (Fig. 4j); wing membrane infuscate, pterostigma and veins dark brown (Fig. 4a, b).

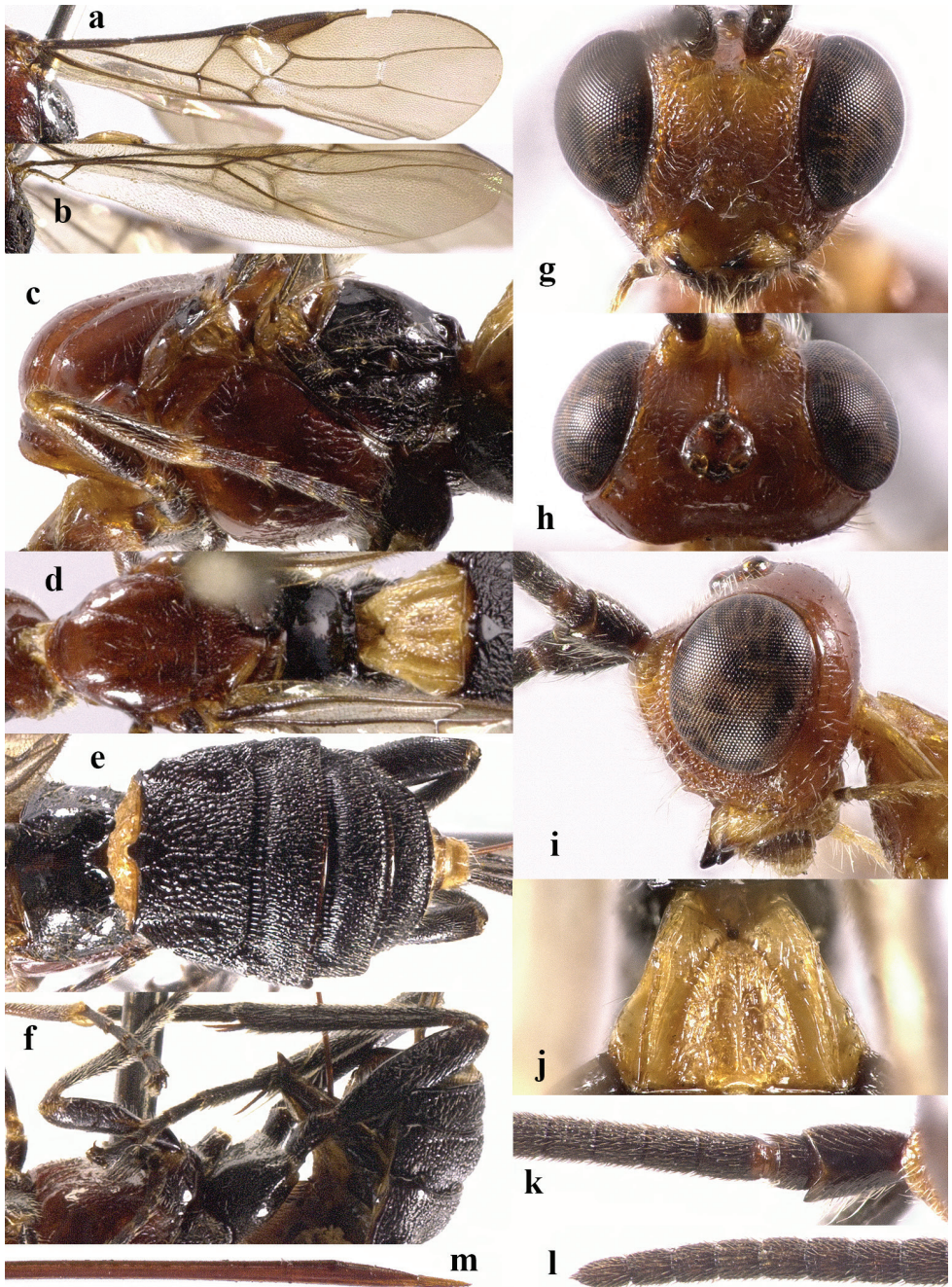


Figure 4. *Indabracon discolor* sp. nov., ♀, holotype **a** fore wing **b** hind wing **c** mesosoma, lateral view **d** mesosoma, dorsal view **e** metasoma, dorsal view **f** hind leg, lateral view **g** head, front view **h** head, dorsal view **i** head, lateral view **j** first metasomal tergite, dorsal view **k** scapus outer side, lateral view **l** apex of antenna **m** apex of ovipositor, lateral view.

Variation. Length of body of female 7.3–9.7 mm, of fore wing of female 6.8–9.1 mm, and of ovipositor sheath 2.7–5.6 mm; ovipositor sheath 0.4–0.6 times as long as fore wing; fore femur and tibia sometimes reddish yellow ventrally.

Biology. Unknown.

Distribution. China (Yunnan).

Etymology. Named after the T1 whitish yellow, while the remainder tergites black: “discolor” is Latin for “not of the same color”.

***Indabracon nigricans* sp. nov.**

<http://zoobank.org/3AD4EAE3-A4EE-453A-A4C3-D4FB71EDE1DD>

Figs 5, 6

Type material. **Holotype.** ♀, China, Yunnan Prov., Xishuangbanna Yunjinghong, 650m, 23.VII.1957, Zang Lingchao, No. IOZ(E)1964520 (IZCAS). **Paratype:** 1♀, China, Yunnan Prov., Xishuangbanna Cheli-Damenglong, 600m, 29.IV.1957, Liu Dahua, No. IOZ(E)1964541 (IZCAS).

Diagnosis. This new species is very similar to *I. bicolor* Yang et Chen, 2006, but can be separated from the latter by the following characters: scutellum black medially and remainder yellow, (entirely yellow in *I. bicolor*); apical third of pterostigma largely blackish (apical half of pterostigma dark brown and remainder yellow in *I. bicolor*); fore wing vein CU1b relatively short, 0.5 times as long as vein 3-CU1 (0.8 times in *I. bicolor*); T1 reddish yellow laterally (whitish yellow in *I. bicolor*) and medio-basal area of T2 rugose (smooth in *I. bicolor*).

Description. Holotype, ♀, length of body 9.2 mm, of fore wing 8.7 mm, of ovipositor sheath 5.6 mm.

Head. Antenna incomplete, 49 segments remaining; third segment 1.2 and 1.3 times longer than fourth and fifth, respectively, the latter 1.1 times longer than wide; length of maxillary palp 0.9 times height of head; malar suture rather weak, sculptured, and with short setae (Fig. 6i); clypeus height: inter-tentorial distance: tentorio-ocular distance = 6: 10: 7; clypeus with dense, long setae; eye weakly emarginated (Fig. 6g); face punctate, especially laterally (Fig. 6g); eye height: shortest distance between eyes: head width = 14: 15: 30; frons largely smooth except for a few weak punctures, with some sparse short setae and a strong median groove (Fig. 6h); vertex largely smooth except for a few weak punctures, and with some sparse short setae; POL: OD: OOL = 4: 5: 12; length of malar space 1.4 times basal width of mandible; length of eye 2.0 times temple in dorsal view; temples largely glabrous except for a few long setae, and subparallel-sided behind eyes (Fig. 6h).

Mesosoma. Length of mesosoma 1.6 times its height (Fig. 6c); notauli impressed anteriorly half (Fig. 6d); mesoscutum largely smooth except for a few weak punctures, with sparse short setae (Fig. 6d); scutellar sulcus moderately narrow, deep, and with crenulae (Fig. 6d); scutellum distinctly convex, punctate especially posteriorly;



Figure 5. *Indabracon nigricans* sp. nov., ♀, holotype, habitus lateral.

metanotum strongly convex medially, and with a short median carina anteriorly (Fig. 6d); propodeum largely smooth except for a few weak punctures and some crenulae posteriorly, and with sparse setae medially, and dense, long setae laterally (Fig. 6d).

Wings. Fore wing (Fig. 6a): SR1: 3-SR: r = 23: 16: 3; 1-SR+M strongly bent after arising from 1-M, and 1.7 times longer than 1-M; 2-SR: 3-SR: r-m = 6: 16: 5; CU1b 0.5 times as long as 3-CU1; cu-a weakly postfurcal, and nearly not bent basally. Hind wing (Fig. 6b): 1r-m straight or nearly so; SC+R1: 2-SC+R: 1r-m = 14: 4: 9.

Legs. Length of fore femur: tibia: tarsus = 11: 13: 16; length of hind femur: tibia: basitarsus = 27: 42: 14; length of femur, tibia and basitarsus of hind leg 3.0, 6.0 and 3.5 times their maximum width, respectively.

Metasoma. Length of T1 0.9 times its apical width, median area convex and strongly coarsely rugose, medio-longitudinal carina only present posteriorly, lateral areas relatively narrow and smooth (Fig. 6j); lateral grooves of T1 distinctly crenulate (Fig. 6j); T2 coarsely sculptured including medio-basal area (Fig. 6e); antero-lateral grooves of T2 strongly developed and crenulate (Fig. 6e); second suture deep and crenulate, wide and curved medially, narrow laterally (Fig. 6e); T3–4 with antero-lateral grooves, and latero-posterior corner medium-sized; T3–5 coarsely sculptured, and with crenulate transverse subposterior groove (Fig. 6e); T6–7 largely rugose, and with dense long setae posteriorly; hypopygium acute apically, not reaching level of apex of metasoma; ovipositor sheath 0.6 times as long as fore wing.

Colour. Largely black (Fig. 5); head largely yellow, except for antenna (but scapus yellow ventrally), eyes, stemmaticum and apex of mandible black (Fig. 6g, h, k); pro-

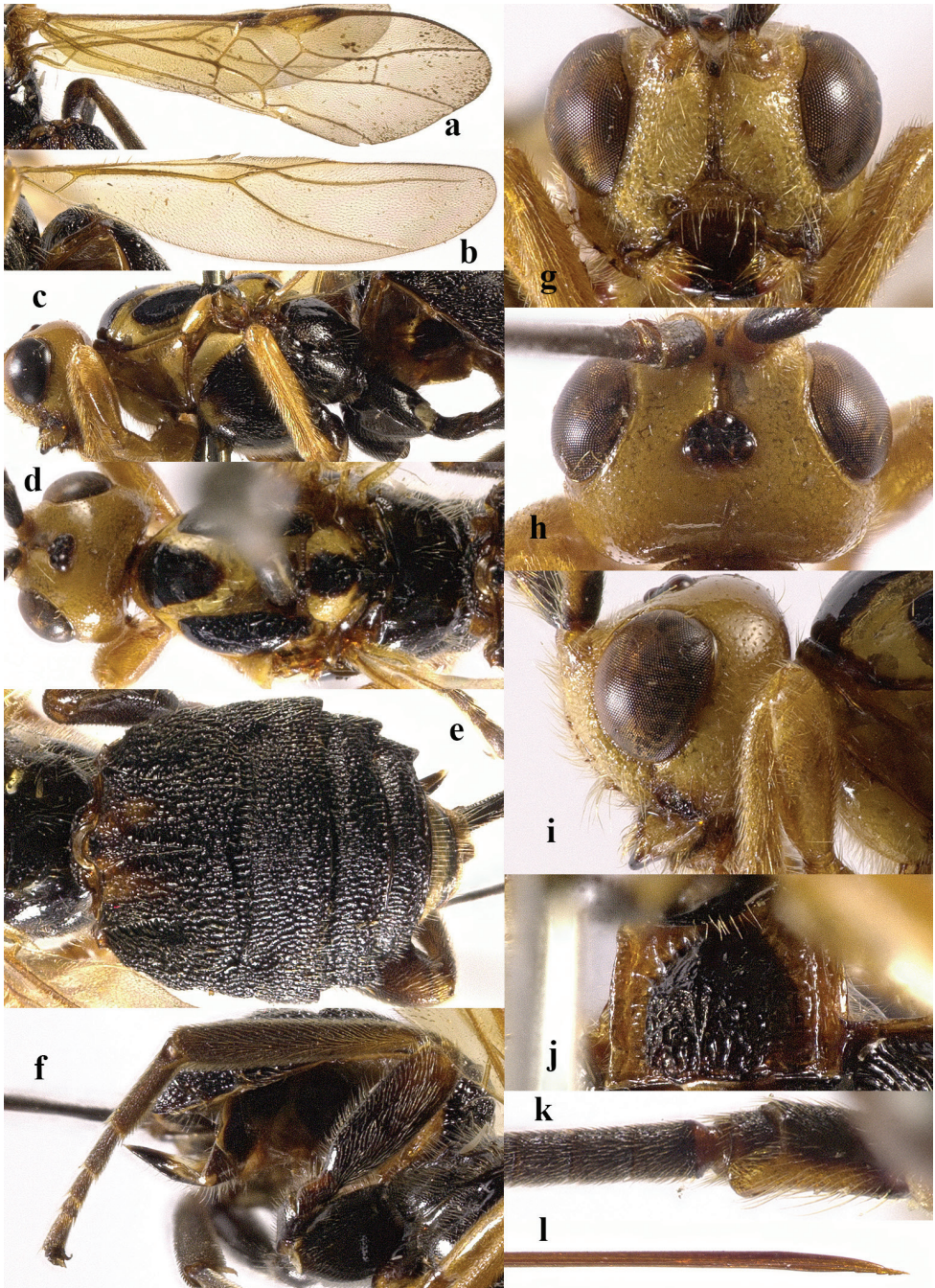


Figure 6. *Indabracon nigricans* sp. nov., ♀, holotype **a** fore wing **b** hind wing **c** mesosoma, lateral view **d** mesosoma, dorsal view **e** metasoma, dorsal view **f** hind leg, lateral view **g** head, front view **h** head, dorsal view **i** head, lateral view **j** first metasomal tergite, dorsal view **k** scapus outer side, lateral view **l** apex of ovipositor, lateral view.

thorax, notaulic area, median mesoscutal lobe posteriorly, tegulae, and scutellum laterally yellow (Fig. 6c, d); fore (except for black claws) and middle legs (but coxa and claws black) yellow; T1 yellowish brown anteriorly and laterally, T6–7 pale yellow (Fig. 6e, j); wing membrane infusate, and pterostigma (but blackish apically) yellow, veins dark brown (Fig. 6a, b).

Variation. Length of body of female 9.2–9.4 mm, of fore wing of female 8.4–8.7 mm, and of ovipositor sheath 5.6–6.2 mm; antenna with 51 segments; apical antennal segment acute, twice longer than wide; length of mesosoma 1.6–1.7 times its height; ovipositor sheath 0.6–0.7 times as long as fore wing.

Biology. Unknown.

Distribution. China (Yunnan).

Etymology. Named after the blackish colour of the metasomal tergites: “nigricans” is Latin for “blackish”.

***Indabracoon semicircularis* sp. nov.**

<http://zoobank.org/6609AFE3-BA4B-4F79-B93D-143E8B2E637A>

Figs 7, 8

Type material. Holotype. ♀, China, Yunnan Prov., Xishuangbanna Meng’^a, 1050–1080m, 13.X.1958, Wang Shuyong, No. IOZ(E)1964518 (IZCAS).

Diagnosis. This new species is very similar to *I. bicolor* Yang et Chen, 2006, but can be separated from the latter by the following characters: pterostigma largely yellow (apical half of pterostigma dark brown in *I. bicolor*); fore wing vein 1-SR+M strongly curved basally (at most weakly curved basally in *I. bicolor*); T1 black laterally (whitish yellow laterally in *I. bicolor*); T2 with sub-lateral areas (sub-lateral areas absent in *I. bicolor*); and ovipositor sheath 0.8 times as long as fore wing (0.6 times in *I. bicolor*).

Description. Holotype, ♀, length of body 10.0 mm, of fore wing 8.8 mm, of ovipositor sheath 7.2 mm.

Head. Antenna with 54 segments; apical antennal segment acute, 2.1 times longer than its maximum width (Fig. 8l); third segment 1.2 and 1.3 times longer than fourth and fifth, respectively, the latter 1.1 times longer than wide; length of maxillary palp 0.8 times height of head; malar suture moderately developed, sculptured and with dense, short setae (Fig. 8i); clypeus height: inter-tentorial distance: tentorio-ocular distance = 5: 12: 10; clypeus with sparse, long setae; eye weakly emarginated (Fig. 8g); face punctate, and with dense, short setae (Fig. 8g); eye height: shortest distance between eyes: head width = 18: 18: 37; frons largely smooth except for a few weak punctures, with a strong median groove (Fig. 8h); vertex largely smooth except for some sparse punctures, and with some sparse short setae; POL: OD: OOL = 4: 5: 14; length of malar space 1.7 times basal width of mandible; length of eye 1.5 times temple in dorsal view; temples smooth, with some long setae, and rather weakly narrowed behind eyes (Fig. 8h).

Mesosoma. Length of mesosoma 1.7 times its height (Fig. 8c); anterior half of notauli impressed (Fig. 8d); mesoscutum smooth, with sparse long setae (Fig. 8d);



Figure 7. *Indabracon semicircularis* sp. nov., ♀, holotype, habitus lateral.

scutellar sulcus moderately wide, deep, and with crenulae (Fig. 8d); scutellum distinctly convex, smooth, and with some short setae posteriorly; metanotum strongly convex medially, and with a short median carina anteriorly (Fig. 8d); propodeum largely smooth except for some crenulae posteriorly, and with sparse setae medially, and dense, long setae laterally (Fig. 8d).

Wings. Fore wing (Fig. 8a): SR1: 3-SR: r = 22: 16: 3; 1-SR+M distinctly bent after arising from 1-M, and 1.7 times longer than 1-M; 2-SR: 3-SR: r-m = 7: 16: 6; CU1b 0.7 times as long as 3-CU1; cu-a subinterstitial, and nearly straight basally. Hind wing (Fig. 8b): 1r-m more or less straight; SC+R1: 2-SC+R: 1r-m = 6: 2: 3.

Legs. Length of fore femur: tibia: tarsus = 19: 22: 28; length of hind femur: tibia: basitarsus = 30: 47: 17; length of femur, tibia and basitarsus of hind leg 3.7, 9.4 and 4.9 times their maximum width, respectively.

Metasoma. T1 as long as its apical width, median area convex and strongly coarsely rugose, with a few carinae, medio-longitudinal carina only present posteriorly, lateral areas relatively narrow and smooth (Fig. 8j); lateral grooves of T1 distinctly crenulate (Fig. 8j); T2 largely coarsely striate-rugose except for smooth medio-basal area (Fig. 8e); antero-lateral grooves of T2 wide but rather shallow, weakly crenulate (Fig. 8e); second suture deep and crenulate, wide and more or less straight medially, narrow laterally (Fig. 8e); T3–4 with antero-lateral grooves, and latero-posterior corner medium-size; T3–4 striate-rugose (T4 relatively weak so); T3–5 with crenulate transverse sub-

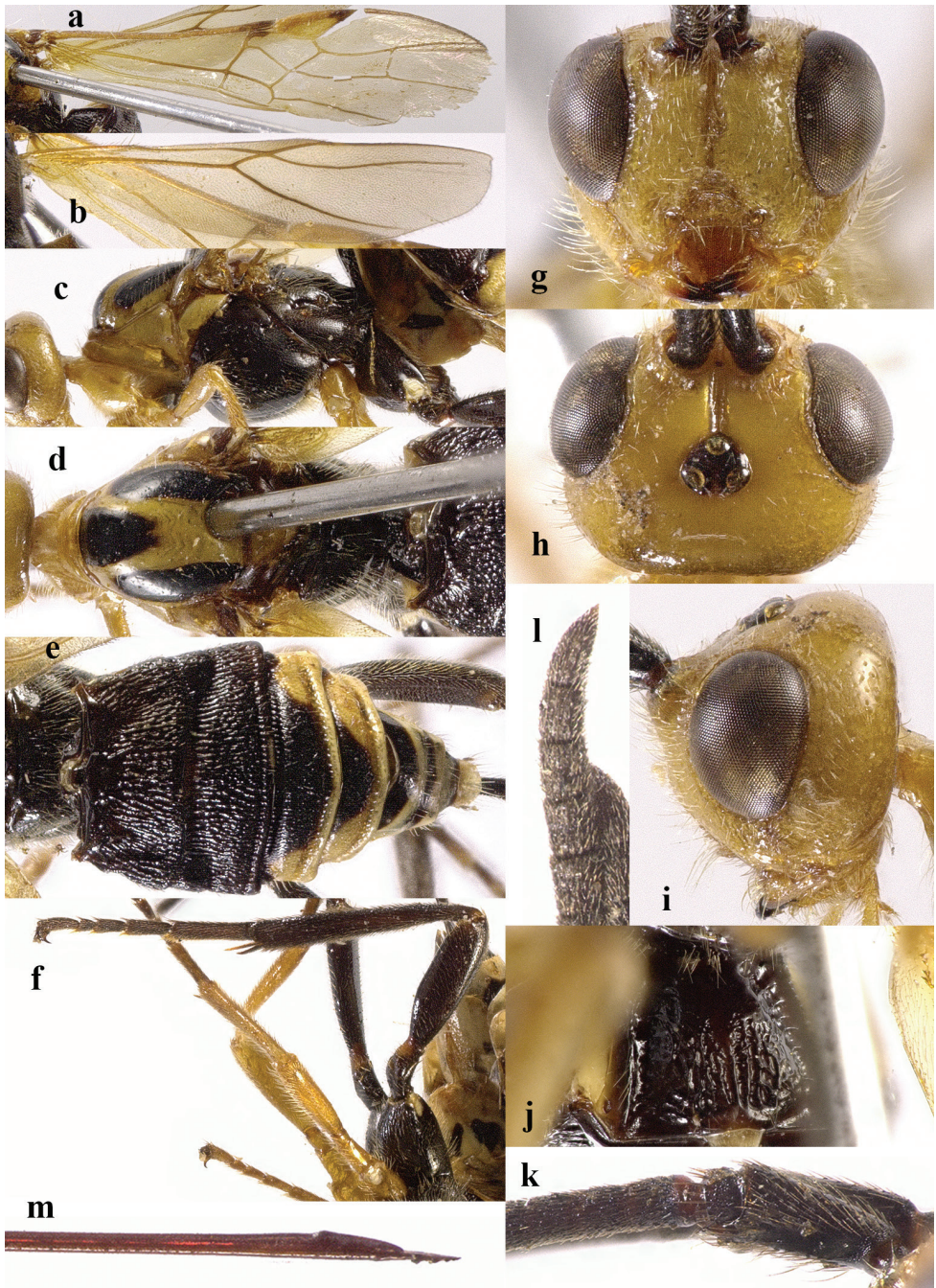


Figure 8. *Indabracon semicircularis* sp. nov., ♀, holotype **a** fore wing **b** hind wing **c** mesosoma, lateral view **d** mesosoma, dorsal view **e** metasoma, dorsal view **f** hind leg, lateral view **g** head, front view **h** head, dorsal view **i** head, lateral view **j** first metasomal tergite, dorsal view **k** scapus outer side, lateral view **l** apex of antenna **m** apex of ovipositor, lateral view.

posterior groove (Fig. 8e); T5–7 largely smooth, and with some long setae posteriorly; hypopygium acute apically, not reaching level of apex of metasoma; ovipositor sheath 0.8 times as long as fore wing.

Colour. Largely black (Fig. 7); head largely yellow, but antenna, eyes, stemmaticum and apex of mandible black (Fig. 8g, h); prothorax, notaulic area, median mesoscutal lobe posteriorly, tegulae, and scutellum yellow (Fig. 8c, d); fore (but claws black) and middle legs (but tarsi and claws blackish) yellow; T4–5 yellow, but T4 black medially (except for posterior margin) and T5 with a half-rounded black spot medio-basally (Fig. 8e); posterior margins of T6–7 pale yellow (Fig. 8e); wing membrane yellowish, pterostigma (except for apical dark brown spot) yellow, veins largely yellow, hind wing vein 2-M dark brown (Fig. 8a, b).

Biology. Unknown.

Distribution. China (Yunnan).

Etymology. Named after the shape of the black spot on the T5: “semi” and “circularis” are Latin for “half” and “round”, respectively.

Indabracon trimaculatus (Cameron, 1900)

Spinaria trimaculata Cameron, 1900: 81; Shenefelt 1975: 1259 (generic position doubtful); Quicke et Walker, 1991: 420 (comparison with *Bicariniabracon*).

Indabracon trimaculatus (Cameron): van Achterberg, 1992: 387; Chen et Yang, 2006: 125.

Biology. Unknown.

Distribution. China (Fujian); India.

Note. Chen et Yang (2006) reported the species from Fujian (SE China).

Acknowledgements

We thank Dr. Kees van Achterberg for his help during the course of study and critical reading of the manuscript. We also thank Mrs Hong Liu (IZCAS) for the loan of specimens. This research was supported by the Key International Joint Research Program of National Natural Science Foundation of China (31920103005), the General Program of National Natural Science Foundation of China (31702035), and the National Key Research and Development Plan (2017YFD0201000).

References

Cameron P (1900) Hymenoptera Orientalia, or Contributions to the knowledge of the Hymenoptera of the Oriental zoological region, Part IX. The Hymenoptera of the Khasia Hills.

- Part II. Section I. Memoirs and Proceedings of the Manchester Literary and Philosophical Society 44(15): 1–114.
- Chen J-H, Yang J-Q (2006) Systematic studies on Braconinae of China (Hymenoptera: Braconidae). Fujian Science and Technology Publishing House, Fujian, 304pp.
- Chen X-X, van Achterberg C (2019) Systematics, phylogeny and evolution of braconid wasps: 30 years of progress. *Annual Review of Entomology* 64: 335–358. <https://doi.org/10.1146/annurev-ento-011118-111856>
- Quicke DLJ, Walker C (1991) A new Indo-Australian genus of Braconinae (Insecta, Hymenoptera, Braconidae). *Zoologica Scripta* 20: 419–424. <https://doi.org/10.1111/j.1463-6409.1991.tb00305.x>
- Shenefelt RD (1975) Braconidae 8. Exothecinae, Rogadinae. *Hymenopterorum Catalogus* (nova editio). Pars 12, 1115–1262.
- van Achterberg C (1988) Revision of the subfamily Blacinae Foerster (Hymenoptera, Braconidae). *Zoologische Verhandelingen Leiden* 249: 1–324.
- van Achterberg C (1990) Illustrated key to the subfamilies of the Holarctic Braconidae (Hymenoptera: Ichneumonoidea). *Zoologische Mededelingen Leiden* 64: 1–20.
- van Achterberg C (1992) Four new genera of the subfamily Braconinae (Hymenoptera: Braconidae) from the Indo-Australian region. *Zoologische Mededelingen Leiden* 66(16–40): 381–397.
- van Achterberg C (1993) Illustrated key to the subfamilies of the Braconidae (Hymenoptera: Ichneumonoidea). *Zoologische Verhandelingen Leiden* 283: 1–189.
- Yang J-Q, Chen J-H, Liu J-J (2006) The discovery of the genus *Indabracon* van Achterberg (Hymenoptera: Braconidae: Braconinae) in China, with description of one new species. *Insect Science* 13(4): 319–323. <https://doi.org/10.1111/j.1744-7917.2006.00100.x>
- Yu DS, van Achterberg C, Horstmann K (2016) Taxapad 2016, Ichneumonoidea 2015. Database on flash-drive. Nepean, Ontario, Canada. <http://www.taxapad.com>

Two new species of *Ooencyrtus* (Hymenoptera, Encyrtidae), egg parasitoids of the bagrada bug *Bagrada hilaris* (Hemiptera, Pentatomidae), with taxonomic notes on *Ooencyrtus telenomicida*

Serguei V. Triapitsyn¹, Sharon A. Andreason², Nancy Power¹, Fatemeh Ganjisaffar¹,
Lucian Fusu³, Chrysalyn Dominguez¹, Thomas M. Perring¹

1 Department of Entomology, University of California, Riverside, California, 92521, USA **2** USDA ARS U.S. Vegetable Laboratory, 2700 Savannah Highway, Charleston, South Carolina, 29414, USA **3** Alexandru Ioan Cuza University, Faculty of Biology, Bd. Carol I no. 11, 700506, Iași, Romania

Corresponding author: Serguei V. Triapitsyn (serguei.triapitsyn@ucr.edu)

Academic editor: P. Jansta | Received 4 November 2019 | Accepted 28 February 2020 | Published 27 April 2020

<http://zoobank.org/24B2A66D-D648-4854-B0B9-4C0489881233>

Citation: Triapitsyn SV, Andreason SA, Power N, Ganjisaffar F, Fusu L, Dominguez C, Perring TM (2020) Two new species of *Ooencyrtus* (Hymenoptera, Encyrtidae), egg parasitoids of the bagrada bug *Bagrada hilaris* (Hemiptera, Pentatomidae), with taxonomic notes on *Ooencyrtus telenomicida*. Journal of Hymenoptera Research 76: 57–98. <https://doi.org/10.3897/jhr.76.48004>

Abstract

In support of a biological control program in California, USA, against the bagrada bug, *Bagrada hilaris* (Burmeister) (Hemiptera, Pentatomidae), an invasive pest of Asian origin, colonies of two species of *Ooencyrtus* Ashmead (Hymenoptera, Encyrtidae) are maintained using *B. hilaris* eggs as host. One of them, *Ooencyrtus mirus* Triapitsyn & Power, **sp. nov.**, is of Pakistani origin. It displays natural preference for bagrada bug eggs and is being evaluated in quarantine as a candidate for classical biological control. The other, *Ooencyrtus lucidus* Triapitsyn & Ganjisaffar, **sp. nov.**, appears to be native to California, and we believe it switched to *B. hilaris* from native pentatomid hosts. Both new species are described and illustrated, as is the Old World species *Ooencyrtus telenomicida* (Vassiliev), for which a neotype is designated. The presented morphometric evidence as well as mitochondrial and nuclear ribosomal DNA sequence data separate *Ooencyrtus mirus* from *O. telenomicida*. A lectotype is designated for *Ooencyrtus californicus* Girault from California, which is morphologically similar to *O. lucidus*.

Keywords

Chalcidoidea, natural enemy, invasive pest, California, Pakistan, biological control, genetic analysis, taxonomy

Introduction

The painted bug, also known as bagrada bug, *Bagrada hilaris* (Burmeister) (Hemiptera, Pentatomidae) (Fig. 1A), is native from western Asia to southern Africa (Howard 1907; Mahmood et al. 2015). It first was discovered in the United States in 2008 in Los Angeles County, California (Arakelian 2008). Since then, its range in the United States has expanded: it has been reported from other regions of California (Reed et al. 2013), Arizona (Palumbo and Natwick 2010; Palumbo et al. 2016), New Mexico (Bundy et al. 2012), Texas (Vitanza 2012), Nevada (Perring et al. 2013), Utah (Reed et al. 2013), and Hawaii (Matsunaga 2014). It also has been identified in Mexico (Sánchez-Peña 2014; Lomeli-Flores et al. 2019). *Bagrada hilaris* is a major pest of cole crops (Palumbo et al. 2016; Bundy et al. 2018), and there is no established biological control program for it. In 2014, in response to the rapid spread of *B. hilaris*, a search was conducted for egg parasitoids within its native range in Pakistan. Three species of parasitoid wasps, *Trissolcus hyalinipennis* Rajmohana & Narendran (Hymenoptera, Scelionidae, Telenominae) (Rajmohana 2006; Ganjisaffar et al. 2018), *Gryon gonikopalense* Sharma (Scelionidae, Scelioninae) (Sharma 1982; Martel et al. 2019), and *Ooencyrtus* sp. (Hymenoptera, Encyrtidae), were collected from *B. hilaris* eggs (Mahmood et al. 2015). Live specimens of the recovered parasitoids were shipped to the United States Department of Agriculture, Agricultural Research Service Quarantine Facility at the National Biological Control Laboratory in Stoneville, Mississippi (Mahmood et al. 2015) to be evaluated as classical biological control candidate agents for *B. hilaris*. In 2016, *Ooencyrtus* sp. was transported under permit to the University of California Riverside (UCR) Quarantine Facility, and we have been studying its biology, host specificity, and risk assessment. In concert with these biological studies, we addressed the taxonomic identification of this insect and describe it as a new species herein.

In addition to the classical biological control efforts with the exotic *Ooencyrtus* sp., surveys for resident egg parasitoids of *B. hilaris* have been conducted throughout California since 2017 using sentinel egg cards. In this project, we collected a variety of parasitoid species from the *B. hilaris* eggs. A species of *Ooencyrtus* Ashmead was recovered from sentinel cards in Riverside, California. Because the taxonomy of the Nearctic species of *Ooencyrtus* is in flux and there are no keys to the 11 described species, the first author physically compared specimens collected in our study to the types and specimens of all described species from North America. In addition, he tried to identify our specimens with keys from other regions (i.e. Neotropical, Oriental, and Palearctic). These efforts were unsuccessful, suggesting that our insect was an undescribed native species. Therefore, we also describe this parasitoid as a new taxon.

During our investigations, we attempted to compare our insects to *Ooencyrtus telenomicida* (Vassiliev) and to other egg parasitoids in the *O. telenomicida* species complex. However, we were unable to locate the type series of *Encyrtus telenomicida* Vassiliev (now *Ooencyrtus telenomicida*). Therefore, we collected *Ooencyrtus* sp. from eggs of *Eurygaster* Laporte, the host genus of *Encyrtus telenomicida*, in the same general habitat as indicated in the original description and matched the morphology of the new collections both with that description and with non-type specimens reared before



Figure 1. **A** *Bagrada hilaris* female and male **B** rearing cages for *Bagrada hilaris* mating pairs and egg production.

1950 from the original host in both Russia and Ukraine, not too far from its type locality. Based on the morphological congruence, we designated a neotype for *Encyrtus telenomicida* and supplement this designation with DNA sequence data necessary for the differentiation of *Ooencyrtus telenomicida* from morphologically similar species in the complex. Throughout the paper we are using the term ‘*O. telenomicida* species complex’ for those species that are genetically and morphologically close to *O. telenomicida*. The group was defined morphologically by Hayat et al. (2014) and later expanded by Samra et al. (2018) using molecular and morphological data.

Materials and methods

Sources of specimens

Ooencyrtus species of Pakistan origin

Compared to other pentatomids, *B. hilaris* has an unusual ovipositional behavior of laying eggs singly or in small clusters on live plant material, in detritus and in soil (Taylor et al. 2014). Knowing this behavior, researchers working in the Toba Tek Singh District of the Punjab Plain in Pakistan noticed *B. hilaris* adults congregating on dry debris of *Brassica juncea* (L.) Czernajew and *Brassica napus* L. The plant debris was collected and shaken onto a plastic sheet, and the resulting leaves, stems and soil were transported to the laboratory and examined for *B. hilaris* eggs (Mahmood et al. 2015). Eggs were collected and placed in glass vials to wait for parasitoid emergence. Mahmood et al. (2015) recovered a uniparental strain of *Ooencyrtus* sp. from the *B. hilaris* eggs on *B. napus* but not from the eggs on *B. juncea*. The emerging parasitoids were reared and shipped to Dr. Walker Jones at the USDA-ARS Quarantine Facility, National Biological Control Laboratory in Stoneville, Mississippi, USA (Mahmood et al. 2015). From there a colony was sent to the UCR Quarantine Facility, where it has been reared continuously on *B. hilaris* eggs since January 2016. The colony is maintained at 26 °C, 14:10 L:D and ~50% RH.

***Ooencyrtus* species native to California**

Sampling surveys for *B. hilaris* parasitoids were initiated in October 2017 and are still in progress. For the present study, *B. hilaris* adults were collected from a greenhouse colony where they were raised on seedlings of broccoli (*Brassica oleracea* L. var. *italica*), canola (*Brassica napus* L.), mustard greens (*Brassica juncea* L.), and sweet alyssum (*Lobularia maritima* (L.) Desvauz). Thirty adult mating pairs were placed in round plastic containers (15 cm diameter × 6 cm depth) (Durphy Packaging Co., Warminster, Pennsylvania, USA) with 2 screen openings on opposite sides for air circulation (Fig. 1B). Paper towels were placed in the bottom of the containers as an ovipositional substrate. The insects were provided organic broccoli florets and moved to new containers daily. Eggs were collected from the plastic containers and paper towels and glued to sentinel cards as described by Ganjisaffar et al. (2018). The cards were deployed in a squash field infested with shortpod mustard weeds, *Hirschfeldia incana* (L.) at the UCR Agricultural Operations on October 26, 2018. One of the cards with 15 glued *B. hilaris* eggs had 12 eggs parasitized, and from these 11 adult parasitoids emerged between November 13 and 15, 2018. These adults were placed in a vial, provided with honey, and given access for 24 hours to 50 *B. hilaris* eggs that had been glued (Elmer's) to a 1.5 × 4 cm white card. Following the 24 hour access period, the card with parasitized eggs was transferred to a new vial for rearing the parasitoids. The original egg parasitoids then were collected and placed in vials containing 95% ethanol and stored in a freezer at -20 °C until they were used for morphological studies or DNA extraction. Primary molecular voucher specimens were slide-mounted in Canada balsam.

***Ooencyrtus telenomicida* (Vassiliev) from Europe**

Specimens of *O. telenomicida*, reared in Russia and Ukraine from eggs of *Eurygaster integriceps* Puton (Hemiptera, Scutelleridae) in 1948 and 1950, were borrowed from the Zoological Institute, Russian Academy of Sciences, Saint Petersburg, Russia. Unfortunately, PCRs failed on all the specimens that were extracted. Therefore, new specimens of *O. telenomicida* were reared in Ipatele, Iași County, Romania, from eggs of *Eurygaster* sp. found on wheat. We were able to extract DNA from these specimens, and the primary molecular vouchers were individually slide-mounted in Canada balsam or chemically dried and point mounted.

Taxonomic studies

For the taxonomic descriptions of the new species, the morphological terms of Gibson (1997) were used, with a few modifications. All wing measurements of length or length:width are given in micrometres (µm). Abbreviations used in the descriptions are: F = funicle segment of the female antenna or flagellomere of the male antenna; mps = multiporous plate sensillum or sensilla on the antennal flagellar segments (= longitudinal sensillum or sensilla, or sensory ridge(s)).

Specimens for morphometric studies were dried from ethanol using a critical point drier, then point-mounted and labeled. Selected specimens then were dissected and slide-mounted in Canada balsam. Slide mounts were examined under a Zeiss Axioskop 2 plus compound microscope (Carl Zeiss Microscopy, LLC, Thornwood, New York, USA) and photographed using the Auto-Montage system (Syncroscopy, Princeton, New Jersey, USA). Photographs were retouched where necessary using Adobe Photoshop (Adobe Systems, Inc., San Jose, California, USA). In addition, the body length of 24 male and 24 female *O. mirus* wasps were measured from the anterior end of the head to the posterior end of the gaster, not including the ovipositor or aedeagus, with a Leica Wild M10 stereoscope using a Bausch & Lomb 0.1 mm and 0.01 mm micrometer.

For the morphometric analysis, we measured characters in adult females and males to determine the following ratios: 1) ovipositor length to mesotibia length; 2) fore wing length to maximum width; 3) scape length to width (excluding the radicle); 4) clava length to width; 5) F1 length to pedicel length; and 6) F2 length to F1 length. For all parameters, the ranges, means, and standard deviations were determined.

For *O. mirus* and *O. telenomicida* we also used multivariate ratio analysis (MRA) (Baur and Leuenberger 2011) because these two species differ mostly in color and very little in body ratios. For this analysis, 15 measurements per specimen were used and 9 female specimens for each species were included in the analysis. Following the approach of Baur et al. (2014) the MRA also served to place the neotype of *O. telenomicida* in the morphospace of specimens from Russia and Ukraine. The complete set of measurements is available as Suppl. material 1 data from the publisher's website.

Specimens examined are deposited in the collections with the following acronyms:

- AICF** Alexandru Ioan Cuza University, Iași, Romania (Lucian Fusu collection);
- BMNH** The Natural History Museum, London, UK;
- EMEC** Essig Museum of Entomology, University of California, Berkeley, California, USA;
- UCRC** Entomology Research Museum, Department of Entomology, University of California, Riverside, California, USA;
- USNM** National Museum of Natural History, Washington, District of Columbia, USA;
- ZIN** Zoological Institute, Russian Academy of Sciences, Saint Petersburg, Russia.

DNA extraction, amplification, and sequencing

Paratype specimens of *O. lucidus* and *O. mirus* were selected for genetic analysis. Genomic DNA from three females (UCRC ENT 311756, 311757, and 311769) and one male (UCRC ENT 311770) *O. lucidus* and three female *O. mirus* (UCRC_ENT 00506189–00506191) was extracted using the non-destructive HotShot method (Truett et al. 2000) as described in Andreason et al. (2019a, 2019b) to preserve specimen integrity for subsequent slide mounting and morphological study. DNA from the neotype female specimen of *O. telenomicida* (UCRC ENT 311776) and a non-type female from the same collection event (UCRC ENT 311775) was extracted using

the non-destructive method described in Triapitsyn et al. (2019). Three more females and one male from the same collection event (AICF vouchers OoIs0101, OoIs0102, OoIs0201, OoIs0202) were extracted with another non-destructive method as detailed in Cruaud et al. (2019); several other specimens are kept at AICF in 96% ethanol at -20°C to preserve DNA integrity for future investigations. DNA extracts were stored at -20°C until PCR amplification was performed.

Paired with morphological descriptions, confirmation of novel species was based on analysis of a fragment of the mitochondrial cytochrome c oxidase subunit I (COI) gene and the nuclear internal transcribed spacer 2 (ITS2) region. PCRs were performed using the reagents at concentrations described in Andreason et al. (2019b) with the primers of Samra et al. (2018), synthesized by Integrated DNA Technologies, Inc. (Coralville, IA, USA), with modified thermal cycling conditions. For COI amplification, thermal cycling was performed at 95°C for 3 m, 40 cycles of 95°C for 30 s, 30°C for 1 m, and 72°C for 1 m 15 s, with a final extension at 72°C for 5 m. For ITS2 reactions, thermal cycling was performed similarly but at a 54°C annealing temperature. Confirmation of amplification by gel electrophoresis, product cleaning, and sequencing were all performed according to Andreason et al. (2019b).

For *O. telenomicida* sequencing of the ITS2 with the primers in Samra et al. (2018) failed, thus we used the primers described in Yara (2006) to obtain a sequence from specimen OoIs0102. For the same species we obtained standard DNA barcodes for specimens OoIs0101, OoIs0102 and OoIs0201 with the primers LCO1490 and HCO2198 (Folmer et al. 1994). Molecular protocols described in Fusu and Ribes (2017) were used, except for the annealing temperature for ITS2 that was set at 45°C . All sequences were deposited in GenBank (accession numbers MN933499–MN933500; MN935769–MN935775; MN947512–MN947518; MN945949–MN945951 [COI]; MN946502 [ITS2]).

Genetic analysis

Interspecific variation among *O. lucidus*, *O. mirus*, *O. telenomicida*, and other populations and species of *Ooencyrtus* was estimated by calculating uncorrected pairwise distances (p-distances) of the COI fragment and ITS2 region and by phylogenetic analysis. MEGA X (Kumar et al. 2018) was used to trim and analyze sequence files obtained in this study, to perform multiple sequence alignments using ClustalW (Thompson et al. 2003), and to construct a phylogenetic tree. For comparisons of the COI and ITS2 regions, *Ooencyrtus* sequences deposited in GenBank by Samra et al. (2018) were aligned with *O. lucidus*, *O. mirus*, and *O. telenomicida* from Romania, and p-distances were calculated using the p-distance model with pairwise deletion of gaps. When comparing COI fragments, all available sequences were analyzed to account for intraspecific differences within species; for ITS2, one sequence was selected from GenBank because the ITS2 region generally has very little, if any, intraspecific variation in Hymenopterans (Campbell et al. 1994; Stouthamer et al. 1999). A phylogeny of the

studied species based on concatenated and unpartitioned COI and ITS2 sequences was inferred using the Maximum Likelihood method based on the Tamura-Nei model with 1000 bootstrap replications (Tamura and Nei 1993). The tree was drawn to scale with the number of substitutions per site estimating the branch lengths. *Ooencyrtus kuvanae* (Howard) was included as an outgroup because it is not part of the *O. telenomicida* complex and for which reliable sequences are available (Samra et al. 2018).

Results

Taxonomy

Ooencyrtus lucidus Triapitsyn & Ganjisaffar, sp. nov.

<http://zoobank.org/98066B3C-9BBB-4BAE-AC92-13A559D58817>

Figs 2–4

Ooencyrtus californicus Girault: Noyes 2010: 402 (misidentification of specimens from Texas).

Type material. *Holotype* female, deposited in UCRC, on slide (Fig. 2B) labeled: 1. “USA: California, Riverside Co. Riverside, T. M. Perring laboratory at UCR, F3 on bagrada bug eggs From colony, ii.2019, F. Ganjisaffar Originally from: UCR Ag. Ops. 33.966002N, 117.343198W Cards with fresh sentinel eggs of *Bagrada hilaris* (Burmeister) placed in squash field 26–29.x.2018 Parasitoids emerged 13–15.xi.2018, F. Ganjisaffar”; 2. “V. V. Berezovskiy 2019 in Canada balsam”; 3. [red] “*Ooencyrtus lucidus* Triapitsyn & Ganjisaffar Holotype ♀”; 4. “Det. by S. V. Triapitsyn 2019”; 5. [barcode database label/unique identifier] “UCRC [bold] UCRC ENT 311771”. The holotype (Figs 2C, 3) is in good condition, complete, dissected under 4 coverslips.

Paratypes. USA, California, Riverside County, Riverside, University of California at Riverside (UCR): Agricultural Operations, 33.966002N, 117.343198W, 304 m, cards with fresh sentinel eggs of *Bagrada hilaris* placed in squash field 26–29.x.2018, parasitoids emerged 13–15.xi.2018, F. Ganjisaffar [4 females on points, 4 females on slides (including 3 molecular vouchers of S. A. Andreason, UCRC ENT 311756, 311757, and 311769) and 1 male on slide (molecular voucher UCRC ENT 311770), UCRC]; T. M. Perring laboratory, from colony, third generation (F3) on bagrada bug eggs, ii.2019, F. Ganjisaffar, originated from the above collection [7 females (1 in BMNH, 1 in EMEC, 3 in UCRC, 1 in USNM, 1 in ZIN), 14 males (2 in BMNH, 2 in EMEC, 6 in UCRC, 2 in USNM, 2 in ZIN) on points and 5 females, 2 males on slides, UCRC].

Other (non-type) material examined. USA: California, Merced County, Merced, 24.viii.1938, R. Rose, “Ex eggs of *Acrosternum hilaris*” [1 female, 1 male, USNM] (misidentified as *O. californicus* Girault by A. B. Gahan). Texas, Presidio County, Presidio, 14.viii.1941, L. W. Noble (from eggs of *Chlorochroa sayi* Stål) (misidentified as *O. californicus* by A. B. Gahan) [2 females, 1 male, UCRC; 6 females, 4 males, USNM].

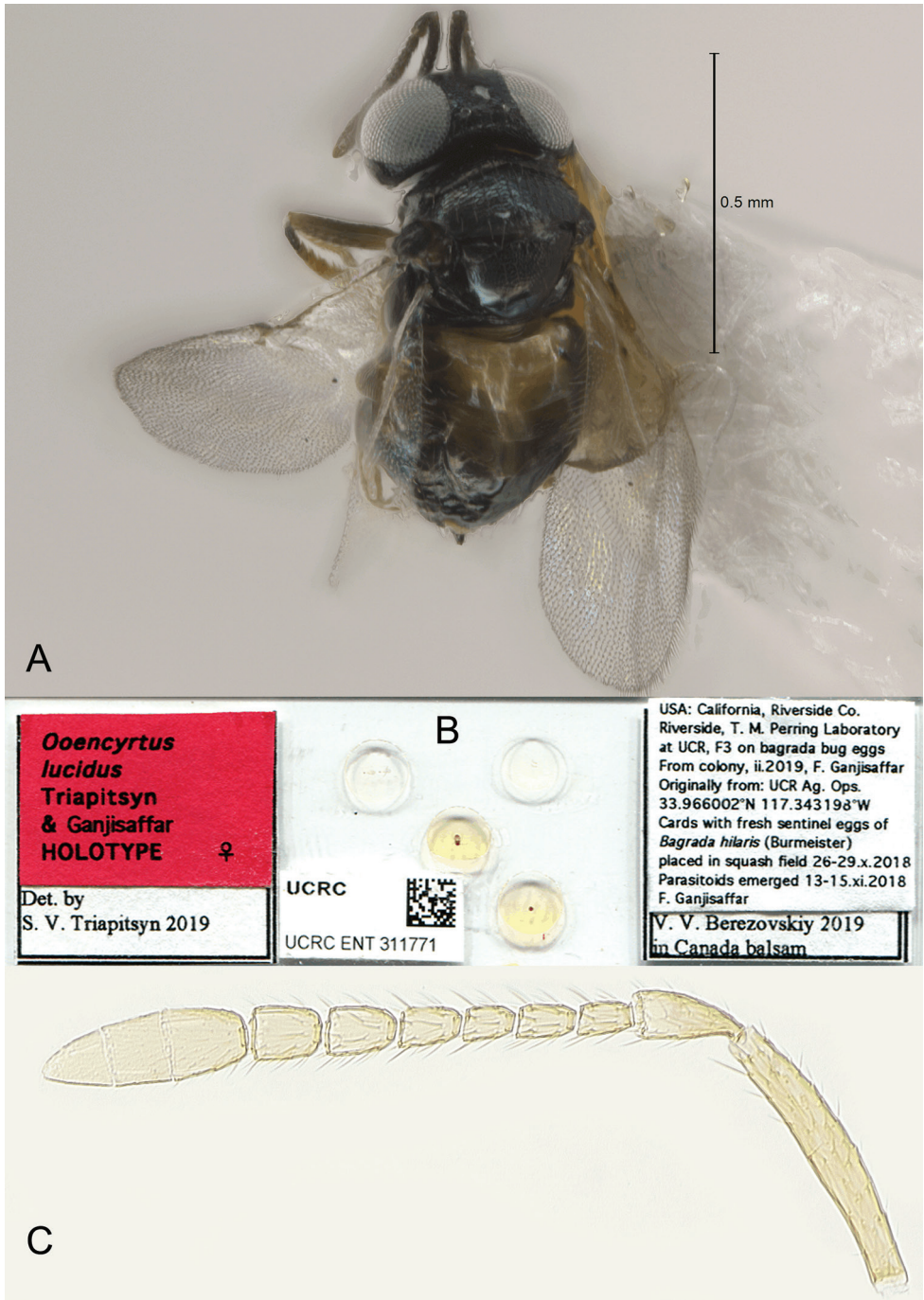


Figure 2. *Ooencyrtus lucidus* sp. nov. female **A** habitus in dorsal view (paratype) **B** holotype slide **C** antenna (holotype).

Diagnosis. There are no comprehensive keys for *Ooencyrtus* in North America and only 3 described species have been identified from California (Zuparko 2015, 2018). Therefore, to confirm that *O. lucidus* was not already collected in North America, the first author visited USNM in February 2019 and compared *O. lucidus* specimens with all the available types of *Ooencyrtus* species; no match was found. Morphologically, *O. lucidus* is most similar to the Nearctic species *O. californicus*, to which its female specimens key in both Noyes (2010) (to the Neotropical species) and Zuparko (2018) (to species in California). However, females of *O. lucidus* differ from *O. californicus* in having the scape at most 7.5× as long as wide (average of 6.6× as long as wide, Table 1) and the F1 is about 1.5× as long as wide (Fig. 2C). For *O. californicus* the scape (Fig. 5C) is about 8.8× as long as wide (as measured from the slide-mounted syntypes, with no significant difference between the four scapes measured; however, these measurements could very well be inaccurate because of the way the specimens were crushed, and the antennae were slide-mounted), and the F1 is a little more than 2.0× as long as wide. In addition, the “base of abdomen encircled by a narrow golden band” described by Girault (1917: 22) for *O. californicus* is not present in *O. lucidus*. Unfortunately, the metasoma of both extant types of *O. californicus* is missing (see below under comments). Instead the base of the gaster has a distinct yellow spot medially. Furthermore, although it is a minor difference, F1 of the female antenna is about 0.5× the length of the pedicel on average in *O. lucidus* (Table 1) whereas in the type specimens of *O. californicus* it is about 0.6× the length of the pedicel. Thus, we are unable to positively attribute our specimens of *O. lucidus* to *O. californicus* based on the available, very limited comparable morphological data.

In Noyes (1985), *O. lucidus* keys to the New World species *O. johnsoni* (Howard), whose entire gaster is shining black, perhaps with a slight greenish tinge. The entire type series of the latter taxon, 2 females and 1 male syntypes, were examined by the first author at USNM; the females are on points, with some parts of them mounted on a slide, and the male is on a slide. It also does not fit any of the described Old World species keyed in the publications mentioned below in the diagnosis of *O. mirus*, and is presumed to be native to the USA.

Description. Female (holotype and paratypes). **Body length** of dry-mounted, critical point-dried paratypes 825–1025 µm, and of slide-mounted paratypes 1045–1125 µm.

Color. Body (Fig. 2A) mostly shining black with some metallic reflections, particularly on mesosoma, except base of gaster always with a distinct yellow, dorsal spot medially (on gastral tergites 1–3) and often with either yellow or light brown areas laterally and ventrally (always separated from medial yellow spot by a brown area); antenna brown; legs mostly yellow to light brown except coxae brown to dark brown basally and protibia and tarsi brownish.

Sculpture. Head with faint, inconspicuous sculpturing; mesoscutum reticulate, with sculpture cells mostly wider than long; axilla and anterior 1/3 or so of scutellum with a rather weak cell-like sculpture, remainder of body smooth.

Table 1. Morphometric ratios and measurements (μm) of *Ooencyrtus lucidus* female morphological characters. All measurements are from slide-mounted specimens.

| | Length ovipositor: length mesotibia | Length: width fore wing | Length: width hind wing | Length: width scape | Length: width clava | Length F1: length pedicel | Length F2: length F1 |
|-------|-------------------------------------|-------------------------|-------------------------|---------------------|---------------------|---------------------------|----------------------|
| Range | 1.0–1.2 | 2.2–2.5 | 4.7–5.3 | 5.7–7.5 | 2.9–3.6 | 0.45–0.55 | 0.9–1.1 |
| Mean | 1.1 | 2.4 | 4.9 | 6.6 | 3.2 | 0.5 | 1.0 |
| n | 10 | 9 | 8 | 10 | 10 | 10 | 10 |
| | Length F1 | Length F2 | Length F3 | Length F4 | Length F5 | Length F6 | |
| Range | 29–35 | 27–38 | 24–36 | 34.85–39.39 | 41–45 | 38–42 | |
| Mean | 33 | 33 | 32 | 37 | 43 | 41 | |
| n | 10 | 10 | 10 | 10 | 10 | 10 | |

Pubescence. Frontovortex, pronotum, mesoscutum, axilla, and scutellum with short, dark setae except scutellum with a few pairs of long, dark setae in posterior half.

Head (Fig. 3A) about 1.2 \times as wide as high. Minimum width of frontovortex about 0.3 \times head width. Toruli just below level of lower eye margin. Ocelli in an obtuse triangle. Maxillary palpus 4-segmented, labial palpus 3-segmented. Mandible with 2 teeth and a broad truncation.

Antenna (Fig. 2C) with radicle about 3.2 \times as long as wide, rest of scape slender, slightly wider in the middle, 5.7–7.5 \times (5.9 \times in the holotype) as long as wide; pedicel about 2.2 \times as long as wide, notably longer than any funicular segment (F1 0.45–0.55 \times length of pedicel, Table 1); funicle segments all longer than wide, F1–F3 usually subequal in length (F2 0.9–1.1 \times length of F1, Table 1) although often F3 the shortest, F5 the longest funicular segment (Table 1), F1–F3 without mps, F4 with 1 mps, F5–F6 each with 2 mps; clava 3-segmented, 2.9–3.6 \times (2.9 \times in the holotype) as long as wide and about as long as combined length of F4–F6, each claval segment with several mps.

Mesosoma (Fig. 3B, C). Mesoscutum about 2.5 \times as wide as long; scutellum a little shorter than wide and slightly longer than mesoscutum, placoid sensilla close to each other and about in the middle of scutellum.

Wings (Fig. 3D) not abbreviated, fore wing extending beyond apex of gaster. Fore wing 2.2–2.5 \times as long as wide (2.3 \times in the holotype), disc hyaline; costal cell about 12 \times as long as wide; marginal vein punctiform; inconspicuous postmarginal vein much shorter than stigmal vein; linea calva closed posteriorly by 2 rows of short, inconspicuous setae; filum spinosum usually with 3 setae, rarely with 4 or 5 setae; longest marginal seta about 0.09 \times maximum wing width. Hind wing 4.7–5.3 \times as long as wide (4.9 \times in the holotype), disc hyaline.

Legs. Mesotibial spur about as long as mesobasitarsus.

Gaster (Fig. 3C) longer than mesosoma. Ovipositor occupying 0.6–0.7 length of gaster, a little exerted beyond its apex, and 1.0–1.2 \times (about 1.1 \times in the holotype) as long as mesotibia.

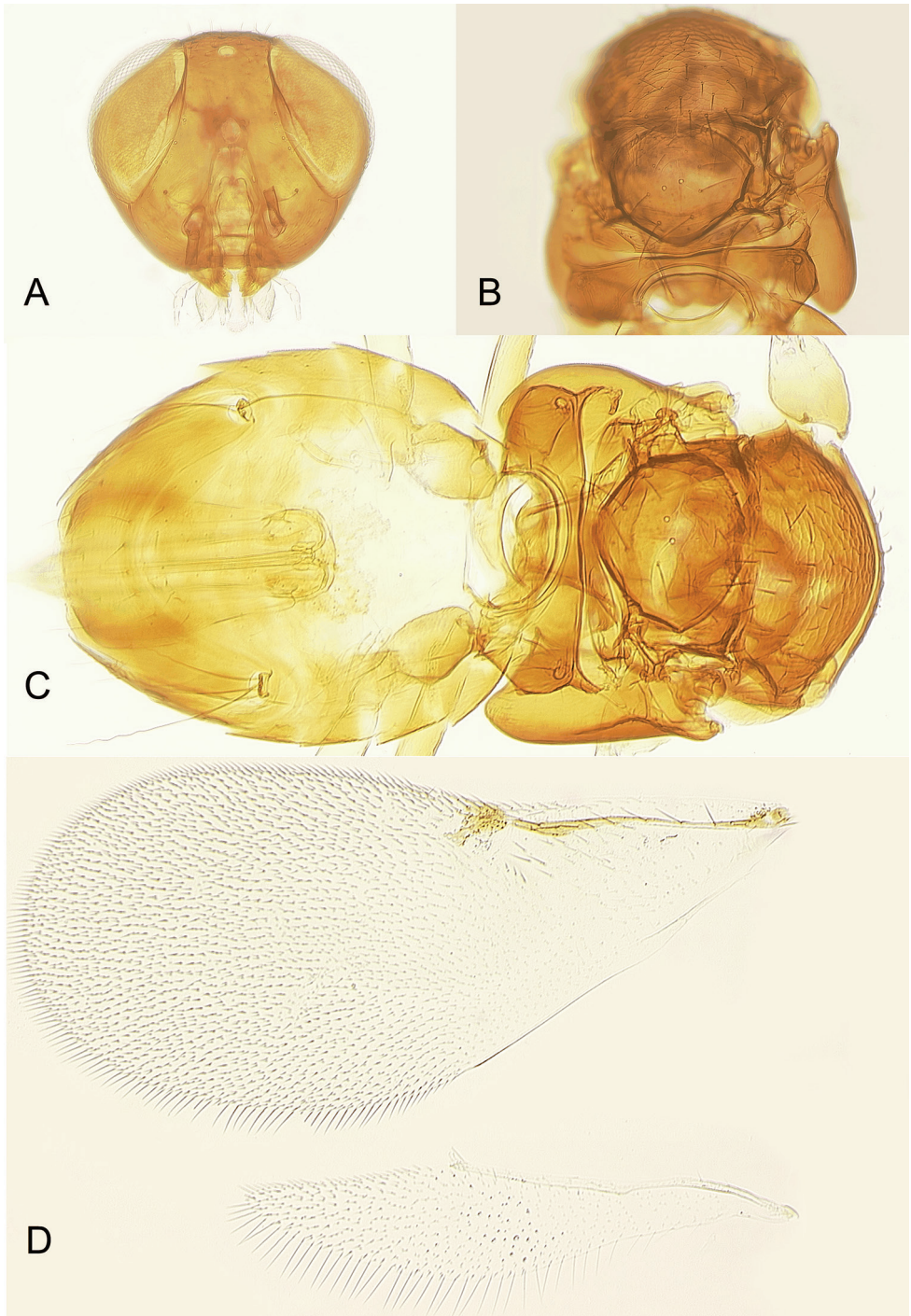


Figure 3. *Ooencyrtus lucidus* sp. nov. female (holotype) **A** head in frontal view **B** mesosoma **C** mesosoma and metasoma **D** fore and hind wings.

Measurements (μm) of the holotype. Mesosoma 394; gaster 480; ovipositor 379; mesotibia 358. Antenna: radicle 48; rest of scape 179; pedicel 70; F1 35; F2 38; F3 30; F4 38; F5 45; F6 42; clava 129. Fore wing 852:369; longest marginal seta 33. Hind wing 603:123; longest marginal seta 48.

Male (paratypes). **Body length** of dry-mounted, critical point-dried paratypes 595–795 μm , and of slide-mounted paratype 940 μm . **Head** and **mesosoma** shining black with metallic reflections (Fig. 4B), **gaster** dark brown; legs mostly yellow or light brown except coxae brown to dark brown and tarsi brownish. **Head** with toruli slightly above lower eye margin. **Antenna** (Fig. 4C) with scape minus short radicle 3.7–4.0 \times as long as wide (Table 2); funicle segments all longer than wide and more or less subequal in length (proximal segments a little shorter), F1–F3 apparently without mps, F4–F6 with at least 2 mps each; clava entire, 3.1–3.2 \times as long as wide, with several mps; flagellar segments all with numerous long setae. Fore **wing** (Fig. 4D) 2.25–3.1 \times as long as wide, with linea calva open posteriorly; hind wing 4.1–4.2 \times as long as wide. **Genitalia** (Fig. 4A) length 171–182 μm .

Etymology. *Bagrada hilaris* populations have declined in California. We believe that parasitoids like *O. lucidus* are responsible for this decline. “Lucidus” is an adjective derived from Latin, meaning “lucid, clear.” It is chosen for this species name referring to the elucidation of why populations of *B. hilaris* have declined in California.

Distribution. Nearctic region: USA (California and Texas).

Hosts. Pentatomidae: *Bagrada hilaris* (Burmeister), *Chinavia hilaris* (Say), and *Chlorochroa sayi* Stål. In California, *O. lucidus* apparently switched from its native host(s), such as the green stink bug *Chinavia hilaris*, to parasitize eggs of the invasive bagrada bug.

Comments. The following specimens of *O. californicus* have been examined. Lectotype female [USNM], here designated to avoid the existing ambiguity regarding the status of the type specimens of this species, on slide (Fig. 5A) labeled: 1. [red] “Type no. 20859 U.S.N.M.”; 2. “*Ooencyrtus californicus* Girault. ♀ type.”. Of the two crushed type female specimens (Fig. 5B) on this slide (because 4 scapes are present), only parts of 4 antennae and a slightly damaged fore wing (Fig. 5D) remain; the lectotype is constituted by the remains of one of them, circled in India ink, with the most intact antenna (Fig. 5C); remains of the other specimen are those of the paralectotype, and the single fore wing (Fig. 5D) can belong to either of them. The species was poorly described (Girault 1917: 22 [as *Oenocyrtus californicus*, sic]) from the unspecified number of “Types” under this catalog number in USNM; the type series was reared in Sacramento, California, USA from bug eggs on *Pinus sabiniana* (Douglas) D. Don (Pinaceae). The whereabouts of the other specimens of the type

Table 2. Morphometric ratios and measurements (μm) of *Ooencyrtus lucidus* male morphological characters. All measurements are from slide-mounted specimens.

| | Length genitalia | Length: width fore wing | Length: width scape |
|-------|------------------|-------------------------|---------------------|
| Range | 171–182 | 2.25–2.3 | 3.7–4.0 |
| Mean | 176 | 2.3 | 3.9 |
| n | 3 | 3 | 2 |

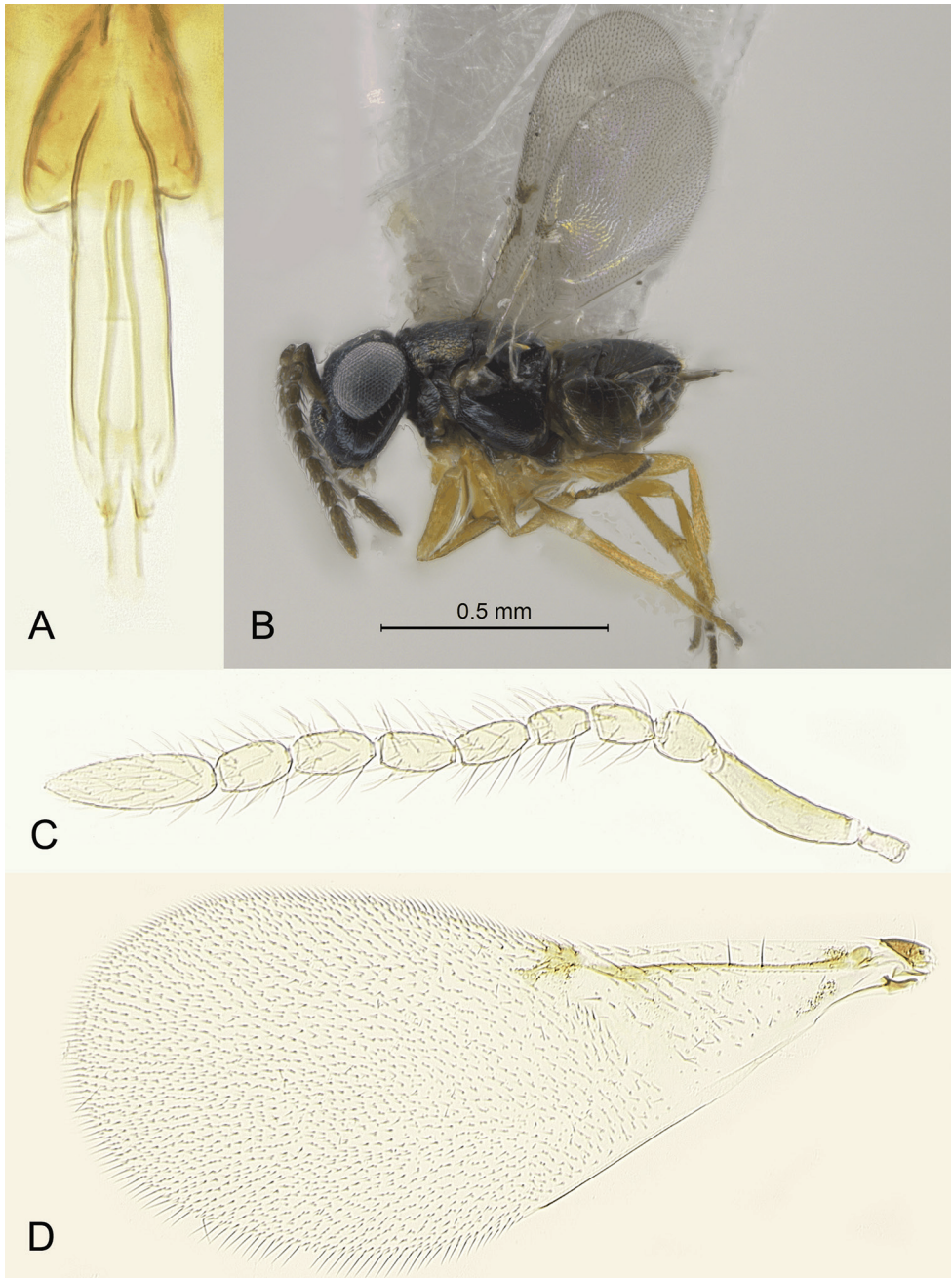


Figure 4. *Ooencyrtus lucidus* sp. nov. male (paratypes) **A** genitalia **B** habitus in lateral view **C** antenna **D** fore wing.

series, if they ever existed, are unknown; however, it is quite likely that these two females were the only original “types”. Thus, all other identifications of this species could be regarded to be tentative at best: for instance, specimens belonging to

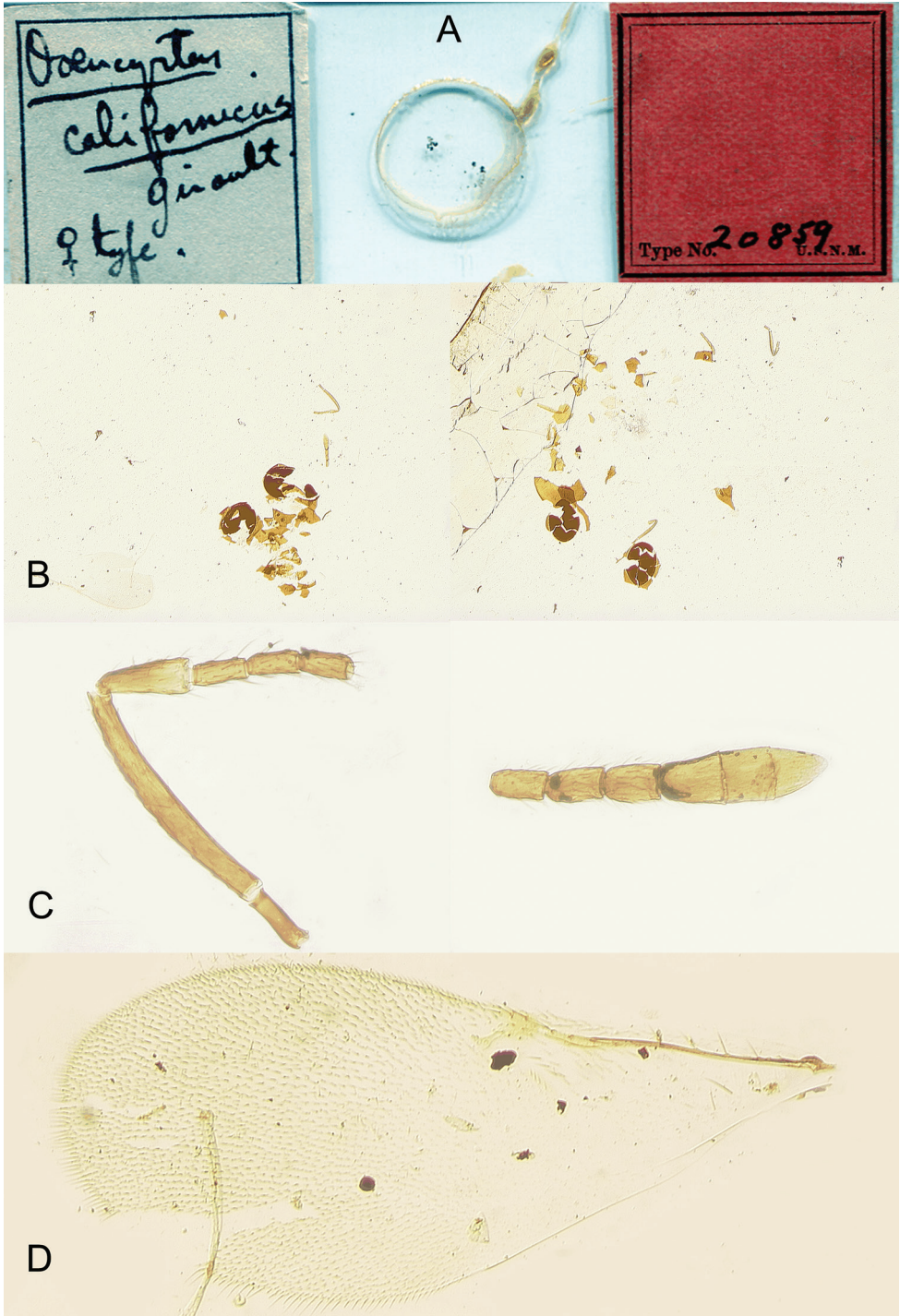


Figure 5. *Ooencyrtus californicus* female **A** lectotype/paralectotype slide **B** lectotype and paralectotype **C** antenna (lectotype) **D** fore wing (lectotype or paralectotype).

perhaps three different species of *Ooencyrtus* stand under *O. californicus* in UCRC. Zuparko (2015: 44) commented on the difficulties of identifying this species and the poor condition of the “holotype” female of *O. californicus* in USNM, noting that a species similar to it was collected in several counties in California including Riverside County. To be fully recognizable (since the original syntypes are incomplete), *O. californicus* will need to be re-described and thoroughly illustrated based on fresh specimens collected in the Sacramento area of California on the original host plant. DNA sequences will need to be compared with those of *O. lucidus* and other species of *Ooencyrtus*. Until that happens (keeping in mind that the true *O. californicus* may never be re-collected and thus would be impossible to be properly recognized), this species is treated as a *nomen dubium*, and making positive identifications of any specimens as *O. californicus* is not currently feasible. Therefore, we chose to describe *O. lucidus*, for which many good quality specimens and DNA sequences are available, as a new species that can be easily and positively recognized using a combination of morphological features and genetic data. The other option, i.e. trying to match our specimens with the incomplete original syntypes of *O. californicus* for which desired DNA sequences are not available, is impossible given the latter nominal species cannot be positively identified.

Noyes (2010) reported 2 females of *O. californicus* (determined as such by A. B. Gahan) from Presidio, Texas, USA, reared from eggs of *Chlorochroa sayi*, but closer examination of the specimens from the same series revealed that they are conspecific with *O. lucidus*.

Also present in UCRC is a series of 9 females misidentified (probably by H. Compere) as *O. californicus*, reared 1.ix.1937 in Riverside, Riverside County, California, USA by J. D. Maple from eggs of *Anasa tristis* (De Geer) (Hemiptera: Coreidae) and reported as *O. californicus* by Maple (1947: 105); these are neither *O. californicus* nor *O. lucidus* because their entire gaster is dark, without any yellow spot or band, and in this regard are more similar to *O. johnsoni*.

***Ooencyrtus mirus* Triapitsyn & Power, sp. nov.**

<http://zoobank.org/C22A1533-33B2-43F5-84E4-CAEC9A986247>

Figs 6–9

Type material. *Holotype* female, deposited in UCRC, on slide (Fig. 7A) labeled: 1. “USA: California, Riverside Co. Riverside, UCR Quarantine Lab. 27.ii.2019, N. Power, from colony on bagrada bug, *Bagrada hilaris* (Burmeister). Of Pakistan origin via USDA-ARS Lab., Stoneville, Mississippi, USA. Received 3.xii.2015, S&R # N-15–30 *Ooencyrtus* sp., females, ca. F44”; 2. “Mounted by V. V. Berezovskiy 2018 in Canada balsam”; 3. [red] “*Ooencyrtus mirus* Triapitsyn & Power Holotype ♀”; 4. “Det. by S. V. Triapitsyn 2018”; 5. [barcode database label/unique identifier] “UCRC [bold] UCRC ENT 311772”. The holotype (Figs 7B, D, E, 8A) is in good condition, complete, dissected under 4 coverslips.

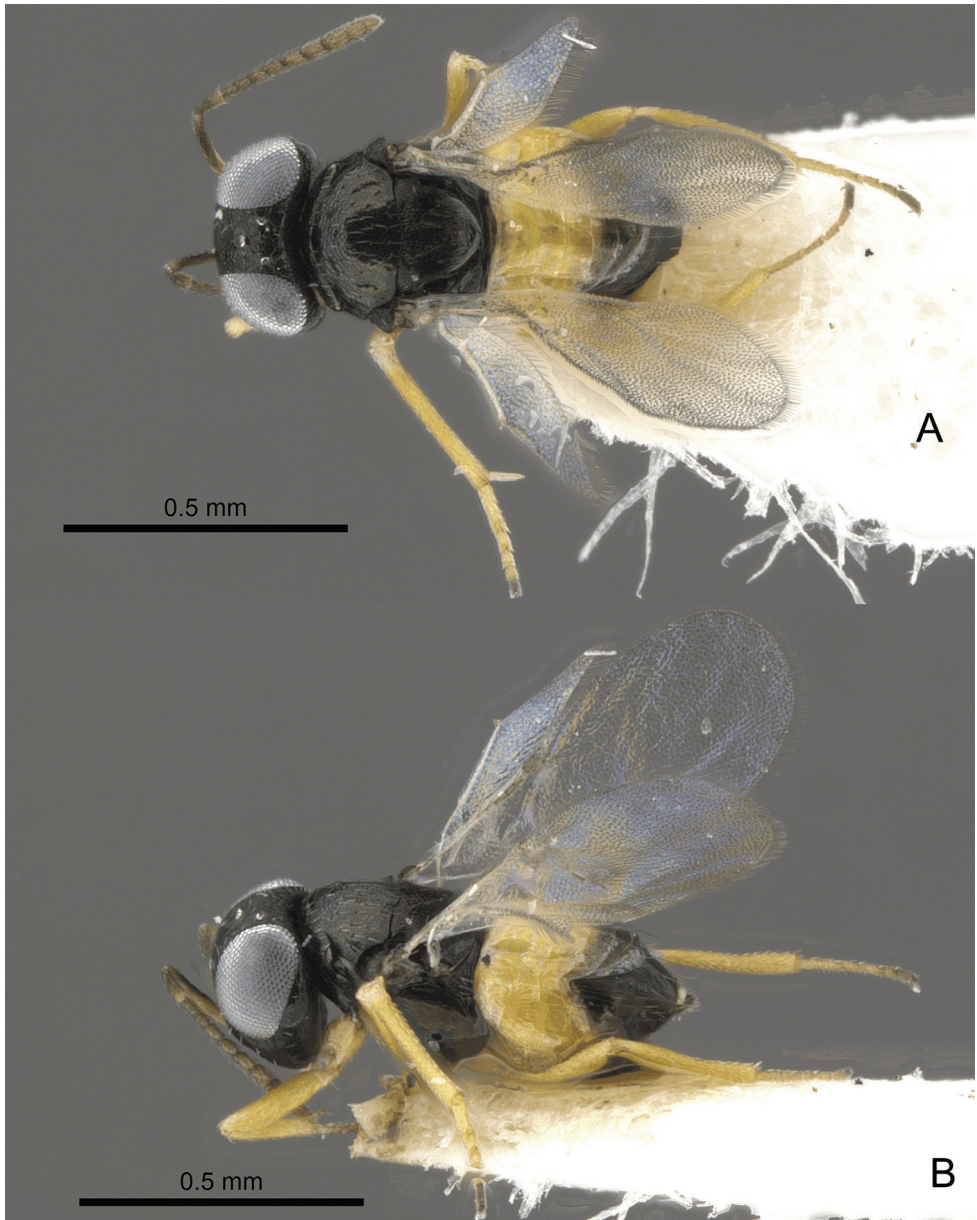


Figure 6. *Ooencyrtus mirus* sp. nov. female (paratype) **A** habitus in dorsal view **B** habitus in lateral view.

Paratypes. USA: California, Riverside Co., Riverside, UCR Quarantine laboratory, N. Power, from colony on *Bagrada hilaris* of Pakistan origin (via USDA ARS laboratory, Stoneville, Mississippi, USA), received 3.xii.2015, S&R # N-15-30: 3.ii.2017 [6 females on points and 2 females on slides, UCRC]; 13.ii.2017 [1 male on point and 2 males on slides, UCRC] (obtained by rearing females with a small dose of antibiotic at 30 °C); 8.iii.2017 [3 females, 7 males on points, UCRC]; 1–7.ii.2019, F. Ganjisaffar [3 females in 95% ethanol in the freezer (molecular vouchers UCRC_ENT 00506189–

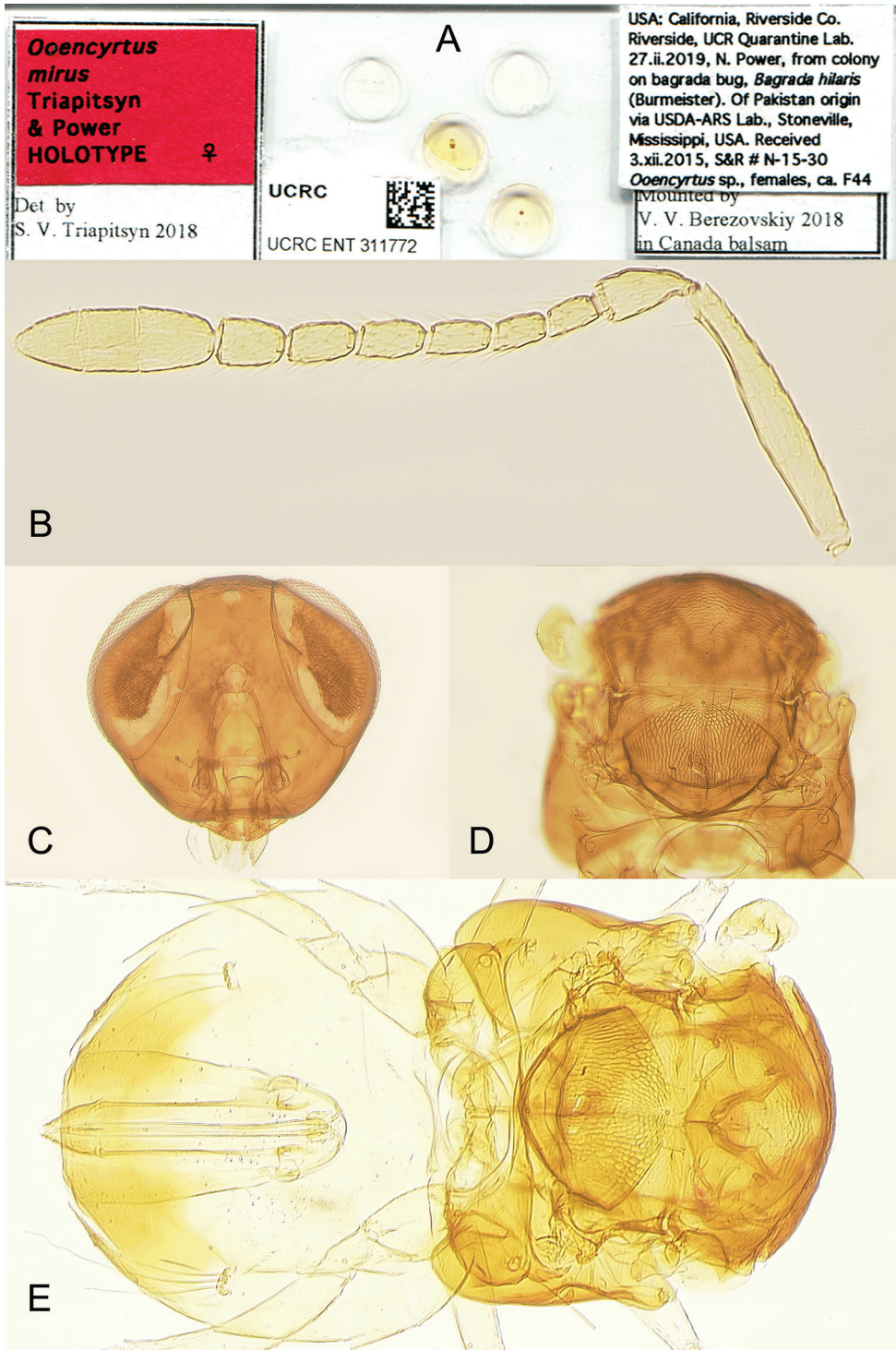


Figure 7. *Ooencyrtus mirus* sp. nov. female **A** holotype slide **B** antenna (holotype) **C** head in frontal view (paratype) **D** mesosoma (holotype) **E** mesosoma and metasoma (holotype).

00506191), UCRC]; 27.ii.2019, ca. F44 [30 females (2 in BMNH, 2 in EMEC, 22 in UCRC, 2 in USNM, 2 in ZIN), 18 males on points (2 in BMNH, 2 in EMEC, 10 in UCRC, 2 in USNM, 2 in ZIN) and 7 females, 2 males on slides, UCRC] (males obtained by rearing females at 36 °C).

Diagnosis. This new species is close to a small group of species of *Ooencyrtus* which are similar to *O. telenomicida* (Vassiliev), as defined by Hayat et al. (2014), although its female legs are entirely yellow. *Ooencyrtus mirus* keys to *O. telenomicida* in Ferrière and Voegelé (1961), Trjapitzin (1989), Huang and Noyes (1994), Zhang et al. (2005), Hayat and Mehrnejad (2016), and Samra et al. (2018). Morphologically, females of *O. mirus* differ from those of *O. telenomicida* mainly in having at least the proximal half of the gaster yellow, with only the apex (from the cercal plates) being brown to dark brown (Figs 6, 7E). In *O. telenomicida*, the yellow or light brown is present as a narrow, transverse basal band (Figs 10A, C, 12A, B, 13C), and this band is practically never extending to the cercal plates. Otherwise, females of these two species are quite similar although there are some differences in the lengths of their funicular segments (Table 3). In the multivariate ratio analysis *O. mirus* is well separated from *O. telenomicida* using the shape PCA (Fig. 16B). However, the scatterplot of isosize against the first shape PC (Fig. 16A) shows that *O. mirus* is also slightly smaller than *O. telenomicida*. This plot thus shows a certain amount of allometric variation and part of the separation is probably based on size rather than shape, and this might be a case of allometric scaling rather than true separation. The next two analyses indicated the same aspect. The PCA ratio spectrum for PC1 (Fig. 16C) identified as most relevant the ratio between propodeum length and scape width (variables lying at the opposite ends of the spectrum are the most relevant), while at the same time this is also the most allometric ratio as shown by the allometry ratio spectrum (Fig. 16D).

The LDA ratio extractor, which is a tool for identifying the best ratios for separating two groups, found that the best ratio to separate the two species is scape width / F5 length, the ratios being almost non-overlapping (Table 8).

Because the commonly used morphometric parameters and ratios of *O. telenomicida* and *O. mirus* are so similar, the importance of their clear separation based on the presented genetic data can not be overestimated.

Table 3. Morphometric ratios and measurements (µm) of *Ooencyrtus mirus* female morphological characters. All measurements are from slide-mounted specimens.

| | Length ovipositor: length mesotibia | Length: width fore wing | Length: width hind wing | Length: width scape | Length: width clava | Length F1: length pedicel | Length F2: length F1 |
|-------|-------------------------------------|-------------------------|-------------------------|---------------------|---------------------|---------------------------|----------------------|
| Range | 0.92–1.02 | 2.28–2.48 | 4.52–4.97 | 5.64–6.89 | 3.00–3.71 | 0.48–0.60 | 0.91–1.08 |
| Mean | 0.95 | 2.36 | 4.75 | 6.33 | 3.30 | 0.54 | 1.00 |
| n | 10 | 10 | 10 | 10 | 10 | 10 | 10 |
| | Length F1 | Length F2 | Length F3 | Length F4 | Length F5 | Length F6 | |
| Range | 28–40 | 28–40 | 34–46 | 39–51 | 40–49 | 40–50 | |
| Mean | 35 | 35 | 41 | 45 | 45 | 45 | |
| n | 10 | 10 | 10 | 10 | 10 | 10 | |

In Hayat et al. (2017), the female of *O. mirus* keys to *O. utuna* Hayat & Zeya from southern India (Karnataka and Tamil Nadu), but the latter has a linea calva closed posteriorly by 1–2 lines of setae (the linea calva is open posteriorly in *O. mirus*).

Description. Female (holotype and paratypes). **Body length** of dry-mounted, critical point-dried paratypes 595–1025 μm .

Color. Head and mesosoma (Fig. 6) mostly black with some metallic reflections, particularly on mesosoma, except mesopleuron with a strong violet luster; most of gaster yellow except brown to dark brown apically (from cercal plates); antenna brown; legs yellow.

Sculpture. Head with faint cell-like sculpture; mesoscutum reticulate, more so anteriorly; axilla reticulate; scutellum more strongly reticulate than mesoscutum or axilla (except sometimes almost smooth at apex), remainder of body more or less smooth.

Pubescence. Frontovortex, pronotum, mesoscutum, axilla, and scutellum with short, inconspicuous, not very dark setae except scutellum with a few pairs of long, dark setae.

Head (Fig. 7C) about $1.1\times$ as wide as high. Minimum width of frontovortex $0.26\text{--}0.28\times$ head width. Toruli just below level of lower eye margin. Ocelli in an obtuse triangle. Maxillary palpus 4-segmented, labial palpus 3-segmented. Mandible with 1 larger tooth, 1 very small, inconspicuous tooth and a broad truncation.

Antenna (Fig. 7B) with radicle about $2.8\times$ as long as wide, rest of scape slender, a little wider in the middle and narrowing towards apex, $5.6\text{--}6.9\times$ ($6.3\times$ in the holotype) as long as wide; pedicel about $2.0\times$ as long as wide, longer than any funicular segment (F1 $0.5\text{--}0.6\times$ length of pedicel, Table 3); funicle segments all longer than wide, F1 usually about as long as F2 and slightly shorter than following funicular segments (F2 $0.9\text{--}1.1\times$ length of F1, Table 3), F3–F6 subequal in length although F3 usually slightly shorter than following funicular segments (Table 3), F1–F2 without mps, F3–F4 each with 1 mps, F5–F6 each with 2 mps; clava 3-segmented, $3.0\text{--}3.7\times$ ($3.1\times$ in the holotype) as long as wide and almost as long as combined length of F4–F6, each claval segment with several mps.

Mesosoma (Fig. 7D, E). Mesoscutum about $2.8\times$ as wide as long; scutellum wider than long and a little shorter than mesoscutum, placoid sensilla close to each other and closer to posterior margin of scutellum. Propodeum smooth and very narrow medially, less than $0.1\times$ as long as scutellum.

Wings (Fig. 8A) not abbreviated, fore wing extending well beyond apex of gaster. Fore wing $2.3\text{--}2.5\times$ as long as wide ($2.3\times$ in the holotype), disc hyaline; costal cell about $12\times$ as long as wide; marginal vein punctiform; postmarginal vein shorter than stigmal vein; linea calva open posteriorly; filum spinosum usually with 3 setae, sometimes with 4 or, rarely, with 2 setae; longest marginal seta about $0.1\times$ maximum wing width. Hind wing $4.5\text{--}6.7\times$ as long as wide ($4.65\times$ in the holotype), disc hyaline.

Legs. Mesotibial spur about as long as mesobasitarsus.

Gaster (Fig. 7E) a little longer than mesosoma. Ovipositor occupying $0.6\text{--}0.7$ length of gaster, at most barely exerted beyond its apex, and $0.9\text{--}1.0\times$ ($0.9\times$ in the holotype) as long as mesotibia.

Measurements (μm) of the holotype. Mesosoma 400; gaster 431; ovipositor 321; mesotibia 351. Antenna: radicle 43; rest of scape 194; pedicel 68; F1 37; F2 40; F3 46;

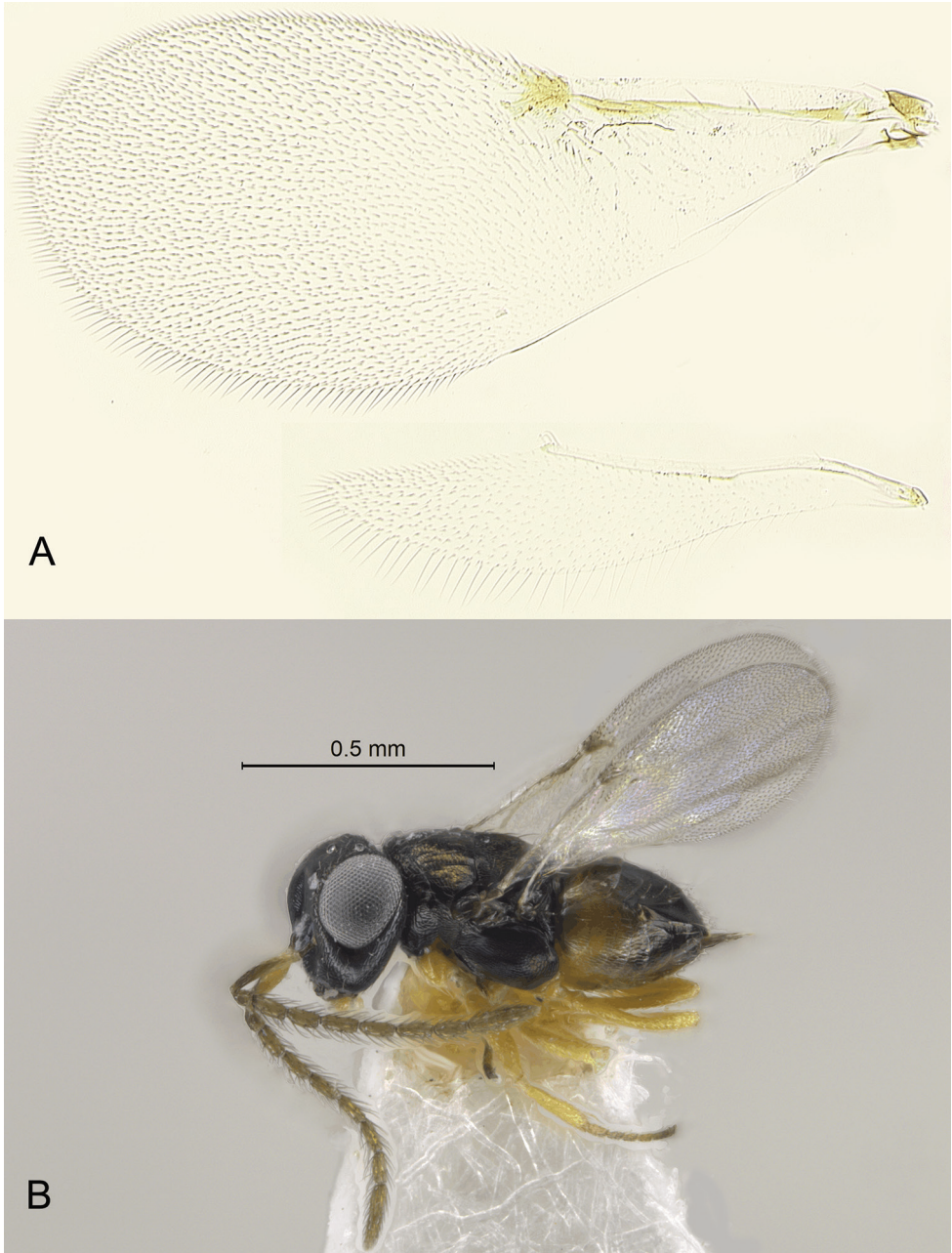


Figure 8. *Ooencyrtus mirus* sp. nov. **A** female fore and hind wings (holotype) **B** male habitus in lateral view (paratype).

F4 49; F5 48; F6 46; clava 135. Fore wing 839:369; longest marginal seta 36. Hind wing 601:129; longest marginal seta 51.

Male (paratypes). **Body length** of dry-mounted, critical point-dried paratypes 660–890 μm , and of slide-mounted paratypes 950–960 μm . **Head** and **mesosoma** black with

metallic reflections (Fig. 8B), *gaster* mostly dark brown to black except yellow to light brown or brown basally; antenna brown except scape light brown ventrally and often dark brown dorsally; legs yellow. *Antenna* (Fig. 9A) with scape minus short radicle 3.4–3.8× as long as wide (Table 4); funicle segments all longer than wide, more or less subequal in length and each with several mps; clava entire, 3.6–3.8× as long as wide, with several mps; flagellar segments all with numerous long setae. Fore *wing* (Fig. 9B) 2.2–2.4× as long as wide; hind wing 4.6–4.8× as long as wide. *Genitalia* (Fig. 9C) length 171–191 μm .

Variation (female and male body length, non-type specimens from the colony in UCR quarantine laboratory). The female body lengths, male body lengths, and paired differences, analyzed by the Shapiro-Wilks normality test in R (R Core Team 2018), all had normal distributions. The mean lengths were 849 μm for the females and 795 μm for the males, with a mean difference of 54 μm . A paired t-test in R showed that the males were significantly shorter in length than the females ($P < 0.001$).

Etymology. The name is an adjective meaning “remarkable” or “amazing.” The name is given to this species because the authors find its biology to be quite remarkable.

Distribution. Oriental region: Pakistan. The population in the quarantine laboratory in UC Riverside that served for the description of this species originated from the Toba Tek Singh District, Punjab, Pakistan.

Hosts. Pentatomidae: *Bagrada hilaris* (Burmeister). We conducted host studies on *O. mirus* and found it to reproduce on the eggs of eight other species in Pentatomidae, one species in Rhopalidae, and one species in Coreidae (Hemiptera), as well as on one species in Noctuidae (Lepidoptera). Of all the potential host species we evaluated, only one, in Pyralidae (Lepidoptera), was not utilized as a host, likely because its eggs were too small. These findings show *O. mirus* to be a generalist parasitoid, although it prefers and reproduces more successfully on *B. hilaris* than on the other hosts evaluated.

Biology. *Ooencyrtus mirus*, a uniparental species, typically produces about 99% females. However, the percentage of males can be increased by providing new eggs to the same female wasps daily for more than two weeks. This depletes the supply of *Wolbachia* bacteria in the ovaries (Lindsey and Stouthamer 2017), and the eggs, all unfertilized, then produce males instead of females.

Comments. This species was initially identified from digital images of both dry- and slide-mounted specimens as *Ooencyrtus telenomicida sensu lato* (J. S. Noyes and E. Guerrieri, personal communications). This determination was ambiguous, however, since *O. telenomicida* was not clearly defined prior to this communication, despite the availability of its numerous diagnoses and redescriptions (e.g., Ferrière and Voegelé 1961; Huang and Noyes 1994; Hayat and Mehrnejad 2016). Thus, until a neotype of *O. telenomicida* was properly designated, and respective DNA sequences were ob-

Table 4. Morphometric ratios and measurements (μm) of *Ooencyrtus mirus* male morphological characters. All measurements are from slide-mounted specimens.

| | Length body | Length genitalia | Length: width fore wing | Length: width scape |
|-------|-------------|------------------|-------------------------|---------------------|
| Range | 947–959 | 172–191 | 2.2–2.4 | 3.4–3.8 |
| Mean | 953 | 181 | 2.3 | 3.6 |
| n | 2 | 4 | 4 | 3 |

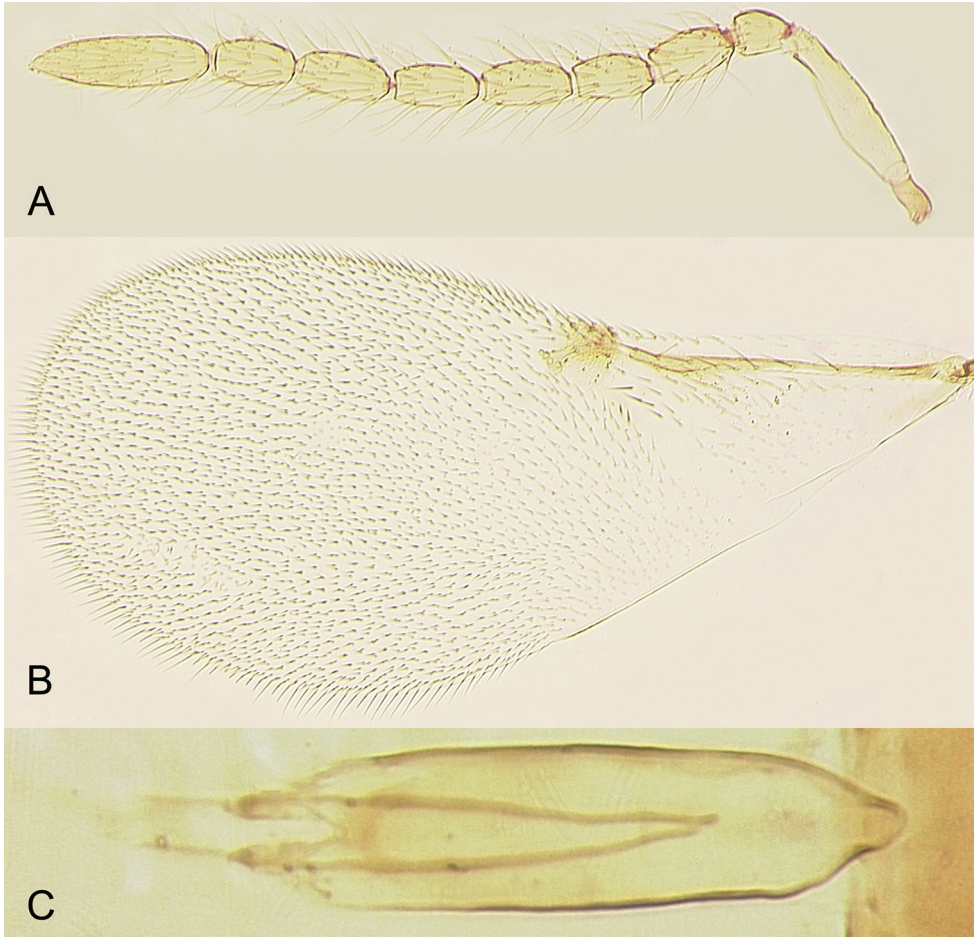


Figure 9. *Ooencyrtus mirus* sp. nov. male (paratypes) **A** antenna **B** fore wing **C** genitalia.

tained, *O. telenomicida* was not defined. We emphasize the importance of obtaining DNA sequences from the neotype since the only specimen defining this species is morphologically very similar to other species in the complex. Samra et al. (2018) provided a diagnosis and DNA sequences for “*O. telenomicida*” reared from Lepidoptera, rather than Pentatomidae, eggs collected in Israel and Turkey, countries with a different climate from that in the type locality. Thus, their conspecificity with *O. telenomicida* from Eastern Europe, reared from eggs of *Eurygaster integriceps*, needed confirmation.

***Ooencyrtus telenomicida* (Vassiliev, 1904)**

Figs 10–15

Encyrtus telenomicida Vassiliev, 1904: 117–108. Original type locality: Kupiansk, Kharkov oblast', Ukraine (as “Kupjansk”, “Gouvern. Charkov” [then Kharkov Govern-

rate of the Russian Empire]). Unspecified number of syntype females and males [type depository not indicated in the original description], lost (not examined).

Schedius flavofasciatus García Mercet, 1921: 315–318. Type locality (of the lectotype designated by Noyes 1981: 182, not examined): Cercedilla, Madrid, Spain. Synonymy by Ferrière and Voegelé 1961: 32.

Ooencyrtus telenomicida (Vassiliev): Romanova 1953: 239–247 (host associations and biology); Ferrière and Voegelé 1961: 28 (key), 30 (illustrations), 32–35 (illustrations, redescription, distribution); Noyes 1978: 11–12 (illustration, comparison with *O. brunneipes* Noyes); Trjapitzin 1989: 202–203 (key, distribution, hosts); Huang and Noyes 1994: 78–79 (diagnosis, hosts, distribution), 130 (illustrations); Hayat and Mehrnejad 2016: 200 (key), 207–209 (redescription, illustrations, hosts); Samra et al. 2018: 8 (key), 12–14 (illustrations, diagnosis, hosts, distribution).

Type material. Neotype female [BMNH], here designated (see “Comments” below for the justification) to stabilize the usage of the name, on slide (Fig. 11A) labeled: 1. “ROMANIA: Iași County, Ipatele 46.918781N, 27.442949E 317 m, 10.vi.2017, L. Fusu, O. A. Popovici, V. Chinan From eggs of *Eurygaster* sp. On wheat, egg mass # 32”; 2. [salmon] “DNA Voucher D # 6875 UCR, J. M. Heraty [Laboratory]”; 3. “Mounted by V. V. Berezovskiy 2019 in Canada balsam”; 4. [red] “*Ooencyrtus telenomicida* Vassiliev, 1904 Neotype ♀ = *Ooencyrtus telenomicida* (Vassiliev)”; 5. “Det. by S. V. Triapitsyn 2019”; 6. [barcode database label] “UCRC ENT 311776”. The neotype (Figs 10A, C, 11B–F) is in good condition although lacking apex of one hind wing, dissected under 2 coverslips.

Material examined. ROMANIA, Iași County, Ipatele, 46.918781N, 27.442949E, 317 m, 10.vi.2017, L. Fusu, O. A. Popovici, V. Chinan (from eggs of *Eurygaster* sp. on wheat) [3 females, two from egg mass # 22, one from # 32, BMNH, UCRC, including one from egg mass # 22 as DNA voucher D # 6874 (UCRC ENT 311775); 2 females from egg mass # 22 as DNA vouchers OoIs0101 and OoIs0102, AICF; 1 female and 1 male from egg mass # 32 as DNA vouchers OoIs0201 and OoIs0202, AICF]. RUSSIA: Krasnodarskiy kray, Slavyansk-na-Kubani (as [stanitsa] “Slavyanskaya” on the original label), Karpova, 1950 (from eggs of *Eurygaster integriceps*; air dried specimens remounted in UCRC on points and slides from a small vial) [9 females, 5 males, UCRC, ZIN] Orenburgskaya oblast’, Orsk, 5.vii.1935, G. Ya. Bey-Bienko (on *Elytrigia* sp.) [1 female, ZIN]. Stavropol’skiy kray: Karpova, Kamenkova 1950 (from eggs of *Eurygaster integriceps*; air dried specimens remounted in UCRC on points and slides from a small vial) [numerous females and males, AICF, UCRC, ZIN]. SPAIN, Madrid: Casa de Campo [park], 15–23.x.1978, J. S. Noyes [1 female, 2 males, UCRC] (determined by J. S. Noyes in 1979); Fuencarral-El Pardo, El Pardo, R. García Mercet [1 female, UCRC] (identified by R. García Mercet as *Schedius flavofasciatus* García Mercet). UKRAINE, Nikolaevskaya oblast’, 2.vi.1948 (from eggs of *E. integriceps*) [5 females, ZIN]. Taxonomic identifications of *O. telenomicida* from Russia and Ukraine were made by M. N. Nikol’skaya and/or V. A. Trjapitzin.

Description of the neotype female. *Color.* *Body* (Fig. 10A) mostly very dark brown with some metallic reflections (mainly dark bluish and some greenish) on fron-

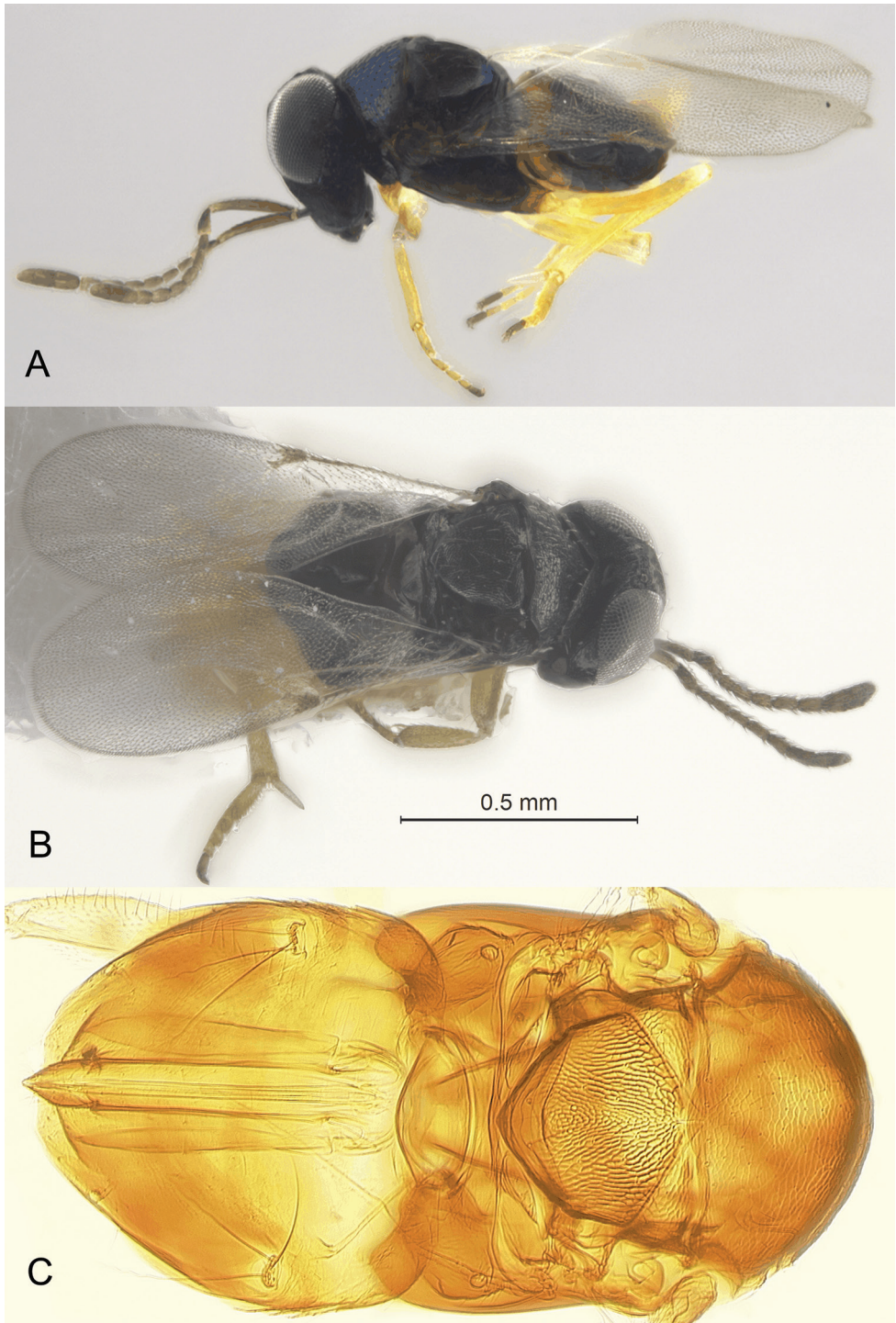


Figure 10. *Ooencyrtus telenomicida* female (from Romania) **A** habitus in lateral view (neotype, prior to DNA extraction) **B** habitus in dorsal view (non-type) **C** mesosoma and metasoma (neotype).

tovertex, mesoscutum, and scutellum except tegula brown and base of gaster with a narrow, light brown band on the first gastral tergite; antenna brown except radicle dark brown; legs mostly yellow except meso- and metacoxa brown basally and tarsi partially light brown.

Sculpture. Head with stronger sculpture on frontovertex; mesoscutum and axilla reticulate; scutellum (Fig. 11D) more strongly reticulate but almost smooth at apex.

Pubescence. Frontovertex, pronotum, mesoscutum, axilla, and scutellum with short, inconspicuous, fine, light setae except scutellum with a pair of longer, dark setae.

Head (Fig. 11C) about 1.1× as wide as high. Minimum width of frontovertex 0.25× head width. Toruli just below level of lower eye margin. Ocelli in slightly obtuse triangle, distance from posterior ocellus to eye margin about equal to ocellus diameter. Maxillary palpus 4-segmented, labial palpus 3-segmented. Mandible with 1 larger tooth, 1 smaller tooth and broad truncation.

Antenna (Fig. 11B) with radicle 2.5× as long as wide, rest of scape slender, slightly wider in the middle and narrowing towards apex, 6.3× as long as wide; pedicel 2.0× as long as wide, longer than any funicular segment (F1 0.6× length of pedicel); funicle segments all longer than wide, F1 as long as F2 and slightly shorter than following funicular segments, F3, F4 and F6 about equal in length, and F5 the longest funicular segment, F1–F2 without mps, F3–F4 each with 2 mps, F5–F6 each with 3 mps; clava 3-segmented, 3.0× as long as wide and almost as long as combined length of F4–F6, each claval segment with several mps.

Mesosoma (Fig. 10C). Mesoscutum about 2.3× as wide as long; scutellum (Fig. 11D) slightly wider than long and a little longer than mesoscutum, placoid sensilla close to each other and closer to posterior margin of scutellum. Propodeum (Fig. 11D) smooth and very narrow medially, less than 0.1× as long as scutellum.

Wings not abbreviated, fore wing extending well beyond apex of gaster. Fore wing (Fig. 11E) 2.4× as long as wide, its disc hyaline; costal cell about 11× as long as wide; marginal vein punctiform; postmarginal vein a little shorter than stigmal vein; lineal calva almost closed posteriorly by a row of short, inconspicuous setae; filum spinosum with 3 setae on one wing and 5 on the other; longest marginal seta 0.09× maximum wing width. Hind wing 5.4× as long as wide, disc hyaline.

Legs. Mesotibial spur almost as long as mesobasitarsus (Fig. 11F).

Gaster (Fig. 10C) almost as long as mesosoma. Ovipositor occupying more than 0.9 length of gaster, not exerted beyond its apex, and almost 1.0× as long as mesotibia.

Measurements (µm) of the neotype. Mesosoma 418; gaster 400; ovipositor 370; mesotibia 375. Antenna: radicle 45; rest of scape 200; pedicel 70; F1 40; F2 40; F3 50; F4 50; F5 60; F6 50; clava 140. Fore wing 900:370; longest marginal seta 33. Hind wing 725:135; longest marginal seta 48.

Taxonomic notes. Female. Variation (non-type specimens from Romania, Russia, and Ukraine). Body length of dry-mounted, air-dried specimens 860–925 µm. Body (Figs 10B, 12A, B, 14B) mostly very dark brown with some bluish and greenish metallic reflections on mesoscutum, except tegula and mesopleuron brown and base of gaster usually with a complete, narrow, yellowish or light brown band (dorsally almost

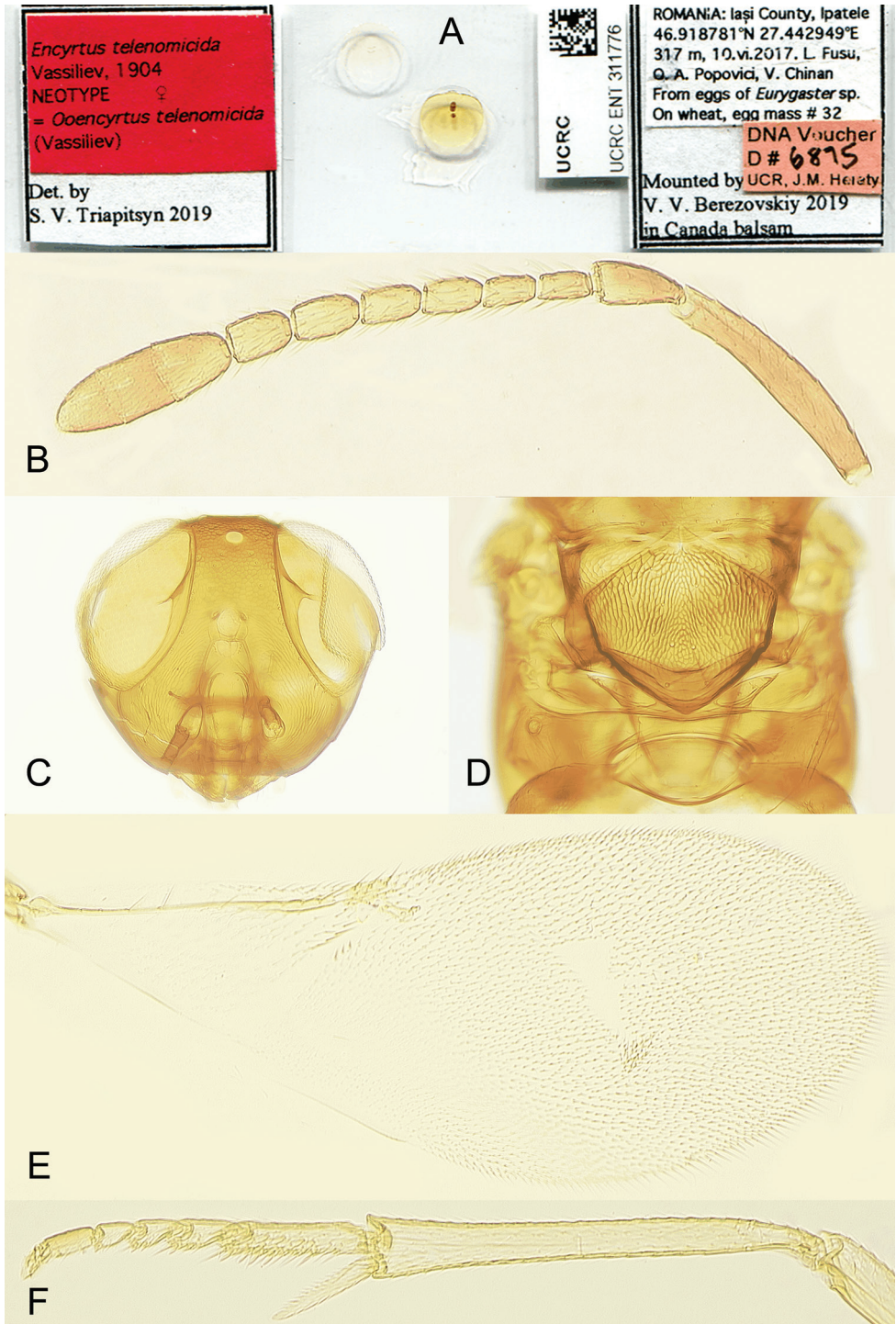


Figure 11. *Ooencyrtus telenomicida* female (neotype) **A** slide **B** antenna **C** head in frontal view **D** axillae, scutellum and propodeum **E** fore wing **F** mesotibia and mesotarsus.

always at most on the first and second gastral tergites, usually only on the first) and often brown (but never yellow) between the yellow basal band and cercal plates dorsally, but occasionally base of gaster entirely dark (Fig. 10B) or, very rarely (observed only in one specimen from Ukraine) the yellow band extends almost to cercal plates (in the absence of molecular data for this historical specimen, it cannot be excluded that it might belong to another species); antenna brown except apex of pedicel a little lighter (light brown); legs mostly yellow except meso- and metacoxa often brown basally, tarsi partially light brown. Minimum width of frontovertex 0.25–0.28× head width (Figs 13A, 14A). Antenna (Fig. 12C) with scape minus radicle 6.0–8.75× as long as wide; F1 the shortest funicular segment, 0.5–0.65× length of pedicel; F2 1.0–1.1× length of F1 (Tables 5, 7), F1–F2 without mps, F3–F6 each with at least 2 mps; clava 2.6–4.1× as long as wide. Fore wing (Fig. 13D) 2.2–2.7× as long as wide; filum spinosum with 3–5 setae. Hind wing 4.2–4.4× as long as wide, its disc hyaline. Ovipositor occupying 0.7–0.9 length of gaster (Fig. 13C), at most barely exerted beyond its apex, and 0.9–1.0× as long as mesotibia.

Male (non-type specimens from Russia). Body length of dry-mounted, air-dried specimens 600–900 µm. Body (Fig. 15A) black with metallic reflections, particularly on mesosoma; antenna brown except scape light brown ventrally and dark brown dorsally; legs yellow except most of coxae and metafemur brown. Antenna (Fig. 15B) with scape minus short radicle 3.6–3.7× as long as wide; funicle segments all longer than

Table 5. Morphometric ratios and measurements (µm) of morphological characters of female *Ooencyrtus telenomicida* from Russia and the Ukraine. All measurements are from slide-mounted specimens.

| | Length ovipositor: length mesotibia | Length: width fore wing | Length: width hind wing | Length: width scape | Length: width clava | Length F1: length pedicel | Length F2: Length F1 |
|-------|-------------------------------------|-------------------------|-------------------------|---------------------|---------------------|---------------------------|----------------------|
| Range | 0.89–1.02 | 2.22–2.71 | 4.13–5.20 | 6.19–8.75 | 2.56–4.09 | 0.47–0.65 | 1.00–1.17 |
| Mean | 0.94 | 2.43 | 4.6 | 7.2 | 3.4 | 0.55 | 1.09 |
| n | 12 | 9 | 10 | 10 | 10 | 10 | 10 |
| | Length F1 | Length F2 | Length F3 | Length F4 | Length F5 | Length F6 | |
| Range | 34–49 | 37–51 | 40–55 | 43–58 | 49–65 | 46–62 | |
| Mean | 39 | 43 | 50 | 52 | 55 | 52 | |
| n | 10 | 10 | 10 | 10 | 10 | 10 | |

Table 6. Morphometric ratios and measurements (µm) of morphological characters of male *Ooencyrtus telenomicida* from Russia. All measurements are from slide-mounted specimens.

| | Length body | Length genitalia | Length: width scape | | | |
|-------------|-------------|------------------|---------------------|-----------|-----------|-----------|
| Range/Value | 836 | 175 | 2.9–6.3 | | | |
| Mean | – | – | 4.6 | | | |
| n | 1 | 1 | 2 | | | |
| | Length F1 | Length F2 | Length F3 | Length F4 | Length F5 | Length F6 |
| Range/Value | 74 | 74–80 | 74 | 74 | 74–77 | 65 |
| Mean | 1 | 77 | 74 | 74 | 75 | 1 |
| n | – | 2 | 2 | 2 | 2 | – |

Table 7. Morphometric ratios and measurements of morphological characters of two female *Ooencyrtus telenomicida*, including the neotype, from Romania. All measurements are from slide-mounted specimens.

| | Body length | Length: ovipositor: length mesotibia | Length: width fore wing | Length: width scape | Length: width clava | Length F1: length pedicel | Length F2: length F1 |
|-------|-------------|--------------------------------------|-------------------------|---------------------|---------------------|---------------------------|----------------------|
| Range | 978 | 0.92–0.96 | 2.45–2.49 | 6.0–8.0 | 3.0–3.4 | 0.60–0.64 | 1.0 |
| Mean | – | 0.94 | 2.47 | 7.0 | 3.2 | 0.62 | 1.0 |
| n | 1 | 2 | 2 | 2 | 2 | 2 | 2 |
| | Length F1 | Length F2 | Length F3 | Length F4 | Length F5 | Length F6 | |
| Range | 43 | 43 | 49 | 49 | 52–55 | 49–54 | |
| Mean | 43 | 43 | 49 | 49 | 54 | 51 | |
| n | 2 | 2 | 2 | 2 | 2 | 2 | |

wide, more or less subequal in length (Table 6) and each with several mps; clava entire, 2.9–3.2× as long as wide, with several mps; flagellar segments all with numerous long setae. Fore wing (Fig. 15C) about 2.3× as long as wide; hind wing about 5.0× as long as wide. Genitalia (Fig. 13B) length 175–200 μm.

Distribution. Confirmed records of *O. telenomicida* are from Romania, Russia, Spain and Ukraine; those from other countries in the Palearctic and Oriental regions were summarized by Samra et al. (2018), but many of them will need to be verified using molecular methods.

Hosts. Scutelleridae (Hemiptera): *Eurygaster integriceps* Puton (Vassiliev 1904; Romanova 1953; Trjapitzin 1989), *Eurygaster* sp., as well as some Telenominae (Scelionidae) primary egg parasitoids of *E. integriceps*, such as *Telenomus* spp. and *Trissolcus* spp. (Vassiliev 1904; Romanova 1953), keeping in mind that their species identifications were likely incorrect. Samra et al. (2018) listed some other Heteroptera (Hemiptera) as hosts of *O. telenomicida*; however, identification of the parasitoids will need to be verified using molecular methods.

Biology. *Ooencyrtus telenomicida* is a facultative hyperparasitoid of *Eurygaster integriceps*, being either a primary egg parasitoid (more so earlier in the season when unparasitized eggs of the host are readily available and prevalent) or a secondary parasitoid via the telenomine primary egg parasitoids, particularly later in the season when many of the host eggs are parasitized (Romanova 1953).

Comments. According to V. A. Trjapitzin (personal communication), the entire type series of *O. telenomicida*, if such ever existed, has never been located and is certainly lost. The dire necessity of a proper recognition of this nominal species, which has been impossible with any confidence from some other members of the *O. telenomicida* species complex (e.g., according to Huang and Noyes (1994), from *O. gonoceri* Viggiani and *O. acastus* Trjapitzin), leaves no choice but to designate a neotype for *O. telenomicida*, complemented with the much needed DNA sequence data from it. That is done herein from the specimen reared from an egg of a species of *Eurygaster* Laporte,

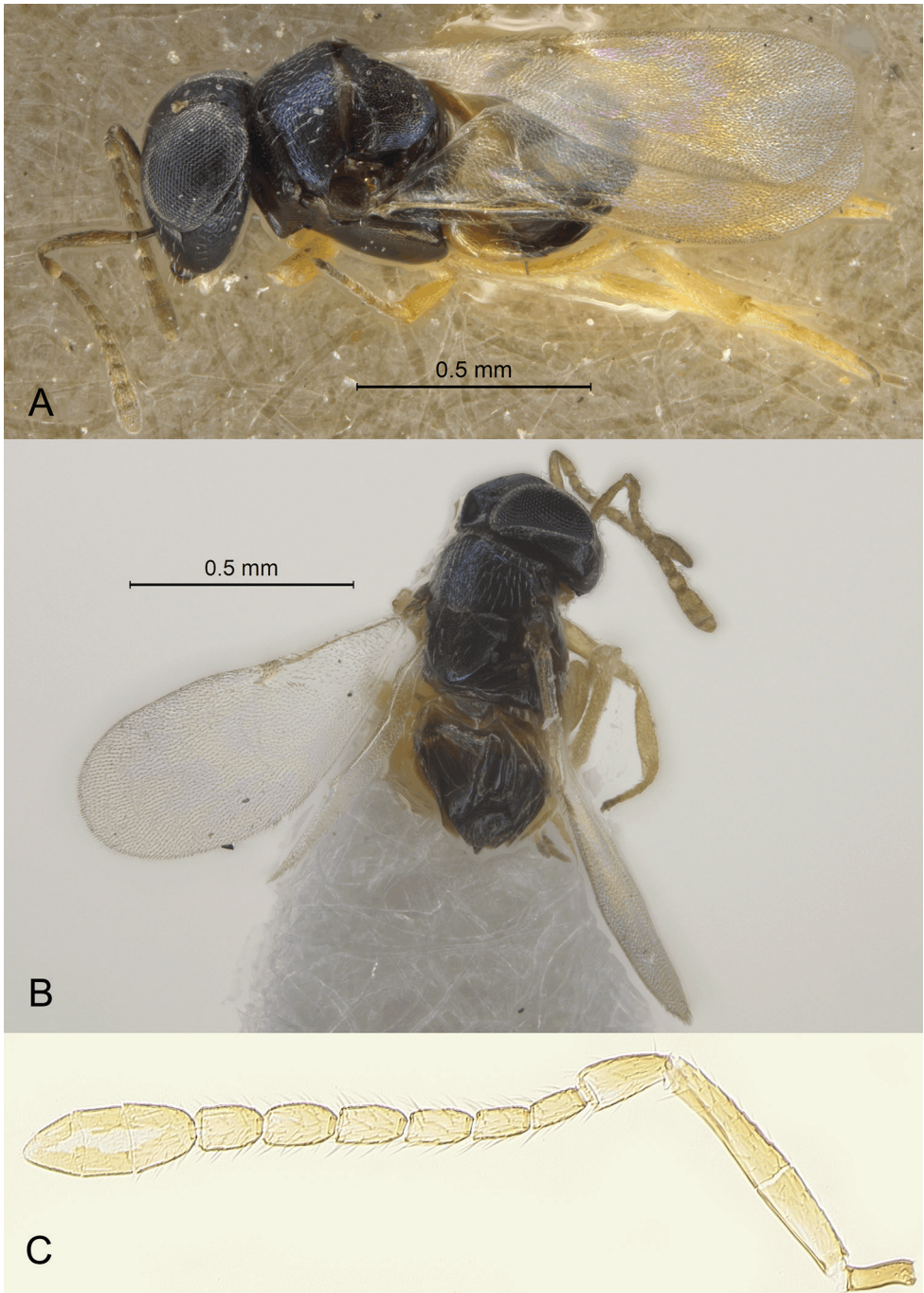


Figure 12. *Ooencyrtus telenomicida* female **A** habitus in lateral view (from Nikolaevskaya oblast', Ukraine) **B** habitus in dorsolateral view (from Krasnodarskiy kray, Russia) **C** antenna (from Stavropol'skiy kray, Russia).

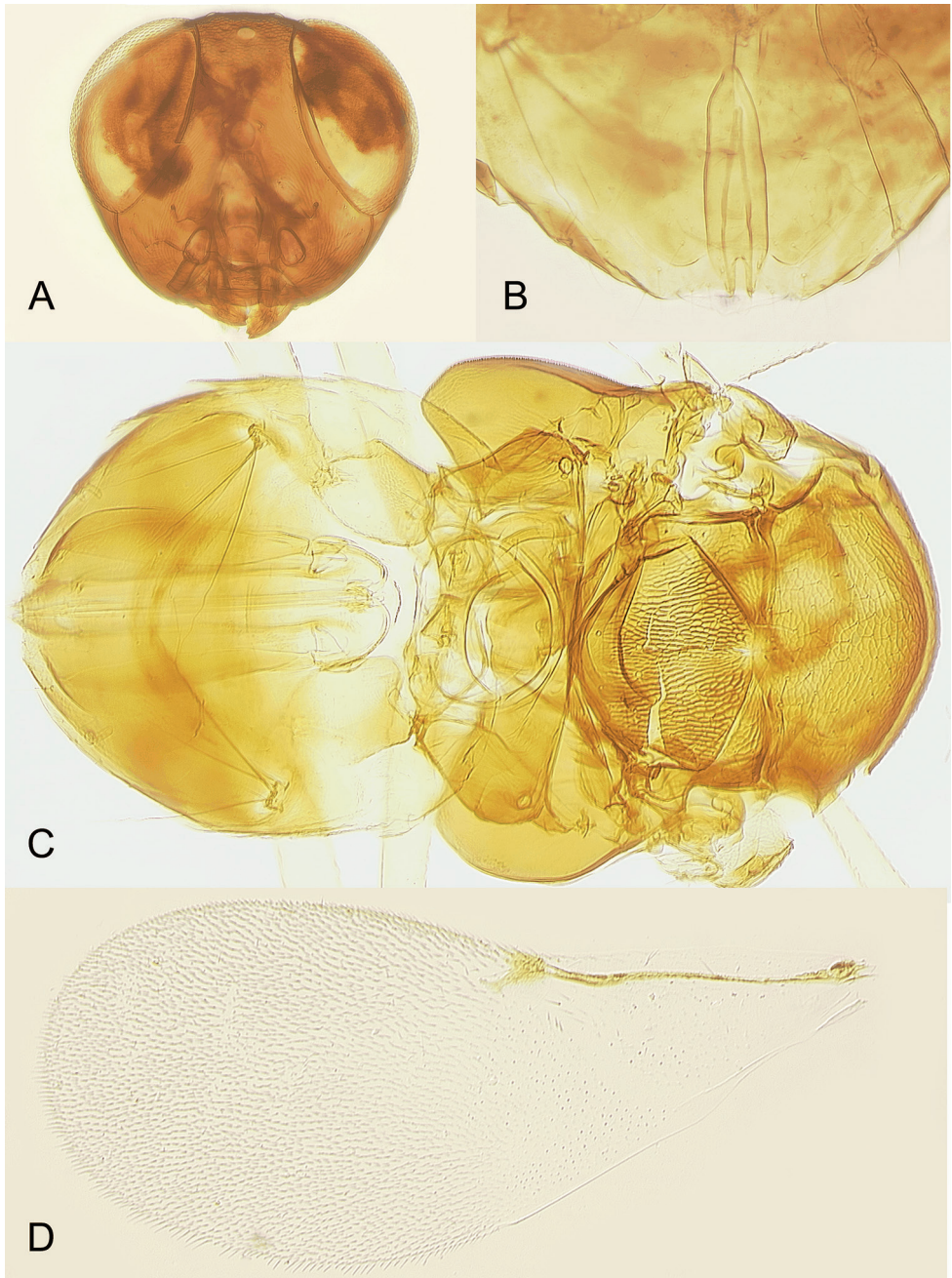


Figure 13. *Ooencyrtus telenomicida* (from Stavropol'skiy kray, Russia) **A** female head in frontal view **B** male genitalia **C** female mesosoma and metasoma **D** female fore wing.

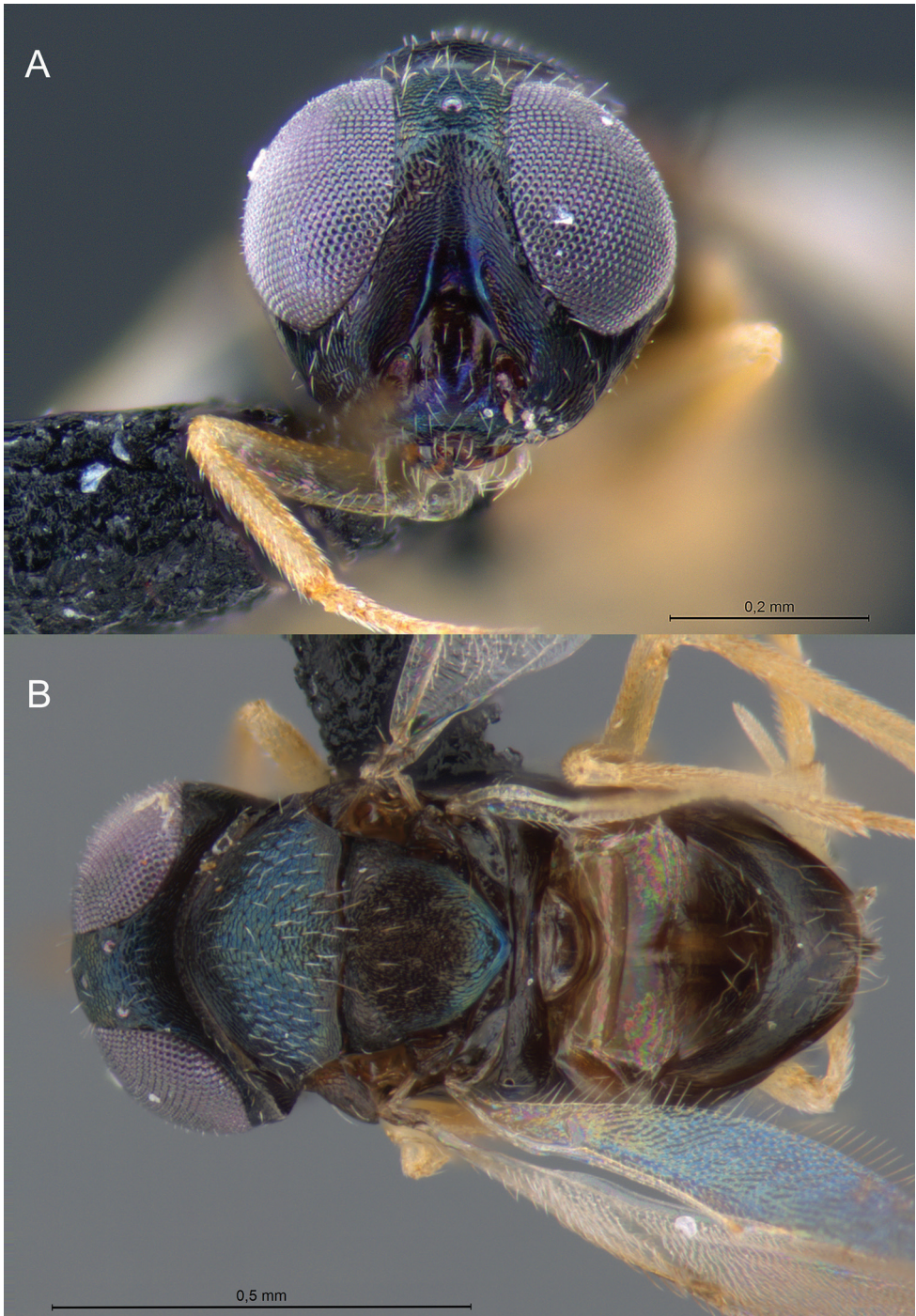


Figure 14. *Ooencyrtus telenomicida* female (from Romania, non-type) **A** head in frontal view **B** body in dorsal view.

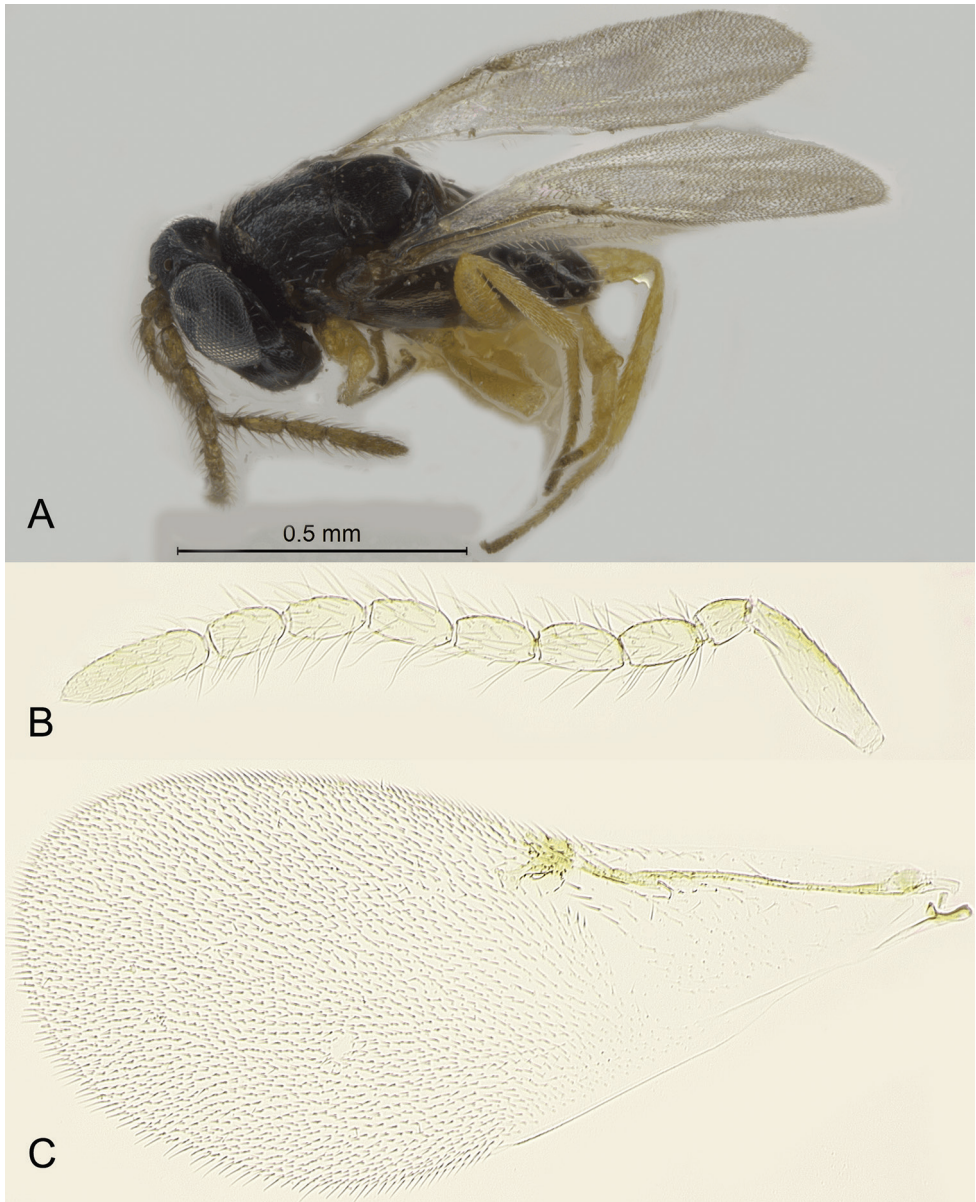


Figure 15. *Ooencyrtus telenomicida* male (from Stavropol'skiy kray, Russia) **A** habitus in lateral view **B** antenna **C** fore wing.

which is the genus from which the originally described *O. telenomicida* emerged. Furthermore, the insects were collected in northeastern Romania which is relatively close to the original collection site in Kharkov oblast' of Ukraine. Importantly, the collections were made in the same general habitat (sylvo-steppe biome) as the originally described species. Morphologically, female specimens from Romania (Figs 10, 11; Ta-

ble 7) are identical to those from Russia and Ukraine reared from eggs of *Eurygaster integriceps* in the late 1940s and early 1950s (Figs 12, 13A, C, D; Table 5). The neotype and especially a second specimen from the same collecting event ('topotype') grouped together with the specimens from Russia and Ukraine (Fig. 16A, B) in the shape PCA of the multivariate ratio analysis.

Based on this information, a genetic library of other members of the complex can be constructed, and their identity determined.

Molecular analyses

COI fragment sequences of *O. lucidus*, *O. mirus*, and *O. telenomicida* from Romania were trimmed for alignment and analysis with sequences of *O. telenomicida*, *O. pistaciae* Hayat & Mehmejad, *O. pityocampae* (García Mercet), *O. mevalbelus* Guerrieri & Samra, *O. zoeae* Guerrieri & Samra, and *O. kuvanae* (Howard) from Samra et al. (2018), to be able to provide continuity and to have comparable data. The four molecular vouchers of *O. lucidus* and those of *O. mirus* demonstrated no intraspecific sequence differences (Table 9). In contrast, the neotype and one non-type *O. telenomicida* specimens from Romania had 3.1% pairwise sequence differentiation (Table 9), indicating high intraspecific variation (these two specimens were obtained from two distinct egg masses found in close proximity). The standard barcode region, obtained from other three specimens but from the same two egg masses, confirms this genetic differentiation (4.4% p-distance). This genetic divergence is at a level that has been demonstrated for other *Ooencyrtus* species, e.g. *O. pistaciae* clades a and b at 4.4% (Samra et al. 2018). ITS2 sequences of *O. lucidus* and *O. mirus* also had no intraspecific differences among specimens. The ITS2 sequence of only one *O. telenomicida* specimen from Romania was obtained. Intraspecific variation could not be determined, although high variation in this region is not expected within the species.

COI alignment and p-distance calculations among the *Ooencyrtus* species revealed at least 5.9% and 7.3% genetic divergence in *O. mirus* and *O. lucidus*, respectively,

Table 8. First five best ratios found by the LDA ratio extractor for separating *O. mirus* sp. nov. and *O. telenomicida*. Standard distance indicates how well one ratio discriminates compared to another; δ indicates how well shape discriminates compared to size (values close to 0 indicate no influence of size and those close to 1 indicate separation based mainly on size). Ranges were calculated on all available measurements, not only on those from the complete dataset used in the analysis. The ratio marked with * has very little overlap.

| Ratio | Ranges | | Standard distance | δ |
|---------------------|------------------------|-----------------|-------------------|----------|
| | <i>O. telenomicida</i> | <i>O. mirus</i> | | |
| L.mesotibia/L.clava | 7.56–12.36 | 7.29–9.66 | 11.9 | 0.18 |
| W.scape/L.F5* | 0.44–0.63 | 0.61–0.74 | 11.73 | 0.18 |
| L.F4/L.scutel | 0.22–0.31 | 0.25–0.28 | 11.5 | 0.18 |
| W.clava/L.pedicel | 0.46–0.70 | 0.53–0.67 | 11.11 | 0.19 |
| L.F2/L.F3 | 0.75–0.92 | 0.78–1.00 | 10.7 | 0.19 |

Table 9. Uncorrected pairwise-distances between *Ooencyrtus lucidus* sp. nov., *O. mirus* sp. nov., *O. telenomicida*, and other congeneric species. Proportions were determined for a fragment of the mitochondrial cytochrome c oxidase I (COI) gene and the nuclear internal transcribed spacer 2 region (ITS2). Values to the left are the p-distances observed based on the COI gene region, while values to the right are p-distances observed based on the ITS2 region. Values on the diagonal element within the parentheses represent the intraspecific variation observed.

| | 1 | 2 | 3 |
|--|-----------------------|-----------------------|-----------------------|
| 1. <i>O. lucidus</i> | (0.000) / (0.000) | – | – |
| 2. <i>O. mirus</i> | 0.087 / 0.227 | (0.000) / (0.000) | – |
| 3. <i>O. telenomicida</i> Romanian | 0.096 – 0.104 / 0.216 | 0.067 – 0.074 / 0.072 | (0.031) / – |
| 4. <i>O. telenomicida</i> East Mediterranean | 0.080 – 0.086 / 0.224 | 0.060 – 0.070 / 0.077 | 0.056 – 0.076 / 0.062 |
| 5. <i>O. pistaciae</i> | 0.073 – 0.078 / 0.223 | 0.059 – 0.065 / 0.069 | 0.063 – 0.079 / 0.064 |
| 6. <i>O. pityocampae</i> | 0.082 – 0.085 / 0.226 | 0.062 – 0.066 / 0.144 | 0.073 – 0.079 / 0.134 |
| 7. <i>O. mevalbelus</i> | 0.091 – 0.094 / 0.205 | 0.070 – 0.074 / 0.091 | 0.075 – 0.093 / 0.075 |
| 8. <i>O. zoeae</i> | 0.078 – 0.084 / 0.202 | 0.062 – 0.066 / 0.096 | 0.074 – 0.087 / 0.083 |
| 9. <i>O. kuvanae</i> | 0.097 / 0.442 | 0.091 / 0.428 | 0.098 – 0.109 / 0.425 |

from *O. telenomicida* and other analyzed *Ooencyrtus* species (Table 9), indicating species level differentiation in both cases. Sequences of *O. mirus* were most similar to those of *O. pistaciae*, but the species is well differentiated with at least 5.9% difference. COI sequences of *O. lucidus* also were closest to *O. pistaciae*, but were divergent with a minimum of 7.3%. The Pakistani *O. mirus* was unequivocally supported as a distinct species from *O. telenomicida*, both from the Romanian neotype designated herein and the East Mediterranean populations studied by Samra et al. (2018). This is supported by 6.7–7.4% and 6.0–7.0% genetic divergence, respectively. *Ooencyrtus lucidus* had high genetic separation from all compared species.

Analysis of the ITS2 region further demonstrated genetic separation of these species. Intraspecific variation in this region is absent to extremely low, while interspecific variation is expected to be high. Our analysis was based on a partial fragment of the ITS2 region because the full sequence was not obtained for every specimen; however, the region analyzed was flanked by regions of congruence (16 bases at the 5' end and 22 bases at the 3' end; average 385 bp region analyzed for each species). The lowest p-distance between *O. mirus* and all compared species in this region was 0.069 (6.9% pairwise distance), which was demonstrated with *O. pistaciae* (Table 9). Sequence divergence for *O. lucidus* was extremely high with the lowest p-distance at 0.202.

Phylogenetic analysis of *Ooencyrtus* species, inferred using concatenated COI and ITS2 genetic regions, supported *O. mirus* as a sister taxon to *O. telenomicida* from Romania (Fig. 17). These two species formed a larger clade with the sister taxa *O. pistaciae* and East Mediterranean *O. telenomicida*, separated from *O. zoeae* and *O. mevalbelus*. Basal to this clade were *O. pityocampae* and *O. lucidus*; *O. kuvanae* was used to root the tree. Using concatenated COI and ITS2 sequences resulted in a phylogenetic tree with a topology that combined the two separate COI and ITS2 trees of Samra et al. (2018). East Mediterranean *Ooencyrtus telenomicida* and *O. pistaciae* branched in a clade separate from *O. zoeae* and *O. mevalbelus* as seen in both the COI and ITS2 phylogenetic

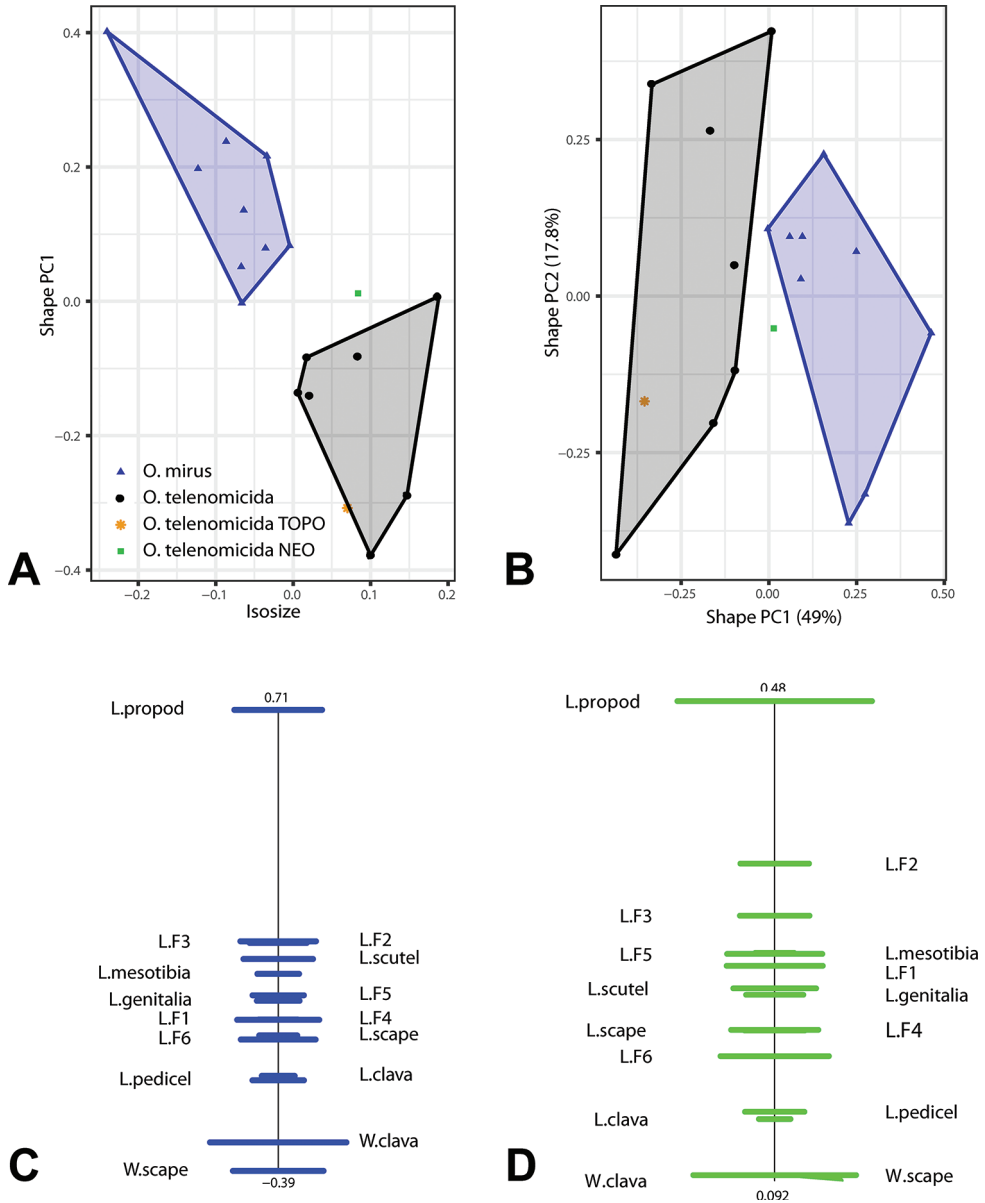


Figure 16. Multivariate ratio analysis for *Ooencyrtus mirus* sp. nov. and *O. telenomicida* **A** scatterplot of isosize against first shape PC **B** shape PCA, scatterplot of first against second shape PC **C** PCA ratio spectrum for PC1, bars represent 68% confidence intervals **D** allometry ratio spectrum; bars represent 68% confidence intervals.

trees, and *O. pityocampae* branched basally as in the ITS2 tree. As suspected, inferring the phylogenetic placement of *O. mirus* and the Romanian *O. telenomicida* (including the neotype) with these species resulted in a clade for the *O. telenomicida* species

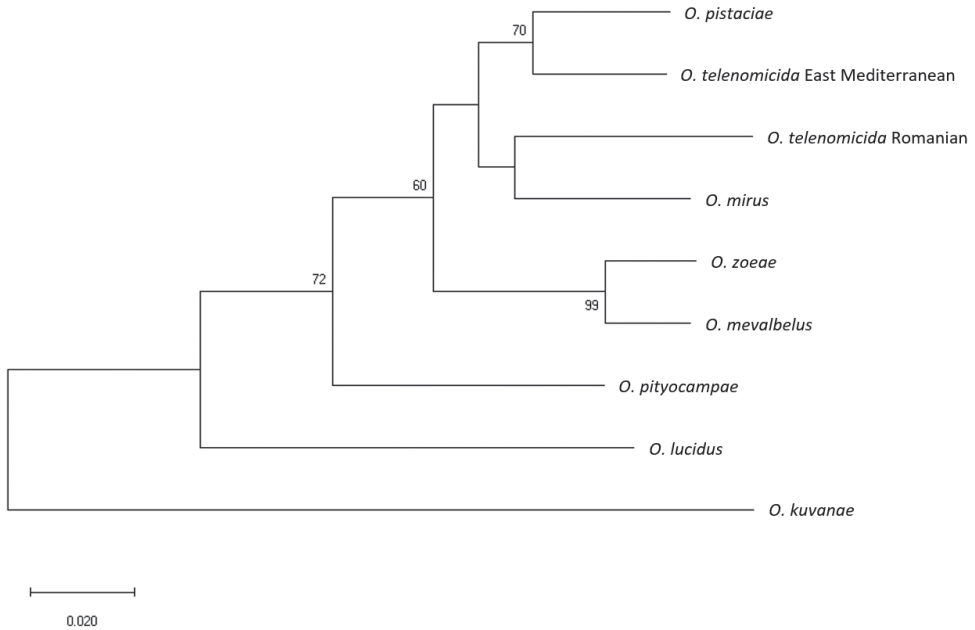


Figure 17. Relationship of *Ooencyrtus lucidus* sp. nov., *O. mirus* sp. nov., and *O. telenomicida* with other congeneric species based on concatenated partial regions of the mitochondrial cytochrome c oxidase I (COI) gene and the nuclear internal transcribed spacer 2 region (ITS2). Optimal maximum likelihood phylogenetic tree based on the Tamura-Nei model. The percentage of replicate trees in which the associated taxa clustered together in the bootstrap test (1000 replicates) are shown next to the branches (values over 50 are shown), and the tree is drawn to scale with branch lengths indicating uncorrected p-distance.

complex. Almost certain of New World origin and completely different from the *O. telenomicida* species complex morphologically, *O. lucidus*, with its high genetic divergence in both COI and ITS2 regions, branched separately. It is basal to all other species in the concatenated phylogenetic tree (as well as in our earlier analyses on single-gene COI and ITS2 trees; data not shown).

Conclusion

Members of the speciose genus *Ooencyrtus*, in which more than 300 currently valid species are known, are notoriously difficult to identify morphologically. That is particularly true for the taxa within the *O. telenomicida* species complex in the Old World. In the New World, identification keys exist only for some Neotropical species (Noyes 1985, 2010) but not for those in the Nearctic region. Moreover, many undescribed species have been recognized (e.g., Zuparko 2015, 2018), and misidentifications of *Ooencyrtus* species are quite common. Whereas molecular methods with both mitochondrial and nuclear gene regions often are necessary for providing reliable identifica-

tion or separation of morphologically similar species, using these methods for positive identifications is useful only if those taxa were correctly identified based on morphological studies of the type specimens and reared material from known hosts. Here we provide both morphological and genetic evidence that has helped to untangle the true identity of the common Old World parasitoid, *O. telenomicida*, and also of two primary egg parasitoids of the bagrada bug, one from California and the other from Pakistan.

Traditionally, the standard DNA barcode region of the COI gene described in Folmer et al. (1994) is analyzed to estimate intraspecific and interspecific difference when comparing metazoan invertebrate species. However, in order to compare our new species with recently described *Ooencyrtus* species, we sequenced the COI region analyzed by Samra et al. (2018). This region is 946-bp in length, whereas the Folmer region is 648-bp long, and these regions share approximately 400-bp overlap allowing comparison of a portion of the two regions. However, we also obtained the standard barcode sequence for three specimens of *O. telenomicida* in order to maximize compatibility with standard DNA barcodes libraries. We found well-supported genetic separation of the two new species described herein from all compared *Ooencyrtus* species in both the full Samra et al. (2018) proposed COI region and the overlapping Folmer region. ITS2 sequences reinforced *O. lucidus* and *O. mirus* as distinct species with high levels of genetic differentiation. Our COI and ITS2 sequence analyses supported and confirmed the morphological differences and morphometric separation observed for these new species. Interestingly, our analysis also demonstrated significant genetic divergence of the neotype of *O. telenomicida* from the likely misidentified *O. telenomicida* specimens previously sequenced. This observation emphasizes the fact that additional work remains to sort out and properly describe and re-describe the species of the *O. telenomicida* species complex, including proposing possible synonymies. That difficult and laborious task, however, is well beyond the scope of this study.

Acknowledgments

We are very grateful to John S. Noyes (BMNH) and Emilio Guerrieri (Istituto per la Protezione Sostenibile delle Piante, Consiglio Nazionale delle Ricerche, Portici, Naples, Italy) for help with the initial identification of *O. mirus* as a species very similar to *O. telenomicida* and valuable discussions. Hannes Baur (Natural History Museum of Bern, Switzerland) is thanked for his advice on using the multivariate ratio analysis. We also thank Ekaterina V. Tselikh (ZIN) for the loans of specimens of *Ooencyrtus telenomicida*, Vladimir A. Trjapitzin (Moscow, Russia) and Robert L. Zuparko (California Academy of Sciences, San Francisco, California, USA) for important information and advice, Vladimir V. Berezovskiy (UCRC) for skillful mounting of specimens, Michael W. Gates (USNM) for providing access to the collection under his care and the loan of material, as well as Natalie Dale-Skey Pappillod (BMNH), Roger A. Burks and Shayla Hampel (UCR) for kind assistance. Thoughtful comments and suggestions by the reviewers helped to improve the manuscript significantly. This research was supported, in

part, by California Department of Food and Agriculture Specialty Crops Block Grant SBC16053. We thank Charlie Pickett (California Department of Food and Agriculture, Sacramento) for his collaboration on this grant. The search for *O. telenomicida* in Romania was supported by the Romanian Executive Agency for Higher Education, Research, Development and Innovation Funding (UEFISCDI) through the project PN-III-P4-ID-PCE-2016-0233.

References

- Andreason SA, Triapitsyn SV, Mendel Z, Protasov A, Levi B, Perring TM (2019a) Expanding the *Anagyrus pseudococci* species complex (Hymenoptera: Encyrtidae): a new species emerges from *Trabutina serpentina* (Hemiptera: Pseudococcidae) on tamarisk on the Dead Sea shore. *Zoology in the Middle East* 65(4): 347–360. <https://doi.org/10.1080/09397140.2019.1648378>
- Andreason SA, Triapitsyn SV, Perring TM (2019b) Untangling the *Anagyrus pseudococci* species complex (Hymenoptera: Encyrtidae), parasitoids of worldwide importance for biological control of mealybugs (Hemiptera: Pseudococcidae): Genetic data corroborates separation of two new, previously misidentified species. *Biological Control* 129: 65–82. <https://doi.org/10.1016/j.biocontrol.2018.09.010>
- Arakelian G (2008) *Bagrada* bug (*Bagrada hilaris*). Los Angeles County Agricultural Commissioner/Weights and Measures Department, CA. http://www.cdfa.ca.gov/plant/PPD/PDF/Bagrada_hilaris.pdf
- Baur H, Kranz-Baltensperger Y, Cruaud A, Rasplus J-Y, Timokhov AV, Gokhman VE (2014) Morphometric analysis and taxonomic revision of *Anisopteromalus* Ruschka (Hymenoptera: Chalcidoidea: Pteromalidae)—an integrative approach. *Systematic Entomology* 39(4): 691–709. <https://doi.org/10.1111/syen.12081>
- Baur H, Leuenberger C (2011) Analysis of ratios in multivariate morphometry. *Systematic Biology* 60(6): 813–825. <https://doi.org/10.1093/sysbio/syr061>
- Bundy CS, Grasswitz TR, Sutherland C (2012) First report of the invasive stink bug *Bagrada hilaris* (Burmeister) (Heteroptera: Pentatomidae) from New Mexico, with notes on its biology. *Southwestern Entomologist* 37(3): 411–414. <https://doi.org/10.3958/059.037.0317>
- Bundy CS, Perring TM, Reed DA, Palumbo JC, Grasswitz TR, Jones WA (2018) *Bagrada hilaris*. In: McPherson J (Ed.) *Biology of Invasive Stink Bugs and Related Species*. CRC Press/Taylor and Francis Books, Boca Raton, 205–241. <https://doi.org/10.1201/9781315371221-3>
- Campbell BC, Steffen-Campbell JD, Werren JH (1994) Phylogeny of the *Nasonia* species complex (Hymenoptera: Pteromalidae) inferred from an internal transcribed spacer (ITS2) and 28S rDNA sequences. *Insect Molecular Biology* 2(4): 225–237. <https://doi.org/10.1111/j.1365-2583.1994.tb00142.x>
- Ferrière C, Voegelé J (1961) Les *Ooencyrtus* parasites des œufs des punaises des cereals au Maroc. *Cahiers de la Recherche Agronomique* 14: 27–36.
- Folmer O, Black M, Hoeh W, Lutz R, Vriienhoek R (1994) DNA primers for amplification of mitochondrial cytochrome C oxidase subunit 1 from diverse metazoan invertebrates. *Molecular Marine Biology and Biotechnology* 3: 294–299.

- Fusu L, Ribes A (2017) Description of the first Palaearctic species of *Tineobius* Ashmead with DNA data, a checklist of world species, and nomenclatural changes in Eupelmidae (Hymenoptera, Chalcidoidea). *European Journal of Taxonomy* 263: 1–19. <https://doi.org/10.5852/ejt.2017.263>
- Ganjisaffar F, Talamas EJ, Bon MC, Gonzalez L, Brown BV, Perring TM (2018) *Trissolcus hyalinipennis* Rajmohana & Narendran (Hymenoptera, Scelionidae), a parasitoid of *Bagrada hilaris* (Burmeister) (Hemiptera, Pentatomidae), emerges in North America. *Journal of Hymenoptera Research* 65: 111–130. <https://doi.org/10.3897/jhr.65.25620>
- García Mercet R (1921) Fauna Ibérica. Himenópteros fam. Encirtidos. Museo Nacional de Ciencias Naturales, Hipódromo, Madrid, 732 pp.
- Gibson GAP (1997) Chapter 2. Morphology and terminology. In: Gibson GAP, Huber JT, Woolley JB (Eds) *Annotated Keys to the Genera of Nearctic Chalcidoidea* (Hymenoptera). NRC Research Press, Ottawa, 16–44.
- Girault AA (1917) *Descriptions stellarum novarum*. Privately printed, 22 pp.
- Cruaud A, Nidelet S, Arnal P, Weber A, Fusu L, Gumovsky A, Huber J, Polaszek A, Rasplus J-Y (2019) Optimised DNA extraction and library preparation for minute arthropods: application to target enrichment in chalcid wasps used for biocontrol. *Molecular Ecology Resources* 19: 702–710. <https://doi.org/10.1111/1755-0998.13006>
- Hayat M, Ahmad Z, Khan FR (2014) Encyrtidae (Hymenoptera: Chalcidoidea) from the Kingdom of Saudi Arabia. *Zootaxa* 3793(1): 1–59. <https://doi.org/10.11646/zootaxa.3793.1.1>
- Hayat M, Mehrnejad MR (2016) *Ooencyrtus* (Hymenoptera: Encyrtidae), egg parasitoids of the pistachio green stink bugs (Hemiptera: Pentatomidae) in Iran. *Zootaxa* 4117(2): 198–210. <https://doi.org/10.11646/zootaxa.4117.2.4>
- Hayat M, Zeya SB, Veenakumari K (2017) The species of *Ooencyrtus* Ashmead (Hymenoptera: Encyrtidae) from India–2. *Journal of Insect Systematics* 4(1): 18–83.
- Howard CW (1907) The *Bagrada* bug (*Bagrada hilaris*). *Transvaal Agricultural Journal* 5: 168–173.
- Huang D-W, Noyes JT (1994) A revision of the Indo-Pacific species of *Ooencyrtus* (Hymenoptera: Encyrtidae), parasitoids of the immature stages of economically important insect species (mainly Hemiptera and Lepidoptera). *Bulletin of the Natural History Museum [London] (Entomology Series)* 63(1): 1–136.
- Kumar S, Stecher G, Li M, Knyaz C, Tamura K (2018) MEGA X: molecular evolutionary genetics analysis across computing platforms. *Molecular biology and evolution* 35(6): 1547–1549. <https://doi.org/10.1093/molbev/msy096>
- Lindsey ARI, Stouthamer R (2017) Penetrance of symbiont-mediated parthenogenesis is driven by reproductive rate in a parasitoid wasp. *PeerJ* 5: e3505. <https://doi.org/10.7717/peerj.3505>
- Lomeli-Flores JR, Rodríguez-Rodríguez SE, Rodríguez-Levy E, González-Hernández H, Garipey TD, Talamas EJ (2019) Field studies and molecular forensics identify a new association: *Idris elba* Talamas, sp. nov. parasitizes the eggs of *Bagrada hilaris* (Burmeister). *Journal of Hymenoptera Research* 73: 125–141. <https://doi.org/10.3897/jhr.73.38025>
- Mahmood R, Jones WA, Bajwa BE, Rashid K (2015) Egg parasitoids from Pakistan as possible classical biological control agents of the invasive pest *Bagrada hilaris* (Heteroptera: Pentatomidae). *Journal of Entomological Science* 50: 147–149. <https://doi.org/10.18474/JES14-28.1>

- Maple JD (1947) The eggs and first instar larvae of Encyrtidae and their morphological adaptations for respiration. University of California Publications in Entomology 8(2): 25–122.
- Martel G, Augé M, Talamas E, Roche M, Smith L, Sforza RFH (2019) First laboratory evaluation of *Gryon gonikopalense* (Hymenoptera: Scelionidae), as potential biological control agent of *Bagrada hilaris* (Hemiptera: Pentatomidae). Biological Control 135: 48–56. <https://doi.org/10.1016/j.biocontrol.2019.04.014>
- Matsunaga JN (2014) Bagrada bug, *Bagrada hilaris* (Burmeister) (Hemiptera: Pentatomidae). State of Hawaii Department of Agriculture, New pest advisory. 14-01, December 2014. <http://hdoa.hawaii.gov/pi/files/2013/01/Bagrada-hilaris-NPA12-9-14.pdf>
- Morse JG, Rugman-Jones PF, Woolley JB, Heraty JM, Triapitsyn SV, Hofshi R, Stouthamer R (2016) Armored scales and their parasitoids on commercial avocados grown in California or imported from Mexico. Journal of Economic Entomology 109: 2032–2042. <https://doi.org/10.1093/jee/tow155>
- Noyes JS (1978) New chalcids recorded from Great Britain and notes on some Walker species (Hym., Encyrtidae, Eulophidae). Entomologist's Monthly Magazine 113 (1352–1355): 9–13.
- Noyes JS (1981) On the types of the species of Encyrtidae described by R. García Mercet (Hymenoptera: Chalcidoidea). EOS. Revista Española de Entomología, Madrid 55/56: 165–189.
- Noyes JS (1985) A review of the Neotropical species of *Ooencyrtus* Ashmead, 1900 (Hymenoptera: Encyrtidae). Journal of Natural History 19(3): 533–554. <https://doi.org/10.1080/00222938500770331>
- Noyes JS (2010) Encyrtidae of Costa Rica (Hymenoptera: Chalcidoidea), 3. Subfamily Encyrtinae: Encyrtini, Echthroplexiellini, Discodini, Oobiini and Ixodiphagini, parasitoids associated with bugs (Hemiptera), insect eggs (Hemiptera, Lepidoptera, Coleoptera, Neuroptera) and ticks (Acari). Memoirs of the American Entomological Institute 84: 1–848.
- Palumbo JC, Natwick ET (2010) The Bagrada bug (Hemiptera: Pentatomidae): a new invasive pest of cole crops in Arizona and California. Plant Management Network. <https://doi.org/10.1094/PHP-2010-0621-01-BR>
- Palumbo JC, Perring TM, Millar J, Reed DA (2016) Biology, ecology, and management of an invasive stink bug, *Bagrada hilaris*, in North America. Annual Review of Entomology 61: 453–473. <https://doi.org/10.1146/annurev-ento-010715-023843>
- Perring TM, Reed DA, Palumbo JC, Grasswitz T, Bundy CS, Jones WA, Papes M, Royer T (2013) National Pest Alert-Bagrada Bug. <http://www.ncipmc.org/alerts/bagradabug.pdf>
- Porter CH, Collins FH (1991) Species-diagnostic differences in a ribosomal DNA internal transcribed spacer from the sibling species *Anopheles freeborni* and *Anopheles hermsi* (Diptera: Culicidae). American Journal of Tropical Medicine and Hygiene 45: 271–279. <https://doi.org/10.4269/ajtmh.1991.45.271>
- Rajmohana K (2006) A checklist of the Scelionidae (Hymenoptera: Platygastroidea) of India. Zoos' Print Journal 21: 2506–2513. <https://doi.org/10.11609/JoTT.ZPJ.1570.2506-13>
- R Core Team (2018) R: A language and environment for statistical computing (computer software manual). R foundation for statistical computing, Vienna.
- Reed DA, Palumbo JC, Perring TM, May C (2013) *Bagrada hilaris* (Burmeister), an invasive stink bug attacking cole crops in the southwestern United States. Journal of Integrated Pest Management 4: 1–7. <https://doi.org/10.1603/IPM13007>

- Romanova VP (1953) Egg parasitoids of the sunn pest from observations in Rostov Province. *Zoologicheskii Zhurnal* 32(2): 238–248. [In Russian]
- Rugman-Jones PF, Hoddle MS, Amrich R, Heraty JM, Stouthamer-Ingel CE, Stouthamer R (2012) Phylogeographic structure, outbreeding depression, and reluctant virgin oviposition in the bean thrips, *Caliothrips fasciatus* (Pergande) (Thysanoptera: Thripidae), in California. *Bulletin of Entomological Research* 102: 698–709. <https://doi.org/10.1017/S0007485312000302>
- Samra S, Cascone P, Noyes J, Ghanim M, Protasov A, Guerrieri E, Mendel Z (2018) Diversity of *Ooencyrtus* spp. (Hymenoptera: Encyrtidae) parasitizing the eggs of *Stenozygum colonatum* (Klug) (Hemiptera: Pentatomidae) with description of two new species. *PLoS ONE* 13(11): e0205245. <https://doi.org/10.1371/journal.pone.0205245>
- Sánchez-Peña SR (2014) First record in Mexico of the invasive stink bug *Bagrada hilaris*, on cultivated crucifers in Saltillo. *Southwestern Entomologist* 39: 375–377. <https://doi.org/10.3958/059.039.0219>
- Sharma SK (1982) On some Scelionidae (Proctotrupeoidea: Hymenoptera) from India. *Records of the Zoological Survey of India* 79: 319–342.
- Stouthamer R, Hu J, van Kan FJPM, Platner GR, Pinto JD (1999) The utility of internally transcribed spacer 2 DNA sequences of the nuclear ribosomal gene for distinguishing sibling species of *Trichogramma*. *BioControl* 43: 421–440. <https://doi.org/10.1023/A:1009937108715>
- Tamura K, Nei M (1993) Estimation of the number of nucleotide substitutions in the control region of mitochondrial DNA in humans and chimpanzees. *Molecular Biology and Evolution* 10: 512–526.
- Taylor ME, Bundy CS, McPherson JE (2014) Unusual ovipositional behavior of the stink bug *Bagrada hilaris* (Hemiptera: Heteroptera: Pentatomidae). *Annals of the Entomological Society of America* 107(4): 872–877. <https://doi.org/10.1603/AN14029>
- Thompson JD, Gibson TJ (2003) Multiple sequence alignment using ClustalW and ClustalX. *Current Protocols in Bioinformatics* 2.3.1–2.3.22. <https://doi.org/10.1002/0471250953.bi0203s00>
- Triapitsyn SV, Andreason SA, Dominguez C, Perring TM (2019) On the origin of *Anagyrus callidus* (Hymenoptera: Encyrtidae), a parasitoid of pink hibiscus mealybug *Maconellicoccus hirsutus* (Hemiptera: Pseudococcidae). *Zootaxa* 4671(2): 283–289. <https://doi.org/10.11646/zootaxa.4671.2.9>
- Trjapitzin VA (1989) Parasitic Hymenoptera of the fam. Encyrtidae of Palaearctics. *Opredeliteli po faune SSSR Izdavaemye Zoologicheskim Institutom AN SSSR (Leningrad, Nauka, Leningrad division)* 158: 1–489. [In Russian]
- Truett GE, Heeger P, Mynatt RL, Truett AA, Walker JA, Warman ML (2000) Preparation of PCR Quality Mouse Genomic DNA with Hot Sodium Hydroxide and Tris (HotSHOT). *BioTechniques* 29: 52–54. <https://doi.org/10.2144/00291bm09>
- Vassiliev I (1904) Ueber eine neue, bei den Vertretern der Gattung *Telenomus* parasitierende *Encyrtus*-Art (Hymenoptera, Chalcididae). *Russkoe Entomologicheskoe Obozrenie (Revue Russe d'Entomologie)* 4(2–3): 117–118.
- Vitanza S (2012) Issues in agriculture. *Texas A&M AgriLife Extension Newsletter* 38: 1–8.
- Yara K (2006) Identification of *Torymus sinensis* and *T. beneficus* (Hymenoptera: Torymidae), introduced and indigenous parasitoids of the chestnut gall wasp *Dryocosmus kuriphilus*

- (Hymenoptera: Cynipidae), using the ribosomal ITS2 region. *Biological Control* 36(1): 15–21. <https://doi.org/10.1016/j.biocontrol.2005.08.003>
- Zhang Y-Z, Li W, Huang D-W (2005) A taxonomic study of Chinese species of *Ooencyrtus* (Insecta: Hymenoptera: Encyrtidae). *Zoological Studies* 44(3): 347–360.
- Zuparko RL (2015) Annotated checklist of California Encyrtidae (Hymenoptera). *Zootaxa* 4017(1): 1–126. <https://doi.org/10.11646/zootaxa.4017.1.1>
- Zuparko R (2018) *Ooencyrtus*. [https://essig.berkeley.edu/research/encyrtidae/Ooencyrtus/\[California Encyrtidae\]](https://essig.berkeley.edu/research/encyrtidae/Ooencyrtus/[California%20Encyrtidae])

Supplementary material I

Measurements used in the multivariate ratio analysis for *Ooencyrtus mirus* Triapitsyn & Power and *O. telenomicida* (Vassiliev) (Hymenoptera: Encyrtidae)

Authors: Serguei V. Triapitsyn, Sharon A. Andreason, Nancy Power, Fatemeh Ganjisafar, Lucian Fusu, Chrysalyn Dominguez, Thomas M. Perring

Data type: measurement

Explanation note: The complete set of measurements used in the multivariate ratio analysis for *Ooencyrtus mirus* Triapitsyn & Power and *O. telenomicida* (Vassiliev).

Copyright notice: This dataset is made available under the Open Database License (<http://opendatacommons.org/licenses/odbl/1.0/>). The Open Database License (ODbL) is a license agreement intended to allow users to freely share, modify, and use this Dataset while maintaining this same freedom for others, provided that the original source and author(s) are credited.

Link: <https://doi.org/10.3897/jhr.76.48004.suppl1>

Status and potential distribution of the Asian carpenter bee, *Xylocopa appendiculata* Smith (Apidae, Xylocopini), in the United States

Allan H. Smith-Pardo¹, Glenn A. Fowler¹, Sunil Kumar²

1 United States Department of Agriculture (USDA), Animal and Plant Health Inspection Service (APHIS), Plant Protection and Quarantine (PPQ), Science and Technology (S&T) 801 I Street, Suite 406, Sacramento, California 95814, USA **2** United States Department of Agriculture (USDA), Animal and Plant Health Inspection Service (APHIS), Plant Protection and Quarantine (PPQ), Science and Technology (S&T) Raleigh, North Carolina 27606, USA

Corresponding author: Allan H. Smith-Pardo (allan.h.smith-pardo@usda.gov)

Academic editor: Jack Neff | Received 18 December 2019 | Accepted 8 March 2020 | Published 27 April 2020

<http://zoobank.org/84656D9D-D17C-483C-B697-4040173FECE1>

Citation: Smith-Pardo AH, Fowler GA, Kumar S (2020) Status and potential distribution of the Asian carpenter bee, *Xylocopa appendiculata* Smith (Apidae, Xylocopini), in the United States. Journal of Hymenoptera Research 76: 99–111. <https://doi.org/10.3897/jhr.76.49518>

Abstract

We update the geographical distribution for *Xylocopa appendiculata* Smith, from eastern Asia, which was first reported from the United States of America (USA) in 2013. After the publication by Dahlberg et al. (2013), there have been more sightings supporting the establishment of *X. appendiculata* in northern California. We used plant hardiness zones and maximum entropy (Maxent) modeling to estimate the potential distribution of *X. appendiculata* in the USA using specimen data from multiple occurrences (confirmed data from literature, museum specimens and validated data from Discover Life.org and iNaturalist.org). We include images and a list of diagnostic features for the identification of the subgenus *Alloxylocopa* Hurd and Moure and the species *X. appendiculata* so that it can be identified and reported to corresponding state or federal authorities, if necessary.

Resumen

Se actualizan los datos de distribución de *X. appendiculata* Smith del este de Asia que fue reportada para los Estados Unidos de América por primera vez en 2013; después de este registro, se han presentado más avistamientos lo cual puede ser confirmación de que esta especie de hecho se ha establecido en el norte de California. Se utilizaron datos de “plant hardiness zones” (zonas de resistencias de plantas) y modelo de nichos Maxent para estimar la distribución potencial de esta especie en los EEUU mediante el uso de datos de especímenes de múltiples fuentes (datos confirmados de la literatura, ejemplares en museos

y datos validados en Discover Life.org y iNaturalist.org) una distribución potencial de la especie en los EEUU con base en los datos de distribución original de la especie así como de datos en las bases de datos DiscoverLife.org y en la plataforma iNaturalist además de datos climáticos. Incluimos además imágenes y una lista de características diagnosticas del subgénero *Alloxylocopa* y de la especie *X. appendiculata* de manera que pueda ser identificada y reportada a las entidades federales o estatales en el futuro si es necesario.

Keywords

Biogeography, exotic bees, introduced species, invasive species, Maxent, Xylocopinae

Palabras claves

Biogeography, exotic bees, introduced species, invasive species, Maxent, Xylocopinae

Introduction

Bees of the genus *Xylocopa* Latreille are large and robust, 13–30 mm long (hence the common name of large carpenter bees), and are characterized, among other things, as having strongly sclerotized mouth parts (particularly the galeae), which are used to cut into corollas of tubular flowers to get the nectar (Sampson et al. 2004, Dedej and Delaplane 2004). Females of *Xylocopa* nest in wood, except those of subgenus *Proxylocopa* Hedicke which nest in the ground (Kronenberg and Hefetz 1984, Michener 2007).

Large carpenter bees have broad geographical distributions. They have diversified within tropical and subtropical regions and expanded their distributions to temperate regions (Hurd and Moure 1963). Several species of *Xylocopa* are suspected to have invaded oceanic islands, as only a few species exist within island groups and the distances between the original and their close relative's habitats are relatively short. For example, *Xylocopa sonora* Smith was allegedly transferred by humans from North America to tropical Pacific islands, including Hawaii (Hurd 1958). More recently, Okabe et al. (2010) reported the introduction of the bamboo-nesting carpenter bee *Xylocopa tranquebarorum* (Swederus) in Japan. These authors also suspected that it was likely introduced from either India or China because of the characteristic mites associated with them. More recently, Dahlberg et al. (2013) reported *Xylocopa appendiculata* as introduced in California, United States.

Dahlberg et al. (2013) provided some diagnostic characteristics for the identification of *X. appendiculata* and some ways to separate it from native species in the USA. However, they used mostly coloration and the only picture in that paper is in black and white.

In this contribution, we provide information on the potential distribution of *X. (Alloxylocopa) appendiculata* in the USA. In addition, we include a diagnostic aid with images for the identification of the subgenus *Alloxylocopa* Hurd and Moure, and the species *X. appendiculata* and comments on its distribution, hosts, quarantine importance, and behavior.

Methods

The specimen used for the images and identification aids was collected in San Jose, California in 2012 and cited by Dahlberg et al. (2013). We also received from Mrs. Dahlberg images of males visiting the same garden in two different years (see new records in the results section) and we used them for some of the information provided in the diagnostic aids of the species. The female specimen used in the aids is housed at the California State Collection of Arthropods in the California Department of Agriculture (CDFA) building in Meadowview, Sacramento, California. Images were taken using a Nikon SMZ18 dissection microscope with a Nikon Digital Sight ds-fi2 camera attached. Once a series of 15–20 images per view were taken, they were focus stacked using the program Helicon Focus (Heliconsoft) and edited using Adobe Photoshop CS6.

Potential distribution modeling

To predict areas where *Xylocopa appendiculata* could establish in the USA, we used location data for specimens at the American Museum of Natural History (AMNH, Jerome Rozen and Lance Jones), The Snow Entomological Collection at the University of Kansas Biodiversity and Natural History Museum (SEMC, Jennifer Thomas), and verified distribution data from iNaturalist (2019), Discover Life (2019), and the Global Biodiversity Information Facility (GBIF 2019) for specimens ID validated by taxonomists. For the iNaturalist data, we used research grade detections, which are identifications that over 2/3 of the identifiers agree on (iNaturalist 2019). The combined dataset contained 325 *X. appendiculata* occurrences (duplicate records were removed). We also included in the analysis the type localities for *X. appendiculata* Smith, 1874 which is Ning-po-foo, China and *X. appendiculata circumvolans* (Smith, 1873) which is Hiogo, Japan (Appendix 1).

We used this dataset to predict where *X. appendiculata* could establish in the USA based on the associated Plant Hardiness Zones and Maxent niche modeling. We used two modeling approaches to increase the rigor of the analysis and better account for uncertainty regarding the bee's potential distribution in the USA.

The Plant Hardiness Zones are calculated based on the average annual extreme minimum temperature for an area in 10 °F (5.6 °C) increments (ARS 2012). They can be used to predict where plant pests (e.g., insects) could establish based on the Plant Hardiness Zones that match with the pest's native range (PERAL 2013). We overlaid the 325 *X. appendiculata* occurrence points with a Plant Hardiness Zone layer that was based on average climate data from 1988 to 2017 (Takeuchi et al. 2018). We then mapped the corresponding plant hardiness zones in the United States to predict its distribution.

We used maximum entropy niche modeling (Maxent 3.3.3k; Phillips et al. 2006, 2017) to estimate the potential distribution of *X. appendiculata* in the United States.

We removed duplicate records (>1 presence point within a $\sim 4 \times 4$ km grid cell) and reduced spatial autocorrelation using ‘spatial filtering’ (i.e. reducing density of occurrences) using SDMToolbox (Brown 2014; Kumar et al. 2016). The total occurrences from the native range (Japan, Korean peninsula, and China) and invaded range (California, USA) were reduced from 325 to 158 (Appendix 1). We then calculated a Gaussian Kernel Density layer of occurrence data in ArcMap using SDMToolbox, which we used to account for potential sampling bias in occurrence data. We obtained climatic data from CHELSA website (Climatologies at High resolution for the Earth’s Land Surface Areas; <http://chelsa-climate.org/>; Karger et al. 2017). We downloaded 19 bioclimatic variables data layers ($\sim 4 \times 4$ km spatial resolution) which represent average monthly temperature, precipitation, seasonal variables, and climatic extreme indices data from 1979–2013 (Hijmans et al. 2005; Appendix 2). We examined all 19 variables for cross-correlation (Pearson correlation coefficient, r) and highly correlated variables ($|r| > 0.80$) were excluded to reduce multicollinearity. The decision to exclude or include a variable was based on its potential biological relevance to *X. appendiculata* and its relative predictive power in the model (Appendix 2, 3).

Multiple models were fitted with different feature types and regularization multiplier values, and the best model with the optimal level of complexity was selected. Performance of the model was evaluated using the area under the receiver operating characteristic (ROC) curve (AUC; Peterson et al. 2011). We used the 10-fold cross-validation procedure for evaluating model performance, and reported averaged test AUC values across the ten replicates. Unsuitable areas for *X. appendiculata* were defined using the 100 percent sensitivity threshold (Liu et al. 2013). Therefore, areas with > 0.107 probability of presence in Maxent modeling results were considered as suitable for *X. appendiculata*.

Results

Potential distribution of *X. appendiculata* in the USA

The analysis of potential U.S. areas for *Xylocopa appendiculata* establishment based on plant hardiness zones (Figure 1) predicted that *X. appendiculata* could establish in Plant Hardiness Zones 5 to 10. This area includes most of the contiguous United States, and parts of southern and coastal Alaska (Figure 1). Colder regions like North Dakota, most of Alaska and the Rocky Mountains, and warmer regions like southern Florida and Hawaii were predicted to be unsuitable. *Xylocopa appendiculata*’s predicted cold hardiness is due to its occurrence in colder parts of Japan.

The plant hardiness zone model likely represents a worst case scenario for *X. appendiculata*’s potential U.S. distribution due to the coarseness of the approach. This conclusion is supported by the fact that no western species of *Xylocopa* reach Canada, except for *X. virginica* which is present in the most southern parts of Ontario and Quebec.

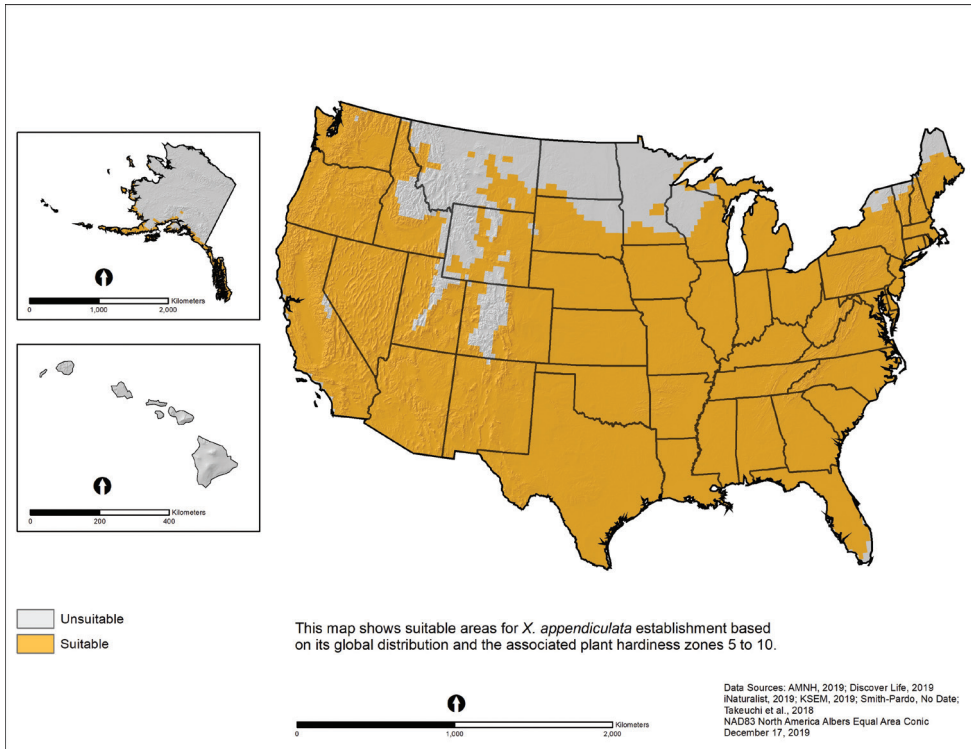
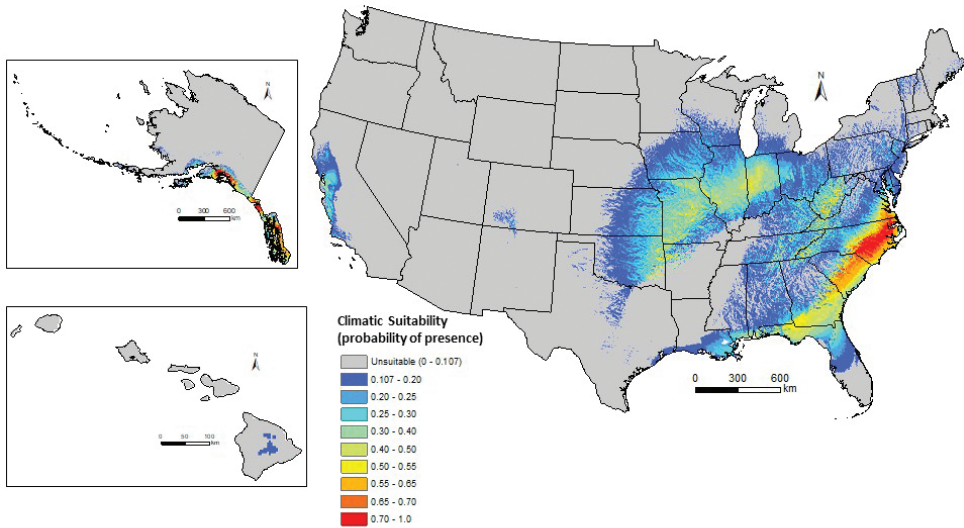


Figure 1. Suitable U.S. areas for *Xylocopa appendiculata* establishment based on plant hardiness zones – This map shows suitable areas for *X. appendiculata* establishment based on its global distribution and the associated plant hardiness zones 5 to 10.

The second analysis, or Maxent model, predicted climatically suitable areas for *X. appendiculata* in the eastern United States, parts of California, southwestern Alaska, and parts of Hawaii (Figure 2). Our model indicated medium to low climatic suitability (probability between 0.40–0.10) in parts of California, and very low suitability in Hawaii (probability 0.10–2.0) (Figure 2). The Maxent model for *X. appendiculata* performed well with a test AUC value of 0.98 (an AUC value of 1.0 indicates superior performance, and 0.5 indicates performance no better than random; Peterson et al. 2011). Precipitation of warmest quarter (Bio18) and temperature seasonality (Bio4) were the two top predictors associated *X. appendiculata*'s distribution, with 45% and 28% contributions, respectively (Appendix 2).

The climatic response curves fitted by the Maxent model suggest that areas with average annual temperatures (Bio1) between 4 °C and 22 °C, and average annual precipitation (Bio12) between 200 mm and 3,800 mm are likely suitable for *X. appendiculata* (Appendix 3). The distinct contrast in the patterns in predicted climatic suitability for *X. appendiculata* in northeastern Texas, Arkansas, northern Louisiana, western Mississippi and Tennessee, is probably due to variation in average summer



This map visualizes the predicted climatic suitability (probability of presence) for *Xylocopa appendiculata* in the United States. The global occurrence data (triangles) were integrated with climatic data using Maxent ecological niche model to produce probability of presence.

Sources: ESRI, No Date; Karger et al. (2017); AMNH, 2019; Discover Life, 2019; iNaturalist, 2019; KSEM, 2019; Smith-Pardo, No Date
NAD83 Albers Equal Area Conic
December 17, 2019

Figure 2. Predicted climatic suitability for *Xylocopa appendiculata* in the United States.

precipitation (June, July and August) in that part of the country (Appendix 4). Based on where the plant hardiness zone and Maxent models agree, the areas at greatest risk for *X. appendiculata* establishment include parts of southern Alaska and portions of eastern Virginia and the Carolinas (Figures 1, 2). Other at-risk areas include portions of western California and the eastern, north central, and central United States.

New observations and distribution records

USA records

USA. 1♀; California: San Jose; Sept. 2012; on flowers of *Salvia azurea* Michx. ex Lam. (Lamiaceae). 1♂; same locality data; May 2013; on flowers of *Erysimum linifolium* (Pers.) J. Gay (Brassicaceae). 2♂; same locality data; Apr. 2015; on flowers *Erysimum linifolium* (Brassicaceae). 1♀; same locality data; Mar.2017; on flowers of *Prunus cerasifera* Ehrh (Rosaceae). 1♀; same locality data; May 2019; on flowers *Erysimum linifolium* (Brassicaceae).

USA. 1♀; California: Castro Valley; 37°42'13"N, 122°03'35"W; Sept. 2017; on flowers of *Grewia occidentalis* L. (Malvaceae). 1♀; same locality data; Aug. 2018; on flowers of *Passiflora* sp. L. (Passifloraceae). These two records show the movement of the species further north (~32–45 kilometers) from where the species was first reported in northern California.

Diagnostic aid for the identification of *Xylocopa appendiculata*

Bees of the subgenus *Alloxylocopa* Hurd and Moure (before the introduction of *X. appendiculata*, the subgenus was not known to be present in the Western hemisphere) can be distinguished from all other *Xylocopa* subgenera that are present in the USA and Canada by the following combination of characters: (*female*) pygidial plate without sub-apical spines (Fig. 3d, pp: pygidial plate), (*both sexes*) mesoscutellum with sub-horizontal dorsal surface abruptly and angularly separated from sub-vertical surface (Fig. 3e), postero-dorsal margin of mesoscutellum not surpassing posterior margin of metanotum and not projecting posteriorly beyond its posterior surface as a thin-edged flange., vertical fold of metasomal tergum 1 with foveate, hollow-like depression (Fig. 3f, arrow),

Specimens of *X. appendiculata* can be distinguished from native U.S. species of carpenter bees by the following combination of features: mandible with two teeth (Fig. 3g, arrow); clypeus and paraoxular areas strongly punctate (Fig. 3b, square); occipital area, mesosoma and external side of fore tibiae with pubescence bright yellow, black on most of metasoma (Fig. 3a), except for few light brown setae close to pygidial plate

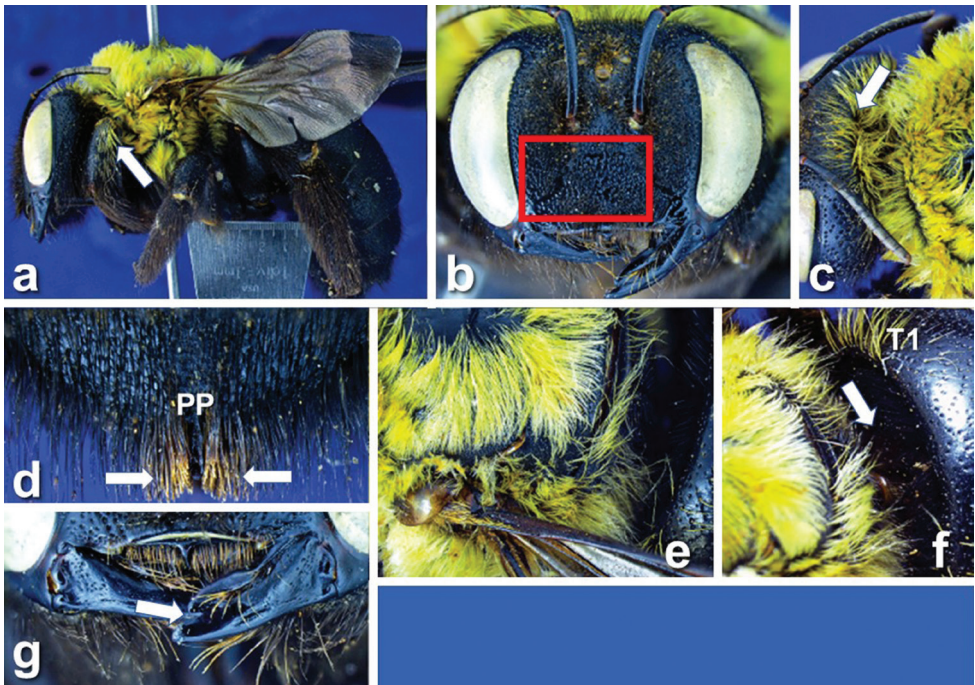


Figure 3. Some of the diagnostic features of *Xylocopa appendiculata* Smith: **a** lateral habitus showing coloration of pubescence on mesosoma and metasoma (the yellow coloration may not be as fluorescent in field specimens and is mostly due to reflections from the imaging system) **b** face showing integument sculpturing of clypeus and paraoxular area **c** coloration of pubescence around occipital area (arrow) **d** pygidial plate (pp) and coloration of pubescence close to it (arrows) **e** shape of mesoscutellum from lateral view **f** Shape of metasomal tergum 1 (T1) from antero-lateral view and the presence of a foveate, hollowed like depression (arrow) **g** dentation of mandibles (arrow showing the two teeth on mandible).

on female (Fig. 3d, arrows); (Fig. 3c, arrow), Fig. 3a, e) and (Fig. 3a, arrow). The mesosoma of the native, North American species can be covered with black, grayish, brownish, or pale yellow setae and often have pale hairs elsewhere on the body and/or metallic highlights on the integument (Hurd and Moure 1963). The most similar of the native carpenter bees in the U.S. is *Xylocopa virginica* L. (the Eastern carpenter bee) which also has two mandibular teeth and a strongly punctuate clypeus, but differs from *X. appendiculata* because it lacks the extensive bright yellow hairs in the mesosoma and vertex. The males of *X. appendiculata* also lack the extensive bluish or greenish reflections of the body present in males of *X. virginica*.

Floral hosts

Little is known about the preferred plants visited and pollinated by *X. appendiculata* in its native range, but based on the observations of visits in the USA this species seems, at least potentially, polylectic in its floral preferences. In the new habitat in the Bay Area this species was seen visiting flowers of introduced plants such as *Grewia occidentalis* (originally from Africa) and *Passiflora* sp. (originally from tropical America). Both plants were in the senior author's bee garden in Castro Valley, CA.

Discussion

Dahlberg et al. (2013) provided a list of all the U.S. species of *Xylocopa* and their distributions by the state. The potential distribution maps show that *X. appendiculata* could establish in all the states where native species of carpenter bees occur according to the distribution records in literature. This is especially true in the east coast where it could broadly overlap with the common species *X. virginica*. Due to their morphological similarities successful diagnosis would require careful examination and the use of the diagnostic aids provided here.

As with all new introduced species, there is a risk that *X. appendiculata* will be better at competing for foraging plants and nesting sites (dry or rotten wood), which may limit resources for native bees. In addition, carpenter bees can be a nuisance because they can nest in human made structures such as fences and roofs. Due to their large size, females of *X. appendiculata* can also damage flowers while feeding without pollinating them.

There is evidence of introduced carpenter bees bringing new parasites (and possibly diseases) to invaded areas (Okabe et al. 2010; Kontschán et al. 2016). There may be new parasites associated with this species that do not occur in the USA that can be potentially damaging to our native *Xylocopa* species.

As is the case with other wood nesting bees that have been introduced into the USA, *X. appendiculata* will likely compete with native species for empty nesting sites or even usurp them when sites are limited (Mangum and Brooks 1997; Batra 1998; Laport and Minckley 2012).

In addition, *Xylocopa appendiculata* also nests in wood, twigs and large stalks of dead plants commonly used to make shipping crates and woodcrafts, which could increase its rate of spread over long distances and across natural barriers such as oceans and mountain ranges.

Given *X. appendiculata*'s potential to establish in the United States and outcompete native carpenter bees it is important to continue monitoring its spread. In this regard, our analysis can assist with *X. appendiculata* identification and informing surveys.

Acknowledgements

We thank Dr. Martin Hauser from CDFA in Sacramento for lending us the original specimen of *X. appendiculata* collected in San Jose for this study. We thank the museum curators and curatorial assistants, listed under methods, for providing us the distribution data for specimens in their collections. We also thank Mr. Timothy Torbett, Botanist with the USDA-APHIS in South San Francisco, for his identifications of the plants visited by the species in Castro Valley. This is a contribution of Science and Technology, Center for Plant Health Science and Technology (CPHST- S&T) of the United States Department of Agriculture, Animal and Plant Health Inspection Service, Plant Protection and quarantine (USDA-APHIS-PPQ).

References

- ARS (2012) USDA Plant Hardiness Zone Map. United States Department of Agriculture, Agricultural Research Service (ARS). Last accessed April 30, 2019, <https://planthardiness.ars.usda.gov>
- Batra SWT (1998) Biology of the giant resin bee, *Megachile sculpturalis* Smith, a conspicuous new immigrant in Maryland. *Maryland Naturalist* 42: 1–3.
- Brown JL (2014) SDMtoolbox: a python-based GIS toolkit for landscape genetic, biogeographic and species distribution model analyses. *Methods in Ecology and Evolution* 5(7): 694–700. <https://doi.org/10.1111/2041-210X.12200>
- Dahlberg L, Hauser M, Yanega D (2013) Japanese carpenter bee, *Xylocopa appendiculata* Smith 1852 (Hymenoptera: Apidae) potentially established in Santa Clara County, first record for North America. *Pan Pacific Entomologist* 89(4): 226–229. <https://doi.org/10.3956/2013-22.1>
- Dedej S, Delaplane KS (2004) Nectar-Robbing Carpenter Bees Reduce Seed-Setting Capability of Honey Bees (Hymenoptera: Apidae) in Rabbit eye Blueberry, *Vaccinium ashei*, 'Climax. *Environmental Entomology* 33(1): 100–106. <https://doi.org/10.1603/0046-225X-33.1.100>
- Discover Life (2019) <https://www.discoverlife.org/> [Accessed October 2019]
- GBIF (2019) Global Biodiversity Information Facility (GBIF). GBIF Secretariat. <https://www.gbif.org/> [Accessed October 2019]
- Hijmans RJ, Cameron SE, Parra JL, Jones PG, Jarvis A (2005) Very high resolution interpolated climate surfaces for global land areas. *International Journal of Climatology* 25(15): 1965–1978. <https://doi.org/10.1002/joc.1276>

- Hurd PD, Moure JS (1963) A classification of the large carpenter bees (Xylocopini) (Hymenoptera: Apoidea). University of California Publications in Entomology 29: 1–365.
- Hurd PD (1958) The carpenter bees of the eastern pacific oceanic islands. Journal of the Kansas Entomological Society 31: 249–255.
- iNaturalist (2019) <https://www.inaturalist.org/> [Accessed October 2019]
- Karger DN, Conrad O, Böhrner J, Kawohl T, Kreft H, Soria-Auza RW, Zimmermann NE, Linder HP, Kessler M (2017) Climatologies at high resolution for the earth's land surface areas. Scientific Data 4: 170–122. <https://doi.org/10.1038/sdata.2017.122>
- Kearse T (2010) Large Carpenter Bees as Agricultural Pollinators. Psyche 2010 (927463): 7 pp. <https://doi.org/10.1155/2010/927463>
- Kontschán J, Jeon MJ, Hwang JM, Seo HY (2016) First record of four bee (Hymenoptera: Apidae) associated mite species (Acari) from Democratic People's Republic of Korea. Journal of Species Research 5 (1): 27–30. <https://doi.org/10.12651/JSR.2016.5.1.027>
- Kronenberg S, Hefetz A (1984) Comparative analysis of Dufour's gland secretions of two carpenter bees (Xylocopinae: Anthophoridae) with different nesting habits. Comparative Biochemistry and Physiology, B, Comparative Biochemistry 79(3): 421–425. [https://doi.org/10.1016/0305-0491\(84\)90399-7](https://doi.org/10.1016/0305-0491(84)90399-7)
- Kumar S, Yee WL, Neven LG (2016) Mapping global potential risk of establishment of *Rhagoletis pomonella* (Diptera: Tephritidae) using MaxEnt and CLIMEX niche models. Journal of Economic Entomology 109(5): 2043–2053. <https://doi.org/10.1093/jee/tow166>
- Laport RG, Minckley RL (2012) Occupation of active *Xylocopa virginica* nests by the recently invasive *Megachile sculpturalis* in Upstate New York. Journal of the Kansas Entomological Society 85(4): 384–386. <https://doi.org/10.2317/0022-8567-85.4.384>
- Liu C, White M, Newell G (2013) Selecting thresholds for the prediction of species occurrence with presence-only data. Journal of Biogeography 40: 778–789. <https://doi.org/10.1111/jbi.12058>
- Mangum WA, Brooks RW (1997) First records of *Megachile (Callomegachile) sculpturalis* Smith (Hymenoptera: Megachilidae) in the continental United States. Journal of the Kansas Entomological Society 70: 146–148.
- Michener CD (2007) The Bees of the World (2nd ed.) Johns Hopkins University Press, Baltimore and London, 953 pp.
- Okabe K, Masuya H, Kawazoe K, Makino S (2010) Invasion pathway and potential risks of a bamboo-nesting carpenter bee, *Xylocopa tranquebarorum* (Hymenoptera: Apidae), and its micro-associated mite introduced into Japan. Applied Entomology and Zoology 45(2): 329–337. <https://doi.org/10.1303/aez.2010.329>
- PERAL (2013) Guidelines for Plant Pest Risk Assessment of Imported Fruit & Vegetable Commodities (08/2012-01). United States Department of Agriculture, Animal and Plant Health Inspection Service, Plant Protection and Quarantine, Center for Plant Health Science and Technology, Plant Epidemiology and Risk Analysis Laboratory (PERAL), Raleigh, NC. 142 pp.

- Peterson AT, Soberon J, Pearson RG, Anderson RP, Martinez-Meyer E, Nakamura M, Araujo MB (2011) Ecological niches and geographic distributions. Princeton University Press, Princeton, N.J. <https://doi.org/10.23943/princeton/9780691136868.003.0003>
- Phillips SJ, Anderson RP, Schapire RE (2006) Maximum entropy modeling of species geographic distributions. *Ecological Modelling* 190(3–4): 231–259. <https://doi.org/10.1016/j.ecolmodel.2005.03.026>
- Phillips SJ, Anderson RP, Dudik M, Schapire RE, Blair ME (2017) Opening the black box: An open-source release of Maxent. *Ecography* 40(7): 887–893. <https://doi.org/10.1111/ecog.03049>
- Sadeh A, Shmida A, Keasar T (2007) The Carpenter Bee *Xylocopa pubescens* as an Agricultural Pollinator in Greenhouses. *Apidologie*: 508–517. <https://doi.org/10.1051/apido:2007036>
- SAFARIS (2019) Spatial Analytic Framework for Advanced Risk Information Systems (SAFARIS). United States Department of Agriculture (USDA) and North Carolina State University (NCSU). <https://safaris.cipm.info/safarispestmodel/StartupServlet?safarishome>
- Sampson BJ, Danka RG, Stringer SJ (2004) Nectar Robbery by Bees *Xylocopa virginica* and *Apis mellifera* Contributes to the Pollination of Rabbit eye Blueberry. *Journal of Economic Entomology* 97(3): 735–740. [https://doi.org/10.1603/0022-0493\(2004\)097\[0735:NRB BXV\]2.0.CO;2](https://doi.org/10.1603/0022-0493(2004)097[0735:NRB BXV]2.0.CO;2)
- Smith F (1852) VIII. Descriptions of some new and apparently undescribed species of Hymenopterous Insects from North China, collected by Robert Fortune, Esq. *Transactions of the Entomological Society of London, New Series v. ii, Vol. 7*: 33–44. <https://doi.org/10.1111/j.1365-2311.1852.tb02208.x>
- Smith F (1873) VIII. Descriptions of Aculeate Hymenoptera of Japan, collected by Mr. George Lewisat Nagasaki and Hiogo. *Transactions of the Entomological Society of London, Vol. 21*: 181–206. <https://doi.org/10.1111/j.1365-2311.1873.tb00641.x>
- Smith-Pardo A (constantly updating) *Xylocopa appendiculata* occurrence (personal observation). United States Department of Agriculture, Animal and Plant Health Inspection Service, Plant Protection and Quarantine, Science and Technology, Sacramento, CA.
- Solomon-Raju AJ, Purnachandra-Rao S (2006) Nesting habits, floral resources and foraging ecology of large carpenter bees (*Xylocopa latipes* and *Xylocopa pubescens*) in India. *Current Science* 90(9): 1210–1217.
- Sugiura N (1995) Burrow construction by the Japanese carpenter bee, *Xylocopa appendiculata circumvolans* Smith, for overwintering (Hymenoptera: Anthophoridae). *Journal of the Kansas Entomological Society* 68(1): 116–119.
- Takeuchi Y, Fowler G, Joseph AS (2018) SAFARIS: Global Plant Hardiness Zone Development. North Carolina State University, Center for Integrated Pest Management; United States Department of Agriculture, Animal and Plant Health Inspection Service, Plant Protection and Quarantine, Science and Technology, Plant Epidemiology and Risk Analysis Laboratory, Raleigh, NC. 6 pp.

Appendix 1

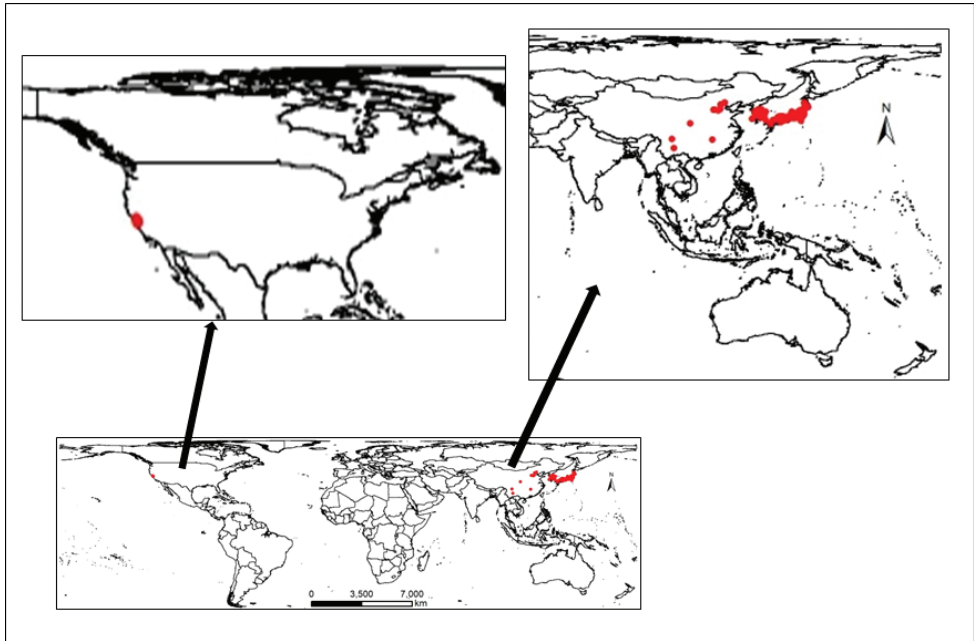


Figure A1. Global distribution of *Xylocopa appendiculata* based on specimens deposited in collections and confirmed records on iNaturalist, GBIF, and Discover Life.org (red circles).

Appendix 2

Table A1. Relative importance of 19 climatic variables considered in *Xylocopa appendiculata* Maxent model. Bold shows the variables used in the Maxent model; other variables were dropped because of high cross-correlations or lower predictive power in the model. Presented values are averages for 10 replicate runs.

| Variable | Percent contribution |
|--|----------------------|
| Precipitation of warmest quarter (Bio18; mm) | 45.3 |
| Temperature seasonality (SD x 100) (Bio4) | 27.9 |
| Mean annual precipitation (Bio12; mm) | 15.0 |
| Mean temperature of driest quarter (Bio9; °C) | 6.0 |
| Precipitation of driest month (Bio14; mm) | 4.5 |
| Precipitation seasonality (CV) (Bio15) | 1.2 |
| Annual mean temperature (Bio1; °C) | – |
| Mean diurnal range in temperature (Bio2; °C) | – |
| Isothermality (Bio3) | – |
| Maximum temperature of warmest month (Bio5; °C) | – |
| Minimum temperature of coldest month (Bio6; °C) | – |
| Temperature annual range (Bio7; °C) | – |
| Mean temperature of wettest quarter (Bio8; °C) | – |
| Mean temperature of warmest quarter (Bio10; °C) | – |
| Mean temperature of coldest quarter (Bio11; °C) | – |
| Precipitation of wettest month (Bio13; mm) | – |
| Precipitation of wettest quarter (Bio16; mm) | – |
| Precipitation of driest quarter (Bio17; mm) | – |
| Precipitation of coldest quarter (Bio19; mm) | – |

Appendix 3

Table A2. Pearson correlation (r) among the six best predictors in the *Xylocopa appendiculata* Maxent model; see Appendix1 for variable names.

| | Bio4 | Bio9 | Bio12 | Bio14 | Bio15 |
|-------|--------|--------|--------|--------|--------|
| Bio9 | -0.787 | | | | |
| Bio12 | -0.568 | 0.289 | | | |
| Bio14 | -0.265 | 0.085 | 0.732 | | |
| Bio15 | -0.133 | 0.254 | -0.298 | -0.527 | |
| Bio18 | -0.241 | -0.030 | 0.727 | 0.593 | -0.273 |

Appendix 4

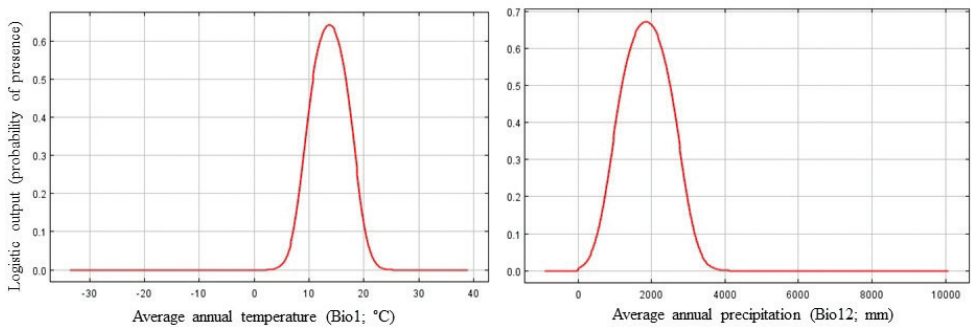


Figure A2. Climatic variables’ response curves fitted by Maxent model for *Xylocopa appendiculata*.

Appendix 5

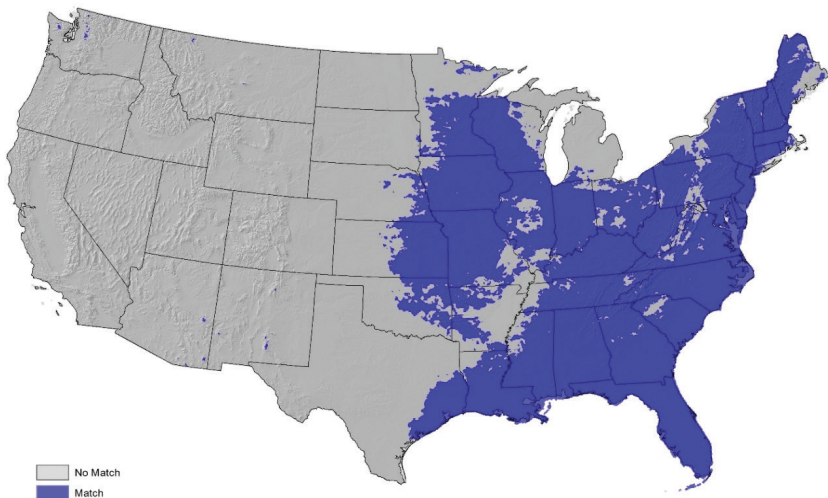


Figure A3. Summer Precipitation Patterns in the USA: Average summer precipitation (June, July and August) was calculated using PRISM climate data with the Spatial Analytic Framework for Advanced Risk Information Systems (SAFARIS 2019). Areas with ≥ 300 mm of precipitation between June and August (blue) based on average data from 2000 to 2019.

Nest structure, pollen utilization and parasites associated with two west-Mediterranean bees (Hymenoptera, Apiformes, Megachilidae) nesting in empty snail shells

Petr Bogusch¹, Lucie Hlaváčková¹, Libor Petr², Jordi Bosch³

1 University of Hradec Králové, Faculty of Science, Rokitanského 62, CZ-500 03 Hradec Králové, Czech Republic **2** Department of Botany and Zoology, Masaryk University, Kotlářská 2, CZ-611 37 Brno, Czech Republic **3** CREA – Centre de Recerca Ecològica i Aplicacions Forestals, Edifici C Campus de Bellaterra, 08193, Barcelona, Spain

Corresponding author: Petr Bogusch (bogusch.petr@gmail.com)

Academic editor: J. Neff | Received 20 December 2019 | Accepted 22 February 2020 | Published 27 April 2020

<http://zoobank.org/6C3DF670-8D3A-4524-972C-25D3B76A5E4D>

Citation: Bogusch P, Hlaváčková L, Petr L, Bosch J (2020) Nest structure, pollen utilization and parasites associated with two west-Mediterranean bees (Hymenoptera, Apiformes, Megachilidae) nesting in empty snail shells. *Journal of Hymenoptera Research* 76: 113–125. <https://doi.org/10.3897/jhr.76.49579>

Abstract

Around thirty species of European solitary bee species in the family Megachilidae nest in empty gastropod shells. We surveyed this group of bees in semi-natural sites adjacent to almond orchards near Lleida (north-eastern Spain) and collected 35 *Hoplitis fertoni* and 58 *Osmia ferruginea* nests in shells of six snail species. We describe the nest structure and report the identity of pollens collected by the two bee species. Both species adjust the number of brood cells to the size of the shell and occasionally build intercalary (empty) cells. *H. fertoni* uses clay and *O. ferruginea* chewed plant leaves for building cell partitions and nest plugs. Most nests of both species were built in *Sphincterochila candidissima* shells. Analysis of the pollen of selected nests confirmed that *H. fertoni* is oligolectic on Boraginaceae (in our study all pollen was from *Lithodora fruticosa*) and *O. ferruginea* is a polylectic species (collecting mostly pollen from Cistaceae, Fabaceae, and Lamiaceae in our study area). Nests of *H. fertoni* were parasitized by five species, the golden wasp *Chrysura hybrida*, the cuckoo bee *Dioxys moesta*, the velvet ants *Stenomutilla collaris* and *Stenomutilla hotentotta*, and the bee-fly *Anthrax aethiops*; nests of *O. ferruginea* were parasitized by the sapygid wasp *Sapyga quinquepunctata* and *A. aethiops*. Except for *C. hybrida* these are newly recorded host-parasite associations. Our results confirm previous information and bring new findings on the ecology of both species.

Keywords

Spain, Lleida, *Hoplitis fertoni*, *Osmia ferruginea*, parasitoid, cleptoparasite, pollen specialization

Introduction

Bees (Anthophila/Apiformes) are a very speciose clade of Hymenoptera, with more than 20,000 species worldwide (Michener 2007). Most of these species are solitary and build their nests underground (Michener 2007; Danforth et al. 2019). However, about a third of the solitary bee species nest above-ground, mostly in pre-established cavities (Bogusch and Horák 2018). Among these, a small group of species have specialized in nesting in empty gastropod shells. This behaviour is widespread in the Old World (Müller et al. 2018), including the Palaearctic and Southern Africa (Gess and Gess 1999, 2008), but much rarer in the New World (Michener, 2007). In Europe about 30 species in the genera *Osmia*, *Hoplitis*, *Protosmia* and *Rhodantidium* are known to construct nest in gastropod shells. The majority of these species have distributions restricted to the southernmost part of the continent (Müller 1994; Müller et al. 2018). Most of these species are very specialized in their nesting substrate choice and rarely use other cavity types (but see Bosch et al. 1993). The nesting biology of species occurring in central Europe is fairly well-known. Several species display a series of behaviours related to the manipulation, translocation, and camouflaging of the nest shells (Bellmann 1981; Müller et al. 2018). Various species of *Chrysura* golden wasps have been reported as parasitoids of these species (Müller 1994; Westrich 2018; Bogusch et al. 2019). However, the nesting biologies of species occurring only in southern Europe remain poorly known (Müller et al. 2018). During our studies on shell-nesting bees near Lleida (Catalonia) in northeast Spain we collected a good number of nests of *Hoplitis fertoni* and *Osmia ferruginea*, two species with a Mediterranean distribution.

Hoplitis fertoni occurs in North Africa, Spain, Portugal, and Sicily, and may be locally abundant. It builds its nests in shells of large snail species (such as *Eobania*, *Otala* and *Theba*), and uses mud to build brood cell partitions and to close the nest (Ferton 1908; Le Goff 2003; Müller et al. 2018). *H. fertoni* nests in spring and does not move or cover its nesting shells (Le Goff 2003). Cuckoo wasps *Chrysura hybrida*, *Chrysura cuprea* and *Chrysura trimaculata* are parasitoids of *Hoplitis fertoni* and several other bees nesting in empty shells (Berland and Bernard 1938; Petit 1969, 1980; Le Goff 2003; Wiśniewski 2014).

Osmia ferruginea occurs in all countries around the Mediterranean and may be locally common in the West-Mediterranean region (Müller 2019). It flies in the spring and utilizes shells of a high number of snail species of various sizes, where it builds 1–10 brood cells separated by partitions of masticated plant matter (Ferton 1905; Saunders 1908; Alfken 1914; Benoist 1931; Mavromoustakis 1952; Grandi 1961; Haesslerer 1997; Moreno-Rueda et al. 2008). Although this species is widespread in South Europe, no associated parasitoid species are known (Müller 2019).

Here, we describe the nest structure of *Hoplitis fertoni* and *Osmia ferruginea*, and report on the snail shells used and the pollens collected by these two species. We also report on several parasitoids and nest cleptoparasites reared from the collected nests. We discuss our results in relation to previous information available for these two species (Ferton 1905, 1908; Benoist 1931; Grandi 1961; Haessler 1997; Le Goff 2003; Moreno-Rueda et al. 2008; Müller et al. 2018; Müller 2019).

Methods

In March 2019 we collected more than 500 large gastropod shells (the size of semiadult *Cerneuella virgata*, 8 mm, or bigger) in 10 semi-natural sites with high shell availability around almond orchards near Lleida. We also collected 434 shells in three additional localities in which shell availability was lower. Some of the shells contained *Hoplitis fertoni* nests built in the previous year (with cocoons). Other shells contained fresh *Osmia ferruginea* nests (with provisions and eggs/larvae).

Hoplitis fertoni nests were dissected 0–8 days after collection. The number of brood cells, their shape and positions within the shell and the number of larvae, pupae and adults were recorded. Some remnants of pollen provisions were collected and placed inside plastic micro-tubes for later identification. Some *O. ferruginea* nests were also dissected 0–8 days after collection. The rest were dissected at biweekly intervals until May 11th, when all nests contained mature larvae in cocoons (prepupae). All brood was kept under laboratory conditions until adult eclosion which occurred by September the same year. The cocoons were opened in September 2019, when all bees and their parasites developed into adults and were alive inside the cocoons, two specimens of the brood parasite *Sapyga quinquepunctata* spontaneously hatched and left the cocoons a few days before we opened them.

Pollen samples were prepared using a standard acetolysis method (Moore et al. 1991). Pollen were boiled for 5 min. in an acetolysis mixture of sulphuric acid (H₂SO₄) and acetic anhydride (CH₃CO)₂O (1 : 9 ratio). Samples were then transferred to a mixture of water and glycerol. Slides were observed at 400× magnification. Pollen grains were determined using pollen identification keys (Punt and Clarke 1984; Moore et al. 1991; Reille 1992; Beug 2004) and the reference collection of the Institute of Botany of the Czech Academy of Sciences.

Photos of shells containing nests, closing plugs, and dissected nests were taken with a digital camera Nikon Coolpix B500. Photos of larvae, brood cells, and nest details were taken with a digital camera Canon EOS 550 and a macro-objective equipped with LED goose-neck light. Final figures were created from multiple level-photos stacked by Zerene Stacker software. We drew figures of nest structure using pen-drawing and colouring in Adobe Photoshop. Photos of pollen grains were taken under a light microscope Delphi X-Observer DX 2153-PLi with a camera Moticam 5+ and software for photo analysis.

Results

Hoplitis fertoni

Nest structure. We collected 35 gastropod shells with nests of *H. fertoni* in three of the 13 localities surveyed. All of the localities were situated in dry hilly region. All shells were found on the ground surface and were not hidden. The closing plug was made of soil of light-brownish or greyish colour (Fig. 1A). In most nests (32) the closing plug was placed at the shell aperture. In the remaining three shells it was placed a few mm inside the shell. Several nests had a vestibular (empty) cell below the plug. The rest of the shell was filled with brood cells. Some nests had one or more empty intercalary cells. The brood cell walls were fully lined with soil and inter-cell partitions were double (Fig. 1D). The brood cells were arranged longitudinally along the spire of the shell cavity but some nests had two or more cells arranged transversally close to the nest aperture. Brood cell partitions were 2–5 mm thick (mean 2.6 mm) and the closing plug 3,5–8 mm thick (mean 4.9 mm) (Fig. 1D).

Shell choice. The majority (26, 74.3%) of the nests were built in shells of *Sphincterochila candidissima*. Other snail species used were *Eobania vermiculata* (4, 11.4%), *Cerneuella* sp. (3, 8.6%) and *Otala lactea* (1, 2.9%). The 35 nests collected contained 217 brood cells (mean \pm SD: 6.2 ± 2.24 ; range: 2–10 brood cells per nest). The nests in *S. candidissima* shells contained 4–9 brood cells (mean 6.4, median 7), and those in *E. vermiculata* shells 5–10 brood cells (mean 5.8, median 6). Nests in the smaller *Cerneuella* sp. shells contained fewer cells (range 2–3, mean 2.3, median 2).

Nest associates. Altogether 58 (26.7%) brood cells contained dead, dry or mouldy contents. Of the remaining brood cells, 126 contained pupae or adults of *H. fertoni*, and 33 were parasitized (25.8% of brood cells containing live insects). The golden wasp *Chrysura hybrida* (Chrysididae) was the most common parasitoid (21 cells in 14 nests). Cells parasitized by *C. hybrida* were recognizable by the presence of a semi-transparent brownish cocoon with a whitish spot within the thicker brownish cocoon of *H. fertoni*. We also found five nests parasitized by the velvet ant *Stenomutilla collaris* (seven cells) and one nest by *Stenomutilla hotentotta* (one cell) (Mutillidae). Velvet ants pupated and became adults by late spring (late May – June). *Stenomutilla* cocoons were very similar to those of *C. hybrida* but harder and darker and did not have whitish marks. We also found three nests parasitized by the cuckoo bee *Dioxys moesta* (Megachilidae) (one cell per nest). The cocoons of this species were composed of a single whitish layer sparsely covered with dark brownish faecal particles. Pupation and adult eclosion occurred more or less at the same time as in *H. fertoni*. Finally, we found one nest with one cell parasitized by the bee-fly *Anthrax aethiops* (Bombyliidae). The structure of all nests is illustrated in Fig. 2.

Pollen contents. We analysed pollen samples (remnants of unconsumed provisions) from six nests from two localities (S35 and S37). All pollen grains identified were *Lithodora fruticosa* (Boraginaceae) (Fig. 3A). During of March 2019 we repeatedly observed *Hoplitis fertoni* females collecting pollen only on flowers of this species in various localities.

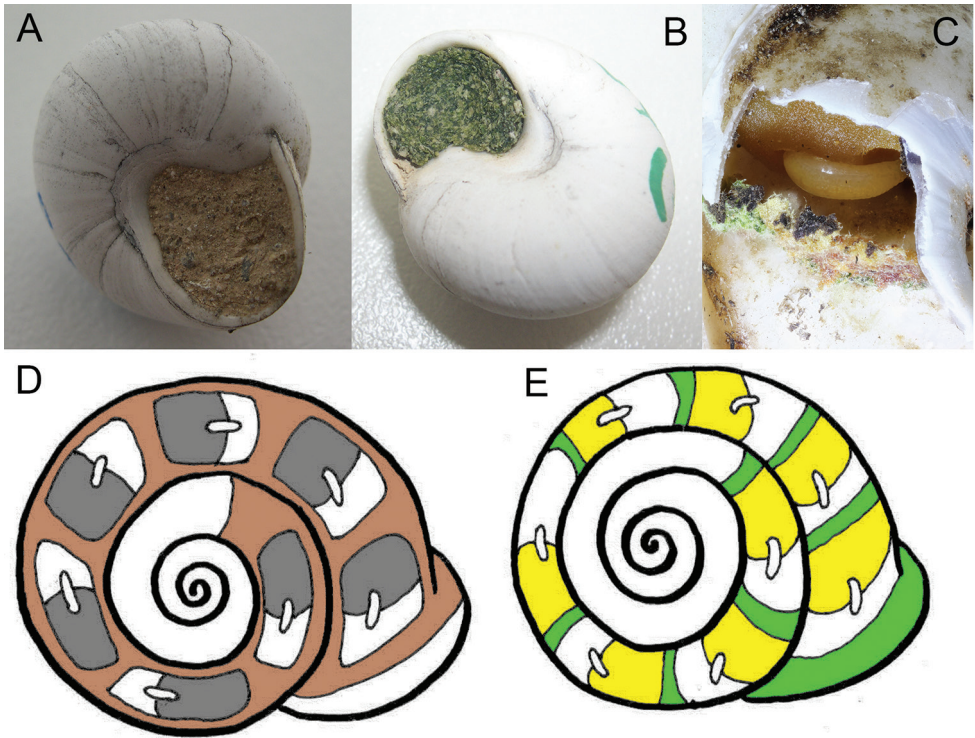


Figure 1. Structure of *Hoplitis fertoni* (A, D) and *Osmia ferruginea* (B, C, E) nests A shell of *Sphincterochila candidissima* with nest of *H. fertoni* B shell of *S. candidissima* with nest of *O. ferruginea* C larva of *O. ferruginea* on pollen-nectar provision D nest structure of *H. fertoni* E nest structure of *O. ferruginea*. Photos and drawings by P. Bogusch.

Osmia ferruginea

Nest structure. We collected 58 shells with nests of *O. ferruginea* in nine of the 13 localities surveyed. Most nests (48) were collected in the localities of a dry hilly area. The remaining 10 nests were collected in the river floodplains. All nests were found exposed (not hidden) at ground level. The surface of the shells had no traces of masticated leaf matter. The closing plug was made of green masticated leaf matter (Fig. 1B). In most nests (38) it was placed at the shell aperture, but in some it was placed inside the shell. All nests had a vestibular (empty) cell below the plug. Brood cells were separated by narrow single partitions of masticated plant matter and the side walls of the brood cells were not lined (Fig. 1C). At the time nests were dissected (March 2019), each cell contained a yellow to light yellow spherical pollen provision with an egg or a young larva (Fig. 1C). The brood cells were always placed longitudinally along the spire of the shell. Brood cell partitions were around 1 mm thick and the closing plug 1.5–3 mm thick (mean 2.1 mm) (Fig. 1E).

Shell choice. Most nests (28, 48.3%) were built in *Sphincterochila candidissima* shells. The remaining nests were placed in shells of *Eobania vermiculata* (13, 22.4%),

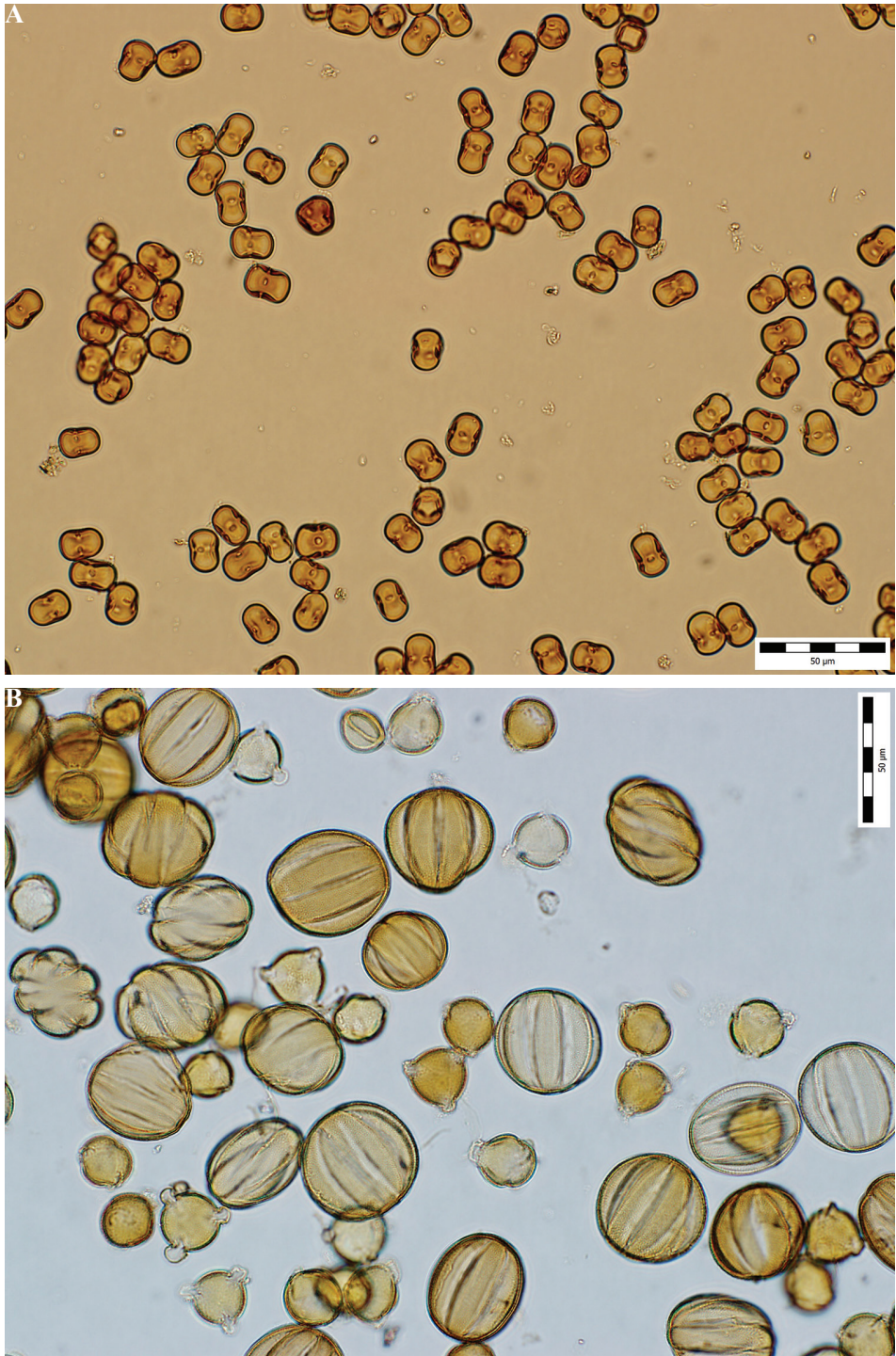


Figure 3. **A** Macrophotography of pollen of *Lithodora fruticosa* from a *Hoplitis fertoni* nest (locality S35). Photo by L. Petr. **B** macrophotography of pollen from an *Osmia ferruginea* nest (locality S7). Larger pollen grains are *Thymus vulgaris*; smaller grains are *Cistus albidus*. Photo by L. Petr.

Table 1. Pollen composition of six provision samples from *Osmia ferruginea* nests.

| Site | Pollen contents |
|------|--|
| S35 | <i>Cistus albidus</i> (Cistaceae) ca. 100%, Asteraceae and <i>Thymus vulgaris</i> (Lamiaceae) |
| S37 | <i>Cistus albidus</i> (Cistaceae) 37 %, <i>Cytisus scoparius</i> (Fabaceae) 37 %, <i>Olea europaea</i> (Oleaceae) 26 % |
| S37 | <i>Cistus albidus</i> (Cistaceae) 50%, <i>Cytisus scoparius</i> (Fabaceae) 40%, <i>Olea europaea</i> (Oleaceae) 10% |
| S7 | <i>Cistus albidus</i> (Cistaceae) 48 %, <i>Cytisus scoparius</i> (Fabaceae) 27 %, <i>Olea europaea</i> (Oleaceae) 22 %, <i>Thymus vulgaris</i> (Lamiaceae) 12 %, contamination of three pollen types of Asteraceae |
| S7 | <i>Thymus vulgaris</i> (Lamiaceae) 51 %, <i>Cytisus scoparius</i> (Fabaceae) 49 % |
| S7 | <i>Cytisus scoparius</i> (Fabaceae) 77 %, <i>Thymus vulgaris</i> (Lamiaceae) 23 % |

T. pisana contained fewer cells (range 1–5, mean 2.1, median 2 and range 2–3, mean 2.5, median 2–3, respectively).

Nest associates. Altogether 56 (20.9%) of the brood cells contained dead, dry or mouldy contents. Most of the remaining brood cells (203) contained pupae or adults of *O. ferruginea*, while 19 contained parasitoids (9% of brood cells containing alive insects). The main parasitoid species was *Sapyga quinquepunctata* (Sapygidae; 18 cells from 11 nests, all from locality S7; 19% parasitism). All the individuals of this cleptoparasitic species reached adulthood by late summer or beginning of autumn (September). Brood cells parasitized by *S. quinquepunctata* were recognizable by the dark brown oval-shaped cocoon, distinct from the cubic cocoons of *O. ferruginea*. The bombyliid *Anthrax aethiops* was recorded in a single cell of one nest. The structure of all nests is illustrated on Fig. 2.

Pollen contents. We analysed six pollen samples from nests collected at three different localities. Most pollen grains were of Cistaceae, Fabaceae (*Cytisus* type), and Lamiaceae (Table 1; Fig. 3B).

Discussion

Nest structures of both species correspond to the nest descriptions published by previous authors (Ferton 1905, 1908; Benoist 1931; Grandi 1961; Haesslerer 1997; Le Goff 2003; Moreno-Rueda et al. 2008; Müller et al. 2018; Müller 2019). Both *Hoplitis fertoni* and *Osmia ferruginea* belong to the group of species building high numbers of brood cells per nest. Most bee species nesting in empty gastropod shells build low numbers of brood cells per shell (usually only one or two) (see Müller et al. 2018). The number of brood cells per nest in both *Hoplitis fertoni* and *Osmia ferruginea* is highly variable depending on the size of the shell utilized. Compared to other middle-sized bee species such as *Osmia rufohirta*, which usually nests in shells of *Xerolenta obvia* and builds one brood cell per nest (Bellmann 1981; Müller et al. 2018; Heneberg et al. 2020), *Hoplitis fertoni* and *Osmia ferruginea* seem to prefer bigger shells (specially *Sphincterochila candidissima*) and build a higher number of cells per nest. *S. candidissima* has also been reported as the most commonly used shell in other studies on shell-nesting bees (Moreno-Rueda et al. (2008), Bogusch et al. (in press).

The number of parasitic species associated with *H. fertoni* (5) in our study is remarkable. The most common parasitoid, *Chrysura hybrida* was already recorded on *H. fertoni* by Le Goff (2003). This species has been associated to several other Osmiini, nesting either in snail shells (*Osmia versicolor*, *Osmia viridana*) or in other types of cavities (*Hoplitis anthocopoides*, *Hoplitis benoisti*, *Hoplitis ravouxi*, *Osmia caeruleascens*, and *Anthocopa villosa*) (Berland and Bernard 1938; Grandi 1961; Petit 1969, 1980). Most of these records are based on observations of the bee and the wasp co-occurring at a given locality but, together with our findings, they suggest that *C. hybrida* specializes on smaller Osmiini, irrespective of the nesting substrate. Other species of *Chrysura* also parasitize bees of the family Megachilidae, and many of them appear to show a strong preference for bees nesting in snail shells (see Müller et al. 2018).

We also reared two species of velvet ants from the nests of *H. fertoni*. Velvet ants are ectoparasitoids and usually have a broad host spectrum. Some species preferentially parasitize either bees or wasps, but others have been recorded on both guilds of hymenopterans (Lelej 1985; Brothers 1989; O'Neill 2001). The biology of *Stenomutilla* is not well-known, but several authors have reported associations with solitary wasps, megachilid bees and chrysomelid beetles of the subfamily Clytrinae (Giner Marí 1944; Brothers 1989). Thus, it is likely that both species of *Stenomutilla* recorded in our study parasitize a wide range of bees and possibly wasps. However, in a broader study in the same geographical area we have examined hundreds of nests of more than ten snail-nesting bees and we found *Stenomutilla* only in nests of *H. fertoni* (Bogusch et al., in press).

The bee-fly *Anthrax aethiops*, has been recorded as a parasitoid in nests of more than ten bee species, some of them nesting in gastropod shells (Austen 1937; Du Merle 1972; Peeters et al. 2012; Müller et al. 2018). Heneberg et al. (2020) found this species to be a frequent parasitoid of *Osmia spinulosa* and two other species nesting in gastropod shells. This parasitoid has probably a broad host spectrum mostly including megachilid bees but also other bees. Although this species has only been reported as a parasitoid of bees, many other representatives of this family are beside bees parasitoids of crabronid wasps (Yeates and Greathead 1997; Bogusch et al. 2015).

Dioxys moesta is a cuckoo bee occurring in south Europe and North Africa. Its host spectrum is unknown. Other *Dioxys* species in Europe and neighbouring regions, are cleptoparasitic on bees of the family Megachilidae, mostly *Hoplitis* and *Osmia* (Westrich 2018), but up to now they were not known to parasitize species nesting in shells. The question whether *D. moesta* specializes on shell-nesting species remains open.

Sapyga quinquepunctata is an unspecialized cleptoparasite in nests of several Megachilidae (Stöckhert 1933; Vicens et al. 1993; Vicens et al. 1994; Gusenleitner and Gusenleitner 1994; Osorio et al. 2018; Müller et al. 2018; Torné-Noguera et al. 2020). Although it has been reared from nests of *Osmia bicolor* (Westrich 2018; Heneberg et al. 2020), it does not appear to be common in nests of shell-nesting species (Bogusch et al. 2019; Heneberg et al. 2020). Our findings of *S. quinquepunctata* and *Anthrax aethiops* in nests of *O. ferruginea* represent the first records of nest parasitism in this species.

Analysis of the pollen provisions yielded contrasting results for the two species studied. Previous studies have reported *Echium* (Boraginaceae) as the only pollen

source of *H. fertoni* (Le Goff 2003, Sedivy et al. 2013; Müller 2019). Both pollen analysis and field observations indicate that in the study area this species visits another Boraginaceae, *Lithodora fruticosa*. Thus, with the information currently available, *H. fertoni* should be considered oligolectic on Boraginaceae, just like most species of the *Hoplitis adunca* species-group (Müller 2019). We have also observed flowering *L. fruticosa* at five localities studied, and three females of *H. fertoni* in three localities (one in each) were observed on flowers of this plant. No species of *Echium* was in flower during our studies (middle March 2019) so *L. fruticosa* is probably the only useful source of pollen for first females of *H. fertoni* provisioning their nests. In other regions, the situation can be different and this species can specialize on other pollen sources, especially of genus *Echium* (as was published by Le Goff 2003 and Müller et al. 2018). *H. fertoni* lacks any of the morphological adaptations usually present in bees that harvest pollen from flowers with included anthers, so it is a question how it is able to efficiently exploit these flowers. Perhaps some behavioral trick that might be revealed by detailed field observation. On the other hand, our results confirm that *O. ferruginea* is a polylectic species with preference for the Fabaceae (Müller 2019). In our nests, all provisions analyzed contained pollen from several plant families. Other species in the subgenus *Pyrosmia* are usually polylectic, but several are oligolectic on Fabaceae (Müller 2019).

The biology of shell-nesting bees from south Europe is poorly known. Our study contributes to filling this gap by providing new records of parasites and pollen use, as well life history and nesting behaviour traits. Interestingly, some of these traits are shared with bees of the same taxa nesting in other types of cavities. For example, *Hoplitis adunca* also lines cell walls, builds double inter-cell partitions and is oligolectic on Boraginaceae (Bosch et al. 2001). For the most part, parasites recorded in this study also seem to be shared by species nesting in other substrates. Nesting behaviour, pollen preferences and host-parasite associations are important sources of information for the reconstruction of phylogenies and for tracking the evolution of behavioural traits in Megachilid bees (Müller 1996; Bosch et al. 2001; Sédivy et al. 2008, Litman et al. 2011; González et al. 2019).

Acknowledgements

We would like to thank Guido Pagliano (Italy) for providing keys on Mutillidae, Lucy Boulton (UK) for the help with the English, and Georgina Alins and Neus Rodriguez-Gasol (IRTA, Lleida) for help with shell collection in the field. This study was supported by the Specific Research Project of University of Hradec Králové Nr. 2101/2019.

References

Alfken JD (1914) Beitrag zur Kenntnis der Bienenfauna von Algerien. Mémoires de la Société Entomologique Belgique 22: 185–237.

- Austen EE (1937) Bombyliidae of Palestine. British Museum of Natural History, London, 188 pp.
- Bellmann H (1981) Zur Ethologie mitteleuropäischer Bauchsammlerbienen (Hymenoptera, Megachilidae): *Osmia bicolor*, *O. aurulenta*, *O. rufobirta*, *Anthidium punctatum*, *Anthidium strigatum*, *Trachusa byssina*. Veröffentlichungen für Naturschutz und Landschaftspflege Baden-Württemberg 53: 477–540.
- Benoist R (1931) Les osmies de la faune française (Hymenopt. Apidae). Annales de la Société Entomologique de France 100: 23–60.
- Berland L, Bernard F (1938) Hyménoptères vespiformes. III. (Cleptidae, Chrysidae, Trigonalidae). Faune de France (Vol. 34). Office Central de Faunistique. Fédération Française des Société des Sciences Naturelles Le Chevalier, Paris, 145 pp.
- Beug HJ (2004) Leitfaden der Pollenbestimmung für Mitteleuropa und Angrenzende Gebiete. Verlag Dr. Friedrich Pfeil, München, 542 pp.
- Bogusch P, Astapenková A, Heneberg P (2015) Larvae and Nests of Six Aculeate Hymenoptera (Hymenoptera: Aculeata) Nesting in Reed Galls Induced by *Lipara* spp. (Diptera: Chloropidae) with a Review of Species Recorded. PLoS ONE 10(6): e0130802. <https://doi.org/10.1371/journal.pone.0130802>
- Bogusch P, Hlaváčková L, Rodriguez-Gasol N, Alins G, Heneberg P, Bosch J (in press) Near-natural habitats near almond orchards with presence of empty gastropod shells are sufficient for solitary shell-nesting bees and wasps. Agriculture, Ecosystems and Environment, submitted.
- Bogusch P, Horák J (2018) Saproxylid Bees and Wasps. In: Ulyshen M (Ed.) Saproxylid Insects. Diversity, Ecology and Conservation. Zoological Monographs, Springer Books, 217–235. https://doi.org/10.1007/978-3-319-75937-1_7
- Bogusch P, Roháček J, Baňar P, Astapenková A, Kouklík O, Pech P, Janšta P, Heller K, Hlaváčková L, Heneberg P (2019) The presence of high numbers of empty shells in anthropogenic habitats is insufficient to attract shell adopters among the insects. Insect Conservation and Diversity 12: 193–205. <https://doi.org/10.1111/icad.12335>
- Bosch J, Maeta Y, Rust RW (2001) A phylogenetic analysis of nesting behavior in the genus *Osmia* (Insecta, Hymenoptera, Megachilidae). Annals of the Entomological Society of America 94: 617–627. [https://doi.org/10.1603/0013-8746\(2001\)094\[0617:APAONB\]2.0.CO;2](https://doi.org/10.1603/0013-8746(2001)094[0617:APAONB]2.0.CO;2)
- Brothers DJ (1989) Alternative life-history styles of mutillid wasps (Insecta, Hymenoptera). In: Bruton M (Ed.) Alternative Life-History Styles of Animals. Springer, Dordrecht, 279–291. https://doi.org/10.1007/978-94-009-2605-9_14
- Danforth BN, Minckley RL, Neff JL (2019) The Solitary Bees: Biology, Evolution, Conservation. Princeton University Press, Princeton. <https://doi.org/10.2307/j.ctvd1c929>
- Du Merle P (1972) Quelques données sur la biologie des Diptères Bombyliidae. Bulletin de la Société entomologique de France 77(7–8): 190–201.
- Ferton C (1905) Notes détachées sur l'instinct des hyménoptères mellifères et ravisseurs (3ème série) avec la description de quelques espèces. Annales de la Société Entomologique de France 74: 56–104. [pl. 3–4]
- Ferton C (1908) Notes détachées sur l'instinct des hyménoptères mellifères et ravisseurs (4ème série) avec la description de quelques espèces. Annales de la Société Entomologique de France 77: 535–586.

- Gess FW, Gess SK (1999) The use by wasps, bees and spiders of shells of *Trigonephrus* Pilsb. (Mollusca: Gasteropoda: Dorcasiidae) in desertic winter-rainfall areas in southern Africa. *Journal of Arid Environments* 43: 143–153. <https://doi.org/10.1006/jare.1999.0549>
- Gess SK, Gess FW (2008) Patterns of usage of snail shells for nesting by wasps (Vespidae: Masarinae and Eumeninae) and bees (Megachilidae: Megachilinae) in Southern Africa. *Journal of Hymenoptera Research* 17: 86–109.
- Giner Marí J (1944) Himenópteros de España. Fams. Apterogynidae y Mutillidae. Instituto Espanol de Entomologia, Madrid, 124 pp.
- Grandi G (1961) Studi di un entomologo sugli imenotteri superiori. *Bollettino dell'Istituto di Entomologia dell'Università di Bologna* 25: 1–659.
- Gonzalez VH, Gustafson GT, Engel MS (2019) Morphological phylogeny of Megachilini and the evolution of leaf-cutter behavior in bees (Hymenoptera: Megachilidae). *Journal of Melittology* 85: 1–123. <https://doi.org/10.17161/jom.v0i85.11541>
- Gusenleitner F, Gusenleitner J (1994) Das Vorkommen der Familie Sapygidae in Österreich (Insecta: Hymenoptera: Sapygidae). *Annalen der Naturhistorischen Museums in Wien* 96B: 173–188.
- Haeseler V (1997) *Osmia rutila*, a wild bee occurring in the coastal area of the southwest Mediterranean where it is now in danger of extinction. In: Garcia Nova F, Crawford RMM, Diaz Barradas MC (Eds) *The Ecology and Conservation of European Dunes*. Ciencias, Sevilla, 169–183.
- Heneberg P, Bogusch P, Hlaváčková L (2020) Experimental confirmation of empty snail shells as limiting resources for specialized bees and wasps. *Ecological Engineering* 142: 105640. <https://doi.org/10.1016/j.ecoleng.2019.105640>
- Le Goff G (2003) Note sur la nidification d'*Hoplitis (Hoplitis) feroni* Pérez dans la province d'Alicante (Espagne) (Hymenoptera; Apoidea, Megachilidae; Osmiini). *L'Entomologiste* 59: 97–102.
- Lelej AS (1985) Mutillidae (Hymenoptera) of the USSR and neighboring countries. Nauka, Leningrad, 268 pp. [in Russian]
- Litman JR, Danforth BN, Eardley CD, Praz CJ (2011) Why do leafcutter bees cut leaves? New insights into the early evolution of bees. *Proceedings of the Royal Society B* 278: 3593–3600. <https://doi.org/10.1098/rspb.2011.0365>
- Mavromoustakis GA (1952) On the bees (Hymenoptera, Apoidea) of Cyprus. Part III. *The Annals and Magazine of Natural History (London)*, ser. 12, 5: 814–843. <https://doi.org/10.1080/00222935208654357>
- Michener CD (2007) *The Bees of the World* (2nd edn.). Johns Hopkins University Press, Baltimore, 992 pp.
- Moore PD, Webb JA, Collingson ME (1991) *Pollen Analysis* (2nd edn.). Blackwell Scientific Publications, Oxford, 216 pp.
- Moreno-Rueda G, Marfil-Daza C, Ortiz-Sanchez FJ, Melic A (2008) Weather and the use of empty gastropod shells by arthropods. *Annales de la Société entomologique del France* 44: 373–377. <https://doi.org/10.1080/00379271.2008.10697573>
- Müller A (1994) Die Bionomie der in leeren Schneckengehäusen nistenden Biene *Osmia spinulosa* (Kirby 1802) (Hymenoptera, Megachilidae). *Veröffentlichungen für Naturschutz und Landschaftspflege Baden-Württemberg* 68/69: 291–334.
- Müller A (1996) Host-plant specialization in Western Palearctic Anthidiine bees (Hymenoptera: Apoidea: Megachilidae). *Ecological Monographs* 66: 235–257. <https://doi.org/10.2307/2963476>

- Müller A (2019) Palaearctic Osmiine Bees, ETH Zürich. <http://blogs.ethz.ch/osmiini>
- Müller A, Praz C, Dorchin A (2018) Biology of the Palaearctic *Wainia* bees of the subgenus *Caposmia* including a short review on snail shell nesting in osmiine bees (Hymenoptera, Megachilidae). *Journal of Hymenoptera Research* 65: 61–89. <https://doi.org/10.3897/jhr.65.27704>
- O'Neill K (2001) *Solitary Wasps: Behavior and Natural History*. Cornell University Press, Ithaca and New York, 406 pp.
- Osorio S, Arnan X, Bassols E, Vicens N, Bosch J (2018) Seasonal dynamics in a cavity-nesting bee-wasp community: shifts in composition, functional diversity and host-parasitoid network structure. *PLoS ONE* 13(10): e0205854. <https://doi.org/10.1371/journal.pone.0205854>
- Peeters TMJ, Nieuwenhuijsen H, Smit J, Van der Meer F, Raemakers IP, Heitmans WRB, Van Achterberg C, Kwak M, Loonstra AJ, De Rond J, Roos M, Reemer M (2012) *De Nederlandse bijen*. Naturalis Biodiversity Center & European Invertebrate Survey, Leiden, 544 pp.
- Petit J (1969) Notes sur quelques Hyménoptères rares recoltés en Haute Belgique. *Lambillionea* 67: 70–74.
- Petit J (1980) Hyménoptères Aculéates intéressants pour la faune de la Belgique et des régions limitrophes. *Lambillionea* 79: 56–61.
- Punt W, Clarke GCS (1984) *The Northwest European Pollen Flora, IV*. Elsevier, Amsterdam, 364 pp.
- Reille M (1992) *Pollen et Spores d'Europe et d'Afrique du nord*. Laboratoire de Botanique Historique et Palynologie, Marseille, 543 pp.
- Saunders E (1908) Hymenoptera aculeata collected in Algeria by the Rev. A.E. Eaton, M.A., F.E.S. and the Rev. Francis David Morice, M.A., F.E.S. Part III. Anthophila. *Transactions of the Entomological Society of London* 1908: 177–274.
- Sedivy C, Praz CJ, Müller A, Widmer A, Dorn S (2008) Patterns of host-plant choice in bees of the genus *Chelostoma*: the constraint hypothesis of host-range evolution in bees. *Evolution* 62: 2487–2507. <https://doi.org/10.1111/j.1558-5646.2008.00465.x>
- Sedivy C, Dorn S, Widmer A, Müller A (2013) Host range evolution in a selected group of osmiine bees (Hymenoptera: Megachilidae): the Boraginaceae-Fabaceae paradox. *Biological Journal of the Linnean Society* 108: 35–54. <https://doi.org/10.1111/j.1095-8312.2012.02013.x>
- Stöckert FK (1933) *Die Bienen Frankens (Hym. Apid.)*. Eine ökologisch-tiergeographische Untersuchung. Beiheft Deutsche Entomologische Zeitschrift 1932: 1–294.
- Torné-Noguera A, Arnan X, Rodrigo A, Bosch J (in press) Spatial variability of hosts, parasitoids and their interactions across a homogeneous landscape. *Ecology & Evolution*.
- Vicens N, Bosch J, Blas M (1993) Análisis de los nidos de algunas *Osmia* (Hymenoptera, Megachilidae) nidificantes en cavidades preestablecidas. *Orsis* 8: 41–52.
- Vicens N, Bosch J, Blas M (1994) Biology and population structure in *Osmia tricornis* Latr. (Hymenoptera, Megachilidae). *Journal of Applied Entomology* 117: 300–306. <https://doi.org/10.1111/j.1439-0418.1994.tb00738.x>
- Westrich P (2018) *Die Wildbienen Deutschlands*. Eugen Ulmer, Stuttgart, 842 pp.
- Wiśniowski B (2014) Cuckoo Wasps (Hymenoptera: Chrysididae) of Poland. Ojców National Park, Ojców.
- Yeates DK, Greathead D (1997) The evolutionary pattern of host use in the Bombyliidae (Diptera): a diverse family of parasitoid flies. *Biological Journal of the Linnean Society* 60: 149–185. <https://doi.org/10.1111/j.1095-8312.1997.tb01490.x>

The genus *Lepisiota* Santschi, 1926 of the Arabian Peninsula with the description of a new species, *Lepisiota elbazi* sp. nov. from Oman, an updated species identification key, and assessment of zoogeographic affinities

Mostafa R. Sharaf^{1,2}, Abdulrahman S. Aldawood¹,
Amr A. Mohamed³, Francisco Hita Garcia⁴

1 Department of Plant Protection, College of Food and Agriculture Sciences, King Saud University, Riyadh, Kingdom of Saudi Arabia **2** Division of Invertebrate Zoology, American Museum of Natural History, New York, USA **3** Department of Entomology, Faculty of Science, Cairo University, PO Box 12613, Giza, Egypt **4** Biodiversity and Biocomplexity Unit, Okinawa Institute of Science and Technology Graduate University, Onna-son, Okinawa, Japan

Corresponding author: Mostafa R. Sharaf (antsharaf@gmail.com, mosharaf@ksu.edu.sa)

Academic editor: P. Klimeš | Received 16 January 2020 | Accepted 17 March 2020 | Published 27 April 2020

<http://zoobank.org/4D85CF52-8E50-4D9D-A0E1-38F5E26B6561>

Citation: Sharaf MR, Aldawood AS, Mohamed AA, Hita Garcia F (2020) The genus *Lepisiota* Santschi, 1926 of the Arabian Peninsula with the description of a new species, *Lepisiota elbazi* sp. nov. from Oman, an updated species identification key, and assessment of zoogeographic affinities. Journal of Hymenoptera Research 76: 127–152. <https://doi.org/10.3897/jhr.76.50193>

Abstract

This study updates and summarizes information on the taxonomy and status of the Arabian *Lepisiota* fauna. We describe and illustrate the new species *Lepisiota elbazi* sp. nov. from the Dhofar Governorate, Oman based on the worker caste. The new species is closest to the Arabian species, *L. arabica* Collingwood, 1985 from the southwestern mountains of the Kingdom of Saudi Arabia (KSA) and can be separated by having fewer body hairs (two pairs on the posterior margin of the head, two or three pairs on the promesonotum and, one or two pairs on the first gastral tergite), the longer head, scapes, and propodeal spines, and the shorter mesosoma. We present the first illustrated key to the worker caste of the Arabian species of *Lepisiota* using stacked digital color images to facilitate species determination. The new species is probably endemic to the Dhofar Governorate and seems rare. An up-to-date synoptic checklist of 21 spe-

cies representing the Arabian *Lepisiota* Santschi, 1926 is emended based upon the most recent literature in ant systematics. Five species are excluded from the Arabian *Lepisiota* fauna, *L. arenaria* (Arnold, 1920), *L. erythraea* (Forel, 1910), *L. incisa* (Forel, 1913), *L. sericea* (Forel, 1892a), and *L. simplex* (Forel, 1892) for issues related to previous species misidentification. *Lepisiota carbonaria* (Emery, 1892) is proposed as a senior synonym of *L. depilis* (Emery, 1897) **syn. nov.** The faunal composition of *Lepisiota* species recorded from the Arabian Peninsula can be divided/delineated into two main groups according to their zoogeographical relationships; (1) Afrotropical (11 species--52.38%); (2) Palearctic (10 species--47.62%) elements whereas eight species (~38%) are Arabian endemics.

Keywords

Afrotropical Region, Arabian Peninsula, endemism, Formicinae, key, Middle East, new species, Palearctic Region, zoogeography

Introduction

With 135 described species and subspecies, the ant genus *Lepisiota* Santschi, 1926 is one of the most diverse genera of the subfamily Formicinae (Bolton 2020). Most species are broadly spread worldwide in the grasslands, savannahs or woodlands of the Afrotropical, Indomalayan, and Palearctic regions (Brown 2000; Hita Garcia et al. 2013), where they are found nesting directly into the ground, under stones, or in rotten wood while numerous species attend aphids and coccids (Bolton 1973; Hita Garcia et al. 2013). The genus is diagnosed in the worker caste by the following character states (Bolton 1994): antennae 11-segmented; eyes well-developed, ocelli frequently present but sometimes reduced; propodeum armed with a pair of spines, teeth, or tubercles; petiole a scale-like with the dorsal margin bispinose, bidentate or emarginated; acidopore well-developed.

With the lack of revisionary studies for most of the zoogeographical regions of the World, the taxonomic status of the genus is dreadful. Most contributions are restricted to few treatments including to a limited number of papers including faunal lists, descriptions of new species or taxonomic keys for some regions and countries, such as for the Arabian Peninsula (Collingwood and Agosti 1996; Sharaf et al. 2016), Armenia (Arakelian 1994), the Balkans (Agosti and Collingwood 1987), Bulgaria (Atanassov and Dlussky 1992), China (Wu and Wang 1995; Zhou 2001), Egypt (Finzi 1936), Europe and Algeria (André 1882), India, Sri Lanka and Burma (Bingham 1903), Kingdom of Saudi Arabia (KSA) (Collingwood 1985), and Turkestan (Kuznetsov-Ugamsky 1929).

The *Lepisiota* fauna of Oman is poorly known due to a lack of appropriate specialized research, and the few available records are scattered through the literature or have been gleaned from few field surveys only accidentally or incidentally. *Lepisiota arenaria* (Arnold, 1920) and *L. spinisquama* (Kuznetsov-Ugamsky, 1929) were the first species to be recorded from Oman (Collingwood 1985). However, *L. arenaria* is now excluded from the fauna of the Arabian Peninsula due to misidentification. In their treatment of the ant fauna of the Arabian Peninsula, Collingwood and Agosti (1996) reported 20 species from the region, with ten from Oman, including a description of a new species *L. dhofara* Collingwood and Agosti from the Dhofar Governorate. Sharaf et al. (2016)

described *L. omanensis* Sharaf and Monks from Oman and the United Arab Emirates (UAE) and presented a key to the Arabian *Lepisiota* species.

The Arabian Peninsula, including Oman, sits as a semi-isolated block between Eurasia and Africa that overlaps three of the world's key zoogeographical regions; the Afrotropical (Ethiopian), the Oriental and the Palearctic (Larsen 1984; Delany 1989). It is, certainly, the only area where three such regions intersect. Through the Miocene to the Pliocene, it formed a land bridge between the Afrotropical and Oriental regions, allowing the interchange between the two faunas with a far stronger Afrotropical influence. The Afrotropical forms would have been forced out by invading Palearctic species following the severance of the land bridges and the lowering of temperatures during the Pleistocene glaciations, contracted into relict distributions, or evolved to become what are now southern Arabian endemics. The Palearctic species would have been forced northwards or into mountain refugia through the post-glacial increase in aridity and temperature and the remaining Afro-tropical species would have expanded their ranges.

Across through the Bab el Mandeb straits, further invasions from Africa may have been occurred, perhaps swamping such endemics, but invasions from the Oriental region seem have not occurred (Larsen 1980; Delany 1989). Land features affect species distribution and richness (Bestelmeyer and Schooley 1999; Boulton et al. 2005). Geographically, highlighting Oman, Al-Hajar mountains extended in Northeastern part. While, the Dhofar mountain range extend in the South East to Hadhramaut in Yemen. A large stretch of barren desert, acting as a zoogeographical barrier, lies between them. Boundaries among zoogeographical realms in the Arabian Peninsula is continuously a trending controversial topic (Larsen 1984; Rueda et al. 2013; El-Hawagry and Al Dhafer 2015; Ficetola et al. 2017; El-Hawagry et al. 2019).

Essentially, we describe and illustrate a new *Lepisiota* species from the Dhofar Governorate, Oman based on the worker caste. The data reported herein represents the first real insight into this less studied genus and its assemblages in this nearly isolated region. Besides, a short zoogeographical analysis of *Lepisiota* species from the Arabian Peninsula in relation to the classic zoogeographical realms is given. Such an overview of the zoogeographical affinities of this genus in the region may contribute to the somehow confused issue of the boundaries among the main zoogeographical regions in the Arabian Peninsula. Reasons for the observed spatiotemporal variation in community composition are remarked and notes on species habitat preferences are included.

Material and methods

Measurements

The following measurements and indices follow Sharaf et al. (2016).

EL Eye length; maximum diameter of compound eye measured in oblique lateral view.

- HL Head length; maximum distance from the midpoint of anterior clypeal margin to midpoint of posterior margin of head, measured in full-face view.
- HW Head width; maximum width of head behind eyes in full-face view.
- ML Mesonotum length; maximum length of mesonotum in dorsal view.
- PH Petiole height; measured from petiole sternum to apex in profile.
- PRW Pronotal width; maximum pronotal width in dorsal view.
- PSL Propodeal spine length; in dorsocaudal view the tip of the measured spine, its base, and centre of propodeal concavity between spines must all be in focus. Using a dual-axis micrometre the spine length is measured from tip of spine to a virtual point at its base where spine axis meets orthogonally with a line leading to median point of concavity.
- SL Scape length; maximum scape length excluding basal condyle and neck.
- TL Total length; outstretched body length from mandibular apex to gastral apex in profile.
- WL Weber's length; diagonal length of mesosoma in profile from posteroventral margin of propodeal lobe to anterior most point of pronotal slope, excluding neck.

Indices

- OI Ocular index: $EL / HW \times 100$
- CI Cephalic index: $HW / HL \times 100$
- SI Scape index: $SL / HW \times 100$
- PSLI Propodeal spine index: $PSL / HL \times 100$

Species names and zoogeographical boundaries in this work follow the online catalogue of Bolton (2020). In the present work the term southern Arabian Peninsula refers to the Al Sarawat and the Asir Mountains (KSA), the Hajar Mountains stretching along the northern coast of Oman to the United Arab Emirates (UAE), the Dhofar Governorate (Oman), and Yemen.

Institutional abbreviations

- BMNH** The Natural History Museum (British Museum, Natural History), London, UK.
- KSMA** King Saud University Museum of Arthropods, Plant Protection Department, College of Food and Agriculture Sciences, King Saud University, Riyadh, Kingdom of Saudi Arabia.
- MSNG** Museo Civico di Storia Naturale "Giacomo Doria", Genova, Italy.
- OUMC** Oxford University Museum, Oxford, UK.

Results

Synoptic species list of the Arabian species of *Lepisiota* Santschi, 1926

- Lepisiota arabica* (Collingwood, 1985)
Lepisiota bipartita (Smith, 1861)
Lepisiota canescens (Emery, 1897)
Lepisiota carbonaria (Emery, 1892)
 == *Lepisiota depilis* (Emery, 1897) syn. nov.
Lepisiota dammama Collingwood & Agosti, 1996
Lepisiota dhofara Collingwood & Agosti, 1996
Lepisiota dolabellae (Forel, 1911)
Lepisiota elbazi sp. nov.
Lepisiota elegantissima Collingwood & van Harten, 2011
Lepisiota frauenfeldi (Mayr, 1855)
Lepisiota gracilicornis (Forel, 1892)
Lepisiota harteni Collingwood & Agosti, 1996
Lepisiota karawaiewi (Kuznetsov-Ugamsky, 1929)
Lepisiota nigra (Dalla Torre, 1893)
Lepisiota nigrescens (Karavaiev, 1912)
Lepisiota obtusa (Emery, 1901)
Lepisiota omanensis Sharaf & Monks, 2016
Lepisiota opaciventris (Finzi, 1936)
Lepisiota riyadha Collingwood & Agosti, 1996
Lepisiota spinisquama (Kuznetsov-Ugamsky, 1929)
Lepisiota validiuscula (Emery, 1897)

For zoogeographical affinities analysis, all the listed species were assigned to a zoogeographical realm and analyzed altogether. While some relevant notes and suggestions are given, no systematic attempt has been made to place the current zoogeographical patterns in their historical context.

Key to the Arabian species of the genus *Lepisiota* Santschi

The following illustrated key is based on Collingwood and Agosti (1996) and Sharaf et al. (2016):

- | | | |
|---|---|---|
| 1 | Posterior margin of head distinctly compressed in profile (Fig. 1A) | 2 |
| – | Posterior margin of head convex in profile (Fig. 1B) | 3 |

- 2 Body pilosity abundant, seven pairs of hairs on posterior margin of head, underside of head and petiole each with two pairs, several pairs on mesosomal dorsum (six on promesonotum, four on mesonotum, and two on propodeal dorsum), femur with hairs (Fig. 1C) (KSA) ***L. arabica***
- Body pilosity less abundant, one or two pairs of hairs on posterior margin of head, underside of head and petiole each without hairs, one to three pairs on promesonotum, and one to two pairs on first gastral tergite; femur bare (Fig. 1D) (Oman) ***L. elbazi sp. nov.***
- 3 Antennal scape long, surpassing the posterior margin of head by half its length or more **4**
- Antennal scape shorter, surpassing the posterior margin of head by a third of its length or less **17**
- 4 Dorsum of mesosoma and the first and second gastral tergites without standing hairs (Fig. 1E); antennal scape exceptionally long; SI > 200 **5**
- Dorsum of mesosoma with at least one or two pairs of long hairs on pronotum (Fig. 1F); gaster always with some projecting hairs; antennal scape shorter; SI < 200 **6**
- 5 Uniform dark brown or black-brown species; body parts of moderate lengths (SI 200–205; WL 1.00) (KSA) ***L. riyadha***
- Bicolored species, head and gaster dark brown or black-brown, mesosoma, petiole, antennae and legs orange; body exceptionally long and slender (SI > 375; WL 1.91) (Fig. 2A, B) (Oman, UAE) ***L. elegantissima***
- 6 Bicolored, mesosoma paler than gaster, mainly or entirely reddish **7**
- Whole body dark except a small area of the mesonotum more or less red in a few species **9**
- 7 Body sculpture coarse, general appearance opaque (Fig. 2C) (Greece, India, Iran, Israel, Lebanon) ***L. bipartita***
- All parts of the body shining with superficial reticulate sculpture at most (Fig. 2D) **8**
- 8 Uniform light brown, appendages yellow; mesonotum distinctly narrower anteriorly than posteriorly in dorsal view (Fig. 2E); propodeal and petiolar spines acute (Fig. 2F) (KSA) ***L. dammama***
- Head, petiole and gaster dark brown contrasting with the red mesosoma; mesonotum characteristically rectangular in dorsal view (Fig. 3A); propodeal and petiolar spines blunt (Fig. 3B) (Greece, Iran, Israel, KSA, Turkey) ***L. dolabellae***
- 9 Mesosoma densely sculptured; not shining **10**
- Mesosoma superficially sculptured; at least partially shining, in some species completely shining **11**
- 10 Head and mesosoma densely sculptured and completely opaque; propodeal spines long and curved (Fig. 3C) (Oman) ***L. dhoifara***
- Head and mesosoma superficially sculptured and slightly shining; propodeal armature short and blunt (Fig. 3D) (Balkan Peninsula, Central Asia, Iran, Kazakhstan, Kuwait, UAE) ***L. karawaiewi***

- 11 Body entirely black, with slight reticulate sculpture at most and shining... **12**
- Mesosoma usually with small area of mesonotum red; head and mesosoma distinctly sculptured and not shining **16**
- 12 Propodeal and petiolar spines reduced (Fig. 3E), petiole dorsum narrow and rounded, with reduced armature; antennal scapes shorter, SI 150–155 (Croatia, Egypt, Greece, Iberian Peninsula, Italy, Kyrgyzstan, Macedonia, Montenegro, Oman, UAE) ***L. nigra***
- Propodeal and petiolar armature both well-developed with long curved spines (Fig. 3F); antennal scape long, SI 165–200 **13**
- 13 Propodeum and first gastral tergite with some fine surface sculpture; first gastral tergite with characteristic violet reflection; SI 195–200 (Egypt, Israel, KSA, UAE) ***L. opaciventris***
- Whole body smooth; first gastral tergite without reflection of any type; SI 165–195 **14**
- 14 Propodeal short, less than 0.10 mm, moderately curved; antennal scape long, SI 175–195 (Yemen, Eritrea, Israel, UAE) ***L. gracilicornis***
- Propodeal spines long, more than 0.12 mm, and distinctly curved; antennal scape shorter, SI 165–170 **15**
- 15 Body dark brown; propodeal spines slightly curved, in profile appearing at level of the petiolar spines; body slightly shining; scape shorter (SI 170), cephalic index smaller (CI 79), petiolar height lower in profile (0.41); appressed pubescence abundant on body (Iran, Kazakhstan, KSA, Oman, Socotra) ***L. spinisquama***
- Body black, propodeal spines strongly curved (Fig. 4A), in profile appearing much higher than level of petiolar spines; body more strongly shining; scape longer (SI 230–233), cephalic index greater (CI 86–88), petiolar height larger in profile (0.25–0.37); pubescence on body scattered (Oman, UAE) ***L. omanensis***
- 16 Paler species, mesosoma, legs and antennae orange, distinctly contrasting the brown head and gaster; pronotum with one pair of hairs (Fig. 4B) (widespread in Palearctic region) ***L. frauenfeldi***
- Uniform black or black-brown; pronotum without hairs (Fig. 4C) (Tunisia, UAE) ***L. nigrescens***
- 17 Head and mesosoma densely punctate and dull **18**
- Head and mesosoma smooth or superficially sculptured rugulose, and shining **20**
- 18 Bicolored species, with mesosoma reddish, head, petiole, and gaster brown (Yemen) ***L. harteni***
- Uniform brown or black-brown species **19**
- 19 Propodeal spines reduced or indistinct (Fig. 4D); whole gastral dorsum covered with abundant pale hairs (Fig. 5A) (Ethiopia, Eritrea, Israel, KSA) ***L. obtusa***
- Propodeal spines well-developed in the form of two broadly-based blunt tubercles in profile (Fig. 5B); gastral pilosity restricted to few pairs on the poste-

- rrior margin of tergites (Fig. 5B) (Djibouti, KSA, Oman, Somalia, Yemen)
 *L. carbonaria* (= *L. depilis* syn. nov.)
- 20 Posterior margin of head in full-face view fringed with about seven pairs of
 stiff hairs (Fig. 5C); body pilosity brown (Namibia, Somalia, Yemen, Zimba-
 bwe)..... *L. validiuscula*
- Posterior margin of head in full-face view with only two to three of stiff hairs
 (Fig. 5D); body pilosity yellow (Guinea, Israel, Kenya, KSA, Somalia, Oman,
 Yemen) *L. canescens*

***Lepisiota elbazi* Sharaf & Hita Garcia, sp. nov.**

<http://zoobank.org/218E57C6-A0CA-4C9D-B4E3-EC9EBF831AEC>

Figs 1A, D, 6A–C

Type material. Holotype: pinned worker from OMAN: DHOFAR: Ayn Razat, 17.12443N, 54.23832E, 98 m, 20.xi.2017, CASENT0872069, SF, (M. R. Sharaf).

Paratype: one pinned worker with same data as holotype, CASENT0922860, (King Saud University Museum of Arthropods (KSMA), Plant Protection Department, College of Food and Agriculture Sciences, King Saud University, Riyadh, KSA).

Holotype worker. Measurements (paratype in parentheses): EL 0.17 (0.20); HL 0.82 (0.87); HW 0.57 (0.62); ML 0.50 (0.57); PH 0.30 (0.32); PRW 0.45 (0.50); PSL 0.12 (0.15); SL 1.07 (1.15); TL 3.20 (3.50); WL 1.40 (1.50). Indices: CI 70 (71); OI 30 (32); PSLI 15 (17); SI 188 (185).

Diagnosis. This new species can be distinguished from its regional congeners by the following combination of characters: in profile, posterior margin of head anteroposteriorly compressed; limited number of hair pairs on body: two pairs on posterior margin of head, two to three pairs on promesonotum, and one to two pairs on first gastral tergite.

Description. Worker. Head. Elongate, distinctly more than 1.3–1.6 × longer than broad, with straight posterior margin and feebly convex lateral margins; posterior margin of head, in profile, anteroposteriorly compressed; antennal scapes when laid back from their insertions surpassing posterior margin of head by more than one third of length (SI 185–188); eyes of moderate size (OI 30–32), with the anteriormost point of the eye lies touching the midlength of head in full-face view; anterior clypeal margin strongly convex anteriorly and dorsally, and with raised lateral margins; frontal triangle opened posteriorly; masticatory margin of mandibles armed with four teeth, the first tooth being longest, the third being smallest, the second and fourth teeth are of moderate size and subequal (counting from apex). **Mesosoma.** Promesonotum convex in profile; first half of mesonotal outline descending posteriorly into a concave curve then elevated and descending posteriorly in a straight line to an impressed metanotal groove; propodeal spines long and acute in profile (PSLI 15–17), propodeal spines in profile rising slightly to the rear from the level of the propodeal dorsum. **Petiole.** Acutely dorsally bispinose. **Pilosity.** First two-thirds of scape without hairs, distal quarter with a few stiff hairs, funiculus with dense appressed pubescence; cephalic dorsum

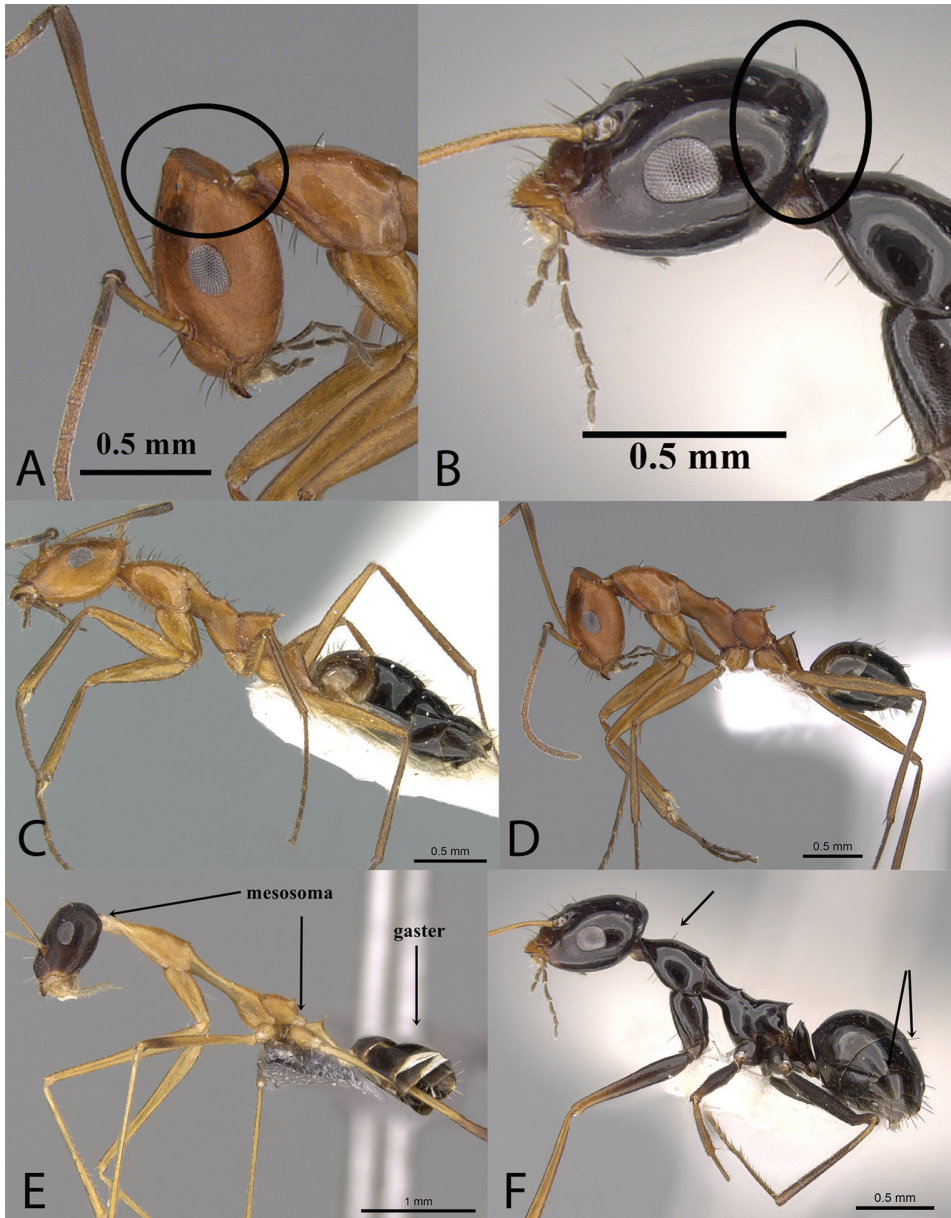


Figure 1. **A** head of *L. elbazi* sp. nov. in profile, [CASENT0922860](#) (Michele Esposito) **B** head of *L. gracilicornis* in profile, [CASENT0906458](#) (Cerise Chen) **C** body of *L. arabica* in profile, [CASENT0906264](#) (Estella Ortega) **D** body of *L. elbazi* sp. nov. in profile, [CASENT0922860](#) (Michele Esposito) **E** body of *L. elegantissima* in profile, [CASENT0922860](#) (Michele Esposito) **F** body of *L. gracilicornis* in profile, [CASENT0906458](#) (Cerise Chen), www.AntWeb.org.

with several pairs of stiff, black, long, blunt hairs (hair length 0.10–0.12) arranged as follow: two on anterior clypeal margin, one on posterior clypeal margin, one at end of frontal carinae; one close to level of anterior margins of eyes; one behind level of

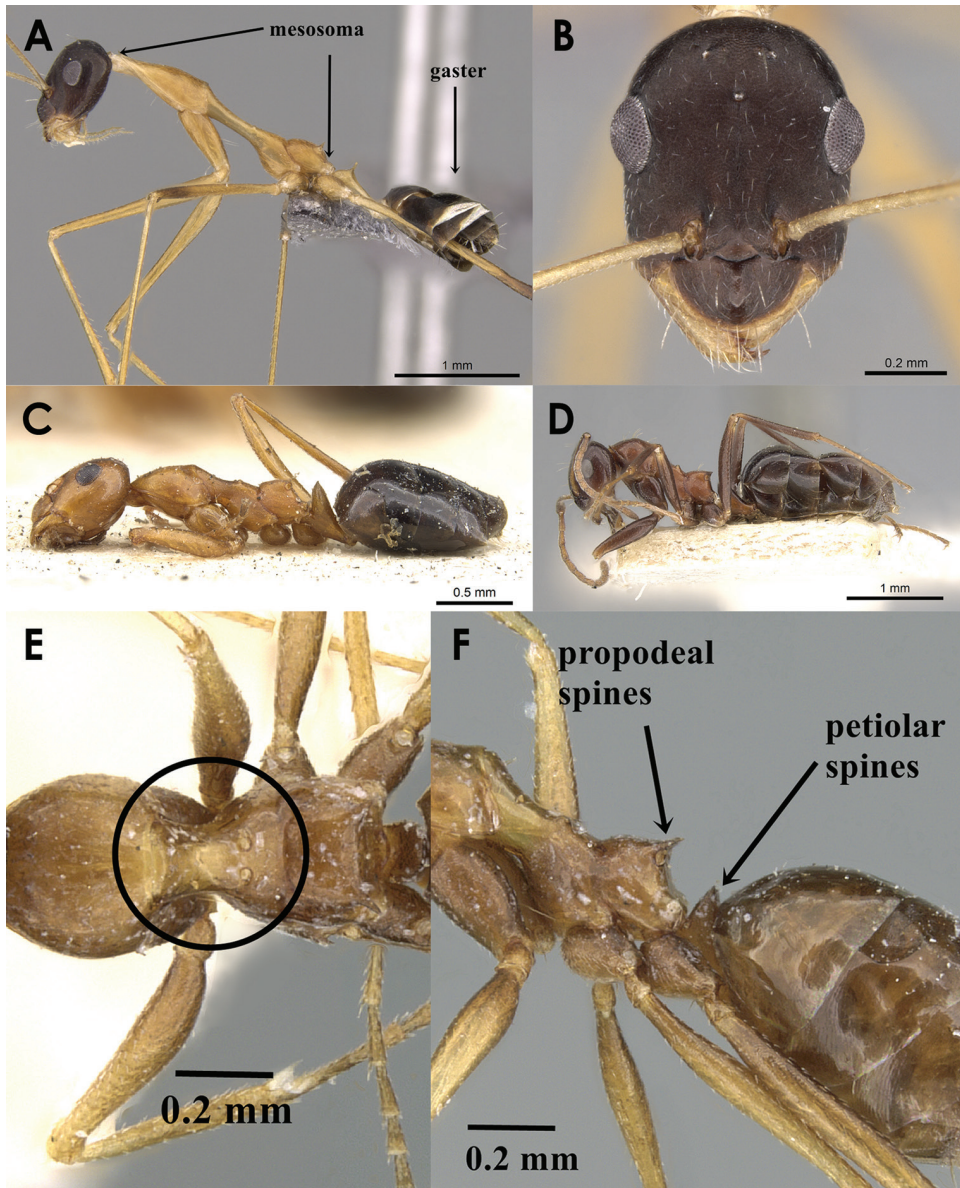


Figure 2A–F. **A** body of *L. elegantissima* in profile, [CASENT0922860](#) (Michele Esposito) **B** head of *L. elegantissima* in full-face view, [CASENT0922860](#) (Michele Esposito) **C** body of *L. bipartita* in profile, [CASENT0903167](#) (Zach Lieberman) **D** body of *L. dolabellae* in profile, [CASENT0249883](#) (Shannon Hartman) **E** mesosoma of *L. dammama* in dorsal view showing mesonotum, [CASENT0906337](#) (Estella Ortega) **F** body of *L. dammama* in profile showing propodeal and petiolar spines, [CASENT0906337](#) (Estella Ortega), www.AntWeb.org.

mid-length of eyes; two at posterior margin of head; promesonotum with one to three pairs of hairs; mandibular surfaces with fine long pale hairs; gaster with several scattered hairs. **Sculpture.** Cephalic, clypeal surfaces, and promesonotal dorsum faintly

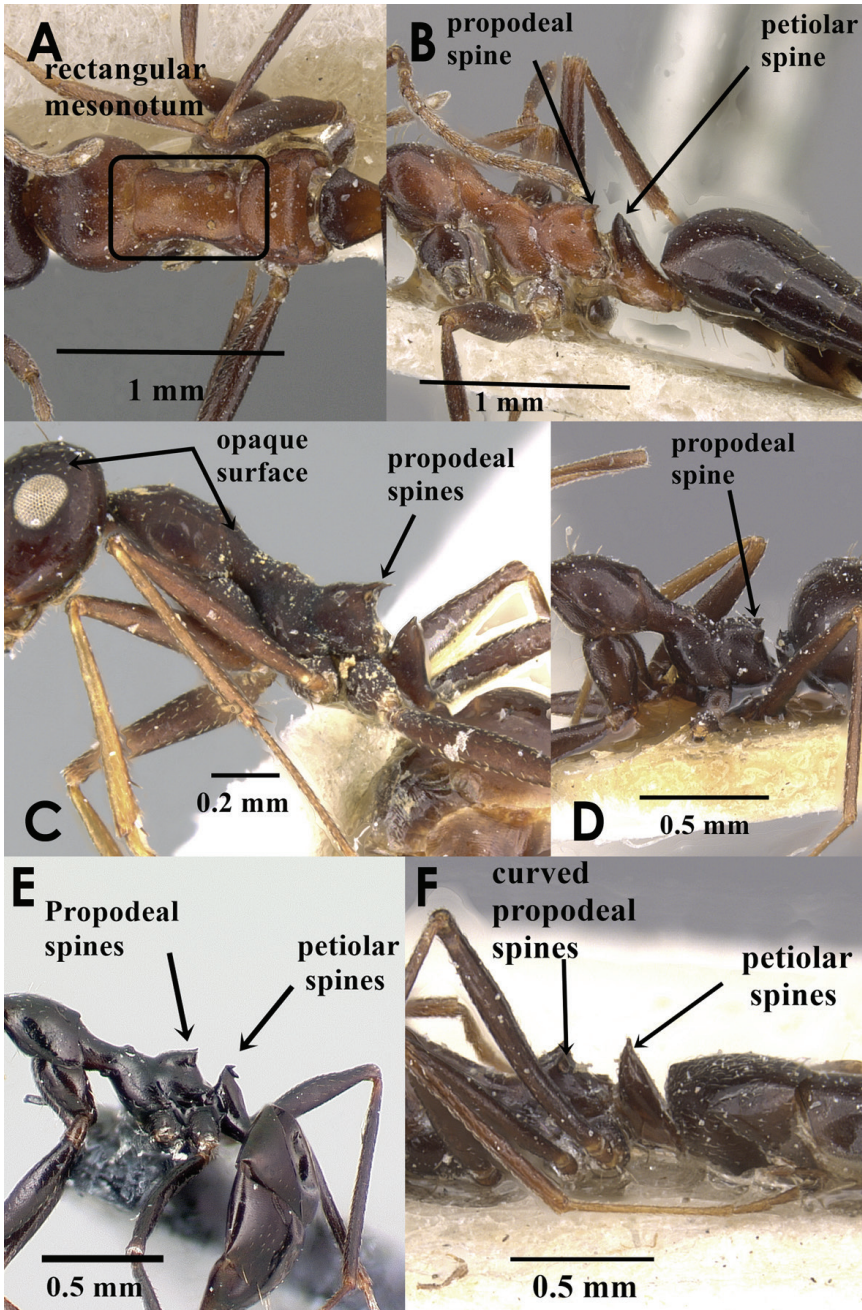


Figure 3A–F. **A** mesosoma of *L. dolabellae* in dorsal view showing mesonotum, [CASENT0909887](#) (Zach Lieberman) **B** body of *L. dolabellae* in profile propodeal and petiolar spines, [CASENT0909887](#) (Zach Lieberman) **C** body of *L. dhofera* in profile showing surface sculpture and propodeal spines, [CASENT0906340](#) (Estella Ortega) **D** mesosoma of *L. karawaiewi* in profile showing propodeal spines, [CASENT0912405](#) (Will Ericson) **E** body of *L. nigra* in profile showing propodeal and petiolar spines, [CASENT0179896](#) (Erin Prado) **F** Body of *L. spinisquama* in profile showing petiolar spines, [CASENT0922270](#) (Michele Esposito), www.AntWeb.org.

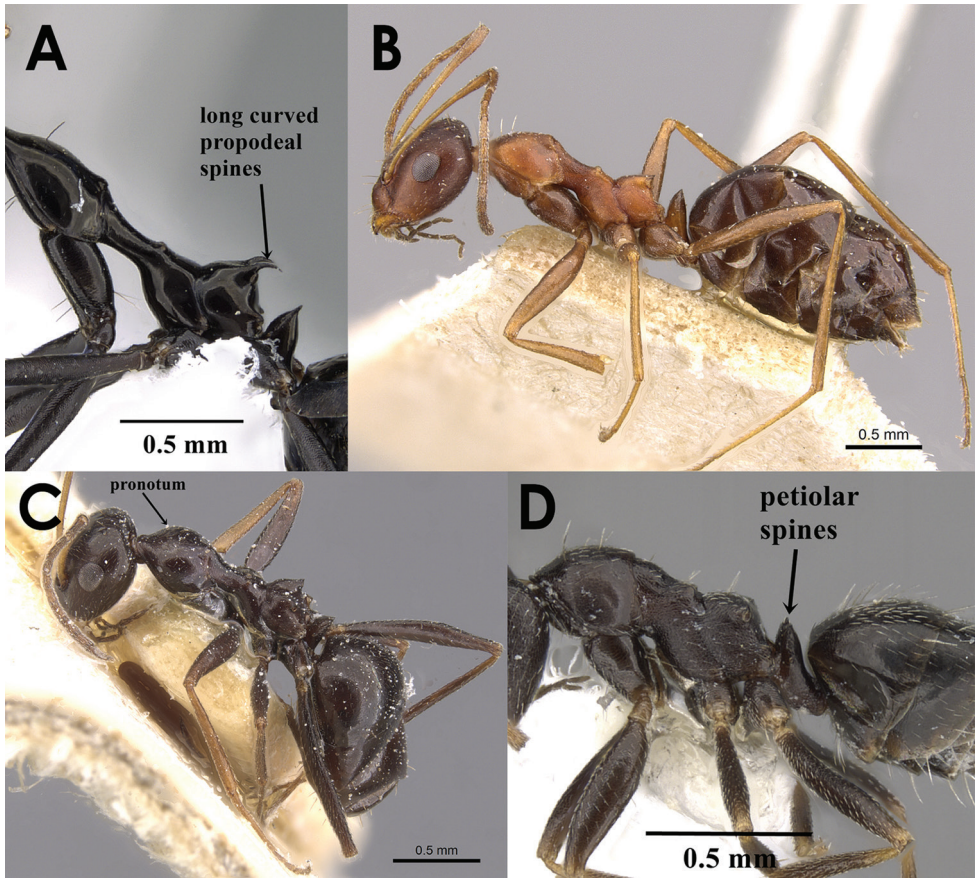


Figure 4A–D. **A** mesosoma of *L. omanensis* in profile showing propodeal spines, [CASENT0922278](#) (Michele Esposito) **B** body of *L. frauenfeldi* in profile propodeal and petiolar spines, [CASENT0909884](#) (Zach Lieberman) **C** body of *L. nigrescens* in profile, [CASENT0912400](#) (Will Ericson) **D** body of *L. obtusa* in profile showing reduced petiolar spines, [CASENT0280477](#) (Shannon Hartman), www.AntWeb.org.

but finely reticulate-rugulose, moderately shiny, mandibular surface smooth and shining; mesonotum, propodeum, and petiole distinctly reticulate-punctate; first gastral tergite smooth and shining. **Color.** Bicolored species, head, mesosoma, petiole yellow or red-yellow, distal end of scapes, first funicular segment and mandibular teeth darker; gaster mostly dark brown to black with first tergite of slightly lighter brown.

Etymology. The patronymic name honors Prof. Farouk El-Baz, the Egyptian space scientist, Boston University, USA in recognition of his distinguished scientific achievements.

Remarks. The occurrence of hairs and their distribution on the surface of the body are diagnostic characters for the recognition of species in many ant genera, notably used in the taxonomy of the genus *Lepisiota* (Collingwood 1985; Collingwood and Agosti 1996). *Lepisiota elbazi* is not similar to any of the known Arabian *Lepisiota*, except the Arabian endemic species *L. arabica* (Collingwood, 1985) described from the

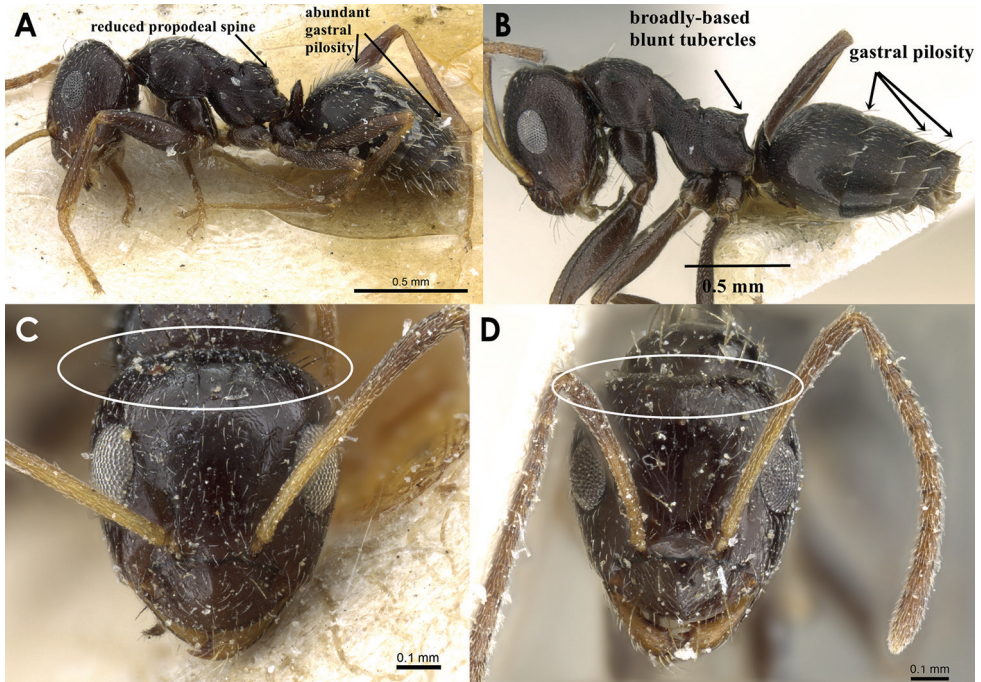


Figure 5A–D. **A** body of *L. obtusa* in profile showing propodeum and gastral pilosity, [CASENT0905150](#) (Zach Lieberman) **B** body of *L. carbonaria* in profile showing propodeal spines and gastral pilosity, [CASENT0906261](#) (Estella Ortega) **C** head of *L. validiuscula* in full-face view showing pilosity on posterior margin, [CASENT0280473](#) (Shannon Hartman) **D** head of *L. canescens* in full-face view showing pilosity on posterior margin, [CASENT0905153](#) (Zach Lieberman), www.AntWeb.org.

southwestern Asir Mountains, KSA. Both species are bicolored and have a compressed posterior margin of the head when seen in profile, acute and long propodeal spines, stiff and blunt hairs, impressed metanotal groove, characteristically paler first gastral tergite and similar body sculpture. The compressed profile of the posterior margin of the head sets the two species apart from any of the Arabian *Lepisiota*, as those all have a rounded profile to the posterior margin of the head.

The two species can be separated by the number of body hairs and dimensions. *Lepisiota elbazi* has fewer hairs on the posterior margin of the head (two pairs), on the mesosoma (two to three pairs on promesonotum), and on the first gastral tergite (one to two pairs). *Lepisiota arabica* has more than seven pairs of hairs on the posterior margin of the head, many pairs scattered on the mesosomal dorsum (six pairs on promesonotum, four pairs on mesonotum, and two pairs on the propodeal dorsum), and several pairs on the first gastral tergite. Additionally, *L. elbazi* has a greater head length (HL 0.82–0.87 vs. HL 0.72–0.77 in *L. arabica*), longer scapes (SL 1.07–1.15, SI 185–188 vs. SL 0.87–0.89, SI 155–159), and relatively longer head (HL 0.82–0.87 vs. HL 0.73–0.75).

Ecological and biological notes. Both workers of the new species were collected at Ayn Razat (Fig. 7) and were foraging in leaf litter covering dry soil under an *Acacia* tree.

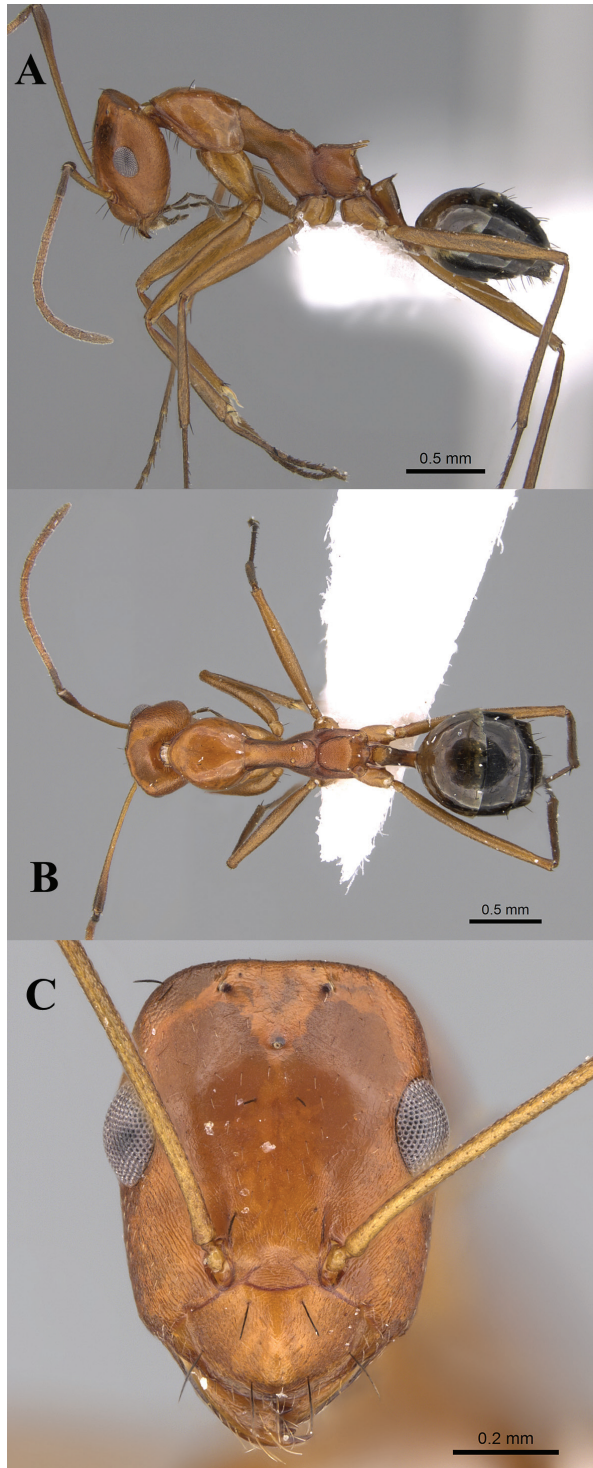


Figure 6A–C. *Lepisiota elbazi* sp. nov. **A** body in profile **B** body in dorsal view **C** head in full-face view, CASENT0922860, (Michele Esposito), www.AntWeb.org.



Figure 7. Ayn Razat, the type locality of *Lepisiota elbazi* sp. nov. (Mostafa Sharaf).

Geographic range. Oman.

Queen and male. Not known.

Newly proposed synonymy

Lepisiota carbonaria (Emery, 1892)

Acantholepis carbonaria Emery, 1892 [Combination in *Lepisiota* by Bolton, 1995]

Acantholepis capensis subsp. *depilis* Emery, 1897 [Raised to species by Collingwood, 1985; Combination in *Lepisiota* by Bolton, 1995] syn. nov.

Material examined of *L. carbonaria*. SOMALIA: 1 syntype worker, Obbia, CASENT0905149, (MSNG); 1 w, Sheikh, 1939, (the Governor), (Pres. By Imp. Inst. Ent.), (B. M. 1946-273), (BMNH, E, 1018291), CASENT0906261; ETHIOPIA: 1 w, Turmi, 04°58'N, 36°29'E, 21.i.2010, (Serge Guiraud), (Hand collecting) (B. Taylor det.) (OUMC); OMAN: 5 w, Dhofar, Ayn Razat, 17.12443N, 54.23832E, 98 m, 20.xi.2017, (M. R. Sharaf), (MRS0399), CASENT0922845 (KSMA).

Material examined of *L. depilis*. SOMALIA: 1 syntype worker, Bricchetti, CASENT0905154, (MSNG).

Remarks. *Lepisiota carbonaria* was originally described by Emery (1892) from Somalia and in 1897 he described *L. depilis* as a subspecies of *Acantholepis capensis* from the same country. Collingwood (1985) was the first to draw the attention of the difference between *L. depilis* and *L. capensis* based on the reduced mesosomal pilosity and the dense mesosomal sculpture of the former which make it sufficiently distinguishable from the later species that has abundant mesosomal pilosity and shining body appearance. However, in his original description of *depilis*, Emery pointed out the remarkable similarities between *depilis* and *carbonaria* which are mainly the dense sculpture on head and mesosoma and dull appearance of these two body parts, and the gastral pilosity which in the form of a row of setae on the posterior margins of the gastral tergites. Emery was correct and our examination of the type material of the two taxa confirms his notes and reveals a straightforward synonymy. The two species have the same body color, dense sculpture, reduced blunt propodeal spines, dull head and mesosoma, and shining gastral tergites with few hairs on margins of tergites. We consider *L. carbonaria* a senior synonym of *L. depilis*.

Species excluded from the Arabian fauna

The following species are excluded from the Arabian *Lepisiota* fauna and are considered as misidentification.

***Lepisiota arenaria* (Arnold, 1920)**

Collingwood and Agosti (1996) wrote “this elegant species with red head and mesosoma” but the type material (CASENT0903150) is no more than uniform dull yellow.

***Lepisiota erythraea* (Forel, 1910)**

Collingwood (1985) stated that this species has a rounded petiole with very shallow emargination, and mesosoma entirely without dorsal hairs. The type material (CASENT0909880) has one pair of long, sharp, triangular petiolar spines and mesosoma with some pairs of hairs.

***Lepisiota incisa* (Forel, 1913)**

This is an eastern African species that seems unlikely to be found in Arabia. Collingwood (1985)’s key mentioned that the mesosomal pilosity is restricted to the pronotum or nil but examination of the type material (CASENT0909876) reveals abundant mesosomal and body pilosity.

***Lepisiota sericea* (Forel, 1892a)**

In their key, Collingwood and Agosti (1996) stated that “this species appeared bicolor- ed with reddish mesosoma lighter than gaster, or entirely reddish. The type material (CASENT0909885) is uniformly dark brown”.

***Lepisiota simplex* (Forel, 1892)**

Collingwood and Agosti (1996) had “mesosoma with pale, thin hairs, that are re- stricted to pronotum”. The type material (CASENT0909878) has several pairs of hairs scattered on the mesosoma including the propodeum.

Zoogeography of the Arabian *Lepisiota*:**Table 1.** Zoogeographic affinities of the Arabian *Lepisiota* (Bolton 2020).

| Species | Type locality | Zoogeography | Afrotropical species recorded from southern Arabian Peninsula | References |
|----------------------------------|----------------------|---------------------------------|---|---|
| <i>Lepisiota arabica</i> | Saudi Arabia | (Endemic) Afrotropical affinity | + | Collingwood 1985 |
| <i>Lepisiota bipartita</i> | Lebanon | Palaearctic | | Collingwood and Agosti 1996 |
| <i>Lepisiota canescens</i> | Somalia | Afrotropical | + | Collingwood 1985; Collingwood and Agosti 1996 |
| <i>Lepisiota carbonaria</i> | Somalia | Afrotropical | + | Collingwood 1985; Collingwood and Agosti 1996 |
| <i>Lepisiota dammama</i> | Saudi Arabia | (Endemic) Palaearctic affinity | | Collingwood and Agosti 1996 |
| <i>Lepisiota dhofara</i> | Oman | (Endemic) Afrotropical affinity | + | Collingwood and Agosti 1996 |
| <i>Lepisiota dolabellae</i> | Turkey | Palaearctic | | Collingwood 1985; Collingwood and Agosti 1996 |
| <i>Lepisiota elbazi</i> sp. nov. | Oman | (Endemic) Afrotropical affinity | + | |
| <i>Lepisiota elegantissima</i> | United Arab Emirates | (Endemic) Afrotropical affinity | + | Collingwood et al. 2011 |
| <i>Lepisiota frauenfeldi</i> | Yugoslavia | Palaearctic | | Collingwood 1985; Collingwood and Agosti 1996 |
| <i>Lepisiota gracilicornis</i> | Yemen | Afrotropical | + | Collingwood 1985; Collingwood and Agosti 1996 |
| <i>Lepisiota harteni</i> | Yemen | (Endemic) Afrotropical affinity | + | Collingwood and Agosti 1996 |
| <i>Lepisiota karawaiewi</i> | Kazakhstan | Palaearctic | | Collingwood and Agosti 1996 |
| <i>Lepisiota nigra</i> | Italy | Palaearctic | | Collingwood and Agosti 1996 |
| <i>Lepisiota nigrescens</i> | Tunisia | Palaearctic | | Collingwood 1985; Collingwood and Agosti 1996 |
| <i>Lepisiota obtusa</i> | Ethiopia | Afrotropical | + | Collingwood 1985; Collingwood and Agosti 1996 |
| <i>Lepisiota omanensis</i> | Oman | (Endemic) Afrotropical affinity | + | Sharaf et al. 2016 |
| <i>Lepisiota opaciventris</i> | Egypt | Palaearctic | | Collingwood 1985; Collingwood and Agosti 1996 |
| <i>Lepisiota riyadha</i> | Saudi Arabia | (Endemic) Palaearctic affinity | | Collingwood and Agosti 1996 |
| <i>Lepisiota spinisquama</i> | Kazakhstan | Palaearctic | | Collingwood 1985; Collingwood and Agosti 1996 |
| <i>Lepisiota validiuscula</i> | Somalia | Afrotropical | + | Collingwood and Agosti 1996 |

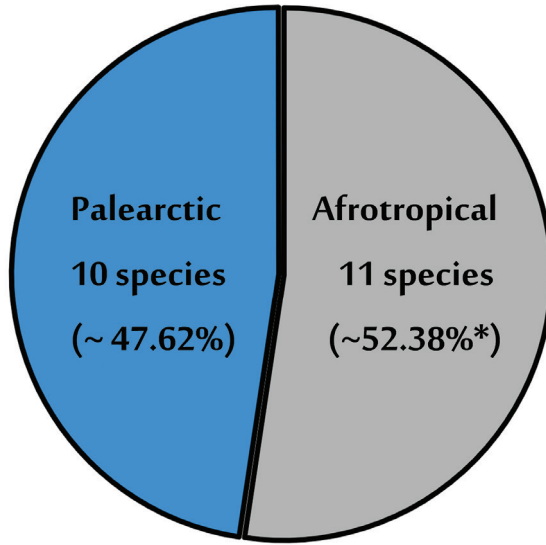
Discussion

The biogeography of the Arabian Peninsula has always been a subject of interest and sometimes controversial by researchers, and this is undoubtedly due to its geographic location at the interchange of three major zoogeographical realms, the Afrotropical, the Palearctic, and the Oriental regions. This pivotal geographical location has made the Arabian Peninsula harbor elements of all zoogeographic regions with a notable influence of the Afrotropical species documented for the southwestern mountains of the Arabian Peninsula, Yemen, the Dhofar Governorate, and Jabal Al Akhdar in Oman (e.g. Guichard 1980; Larsen and Larsen 1980; Larsen 1984; Collingwood 1985; Cowie 1989; Collingwood and Agosti 1996; Pesenko and Pauly 2009; Sharaf and Aldawood 2011, 2012, 2019; Sharaf et al. 2012a, b, c; El-Hawagry et al. 2013, 2016a, b, 2017; Abdel-Dayem et al. 2019).

Our new collections and previous literature records (Collingwood 1985; Collingwood and Agosti 1996; Collingwood et al. 2011) indicate that the *Lepisiota* fauna of the Arabian Peninsula includes 21 species, which is clearly represented by taxa of the Afrotropical and the Palearctic regions (Table 1, Fig. 8). About 53% of these species have strong affinities with the Afrotropical Region (11 species), followed by the Palearctic elements (including western and eastern boundaries of the Palearctic region) with about 48% (10 species). This Afrotropical preponderance has been previously recognized by numerous studies (e.g. Guichard 1980; Larsen and Larsen 1980; Larsen 1984; Collingwood 1985; Cowie 1989; Waterston and Pittaway 1991; Schneider and Krupp 1993; Collingwood and Agosti 1996; Taiti et al. 2000; Hausmann 2009; Pesenko and Pauly 2009; Sharaf and Aldawood 2011, 2012, 2019; Neubert and van Damme 2012; Sharaf et al. 2012a, b, c; El-Hawagry et al. 2013, 2016a, b, 2017; Hájek and Reiter 2014; Ball et al. 2015; Abdel-Dayem et al. 2019). The close Afrotropical affinity of the taxa mentioned in the above studies supports the direct linkage of Afrotropical lineages with the Arabian Peninsula. However, the Oriental influence is absent but it is anticipated some taxa from the region might exist with extensive collecting. The minor Oriental influence is documented by some studies as Larsen (1984) on the Arabian fauna of the butterflies (Larsen 1984), Penati and Vienna (2006) on the Arabian Histeridae, and Abdel-Dayem et al. (2019) on the Carabidae of Shada Al-A'Ala Nature Reserve, Southwestern KSA. Obviously much more collecting efforts must be done to allow an in-depth zoogeographical treatment for confirming speculation.

These distributional patterns indicate that zoogeographically the area of the Arabian Peninsula is not a homogeneous unit. Our analysis of *Lepisiota* zoogeographic affinities generally supports Larsen and Larsen (1980), Larsen (1984), Abdel-Dayem et al. (2019), Cowie (1989), Penati and Vienna (2006), Rueda et al. (2013), Sharaf et al. (2014), Ficitola et al. (2017), Delany (1989), El-Hawagry et al. (2019) arguments that a major zoogeographic discontinuity exists within the region. Despite this, as mentioned above about 38% (8 out of 21 spp.) of the species appear to be endemic to the region.

The geographic location of the Arabian Peninsula at the conjunction of three zoogeographical regions make the delineation of the borders among these three bioregions is a difficult task and this subject is often pay the attention of biogeographers.



***Afrotropical species in southern Arabian Peninsula**
Endemic species are representing ~38.10% of total species
(8 of 21 species)

Figure 8. Zoogeographic analysis of the Arabian *Lepisiota*.

Numerous studies have considered that the southwestern Arabian Peninsula, which includes the Al Sarawat Mountain and the Asir Mountains (KSA) and Yemen, with clear Afrotropical affinities (e.g. Larsen and Larsen 1980; Collingwood 1985; Collingwood and Agosti 1996; Taiti et al. 2000; Hausmann 2009; Pesenko and Pauly 2009; Sharaf and Aldawood 2011, 2012, 2019; Sharaf et al. 2012a, b, c; El-Hawagry et al. 2013, 2016a, b, 2017; Hájek and Reiter 2014; Ball et al. 2015; Abdel-Dayem et al. 2019). Some studies conjoin the Dhofar Governorate, Jebel Akhdar (Oman) and the Hajar Mountains that extend between Oman and the UAE to the Arabian areas of Afrotropical elements but with relatively lesser degrees of Afrotropical affinities (Larsen 1984; Cowie 1989; Delany 1989; Penati and Vienna 2006).

Our available data of the distribution of the Arabian fauna of *Lepisiota* clearly show a confined distribution of all the Afrotropical species and the endemic species to the southern Arabian Peninsula, whereas those Afrotropical species are not represented in the arid regions of the Arabian deserts and obviously are replaced by taxa of the Palearctic region. These data fully coincide with the findings of several studies that draw the boundaries between the Afrotropical and the Palearctic regions of the Arabian Peninsula as a line connecting the mountainous coastal strip that is parallel to the Red Sea in the western Arabian Peninsula starting from Taif and southwards to Yemen, parts of Oman (Dhofar, Jebel Akhdar) and the UAE) (the Hajar Mountains) (Fig. 9) (Larsen 1984; Cowie 1989; Delany 1989; Penati and Vienna 2006).

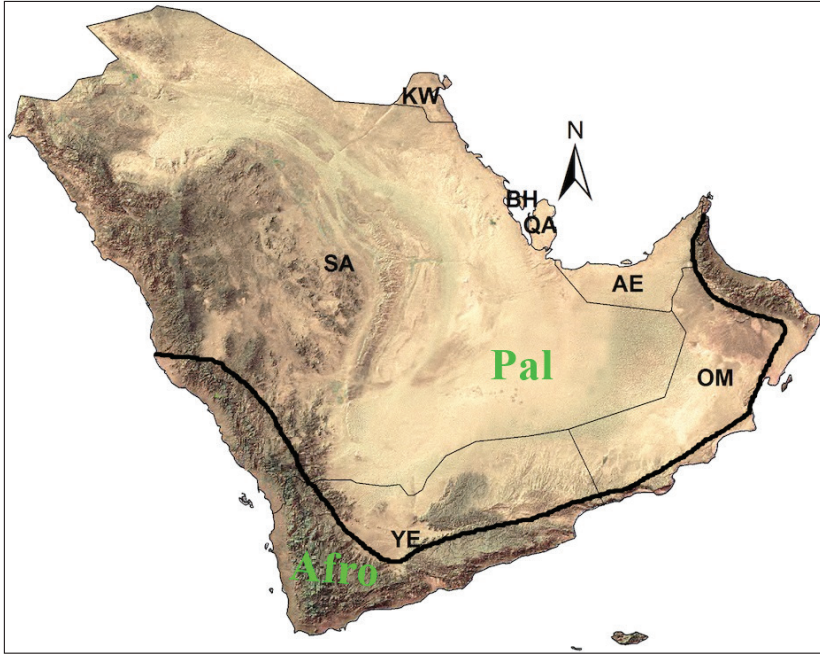


Figure 9. Zoogeographic boundaries between the Afrotropical and the Palearctic regions of the Arabian Peninsula, AE: United Arab Emirates, BH: Bahrain, KW: Kuwait, OM: Oman, QA: Qatar, SA: Saudi Arabia, YE: Yemen.

The distribution pattern of the Arabian *Lepisiota* is restricted to two major regions of the Arabian Peninsula: the forests of the southwestern mountains and the vast surrounding deserts. The distribution of the Afrotropical species is obviously confined to forests of the southern Arabian Peninsula of the KSA, Yemen, and Oman, whereas the Palearctic species are mainly represented outside this geographic range and precisely correlated to the desert ecosystems of the Arabian Peninsula. Hence, while the Afrotropical influence decreases towards the north and east, the Palearctic influence increases correspondingly. This geographic correlation is likely related to habitat availability, soil nature, and vegetation cover in the two ecosystems. Environmental impact obviously favors the spread and maintenance of a species over another and can result in a vast distribution (Larsen 1984; Cowie 1989).

The Arabian *Lepisiota* fauna, however, includes a noteworthy proportion of apparently endemic species (38.10%) represented by eight species, *L. arabica*, *L. dammama*, *L. dhofara*, *L. elbazi* sp. nov., *L. elegantissima*, *L. harteni*, *L. omanensis*, and *L. riyadha*. This high degree of endemism for the Arabian Peninsula is documented for several groups of animals including amphibians (Arnold 1980), reptiles (Šmíd 2010; Melnikov and Pierson 2012), birds (Ball et al. 2015), arthropods of different groups including Isopoda (Taiti et al. 2000), Lepidoptera (Larsen and Larsen 1980; Hausmann 2009), Isoptera (Cowie 1989), Odonata (Waterston and Pittaway 1991; Schneider and Krupp 1993), Coleop-

tera (Hájek and Reiter 2014), and Hymenoptera (Collingwood 1985; Collingwood and Agosti 1996; Pesenko and Pauly 2009; Sharaf and Aldawood 2019).

Our analysis of species endemism is distinctly higher than the degree of endemism of numerous animal groups which include the works of Cowie (1989) for the Arabian Isoptera (24%), Abdel-Dayem et al. (2018) for the Carabidae of Garf Raydah (southern KSA) (19.3%), Larsen (1984) for the Rhopalocera (15.5%), Collingwood (1985) for the Formicidae of the KSA (11%), Collingwood and Agosti (1996) for the Formicidae of the Arabian Peninsula (25%), Abdel-Dayem et al. (2019) for the Carabidae of Shada Al-A'Ala Nature Reserve (KSA) (5.3%), Abdel-Dayem et al. (2017) for the Carabidae of the beetle fauna of Rawdhat Khorim National Park (KSA) (6.0 %), Penati and Vienna (2006) for the Histeridae (7.5%).

The ant genus *Lepisiota* along with two other genera (*Camponotus* Mayr, 1861 and *Cataglyphis* Foerster, 1850) are the most diverse and abundant genera of the subfamily Formicine both in Oman and in the entire Arabian Peninsula (Collingwood 1985; Collingwood and Agosti 1996; Sharaf et al. 2018). They are represented in Oman by the following number of species; *Camponotus* (18), *Cataglyphis* (15) and *Lepisiota* (15). In the Arabian Peninsula the number is as follows; *Camponotus* (25), *Cataglyphis* (28) and *Lepisiota* (26). An inventory in the southwestern mountains of the KSA using several collecting techniques (Pitfall, Malaise, and light traps) revealed a similar pattern of abundance and diversity of the three genera (Sharaf et al. unpublished data).

Among this remarkable abundance and diversity of many species of *Lepisiota*, however, there are some rare species known only from a few specimens, e.g. *Lepisiota arabica* Collingwood, 1985 (5), *L. dhofara* Collingwood & Agosti (1), *L. dammama* Collingwood & Agosti (5), *L. elbazi* sp. nov. (2), and *L. omanensis* Sharaf & Monks, 2016 (5). Not only are there morphological similarities between *L. elbazi* and its congener *L. arabica* but they have similar habitat preferences with both species appearing to prefer the mountainous territories of the Dhofar Governorate for *L. elbazi* and the southwestern mountains of the KSA for *L. arabica*.

The taxonomic keys for the *Lepisiota* fauna of the KSA (Collingwood 1985) and the Arabian Peninsula (Collingwood and Agosti 1996) have some degree of apparent ambiguity in some of their parts, which results in the difficulty of species identification. Therefore, interested workers in the region must be careful when dealing with these two keys.

Acknowledgments

We thank the following colleagues: Barry Bolton for suggestions that improved the work; Brian Taylor, Xavier Espadaler, Boris Kondratieff, and Georg Fischer for valuable comments; Brian Fisher, Michele Esposito (California Academy of Sciences, San Francisco) for imaging the species; Annette Patzelt for appreciated permission to use image of Ayn Sahlanot, Saif Al-Hatmi (Oman Botanic Garden) for support during the field work in Oman, and A. Shams Al Ola for technical assistance. Mostafa Sharaf thanks the following colleagues for making material available for the study and ap-

preciated hospitality in the UK.: James Hogan (OUMC), Andrew Polaszek (BMNH), Stephen Judd, and Tony Hunter (World Museum Liverpool, Liverpool, U.K.). This work was supported by the Deanship of Scientific Research at King Saud University [RG-1438-010].

References

- Abdel-Dayem MS, Fad HH, El-Torkey AM, Elgharbawy AA, Aldryhim YN, Kondratieff BC, Al Ansi AN, Aldhafer HM (2017) The beetle fauna (Insecta, Coleoptera) of the Rawdhat Khorim National Park, Central Saudi Arabia. *ZooKeys* 653: 1–78. <https://doi.org/10.3897/zookeys.653.10252>
- Abdel-Dayem MS, Rasool I, Elgharbawy AA, Nagel P, Aldhafer HM (2018) Faunistic inventory and zoogeographical analysis of the ground beetles (Coleoptera, Carabidae) of Garf Raydah Nature Reserve, Southwestern of Saudi Arabia, and description of a new species of Paussinae. *Zootaxa* 4514(3): 341–371. <https://doi.org/10.11646/zootaxa.4514.3.3>
- Abdel-Dayem MS, Elgharbawy AA, Rasool I, Nagel P, Aldhafer HM (2019) The Carabidae (Coleoptera) of Shada Al-A'Ala Nature Reserve, Southwestern Saudi Arabia, with description of a new species of Paussinae. *ZooKeys* 812: 93–131. <https://doi.org/10.3897/zookeys.812.30937>
- Agosti D, Collingwood CA (1987) A provisional list of the Balkan ants (Hym. Formicidae) with a key to the worker caste. II. Key to the worker caste, including the European species without the Iberian. *Mitteilungen der Schweizerischen Entomologischen Gesellschaft* 60: 261–293.
- André E (1882) Les fourmis [part]. In: André E (Ed.) *Species des Hyménoptères d'Europe et d'Algérie*. Tome Deuxième. Edmond André 919, Beaune, 153–232.
- Arakelian GR (1994) Fauna of the Republic of Armenia. Hymenopterous insects. Ants (Formicidae). *Gitutium*, Erevan, 153 pp. [In Russian.]
- Arnold G (1920a) A monograph of the Formicidae of South Africa. Part IV. Myrmicinae. *Annals of the South African Museum* 14: 403–578.
- Arnold EN (1980) The reptiles and Amphibians of Dhofar, Southern Arabia. *Journal of Oman Studies Special Report No. 2*: 273–332.
- Atanassov N, Dlussky GM (1992) Fauna of Bulgaria. Hymenoptera, Formicidae. *Fauna na Búlgariya* 22: 1–310. [In Bulgarian.]
- Ball L, Al-Fazari W, Borrell JS (2015) Birds of Wadi Sayq, Dhofar, Oman: British Exploring Society Expeditions January-March 2012 and 2013. *Sandgrouse* 37(1): 2–12.
- Bestelmeyer BT, Schooley RL (1999) The ants of the southern Sonoran Desert: community structure and the role of trees. *Biodiversity and Conservation* 8: 643–657. <https://doi.org/10.1023/A:1008873406658>
- Bingham CT (1903) The fauna of British India, including Ceylon and Burma. Hymenoptera (Vol. II). Ants and Cuckoo-wasps. Taylor and Francis, London, 506 pp.
- Bolton B (1973) The ant genera of West Africa: a synonymic synopsis with keys (Hymenoptera: Formicidae). *Bulletin of the British Museum (Natural History). Entomology* 27: 317–368.

- Bolton B (1994) Identification Guide to the Ant Genera of the World. Harvard University Press, Cambridge, 222 pp.
- Bolton B (1995) A New General Catalogue of the Ants of the World. Harvard University Press, Cambridge, 504 pp.
- Bolton B (2020) An online catalog of the ants of the world. <http://antcat.org>. [accessed 9 January 2020]
- Boulton AM, Davis KF, Ward PF (2005) Species richness, abundance, and composition of ground-dwelling ants in northern California grasslands: role of plants, soil, and grazing. *Environmental Entomology* 34: 96–104. <https://doi.org/10.1603/0046-225X-34.1.96>
- Brown Jr WL (2000) Diversity of ants. In: Agosti D, Majer JD, Alonso LE, Schultz TR (Eds) *Ants. Standard Methods for Measuring and Monitoring Biodiversity*. Biological diversity Handbook Series. Smithsonian Institution Press, Washington, 45–79.
- Collingwood CA (1985) Hymenoptera: Fam. Formicidae of Saudi Arabia. *Fauna of Saudi Arabia* 7: 230–302.
- Collingwood CA, Agosti D (1996) Formicidae (Insecta: Hymenoptera) of Saudi Arabia (part 2). *Fauna of Saudi Arabia* 15: 300–385.
- Collingwood CA, Agosti D, Sharaf MR, Van Harten A (2011) Order Hymenoptera, family Formicidae. *Arthropod Fauna of the UAE* 4: 405–474.
- Cowie RH (1989) The zoogeographical composition and distribution of the Arabian termite fauna. *Biological Journal of the Linnean Society* 36: 157–168. <https://doi.org/10.1111/j.1095-8312.1989.tb00488.x>
- Dalla Torre KW (1893) *Catalogus Hymenopterorum Hucusque Descriptorum Systematicus et Synonymicus* (Vol. 7). Formicidae (Heterogyna). W. Engelmann, Leipzig, 289 pp. <https://doi.org/10.5962/bhl.title.8794>
- Delany MJ (1989) The zoogeography of the mammal fauna of southern Arabia. *Mammal Review* 19(4): 133–152. <https://doi.org/10.1111/j.1365-2907.1989.tb00408.x>
- El-Hawagry MS, Khalil MW, Sharaf MR, Fadl HH, Aldawood AS (2013) A preliminary study on the insect fauna of Al-Baha Province, Saudi Arabia, with descriptions of two new species. *ZooKeys* 274: 1–88. <https://doi.org/10.3897/zookeys.274.4529>
- El-Hawagry MS, Al Dhafer HM (2015) Five new records of bee flies (Bombyliidae, Diptera) from Saudi Arabia with zoogeographical remarks. *ZooKeys* 489: 125–133. <https://doi.org/10.3897/zookeys.489.8794>
- El-Hawagry MS, Abdel-Dayem MS, Elgharbawy AA, Dhafer HM (2016a) A preliminary account of the fly fauna in Jabal Shada al-A'la Nature Reserve, Saudi Arabia, with new records and biogeographical remarks (Diptera, Insecta). *ZooKeys* 636: 107–139. <https://doi.org/10.3897/zookeys.636.9905>
- El-Hawagry MS, Sharaf MR, Al Dhafer HM, Fadl HH, Aldawood AS (2016b) Addenda to the insect fauna of Al-Baha Province, Kingdom of Saudi Arabia with zoogeographical notes. *Journal of Natural History* 50(19–20): 1209–1236. <https://doi.org/10.1080/00222933.2015.1103913>
- El-Hawagry MS, Abdel-Dayem MS, El-Sonbati SA, Al Dhafer HM (2017) A preliminary account of the fly fauna in Garf Raydah Nature Reserve, Kingdom of Saudi Arabia, with new

- records and biogeographical remarks (Diptera: Insecta). *Journal of Natural History* 51: 1499–1530. <https://doi.org/10.1080/00222933.2017.1347299>
- El-Hawagry MS, Al Dhafer HM, Abdel-Dayem MS (2019) On the fly fauna of the central region of the Kingdom of Saudi Arabia: new country records from Riyadh Region, with a list of associated fly species and zoogeographical remarks (Insecta: Diptera). *Journal of Natural History* 53: 17–43. <https://doi.org/10.1080/00222933.2019.1568601>
- Emery C (1892) Sopra alcune formiche raccolte dall'Ingegnere L. Bricchetti Robecchi nel paese dei Somali. Dummy reference. *Annali del Museo Civico di Storia Naturale* 32[=(2)12]: 110–122.
- Emery C (1897) Formiche raccolte da Don Eugenio dei Principi Ruspoli, durante l'ultimo suo viaggio nelle regioni dei Somali e dei Galla. *Annali del Museo Civico di Storia Naturale* 38[=(2)18]: 595–605.
- Emery C (1901) Spicilegio mirmecologico. *Bullettino della Società Entomologica Italiana* 33: 57–63.
- Ficetola GF, Mazel F, Thuiller W (2017) Global determinants of zoogeographical boundaries. *Nature Ecology and Evolution* 1: 1–7. <https://doi.org/10.1038/s41559-017-0089>
- Finzi B (1936) Risultati scientifici della spedizione di S. A. S. il Principe Alessandro della Torre e Tasso nell'Egitto e penisola del Sinai. XI. Formiche. *Bulletin. Société Entomologique d'Egypte* 20: 155–210.
- Forel A (1892) Notes myrmécologiques. *Annales de la Société Entomologique de Belgique* 36: 38–43.
- Forel A (1910) Ameisen aus der Kolonie Erythraä. Gesammelt von Prof. Dr. K. Escherich (nebst einigen in West-Abessinien von Herrn A. Ilg gesammelten Ameisen). *Zoologische Jahrbücher. Abteilung für Systematik, Geographie und Biologie der Tiere* 29: 243–274.
- Forel A (1911) Fourmis nouvelles ou intéressantes. *Bulletin de la Société Vaudoise des Sciences Naturelles* 47: 331–400.
- Forel A (1913) Formicides du Congo Belge récoltés par MM. Bequaert, Luja, etc. *Revue Zoologique Africaine (Brussels)* 2: 306–351.
- Guichard KM (1980) A preliminary account of the sphecid wasps of Oman (Hymenoptera, Sphecidae). *The Journal of Oman Studies, Special Report* 2: 223–232.
- Hájek J, Reiter A (2014) Adepagous water beetles (Coleoptera: Gyrinidae, Haliplidae, Noteridae, Dytiscidae) of Yemen and Dhofar region (Oman) with description of a new Hyphydrus from Socotra Island. *Acta Entomologica Musei Nationalis Pragae* 54: 63–99.
- Hausmann A (2009) New and interesting geometrid moths from Dhofar, southern Oman (Lepidoptera, Geometridae). *Mitteilungen der Münchner Entomologischen Gesellschaft* 99: 111–128.
- Hita Garcia F, Wiesel E, Fischer G (2013) The ants of Kenya (Hymenoptera: Formicidae) faunal overview, first species checklist, bibliography, accounts for all genera, and discussion on taxonomy and zoogeography. *Journal of East African Natural History* 101: 127–222. <https://doi.org/10.2982/028.101.0201>
- Karavaiev V (1912) Ameisen aus Tunesien und Algerien, nebst einigen unterwegs in Italien gesammelten Arten. *Russkoe Entomologicheskoe Obozrenie* 12: 1–22.
- Kuznetsov-Ugamsky NN (1929) Die Gattung *Acantholepis* in Turkestan. *Zoologischer Anzeiger* 82: 477–492.

- Larsen TB (1980) The butterflies of Dhofar and their zoogeographic composition. *Journal of Oman Studies Special Report 2*: 153–186.
- Larsen TB, Larsen K (1980) *The Butterflies of Oman*. Bartholomew, Edinburgh, 80 pp.
- Larsen TB (1984) The zoogeographical composition and distribution of the Arabian butterflies (Lepidoptera: Rhopalocera). *Journal of Biogeography* 11: 119–158. <https://doi.org/10.2307/2844685>
- Mayr G (1855) *Formicina austriaca*. Beschreibung der bisher im österreichischen Kaiserstaate aufgefundenen Ameisen, nebst Hinzufügung jener in Deutschland, in der Schweiz und in Italien vorkommenden Arten. *Verhandlungen der Zoologisch-Botanischen Vereins in Wien* 5: 273–478.
- Melnikov D, Pierson T (2012) A new species of *Pseudotrapelus* (Agamidae, Sauria) from Dhofar, Oman. *Current Herpetology* 12: 143–151.
- Neubert E, van Damme D (2012) Palaeogene continental molluscs of Oman. *Contributions to Natural History* 20: 1–21.
- Penati F, Vienna P (2006) An updated catalogue of the Histeridae (Insecta: Coleoptera) of the Arabian Peninsula, with biogeographical remarks. *Zootaxa* 1157: 1–74. <https://doi.org/10.11646/zootaxa.1157.1.1>
- Pesenko YA, Pauly A (2009) A contribution to the fauna of the Nomioidine bees of the Arabian Peninsula (Hymenoptera: Halictidae). *Fauna of Arabia* 24: 217–236.
- Rueda M, Rodríguez MÁ, Hawkins BA (2013) Identifying global zoogeographical regions: lessons from Wallace. *Journal of Biogeography* 40: 2215–2225. <https://doi.org/10.1111/jbi.12214>
- Schneider W, Krupp F (1993) Dragonfly Records from Saudi Arabia with an annotated checklist of the species from the Arabian Peninsula (Insecta: Odonata). *Fauna of Saudi Arabia* 13: 63–78.
- Sharaf MR, Al Dhafer HM, Aldawood AS (2014) First record of the myrmicine ant genus *Meranoplus* Smith, 1853 (Hymenoptera: Formicidae) from the Arabian Peninsula with description of a new species and notes on the zoogeography of southwestern Kingdom Saudi Arabia. *PLoS ONE* 9(11): e111298. <https://doi.org/10.1371/journal.pone.0111298>
- Sharaf MR, Aldawood AS (2011) *Monomorium dryhimi* sp. n., a new ant species (Hymenoptera, Formicidae) of the *M. monomorium* group from Saudi Arabia, with a revised key to the Arabian species of the group. *ZooKeys* 106: 47–54. <https://doi.org/10.3897/zookeys.106.1390>
- Sharaf MR, Aldawood AS (2019) Review of the ant genus *Meranoplus* Smith, 1853 (Hymenoptera: Formicidae) in the Arabian Peninsula with description of a new species *M. mosalahi* sp. n. from Oman. *PeerJ* 7:e6287. <https://doi.org/10.7717/peerj.6287>
- Sharaf MR, Aldawood AS, Taylor B (2012a) A new ant species of the genus *Tetramorium* Mayr, 1855 (Hymenoptera, Formicidae) from Saudi Arabia, including a revised key to the Arabian species. *PLoS ONE* 7(2): e30811. <https://doi.org/10.1371/journal.pone.0030811>
- Sharaf MR, Aldawood AS, El-Hawagry MS (2012b) A new ant species of the genus *Tapinoma* (Hymenoptera, Formicidae) from Saudi Arabia with a key to the Arabian species. *ZooKeys* 212: 35–43. <https://doi.org/10.3897/zookeys.212.3325>

- Sharaf MR, Aldawood AS, El-Hawagry MS (2012c) First record of the ant subfamily Aenictinae (Hymenoptera, Formicidae) from Saudi Arabia, with the description of a new species. *ZooKeys* 228: 39–49. <https://doi.org/10.3897/zookeys.228.3559>
- Sharaf MR, Fisher BL, Al Dhafer HM, Polaszek A, Aldawood AS (2018) Additions to the ant fauna (Hymenoptera: Formicidae) of Oman, updated list, new records and description of two new species. *Asian Myrmecology* 9: e010004. [1–38]
- Sharaf MR, Monks J, Polaszek A, Aldawood SA (2016) A remarkable new species of the genus *Lepisiota* Santschi (Hymenoptera: Formicidae) from Oman and the United Arab Emirates with a key to the Arabian species. *Journal of Natural History* 50(29–30): 1875–1887. <https://doi.org/10.1080/00222933.2016.1180722>
- Šmíd J (2010) New remarkable snake records from Oman. *Herpetology Notes* 3: 329–332.
- Smith F (1861) Descriptions of some new species of ants from the Holy Land, with a synonymic list of others previously described. *Journal and Proceedings of the Linnean Society of London. Zoology* 6: 31–35. <https://doi.org/10.1111/j.1096-3642.1861.tb00926.x>
- Taiti S, Ferrara F, Davolos D (2000) The terrestrial Isopoda (Crustacea: Oniscidea) of Oman. *Fauna of Arabia* 18: 145–163.
- Waterston AR, Pittaway, AR (1991) The Odonata or dragonflies of Oman and neighbouring territories. *Journal of Oman Studies* 10: 131–168.
- Wu J, Wang C (1995) *The ants of China*. China Forestry Publishing House, Beijing, 214 pp. [In Chinese]
- Zhou S (2001) *Ants of Guangxi*. Guangxi Normal University Press, Guilin, 255 pp. [In Chinese]